Evaluating the economics of metal recycling from end-of-life lithium ion batteries in South Africa

By

Mari-Alet Smit

Thesis presented in partial fulfilment
of the requirements for the Degree

of

MASTER OF ENGINEERING
(EXTRACTIVE METALLURGICAL ENGINEERING)

in the Faculty of Engineering
at Stellenbosch University

Supervisor
Prof. Christie Dorfling

Co-Supervisor
Prof. Guven Akdogan

December 2020

DECLARATION

By submitting this thesis electronically, I declare that the entirety of the work contained therein is my own, original work, that I am the sole author thereof (save to the extent explicitly otherwise stated), that reproduction and publication thereof by Stellenbosch University will not infringe any third party rights and that I have not previously in its entirety or in part submitted it for obtaining any qualification.

Date: *November 2020*

PLAGIARISM DECLARATION

1. Plagiarism is the use of ideas, material and other intellectual property of another's work and to present is as my own.

2. I agree that plagiarism is a punishable offence because it constitutes theft.

3. I also understand that direct translations are plagiarism.

4. Accordingly all quotations and contributions from any source whatsoever (including the internet) have been cited fully. I understand that the reproduction of text without quotation marks (even when the source is cited) is plagiarism.

5. I declare that the work contained in this assignment, except where otherwise stated, is my original work and that I have not previously (in its entirety or in part) submitted it for grading in this module/assignment or another module/assignment.

Student number:

Initials and surname: M. Smit

Signature: ……..

Date: November 2020

ABSTRACT

Lithium-ion batteries (LIBs) are used in various electronic equipment as well as electric vehicles. With the rapid growth and development in technology usage, it is not surprising that the generation and safe disposal of end-of-life LIBs have become a global problem. Sustainably recycling spent LIBs will address this problem.

The study aimed to investigate and compare the techno-economic feasibility of mineral acid based and organic acid based hydrometallurgical processes for metal recovery from end-of-life LIBs within a South African context. This was achieved by developing various hydrometallurgical flowsheets, completing associated mass and energy balances, calculating capital and operating costs, evaluating the profitability and performing a sensitivity analysis to investigate the influence of changing market and operating conditions on the profitability criteria.

A LIB feed capacity of 868 ton per year was selected as basis for mass and energy balances. Six flowsheet alternatives using either hydrochloric or citric acid as leaching reagents were evaluated and compared. A LIB recycling facility using citric acid as leaching reagent and four selective precipitation steps for the recovery of manganese oxide, nickel hydroxide, cobalt oxalate and lithium phosphate will be the techno-economically most favorable option returning a Net Present Value (NPV) of $ 16.4 million after 20 years. The proposed process has an estimated Capital Expenditure (CAPEX) of $ 22.8 million, Operating Expenditure (OPEX) of $ 17.0 million per year and revenue of $ 25.5 million per year. The Present Value Ratio (PVR) of 1.8 and Discounted Cashflow Rate of Return (DCFROR) of 28.2% confirmed that profitable operation will be possible.

However, if the aim of the facility is to produce only two metal products (i.e. a combined metal product that could be used in cathode material regeneration and a lithium product), the use of hydrochloric acid as leaching reagent with two subsequent precipitation steps will be most profitable and result in an NPV of $ 5.7 million. A similar flowsheet using citric acid as lixiviant may also be profitable depending on the chosen precipitant.

The sensitivity analysis indicated that the profitability of the proposed facility is most sensitive to fluctuations in the feed capacity, metal selling prices and the fixed capital investment when all other parameters are kept at base values. Monte Carlo simulations evaluated the sensitivity of the profitability criteria to the random interaction between 17 variables. Depending on the simulation input specifications the probability of profitable operation ranged between 58.45% and 99.52%.

It was concluded that citric acid would be a suitable alternative lixiviant for mineral acids in the LIB recycling process. Further research and experimental work should focus on in-depth process development as the current level of process integration and development is only at concept phase. Pilot-plant studies will be the best way to reduce uncertainty in mass and energy balances and to understand the technical challenges that will be faced with large-scale operation. A detailed market analysis to evaluate the current status of LIB recycling in South Africa and correspondence with key stakeholders is recommended.

OPSOMMING

Litium-ioon batterye (LIBe) word in ’n verskeidenheid elektroniese toerusting asook elektriese voertuie gebruik. As gevolg van die vinnige groei en ontwikkeling in die gebruik van tegnologie, is dit nie verbasend dat die toename in LIB afval en die veilige verwydering daarvan ’n wêreldwye probleem geword het nie. Die volhoubare herwinning van LIB afval sal die probleem kan aanspreek.

Hierdie studie het die tegno-ekonomiese lewensvatbaarheid van mineraalsuur- en organiese suur gebaseerde hidrometallurgiese prosesse wat fokus op metaal herwinning uit afval LIBe ondersoek en vergelyk binne ’n Suid-Afrikaanse konteks. Die ondersoek het die volgende behels: ontwikkeling van hidrometallurgiese vloeidiagramme en die gepaardgaande massa- en energiebalanse, berekening van kapitaal- en bedryfskostes, evaluering van winsgewendheid en sensitiwiteitsanalises om die invloed van mark- en bedryfstoestande op die winsgewendheidskriteria te ondersoek.

’n Voer kapasiteit van 868 ton LIB afval per jaar is gekies as basis vir die massa- en energiebalanse. Ses verskillende proses opsies wat soutsuur of sitroensuur as logingsreagens gebruik, is geëvalueer en vergelyk. ’n LIB herwinningsaanleg wat sitroensuur as logingsreagens en 4 selektiewe presipitasie stappe gebruik om mangaandioksied, nikkelhidroksied, kobaltoksalaat en litiumfosfaat as produkte te produseer, is die proses opsie wat die mees finansieel lewensvatbaar sal wees. Die netto huidige waarde van die aanleg is bereken as $ 16.4 miljoen na ’n projekleeftyd van 20 jaar. Die voorgestelde LIB herwinningsaanleg het ’n beraamde kapitaalkoste van $ 22.8 miljoen, jaarlikse bedryfskoste van $ 17.0 miljoen en verwagte jaarlikse inkomste van $ 25.5 miljoen. Die huidige waarde verhouding van 1.8 en die verdiskonteerde kontantvloei opbrengskoers van 28.2% het bevestig dat die projek winsgewend sal kan wees.

Indien die doel van die herwinningaanleg is om net twee metaal produkte (nl. ’n gekombineerde metaal produk wat gebruik kan word in katode materiaal produksie en ’n litium produk) te produseer, sal die gebruik van soutsuur as logingsreagens met twee opeenvolgende presipitasie stappe die mees finansieel lewensvatbare aanleg met ’n netto huidige waarde van $ 5.7 miljoen wees. ’n Soortgelyke sitroensuur gebaseerde aanleg kan ook winsgewend wees afhangende van die gekose presipitasie reagens.

Die sensitiwiteitsanalise het aangedui dat die winsgewendheid van die voorgestelde aanleg die sensitiefste is vir veranderinge in die voer kapasiteit, die metaal produk verkoopspryse en die aanvanklike kapitaal belegging indien alle ander veranderlikes by basis waardes gehou word. Monte Carlo simulasies is gebruik om die sensitiwiteit van die winsgewendheidskriteria vir die lukrake interaksie tussen 17 veranderlikes te evalueer. Afhangende van die simulasie invoer spesifikasies het die waarskynlikheid vir winsgewendheid gewissel tussen 58.45% en 99.52%.

Daar is tot die gevolgtrekking gekom dat sitroensuur ’n geskikte alternatiewe logingsreagens vir mineraalsure in die LIB herwinningsproses is. Toekomstige navorsing en eksperimentele werk moet fokus op gedetailleerde prosesontwikkeling aangesien die huidige stand van proses-integrasie en -ontwikkeling slegs konseptueel is. Proefaanleg-studies sal die beste manier wees om onsekerhede in massa- en energiebalanse uit te skakel en die tegniese uitdagings wat gepaard gaan met grootskaalse aanlegte te

verstaan. ’n Gedetailleerde markanalise wat die huidige status van LIB herwinning in Suid-Afrika evalueer en samewerking met belanghebbendes word aanbeveel.

ACKNOWLEDGEMENTS

All glory belongs to God who gave me the energy and ability to complete this project. Thank you Father for blessing me with joy in my work.

James 1:17 (ESV) – Every good and perfect gift is from above, coming down from the Father of lights with whom there is no variation or shadow due to change.

I would also like to thank the following individuals or institutions:

- Professor Christie Dorfling, for always being available to answer questions and think with me and providing support and guidance throughout my project. It was a privilege working with and learning from you.
- My parents, Pieter and Mariet Smit, for unconditionally loving, supporting, believing in and praying for me. Thank you for being role models to me and giving me opportunities that shaped me to be the person I am today.
- My siblings, Jakobus and Christie, for family dinners away from home. Stellenbosch would not have been the same without having both of you here this year.
- David for many Whatsapp calls, encouraging words, laughter and weekend adventures that made every week's hard work worthwhile.
- The Harry Crossley Foundation for their financial support that made this project possible.
- The administrative staff at the Department of Process Engineering at Stellenbosch University.

TABLE OF CONTENTS

LIST OF FIGURES

LIST OF TABLES

NOMENCLATURE

Symbols		
A	Area	m^2
	Equipment cost parameter	Dimensionless
C_{OL}	Operating labour cost	US $
COM_d	Cost of manufacturing excluding depreciation	US $
C_p^0	Base equipment cost	US $
C_p	Specific heat capacity	kJ/kg.K
C_{RM}	Raw material cost	US $/annum
C_{TOC}	Total operating cost	US $/annum
C_{UT}	Utility cost	US $/annum
C_{WT}	Waste treatment cost	US $/annum
D	Depreciable capital	US $
D_c	Column diameter	m
d	Yearly depreciation	US $
d_k^{SL}	Yearly depreciation calculated with the Straight-Line method	US $
FCI_L	Fixed Capital Investment excluding land	US $
FCI	Fixed Capital Investment	US $
F_M	Material correction factor	Dimensionless
F_P	Pressure correction factor	Dimensionless
F_T	Temperature correction factor	Dimensionless
h	Convective heat transfer coefficient	$W/m^2.K$
H_{tower}	Tower height	m
l_t	Plate spacing	m
$\dot{m}$	Mass flowrate	kg/hr
n	Cost exponent or scaling factor	Dimensionless
	Number of iterations	Dimensionless
	Mole	mole
	Year	Dimensionless
pK_{sp}	Solubility product	Dimensionless
R	Revenue from sales	US $
r	Discount rate	%

S	Salvage Value	US $
	Standard deviation of NPV	US $
	Sensitivity	Million US $/% Change
T	Temperature	°C
ΔT_{lm}	Log mean temperature difference	K
t	Taxation rate	%
u	Velocity	m/s
U	Overall heat transfer coefficient	W/m^2.K
V	Volume	m^3
$\dot{V}$	Volumetric flowrate	m^3/hr
$\dot{Q}$	Heat transfer rate	kW
Z	Z-value related to normal distribution	Dimensionless
Greek symbols		
ρ	Density	kg/L
Subscripts and superscripts		
aq	Aqueous phase	
in	Flow stream into the system	
l	Liquid	
org	Organic phase	
out	Flow stream out of the system	
v	Vapour	
Acronyms and abbreviations		
CAPEX	Capital Expenditure	
CEPCI	Chemical Engineering Plant Cost Index	
CV	Coefficient of Variation	
D2EHPA	Di-(2-ethylhexyl) phosphoric acid	
DCFROR	Discounted Cash Flow Rate of Return	
DEC	Diethyl Carbonate	
DMG	Dimethylglyoxime	
DMSO	Dimethyl Sulfoxide	
EDTA	Ethylene di-amine tetra acetic acid	
EV	Electric Vehicle	
E-Waste	Electronic Waste	
HPS	High pressure steam	
LCA	Life Cycle Analysis	

LCO	Lithium Cobalt Oxide ($LiCoO_2$)
LFP	Lithium Iron Phosphate ($LiFePO_4$)
LIB	Lithium-Ion Battery
LLS	Layered-Layered-Spinel
LMO	Lithium Manganese Oxide ($LiMn_2O_4$)
LNO	Lithium Nickel Oxide ($LiNiO_2$)
MA-1	Mineral Acid process option 1
MA-2	Mineral Acid process option 2
MA-3	Mineral Acid process option 3
NMC	Nickel-Manganese-Cobalt Oxide ($LiNi_xMn_yCo_zO_2$)
NMP	N-methyl pyrrolidone
Ni-DMG	Nickel Dimethylglyoxime complex
Ni-MH	Nickel Metal Hydride
NPV	Net Present Value
OA-1	Organic Acid process option 1
OA-2	Organic Acid process option 2
OA-3	Organic Acid process option 3
O:A	Organic to Aqueous phase ratio
OPEX	Operating Expenditure
PC	Propylene Carbonate
PE	Polyethylene
PFD	Process Flow Diagram
PLS	Pregnant Leach Solution
PP	Polypropylene
ppm	parts per million
PTFE	Polytetrafluoroethylene
PVDF	Polyvinylidene fluoride
PVR	Present Value Ratio
S/L	Solid to Liquid ratio
TBP	Tributyl Phosphate
TOA	Tri-n-octylamine
USD	United States Dollars
WC	Working Capital
WEEE	Waste Electrical and Electronic Equipment

1 Introduction

1.1 Background and problem statement

Lithium-ion batteries (LIBs) are used as devices for energy storage and the conversion of chemical energy to electrical energy in various electrical and electronic equipment since the 1990s. Due to their high energy density, light weight, small volume, long storage life, low self-discharge efficiency, wide range of application temperatures and excellent electrochemical performance, LIBs are a suitable option in both household and industrial applications as well as electric vehicles (Zhang *et al.*, 2018; Zheng *et al.*, 2018).

LIBs used in digital appliances typically have a lifetime of between 1 and 3 years whereas the lifetime of batteries used in electric vehicles range between 5 and 8 years. Based on the assumed LIB lifetime, it was estimated that China will produce 2.5 billion end-of-life LIBs (approximately 500 000 tonnes of waste) by 2020 (Zheng *et al.*, 2018). Knights and Saloojee (2015) predicted that the South African LIB consumption rate will reach 10 000 tonnes per annum in 2020. With the rapid growth in the use of consumer electronics and the anticipated adoption of electric cars in the automotive industry, it is not surprising that the generation and safe disposal of LIBs have become a global problem. The main drivers for LIB recycling in South Africa are:

1. There are currently no LIB recycling facilities focussing on the processing and recovery of valuable metals from end-of-life LIBs in the entire African continent. LIB recycling facilities are mainly located in North America, Asia and Europe. The combined processing capacity of current recycling facilities is less than 30% of the global LIB production (Knights and Saloojee, 2015).
2. E-waste is currently the fastest growing waste stream in South Africa (Cape E-Waste Recyclers, no date) with each South African producing approximately 6.2 kg of e-waste annually (Guy, 2017). Due to the lack of LIB recycling facilities in South Africa, spent LIBs are landfilled or exported to countries where LIBs can be recycled. Thus, South Africa loses out on the economic potential of recycling the LIB waste generated within the country. Local LIB recycling can lead to economic and social benefits for South Africa by contributing to economic growth and creating job opportunities.
3. LIBs contain various valuable metals such as lithium, cobalt, nickel and manganese that can be recycled profitably. Globally the production rates of lithium and cobalt have increased slightly in the last few years. However, the current growth in the demand for lithium and cobalt impose pressure on the supply side of these metals that may lead to shortages in the near future (Lv *et al.*, 2018). Recycling facilities that recover these valuable metals can help to relieve the pressure on the valuable metal supply chain. Recycling LIBs will not only decrease the dependency on raw mineral ores but may also reduce the fossil resource demand with 45.3% and the nuclear energy demand with 57.2% resulting in natural resource savings of 51.3% (Dewulf *et al.*, 2010).
4. More than a third of the manufacturing costs for lithium-ion batteries are related to raw materials costs (Georgi-Maschler *et al.*, 2012). Recovering lithium, cobalt, nickel and manganese from end-of-life LIBs with the aim of producing raw materials suitable for use in the LIB production process may add economic value to the LIB recycling industry.

5. There is a need for a LIB disposal strategy that will not pose risks to human health and safety or the environment. The components of LIBs contain hazardous heavy metals and organic materials as seen in Table 1 below. Knights and Saloojee (2015) stated potential risks associated with the landfilling of LIB waste. When damaged or exposed to high temperatures, LIBs can explode. The groundwater and soil can be contaminated by the heavy metals and toxic electrolytes present in LIB waste. Thus, the handling and treatment of end-of-life LIB materials is of importance for both human and environmental health and safety.

Table 1: Environmental and health hazards associated with spent LIBs (Zheng *et al.*, 2018)

LIB Component	**Material**	**Hazard**
Electrolyte	$LiPF_6$, $LiBF_4$, $LiClO_4$, $LiSO_2$, PC, DEC, DMSO	Very corrosive, hazardous gases (HF, Cl_2, CO and CO_2) is produced when burned, toxic, flammable
Cathode	$LiCoO_2$, $LiNiO_2$, $LiMn_2O_4$, $LiFePO_4$, $LiNi_xCo_yMn_{1-x-y}O_2$	Contains heavy metals (Co, Ni, Mn) that can pose a risk to both human health and the environment
Binder	PVDF or PTFE	HF production when heated

Various recycling strategies involving mechanical, hydrometallurgical or pyrometallurgical treatment can be implemented to recover valuable components from end-of-life LIBs. In hydrometallurgical processes, LIBs are mechanically pre-treated before fed to a process that involves leaching and selective metal recovery from the leach solution to produce high purity metal products. Conventionally, mineral acids such as hydrochloric, sulfuric or nitric acid are used to facilitate the leaching of valuable metals in large-scale recycling facilities. Recently the leaching behaviour of various organic acids has been evaluated as possible alternative eco-friendly leaching reagents for the leaching of valuable metals from LIB waste.

Research currently conducted focusses on the technical aspects related to hydrometallurgical flowsheet development for metal recovery from LIBs. Limited work considering the techno-economic feasibility of possible hydrometallurgical process routes within a South African context has been done. This project aims to investigate and compare the techno-economic feasibility of two broadly defined hydrometallurgical process routes (i.e. mineral acid based processes and organic acid based processes) within a South African context.

1.2 Objectives

The project aims to compare the key economic indicators for different hydrometallurgical process flowsheets suitable for metal recycling from end-of-life LIBs. The project aims to achieve the following specific objectives:

1. Conduct a literature review to gain an overview of hydrometallurgical flowsheet options that can be employed in the LIBs recycling industry. Assess the current status of LIBs recycling in South Africa in terms of waste generation, recycling rates and local value recovery.

2. Develop flowsheets and complete mass and energy balances for various process options within two broadly defined hydrometallurgical process routes (i.e. mineral acid based processes and organic acid based processes).
3. Based on the capital and operating costs, calculate key profitability criteria and economic indicators to determine the economic viability of different flowsheet options. Compare different flowsheet options to make relevant conclusions and recommendations with regards to the techno-economic feasibility of possible LIB recycling options in a South African context.
4. Perform a sensitivity analysis to investigate the effect of changing market and operating conditions on the profitability criteria.

1.3 Key questions

The study aims to answer the following key questions:

1. How do the hydrometallurgical flowsheets and unit operations required for mineral acid based and organic acid based processes differ from each another?
2. How do the capital and operating costs and profitability criteria of various flowsheet options differ from each other?
3. Which hydrometallurgical flowsheet is the best option for valuable metal recovery from end-of-life LIBs in South Africa?
4. How sensitive is the profitability criteria to fluctuations in market and operating conditions?

1.4 Research approach

The research approach or methodology followed to achieve the objectives and answer the key questions are listed below:

1. A literature study was conducted to gain an understanding of LIB recycling and various hydrometallurgical flowsheet options that can be used to recover valuable metals from spent LIBs.
2. Based on published data and literature sources, hydrochloric acid was selected as mineral acid lixiviant and citric acid was selected as organic acid lixiviant. Mineral and organic acid based flowsheets using different mechanisms to sequentially recover the valuable metals from leach solutions were developed.
3. Assumptions were made with regards to the possible LIB feed and operating conditions of unit operations in each flowsheet option. Mass and energy balances were completed for each flowsheet option. Major equipment pieces were sized based on the information gained from the mass and energy balances.
4. Each flowsheet option was evaluated with regards to its techno-economic feasibility by calculating the capital expenditure (CAPEX), operating expenditure (OPEX) and key profitability criteria associated with it.

5. The CAPEX, OPEX and profitability criteria of the evaluated process options were compared to make relevant conclusions and recommendations with regards to the economic feasibility of LIB recycling within a South African context.
6. A sensitivity analysis was performed to investigate the effect of changing market and operating conditions on the profitability criteria. Monte Carlo simulations were used to understand the effect of random multi-variable interaction on the Net Present Value (NPV). Economy of scale was evaluated to calculate the minimum LIB feed that would allow profitable operation.
7. Based on the outcome of the mass and energy balances, economic analyses and sensitivity analysis, the key technical and sustainability challenges and opportunities were identified to focus future efforts in this research and development field.

1.5 Thesis outline

The work in this thesis is presented as follows:

Chapter 2: Literature Review

Various strategies for the recycling of LIB waste are discussed and compared in this chapter. An overview of hydrometallurgical process options with regards to pre-treatment, leaching and metal recovery from leach liquors are discussed.

Chapter 3: Mass and Energy Balances

Different hydrometallurgical flowsheets were developed based on previous experimental studies. The system boundaries are defined, the feed capacity and composition are specified, and the assumptions made to complete the mass and energy balances for each flowsheet option are discussed in this chapter.

Chapter 4: Process Economics

The theory and approach to the economic analysis are presented in this chapter. The correlations and assumptions made regarding equipment selection and preliminary sizing, capital and operating cost estimations and the calculation of profitability indicators are discussed.

Chapter 5: Economic Analysis and Process Comparison

The results of the mass and energy balances as well as the economic analysis performed for each flowsheet option are discussed and compared. Possible reasons for the differences in the metal recovery, product quality, capital and operating expenditure, revenue and economic indicators of the flowsheet options are discussed. The best flowsheet options with regards to techno-economic feasibility within a South African context are selected.

Chapter 6: Sensitivity Analysis

The results of a sensitivity analysis concentrating on the effect of changing market and operating conditions on the profitability criteria are presented in this chapter. The effect of

individual variables as well as multi-variable interaction (assessed with Monte Carlo simulations) are discussed.

Chapter 7: Conclusions and Recommendations

The main conclusions and recommendations concerning the techno-economic feasibility of hydrometallurgical processes for LIB recycling in South Africa based on the results obtained from the economic and sensitivity analysis are presented. The chapter also discuss how each of the objectives set in section 1.2 were met in the study. Recommendations as to improve flowsheets and the reliability of results as well as future work that may add value to the research field are made.

2 Literature Review

2.1 Lithium-Ion battery structure

Lithium-ion batteries typically consist of a cathode, anode, electrolyte and separator within a plastic or metal casing (Zeng, Li and Singh, 2014; Chagnes *et al.*, 2015). Figure 1 below is a simplified diagram showing the main components of a lithium-ion battery. The anode primarily consists of carbon bound to a copper current collector with a polymer binder (Zeng, Li and Singh, 2014). The cathode consists of active material which is a lithium metal oxide ($LiCoO_2$, $LiNiO_2$, $LiMn_2O_4$, $LiFePO_4$ or $LiNi_xCo_yMn_{1-x-y}O_2$) bound to an aluminium current collector. Polyvinylidene fluoride (PVDF) is typically used as polymer binder between the current collectors and electrode active material. The electrolyte consists of a lithium salt (for example $LiPF_6$, $LiBF_4$, $LiClO_4$ or $LiSO_2$) dissolved in an organic solvent (for example ethylene carbonate or propylene carbonate) (Knights and Saloojee, 2015). Micro-perforated plastics such as polyethylene (PE) or polypropylene (PP) are used as separators in LIBs to avoid short circuiting due to direct contact between the cathode and anode (Zheng *et al.*, 2018).

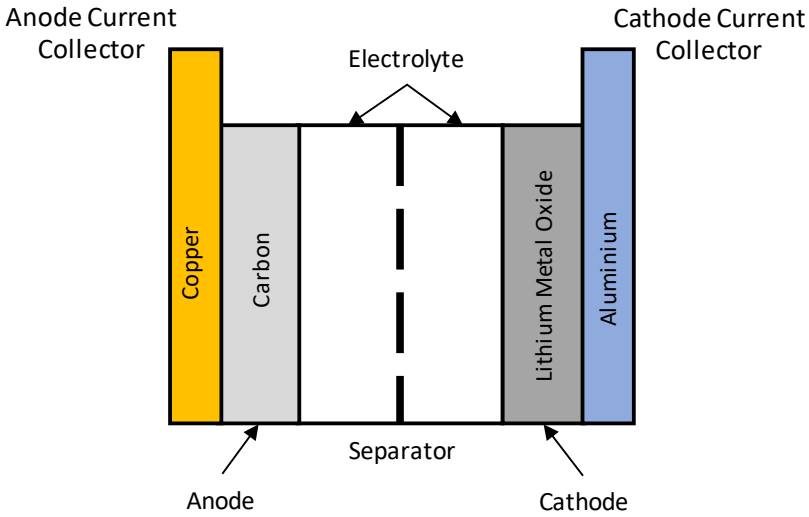

Figure 1: Simplified diagram illustrating the main components of a lithium-ion battery (adapted from Electropaedia, no date)

The performance of a lithium-ion battery is primarily determined by its cathode material (Zou *et al.*, 2013). Historically the market share of cathode materials was dominated by $LiCoO_2$ due to its great performance. The advantages and disadvantages of various cathode materials are summarized in Table 2 below. These factors have an influence on the market trends and demand for each cathode material. Because nickel and manganese are cheaper than cobalt, global cathode markets are shifting towards nickel-manganese-cobalt (NMC) batteries.

The LIB recycling process primarily aims to recover the valuable metals (Co, Ni, Mn and Li) from the active cathode materials. However, other battery components such as paper, plastics, graphite and steel can also be recovered during the process and further recycled in other specialised facilities.

Table 2: Advantages and disadvantages of cathode materials (Zou *et al.*, 2013)

Cathode Material	Advantages	Disadvantages
$LiCoO_2$	1. Simple manufacturing process 2. Better performance in voltage stability, capacity, reversibility, charging efficiency 3. Long cycle life	1. Cobalt is very expensive 2. Environmental issues should be considered
$LiNi_{0.33}Mn_{0.33}Co_{0.33}O_2$	1. Less expensive than $LiCoO_2$ 2. Better safety and performance	-
$LiFePO_4$	1. Cheapest cathode material 2. Environmentally friendly 3. Resource availability 4. High thermal stability	1. Low energy density 2. Low electronic conductivity
$LiMn_2O_4$	1. Low cost 2. Resource availability 3. Environmentally friendly	1. Reduced performance at high temperatures
$LiNiO_2$	1. Less expensive than $LiCoO_2$ 2. Performance similar to $LiCoO_2$	1. Operating window for synthesis is tight 2. Low energy density and poor electrochemical performance 3. Fire/explosion hazard when overcharged

2.2 Process routes for the recycling of LIB waste

Mechanical, hydrometallurgical and pyrometallurgical process routes can be used to extract metals from LIB waste. For optimal metal extraction, two or more of these process routes are usually combined. The sections below shortly discuss the differences between these alternatives. The advantages and disadvantages of the different options are summarized in section 2.2.4.

2.2.1 Mechanical process routes

Mechanical process routes focus on the physical treatment or processing of LIB waste to separate the plastics, paper, separators, current collectors and metal casing from electrode materials (Chagnes *et al.*, 2015). This may include crushing, shredding, milling and screening of LIBs and various separation techniques exploiting differences in material characteristics such as density, magnetism and conductivity (Musariri, 2019). Refer to section 2.3.1 for a more detailed discussion on the different mechanical pre-treatment steps used in the LIB recycling industry.

Most LIB recycling facilities use mechanical process routes or treatment in combination with pyrometallurgy or hydrometallurgy. Examples of facilities or processes that use mechanical pre-treatment of LIB waste are Batrec Industrie AG in Switzerland and Akkuser in Finland (Chagnes *et al.*, 2015).

2.2.2 Pyrometallurgical process routes

Pyrometallurgical process routes use high temperature operation to recover metals from LIB waste. Smelting, pyrolysis, refining and distillation are some of pyrometallurgical unit operations that are used

in industry (Musariri, 2019). Generally cobalt, nickel and copper will be recovered as alloys which will require further refining to produce pure metal products. The slag produced will contain the manganese, lithium and aluminium which can be recovered by hydrometallurgical process steps (Chagnes *et al.*, 2015). Examples of facilities or processes that use pyrometallurgical process routes are Accurec in Germany, Umicore in Belgium and Xstrata (Chagnes *et al.*, 2015).

2.2.3 Hydrometallurgical process routes

Hydrometallurgical processes involve the extraction of valuable metals in an aqueous environment. Leaching is the process whereby metals are dissolved in an aqueous medium (usually acidic). The pregnant leach solution (PLS) rich in dissolved metal species is purified. The aim is to selectively extract metal species from the PLS with mechanisms such as precipitation, solvent extraction, ion-exchange and electrowinning to produce pure metal products. Leaching and hydrometallurgical recovery mechanisms that can be used in the LIB recycling industry are discussed in section 2.3. Examples of facilities or processes that use hydrometallurgical process routes are Recupyl in France and Retriev Technologies (previously known as Toxco) in Canada (Chagnes *et al.*, 2015).

2.2.4 Advantages and disadvantages of different LIB recycling strategies

Table 3 provides a summary of the advantages and disadvantages of the three process routes discussed in the previous sections. Hydrometallurgical LIB recycling is a suitable option for South Africa as it is less energy intensive compared to pyrometallurgy and allows the processing of smaller volumes of LIB waste.

Table 3: Advantages and disadvantages of LIB recycling process routes (continues on next page)

LIB Recycling Strategy	**Advantages**	**Disadvantages**
Mechanical Treatment	1. No change in composition of LIB waste (Musariri, 2019)	1. Batteries can explode during crushing or shredding (Musariri, 2019) 2. Crushing and milling are energy intensive (Musariri, 2019)
Pyro-metallurgy	1. Smelting furnaces can process large volumes of raw LIB waste (Chagnes *et al.*, 2015) 2. No special mechanical pre-treatment required (Chagnes *et al.*, 2015) 3. No sorting or separation of different types of batteries required (Chagnes *et al.*, 2015) 4. Processes consist of fast, simple steps (high efficiency) thus, there is no risk of exposure to toxic LIB electrolytes (Musariri, 2019)	1. Li and Mn cannot be recovered directly as it ends up in the slag phase. Hydrometallurgical treatment of the slag is required for the recovery of Li and Mn (Chagnes *et al.*, 2015) 2. Emission of harmful gases, thus gas trapping and purification equipment is required (Musariri, 2019) 3. High temperature operation, making processes energy intensive (Musariri, 2019)

LIB Recycling Strategy	Advantages	Disadvantages
Hydro-metallurgy	1. Processes are less energy intensive due to operation at low temperatures (Chagnes *et al.*, 2015) 2. Ability to adapt to lower volumes of feed material and fluctuations in feed composition (Chagnes *et al.*, 2015) 3. High recoveries of valuable metals (Musariri, 2019) 4. High purity final products produced (Chagnes *et al.*, 2015; Musariri, 2019) 5. Low gas emissions and generally more environmentally friendly (Musariri, 2019)	1. Requires mechanical pre-treatment of LIB waste (Chagnes *et al.*, 2015) 2. Liquid waste streams are produced that require further treatment (Musariri, 2019)

2.2.5 Current commercial hydrometallurgical LIB recycling processes

There are various companies that are profitably recycling lithium-ion batteries globally of which not a single facility on the African continent. Knights and Saloojee (2015) provide a list of these facilities and their respective recycling capacities. Two examples of commercial hydrometallurgical facilities are discussed in the sections below.

2.2.5.1 Recupyl Process

The Recupyl process (Figure 2) is a hydrometallurgical process that was developed in France and implemented in Singapore (Chagnes *et al.*, 2015).

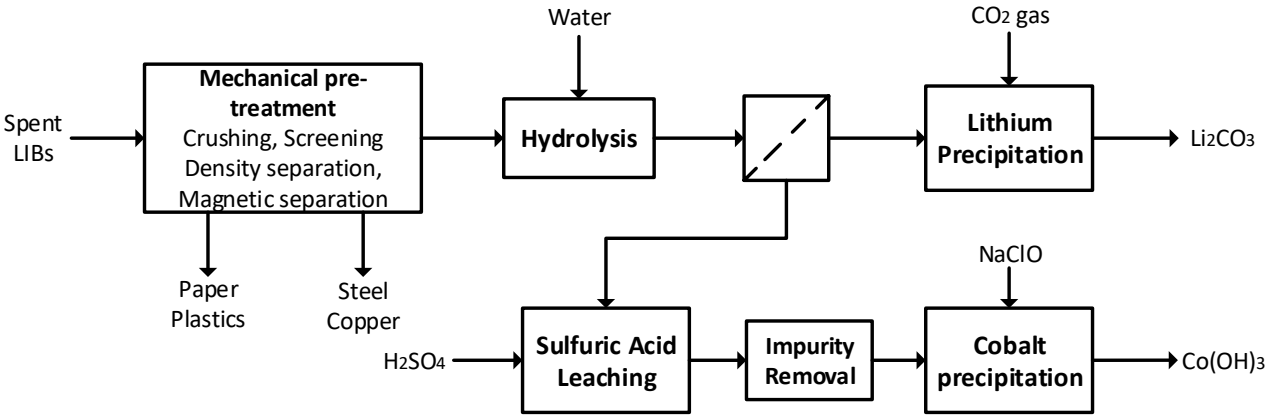

Figure 2: Schematic diagram of Recupyl Process

Spent LIBs are mechanically pre-treated with crushing, screening, density and magnetic separation steps to produce three waste fractions namely: paper and plastics, steel and copper, and a fine material fraction (Chagnes *et al.*, 2015; Knights and Saloojee, 2015). The fine material is treated by hydrolysis to dissolve the lithium. The lithium rich solution is separated from the remaining solids after which Li_2CO_3 is precipitated from the solution using carbon dioxide gas. Sulfuric acid is used to leach cobalt from the

residual solids after solid-liquid separation. The leach solution is purified by removing copper and iron from solution with the aim of increasing the purity of the cobalt hydroxide precipitate formed after the addition of sodium hypochlorite. Electrolysis is an alternative to precipitation for the recovery of cobalt from the leach solution (Knights and Saloojee, 2015).

2.2.5.2 Toxco Process

Retriev Technologies is an LIB recycling industry situated in Canada and was previously known as Toxco (Chagnes *et al.*, 2015). The Toxco process (shown in Figure 3) is a combination of mechanical treatment and hydrometallurgical process steps.

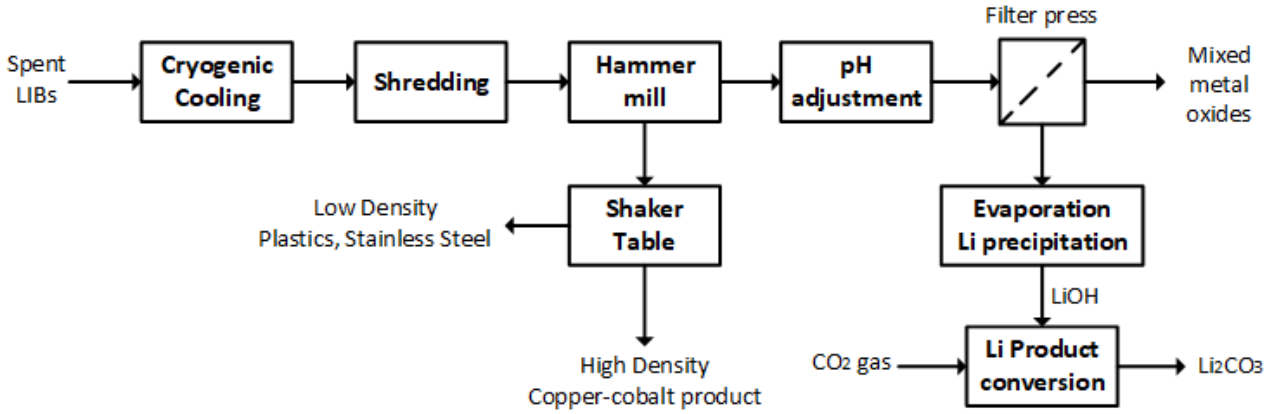

Figure 3: Schematic diagram of Toxco Process (adapted from Gaines *et al.*, 2011)

A cryogenic cooling step is used to cool the spent LIBs to between -175°C and -195°C with liquid nitrogen. This is necessary to ensure that the LIB material is rendered inert as some of the battery components may be reactive (Knights and Saloojee, 2015). The inert and discharged batteries undergo shredding before it is milled in a lithium brine with a hammer mill. The lithium is dissolved in the brine in the hammer mill to form a lithium rich solution that can be separated from the undissolved solids. The undissolved solids are separated into a high-density stream containing a cobalt-copper product and a low-density stream containing the plastics and stainless steel with a shaking table (Knights and Saloojee, 2015).

The pH of the lithium containing solution is controlled at a pH of 10 with the addition of lithium hydroxide. A mixed metal oxide product precipitates from the solution and is removed with a filter press. The evaporation of water from the lithium solution increases the concentration of lithium until lithium salts precipitate out. The addition of carbon dioxide finally converts the LiOH to Li_2CO_3 which can be packaged and sold (Knights and Saloojee, 2015).

2.3 Hydrometallurgical process overview

2.3.1 Pre-treatment of LIB waste

The pre-treatment process of LIB waste can be divided into two main processes: the disintegration of the batteries (by physical dismantling or crushing) and the classification or separation into material fractions with similar properties (Chagnes *et al.*, 2015). The aim is to separate the electrode materials which

contain the valuable metals from the other battery components with the smallest possible loss of valuable metals.

The first step in the pre-treatment process is to discharge the batteries to avoid short-circuits and sparks when the batteries are dismantled or crushed. LIBs are generally discharged through immersion in a salt solution (Zeng, Li and Singh, 2014; Yao *et al.*, 2018). After discharging, the batteries can either be physically dismantled or undergo crushing and screening steps combined with other separation techniques to separate the battery components into various fractions.

Physical dismantling involves removing the cell casings to expose the cell core so that the cathodes, anodes, steel, plastics and organic separators can be separated from each other. For large-scale or commercial recycling facilities, manual dismantling of LIBs will not be viable due to the large quantities of LIBs and the small size of traditional consumer batteries present in electronic devices (Yao *et al.*, 2018). Thus, for large-scale LIB recycling, mechanical processes that involve crushing is advisable.

After dismantling, cathode active material can be separated from the aluminium foil current collector by dissolving the PVDF binder in N-methyl pyrrolidone (NMP). Due to the polarity of both NMP and the PVDF binder, the binder can be dissolved in 1 hour. Other organic solvents that can also be used for LIB binder dissolution are N,N-dimethylformamide (DMF), N,N-dimethylacetamide (DMAC) and dimethyl sulfoxide (DMSO) (Yao *et al.*, 2018). Although great separation between Al foils and cathode material can be achieved, the use of these solvents is not feasible in large-scale recycling facilities. These solvents are very expensive and a single solvent cannot dissolve all types of binders (Yao *et al.*, 2018).

Sodium hydroxide is a cheaper alternative solvent that can be used for the dissolution of the Al foils (Musariri, 2019). Musariri (2019) treated the cathode material with a 10 wt% NaOH solution and solid-to-liquid (S/L) ratio of 100 g/L for 2 hours to dissolve the Al foils. The NaOH selectively dissolves the Al foils leaving behind the electrode material and binder which can be mechanically pre-treated in subsequent process steps.

Various multistage crushing and screening processes have been investigated to optimize the mechanical separation of the valuable cathode materials from the rest of the battery (Shin *et al.*, 2005; Jinhui Li, Shi, *et al.*, 2009; G. Granata *et al.*, 2012; Zhang *et al.*, 2013, 2014; Peng *et al.*, 2018). A disadvantage of using crushing or mechanical pre-treatment instead of physical dismantling is that some of the valuable cathode metals will inevitably be lost during the process.

Magnetic separation can be used to selectively remove the steel casings and iron particles after crushing (Shin *et al.*, 2005; Peng *et al.*, 2018). Density separation can be employed to separate the different components into lighter (plastics and paper) and heavier (metals and steel) fractions as done with the shaking table in the Toxco process (Chagnes *et al.*, 2015). The wet scrubbing separation technique investigated by Dutta *et al.* (2018) is also based on separating particles based on differences in their densities.

Zhang *et al.* (2014) proposed a process that involved air and electromagnetic separation techniques after crushing and sieving. Air separation was used to remove the fraction of particles with a size greater than

2 mm whereas electrostatic separation was used for the fraction of particles with sizes between 0.5 mm and 2 mm (Zhang *et al.*, 2014). Electrodynamic separation of particles with a size greater than 1 mm was investigated in the work done by Granata *et al.* in 2012.

Jinhui Li, Shi *et al.* (2009), Golmohammadzadeh *et al.* (2017), He, Sun, Mu *et al.* (2017), He *et al.* (2015) and He, Sun and Yu *et al.* (2018) investigated the use of ultrasonic washing. The aim was to separate the Al foils from the cathode material and the Cu foils from the graphite anode material. The optimized pre-treatment process suggested by Jinhui Li, Shi *et al.* (2009) included the following steps: crushing with a 12 mm aperture screen, ultrasonic washing with agitation at room temperature for 15 minutes followed by screening with a 2 mm aperture screen. Under these conditions, 92% of the electrode material was removed from their respective Al or Cu foils. The process proposed only used one crushing step in comparison to the two crushing steps employed in the work done by Lee and Rhee (2002) and no thermal pre-treatment is required making it less energy-intensive. Very little waste water or gas will be produced making it an environmentally friendly option (Jinhui Li, Shi, *et al.*, 2009). The optimized ultrasonic washing conditions suggested by another study was 240 W ultrasonic power, 70℃, S/L ratio of 0.1 g/ml and 90 min retention time (He *et al.*, 2015; He, Sun and Yu, 2018).

Thermal pre-treatment is an alternative option that can be used for the removal of organic compounds and graphite. If thermal pre-treatment is performed in the presence of oxygen it is defined as incineration (Chagnes *et al.*, 2015). Incineration can easily be used in large-scale applications due to the simplicity of the process. Various literature sources have investigated the effect of incineration on leaching and overall process performance (Lee and Rhee, 2002; Shin *et al.*, 2005; Paulino, Busnardo and Afonso, 2008; Li, Ge, Wu, *et al.*, 2010; Petranikova *et al.*, 2011; Guo *et al.*, 2016). Thermal pre-treatment reduces the amount of organic compounds and graphite in the LIB feed material, leading to increased metal extraction efficiencies (especially cobalt) achieved during leaching.

Thermal pre-treatment in the absence of oxygen is called pyrolysis (Chagnes *et al.*, 2015). Various studies have considered pyrolysis to determine if it is a suitable alternative for incineration (Sun and Qiu, 2011; Yao *et al.*, 2016). Incineration is associated with high smoke emissions and toxic gas production which will require extra gas trapping and purification equipment if used in large-scale industries (Yao *et al.*, 2018). Pyrolysis seems to be the more environmentally friendly alternative of the two options considering the composition of the organic material present in the battery waste (Chagnes *et al.*, 2015).

Table 4 summarizes the advantages and disadvantages of the pre-treatment methods discussed in this section.

Table 4: Summary of the advantages and disadvantages of pre-treatment mechanisms for LIB waste (Yao *et al.*, 2018; Zheng *et al.*, 2018)

Pre-treatment Process	Advantages	Disadvantages
Organic Solvent Dissolution (NMP)	1. High separation efficiency	1. Environmental hazards due to organic waste water generated 2. High cost of solvent 3. Require a specific solvent for each type of binder
NaOH Dissolution	1. Cheaper than organic solvents 2. Simple operation 3. High separation efficiency	1. Alkali waste water emission 2. Difficult to recover aluminium
Crushing and Sieving	1. Simple and convenient operation 2. Suitable for large-scale LIB recycling from an industrial and economic perspective	1. Toxic gas emissions 2. Cannot separate all components in waste entirely
Ultrasonic Washing	1. Simple operation 2. Environmentally safe, reduced pollution 3. Less energy intensive than crushing or thermal pre-treatment	1. Noise pollution 2. High initial capital investment
Incineration (Thermal Pre-treatment)	1. Simple and convenient operation for large-scale processing	1. Toxic gas and smoke emissions 2. High energy consumption
Pyrolysis (Thermal Pre-treatment)	1. More environmentally friendly than incineration	1. High energy consumption

2.3.2 Mineral acid leaching process

2.3.2.1 Mineral acid leaching

The valuable metal components such as Li, Co, Ni and Mn in lithium-ion batteries can be dissolved in acidic solutions. Mineral acids such as HCl, H_2SO_4 and HNO_3 are conventionally used for the dissolution of these components. The leaching efficiency and metal extraction achieved are affected by variables such as the pH, solid-to-liquid-ratio, residence time, temperature and type of lixiviant (Chagnes *et al.*, 2015). Gao, Liu *et al.* (2018) investigated the influence level of various leaching parameters and concluded that the influence level from high to low are the lixiviant species, acid molarity, leaching time, reductant species and addition, S/L ratio, reaction temperature and stirring speed. Refer to Table 5, Table 6 and Table 7 for the leaching results obtained with HCl, H_2SO_4 and HNO_3 in previous experimental work.

The leaching reactions of $LiCoO_2$ (the most common cathode material) with HCl, H_2SO_4 and HNO_3 are shown in equations 1, 2 and 3 below (Chagnes *et al.*, 2015). Experimental work has shown that the highest leaching efficiencies and metal extraction of Li and Co are achieved with HCl (Sakultung, Pruksathorn and Hunson, 2007). Hydrochloric acid provide high leaching efficiencies because the chloride ions in solution destabilize the formation of a surface layer (Joulié, Laucournet and Billy, 2014).

$$2LiCoO_2 + 6HCl \rightarrow 2CoCl_2 + 2LiCl + 3H_2O + 0.5O_2 \quad [1]$$

$$LiCoO_2 + 1.5H_2SO_4 \rightarrow CoSO_4 + 0.5Li_2SO_4 + 0.25O_2 + 1.5H_2O \quad [2]$$

$$2LiCoO_2 + 6HNO_3 \rightarrow 2Co(NO_3)_2 + 2LiNO_3 + 0.5O_2 + 3H_2O \quad [3]$$

The leaching of cathode materials is challenging due to the strong chemical bonds that exist between the various metal components within the material. Thus, leaching efficiencies can be improved by the addition of a reductive agent. The reductive agent reduces Co^{3+} to Co^{2+}, which enhances the Co extraction during leaching (Chagnes *et al.*, 2015). Hydrogen peroxide is typically used as reductant in mineral acid leaching systems. The oxidation and reduction reactions are represented by equations 4 and 5 shown below (Skoog and West, 1982).

$$H_2O_2 + 2H^+ + 2e^- \leftrightarrow 2H_2O \quad [4]$$

$$Co^{3+} + e^- \leftrightarrow Co^{2+} \quad [5]$$

When hydrogen peroxide is used as reductant, the leaching of $LiCoO_2$ with HCl, H_2SO_4 and HNO_3 can be represented by equations 6, 7 and 8 respectively (Chagnes *et al.*, 2015).

$$2LiCoO_2 + 6HCl + H_2O_2 \rightarrow 2CoCl_2 + 2LiCl + O_2 + 4H_2O \quad [6]$$

$$LiCoO_2 + 1.5H_2SO_4 + 1.5H_2O_2 \rightarrow CoSO_4 + 0.5Li_2SO_4 + O_2 + 3H_2O \quad [7]$$

$$2LiCoO_2 + 6HNO_3 + H_2O_2 \rightarrow 2Co(NO_3)_2 + 2LiNO_3 + O_2 + 4H_2O \quad [8]$$

Various studies have showed the improvement in leaching efficiencies with the addition of a reductant. For example, the experimental work done by Zhang *et al.* (1998) showed that the addition of 1.7 vol% hydrogen peroxide increased the metal extraction of cobalt and lithium with nitric acid from 40% and 50% respectively to 99% for both metals. An increase from 50% to 100% dissolution of cobalt was reported by Dorella *et al.* (2007) with the addition of 1 vol% H_2O_2 to the sulphuric acid leach solution.

Based on the literature values tabulated in Table 5, Table 6 and Table 7, it was concluded that:

1. High leaching efficiencies can be achieved with hydrochloric acid without the addition of a reductant. The addition of a reductant is necessary to achieve high leaching efficiencies of valuable metals with H_2SO_4 and HNO_3.
2. Hydrogen peroxide is the most common reductant used. The optimal H_2O_2 concentration is between 1 and 10 vol% H_2O_2.
3. Generally the optimal leaching conditions for high Li and Co extraction is achieved with 2 to 4 M hydrochloric or sulphuric acid, 1-6 vol% H_2O_2 addition, a temperature of 60-80 ℃ and a leaching time of 1 hour (Chagnes *et al.*, 2015).

Table 5: Hydrochloric acid leaching conditions and metal extraction efficiencies

Reference	Cathode Material Type	Acid Concentration	Tempera-ture (℃)	S/L ratio	Time	H_2O_2 Concentration	Metal Extraction
(Zhang *et al.*, 1998)	$LiCoO_2$	4 M HCl	80	1:10	1 h	-	> 99% Li and Co
(Takacova *et al.*, 2016)	$LiCoO_2$	2 M HCl	60-80	1:50	90 min	-	100% Li and Co
(Joulié, Laucournet and Billy, 2014)	$LiCo_{0.15}Ni_{0.8}Al_{0.05}O_2$	4 M HCl	90	5% (w/v)	18 h	-	100% Li, Co and Ni
(Wang, Lin and Wu, 2009)	$LiCoO_2$, $LiMn_2O_4$, $LiCo_{0.33}Ni_{0.33}Mn_{0.33}O_2$	4 M HCl	80	0.02 g/ml	1 h	-	99.9% Li, 99.5% Co, 99.8% Ni, 99.8% Mn
(Jinhui Li, Shi, *et al.*, 2009)	$LiCoO_2$	4 M HCl	80	-	2 h	-	97% Li, 99% Co
(Sakultung, Pruksathorn and Hunson, 2007)	$LiCoO_2$, Ni-MH batteries	5 M HCl	8	15 g/L	1 h	-	>84% Co, >92% Ni
(Barik, Prabaharan and Kumar, 2017)	$LiCoO_2$, $LiMn_2O_4$	1,75 M HCl	50	20% (w/v)	2h	-	> 99% Li, Co and Ni
(Jinhui Li, Li, *et al.*, 2009)	Mixed batteries	6 M HCl	60	1:8	2 h	$(H_2O_2)/(MeS)$ >2 (molar)	95.5% Co, 96.5% Ni, 96% Mn, 96.3% Fe, 98.5% Cu
(Shuva and Kurny, 2013)	$LiCoO_2$	3 M HCl	80	1:20 (g/ml)	1 h	3.5% H_2O_2	89% LiCoO2
(Porvali *et al.*, 2019)	$LiCoO_2$, $LiMn_2O_4$	4 M HCl	50-80	1:10 – 1:20	2 h	0.133 dm^3/s O_2	60-85% Li, 50-75% Co
(Huang *et al.*, 2016)	$LiFePO_4$, $LiMn_2O_4$	6,5 M HCl	60	1:5	2 h	15% H_2O_2	92.15% Li, 89.95% Mn, 91.73% Fe
(Giuseppe Granata *et al.*, 2012)	$LiCoO_2$	1.5 g HCl/g powder	90	100 g/L	3 h	-	99% Li, 100% Co, Ni, Mn, Cu and 58% Fe
(Contestabile, Panero and Scrosati, 2001)	$LiCoO_2$	4 M HCl	80		1 h	-	-
(Gao, Liu, *et al.*, 2018)	$LiCoO_2$	1 M HCl	80	20 g/L	-	-	97.56% Co, 99.14% Li, 99.40% Al
	$LiCoO_2$	1 M HCl	80	20 g/L	-	4 vol% H_2O_2	99.82% Co, 99.78% Li, 99.51% Al

Table 6: Sulphuric acid leaching conditions and metal extraction efficiencies

Reference	Cathode Material Type	Acid Concentration	Tempera-ture (℃)	S/L ratio	Time	H_2O_2 Concentration	Metal Extraction
(Dutta *et al.*, 2018)	Mixed batteries	2 M H_2SO_4	30	75 g/L	2 h	10% H_2O_2	99.99% Li, 97% Co
(Dorella and Mansur, 2007)	Mixed batteries	6% (v/v) H_2SO_4	65	30 ml/g	1 h	1 vol% H_2O_2	90-95% Li, 70-80% Co, 60-70% Al
(Sattar *et al.*, 2019)	Mixed batteries	2 M H_2SO_4	50	5% pulp density	2 h	4 % H_2O_2	> 98% of all metals
(Yang, Xu and He, 2017)	$LiCo_{0.33}Ni_{0.33}Mn_{0.33}O_2$	2 M H_2SO_4	90	12.5 g/100 ml	2 h	2M H_2O_2	99% Co, 99% Ni, 97% Mn
(Sohn *et al.*, 2006)	-	2 M H_2SO_4	75	75 g/5 L	75 min	10 vol% H_2O_2	>99% Li and Co
(Chen *et al.*, 2011)	$LiCoO_2$	4 M H_2SO_4	85	1:10	2 h	10 vol% H_2O_2	96% Li, 95% Co
(Swain *et al.*, 2007)	$LiCoO_2$	2 M H_2SO_4	75	100 g/L	30 min	5 vol % H_2O_2	94% Li, 93% Co
(Jiangang Li *et al.*, 2009)	$LiCoO_2$	3 M H_2SO_4	70	-	1 h	1.5 M H_2O_2	94.5% Li, 99.5% Co
(Ferreira *et al.*, 2009)	$LiCoO_2$	4% (v/v) H_2SO_4	40	1.3 g/ml	1 h	1 vol% H_2O_2	100% Li, 97% Co
(Kang *et al.*, 2010)	$LiCoO_2$, $LiNiO_2$	2 M H_2SO_4	60	100 g/L	1 h	6 vol% H_2O_2	97% Li, 98% Co
(He, Sun, Song, *et al.*, 2017)	$LiCo_{0.33}Ni_{0.33}Mn_{0.33}O_2$	1 M H_2SO_4	40	40 g/L	1 h	1 vol% H_2O_2	99.7% Li, Co, Ni and Mn
(Jha *et al.*, 2013)	$LiCoO_2$	2 M H_2SO_4	75	100 g/L	1 h	5 vol% H_2O_2	99.1% Li, 70% Co
(Sun and Qiu, 2011)	$LiCoO_2$	2 M H_2SO_4	80	50 g/L	1 h	5 vol% H_2O_2	>99% Li and Co
(Chen, Xu, *et al.*, 2015)	Mixed batteries	2 M H_2SO_4	80	20 ml/g	1 h	2 vol% H_2O_2	-
(Nan, Han and Zuo, 2005)	$LiCoO_2$	3 M H_2SO_4	70	1:5	4 h	-	>95% Co and Li
(Nan *et al.*, 2005)	$LiCoO_2$, Ni-MH batteries	3 M H_2SO_4	70	1:10	5 h	3 wt% H_2O_2	>90%
(Gao, Liu, *et al.*, 2018)	$LiCoO_2$	1 M H_2SO_4	80	20 g/L	-	4 vol% H_2O_2	99.76% Co, 99.05% Li, 99.76% Al
(Chen and Ho, 2018)	$LiCo_{0.33}Ni_{0.33}Mn_{0.33}O_2$	2 M H_2SO_4	70	30 ml/g	90 min	10 vol% H_2O_2	98.5% Co, 98.6% Ni, 99.8% Li, 98.6% Mn

Table 7: Nitric acid leaching conditions and metal extraction efficiencies

Reference	Cathode Material Type	Acid Concentration	Tempera-ture (℃)	S/L ratio	Time	H_2O_2 Concentration	Metal Extraction
(Lee and Rhee, 2002)	$LiCoO_2$	1 M HNO_3	75	-	1 h	1.7 vol% H_2O_2	-
(Lee and Rhee, 2003)	$LiCoO_2$	1 M HNO_3	75	-	1 h	1.7 vol% H_2O_2	> 95% Li and Co
(Castillo *et al.*, 2002)	Li, Mn, Ni (cylindrical spent battery)	2 M HNO_3	80	-	2 h	-	>95% Li, >90% Mn
(Sakultung, Pruksathorn and Hunson, 2007)	$LiCoO_2$, Ni-MH batteries	1-6 M HNO_3	30-90	10-40 g/L	5-120 min	-	-
(Gao, Liu, *et al.*, 2018)	$LiCoO_2$	1 M HNO_3	80	20 g/L	-	-	62.40% Co, 99.65% Li, 99.7% Al
	$LiCoO_2$	1 M HNO_3	80	20 g/L	-	4 vol% H_2O_2	99.24% Co, 99.18% Li, 99.76% Al

2.3.2.2 Manganese recovery

Manganese can be recovered from leach solutions by precipitation or solvent extraction. Refer to Table 8 and Table 9 for previous experimental work done on Mn precipitation and solvent extraction from mineral acid leach solutions. Selective manganese precipitation typically occurs at pH values between 1 and 4. Thus, manganese is generally the first metal selectively recovered from leach solutions in metal recovery flowsheets suggesting manganese precipitation.

Table 8: Manganese recovery by precipitation

Reference	Leaching Media	Precipitant	pH	Tempera-ture (℃)	Time	Mn recovery	Product Purity	Additional Information
(Wang, Lin and Wu, 2009)	HCl	$KMnO_4$	2	40	10 min	100%	98.23%	Molar ratio of Mn^{2+}: $KMnO_4$=2
(Huang *et al.*, 2016)	HCl	0.35M $KMnO_4$	2	-	-	95.27%	98.73%	5% Li lost
(Barik, Prabaharan and Kumar, 2017)	HCl	NaClO	1.5	30	30 min	98.2%	-	NaClO addition: 1.5 times the stoichio-metric requirement
(Sattar *et al.*, 2019)	H_2SO_4	$KMnO_4$	2.5	80	1 h	98%	98.68%	Molar ratio of $KMnO_4$: Mn^{2+} = 1.2:1
(Chen, Xu, *et al.*, 2015)	H_2SO_4	0.5M $KMnO_4$	2	25	1h	99.20%	-	Molar ratio of Mn^{2+}: $KMnO_4$=2
(Nguyen *et al.*, 2014)	H_2SO_4	$KMnO_4$	2-3	-	-	-	-	-
(Chen *et al.*, 2011)	H_2SO_4	10% $(NH_4)_2S_2O_8$	4	70	-	99%	-	Molar ratio of $S_2O_8^{2-}$: Mn^{2+} = 1.8
(Dutta *et al.*, 2018)	H_2SO_4	$(NH_4)_2S_2O_8$	4.2	70	4h	100%	-	Weight ratio of $(NH_4)_2S_2O_8$: Mn = 8:1

Manganese recoveries greater than 98% were achieved with the addition of potassium permanganate at a pH of between 2 and 2.5 in both chloride and sulphate leach media. A selective redox reaction occur between the manganese ions in solution and potassium permanganate according to equation 9 shown below (Wang, Lin and Wu, 2009; Sattar *et al.*, 2019). Due to the high selectivity of $KMnO_4$, very high Mn product purities can be achieved. The co-precipitation of Ni, Co and Li are negligible with the addition of $KMnO_4$ (Wang, Lin and Wu, 2009).

$$3Mn^{2+} + 2MnO_4^- + 2H_2O \rightarrow 5MnO_2 + 4H^+ \quad [9]$$

Ammonium persulfate can remove manganese from a sulphate leaching media at a pH of 4-4.2 according to reaction 10 (Chen *et al.*, 2011; Dutta *et al.*, 2018). However, the use of ammonium persulfate will cause a loss of 1.6% Co according to the results reported by Chen *et al.* (2011).

$$Mn^{2+} + (NH_4)_2S_2O_8 + 2H_2O \rightarrow MnO_2 + (NH_4)_2SO_4 + H_2SO_4 + 2H^+ \quad [10]$$

According to the work done by Dutta *et al.* (2018), iron in solution will react with ammonium persulfate and will be completely removed from solution according to equation 11. Thus, the presence of large amounts of Fe in the feed material may negatively affect the purity of the Mn product obtained if the iron is not removed prior to Mn precipitation. Dutta *et al.* (2018) suggested the addition of NaOH to remove 99% of the iron in solution at a pH of 3 and 95℃ for 2h before the addition of ammonium persulfate.

$$FeSO_4 + (NH_4)_2S_2O_8 \rightarrow Fe_2(SO_4)_3 + (NH)_4SO_4 \quad [11]$$

Barik, Prabaharan and Kumar (2017) evaluated the use of sodium hypochlorite for the recovery of manganese from a chloride leach solution at a pH of 1.5 (equation 12). At pH values greater than 1.5, the recovery of Mn decreased due to the re-dissolution of manganese oxide according to equation 13. High manganese recoveries of greater than 98% is possible when using NaOCl as precipitation additive. However, approximately 30% of the cobalt in solution was co-precipitated with manganese (Barik, Prabaharan and Kumar, 2017). Cobalt co-precipitation negatively affects the Mn product purity and the amount of pure Co that can be recovered in subsequent process steps.

$$MnCl_2 + 2NaOCl \rightarrow MnO_2 + 2NaCl + Cl_2 \quad [12]$$

$$2MnO_2 + 3NaOCl + 2NaOH \rightarrow 2NaMnO_4 + 3NaCl + H_2O \quad [13]$$

Refer to Table 9 for examples of experimental work that have been done on solvent extraction for the recovery of manganese from leach solutions. Solvent extraction is primarily used for metal recovery from sulphate leach liquors. The experimental work performed by Porvali *et al.* (2019) and Yang, Xu and He (2017) aimed to recover Mn, Co and Ni from the leach liquors. Thus, the aim was not to selectively extract manganese in these cases.

Table 9: Manganese recovery from leach solutions using solvent extraction

Reference	Leaching Media	Extractant	Diluent	O:A ratio	pH	Sta-ges	Extraction	Stripping Conditions
(Porvali *et al.*, 2019)	HCl	20 vol% Cyanex 272, 10 vol% TBP	Sulfonated kerosene	1:1	4	1	56.17% Co, 80.3% Mn, 3.15% Ni, 5.26% Li	-
(Chen, Chen, *et al.*, 2015)	H_2SO_4	15 vol% Co-D2EHPA, 5 vol% TBP	Kerosene	1:1	3.2	1	97.1% Mn, <1% Co and Li	0.1M H_2SO_4 O:A=2:1 99% stripping
(Yang, Xu and He, 2017)	H_2SO_4	40 vol% D2EHPA	Sulfonated kerosene	1:1	3.5	3	100% Mn, 99% Co, 85% Ni, 30% Li	0.5M H_2SO_4
(Joo *et al.*, 2015)	H_2SO_4	20 vol% PC88A 25 vol% Versatic 10 acid	Kerosene	1:1	4.5	4	99.5% Mn, small amounts of Li, Ni and Co	0.5M H_2SO_4 O:A=2:1 2 stages
(Tanong *et al.*, 2017)	H_2SO_4	30 vol% D2EHPA 5 vol% TBP	Kerosene	2:1	2.7	2	93.1% Mn, 30.9% Co, 20.8% Ni	1.2M H_2SO_4 O:A=4:1
(Wang *et al.*, 2019)	H_2SO_4	30 vol% P-204	Kerosene	1:1	2.5	3	90% Mn, <4% Co	1M H_2SO_4

Chen, Chen *et al.* (2015) selectively extracted 97.1% Mn with little Co and Li co-extraction (<1%). Dilute oxalic acid (5 w/v% $H_2C_2O_4$ solution) was used to scrub the cobalt ions that were co-extracted from the loaded organic phase. Almost 100% of the cobalt ions were scrubbed into the aqueous phase, producing a pure manganese solution. The high scrubbing efficiency with oxalic acid can be explained by the formation of $CoC_2O_4.2H_2O$ which is a stable precipitate (Chen, Chen, *et al.*, 2015).

Joo *et al.* (2015) reported the extraction of 99.5% manganese with the co-extraction of small amounts of Li, Ni and Co that could be scrubbed from the loaded organic phase with a 0.05-0.2 M EDTA solution. The

co-extracted impurities were completely removed from the organic phase. 0.4% of the extracted manganese was transferred back to the aqueous phase during scrubbing (Joo *et al.*, 2015).

2.3.2.3 Impurity removal

The amount of iron, aluminium and copper present in the electrode material fed to the leaching tank will be dependent on the feed material composition and the type of pre-treatment process selected (Chagnes *et al.*, 2015). These metals are classified as impurities in the leach liquor because they are co-extracted (through precipitation or solvent extraction) with the valuable metals (Li, Co and Ni) and decrease the purity of the products obtained. Thus, it makes sense to reduce the concentration of Fe, Al and Cu in the leach solution before the selective extraction of Co, Ni and Li. The impurities can be removed by precipitation or solvent extraction. The results reported by various literature sources that evaluated impurity removal by selective precipitation are summarized in Table 10 below.

Table 10: Removal of Fe, Al and Cu from leach solutions by precipitation

Reference	Leaching Media	Precipitant	pH	Impurity Removal			Valuable Metals Lost
				Al	Cu	Fe	
(Jinhui Li, Shi, *et al.*, 2009)	HCl	NaOH	4.5	40%	10%	100%	2% Co
			5	75%	55%	100%	2.5% Co
			5.5	92%	98%	100%	5% Co
(Chen, Chen, *et al.*, 2015)	H_2SO_4	2M NaOH	3-3.1	-	-	99.6%	< 1% Mn, Co, Ni, Li
(Porvali *et al.*, 2019)	HCl	2M NaOH	5	80.50%	81.30%	99.60%	1.6% Co, 2.28% Li, 9.6% Ni
(Giuseppe Granata *et al.*, 2012)	HCl	NaOH	5	100%	60%	100%	-
(Kang *et al.*, 2010)	H_2SO_4	4M NaOH	6.5	>99%	>99%	>99%	7% Co, 15% Mn
(Chen *et al.*, 2011)	H_2SO_4	Na_2SO_4	3	-	-	99.99%	<1% Co
	H_2SO_4	NaOH	5.5	-	98.5%	-	-
(Chen, Xu, *et al.*, 2015)	H_2SO_4	1M NaOH	3	-	-	100%	-
(Chen *et al.*, 2011)	H_2SO_4	NaOH	3	-	-	99%	-
	H_2SO_4	NaOH	5.5	-	98.5%	-	-
(Dorella and Mansur, 2007)	H_2SO_4	NH_4OH	5	80%	-	-	20% Co

The results reported in Table 10 confirm that sodium hydroxide is generally used as precipitation agent for the removal of iron, copper and aluminium from solution. However, Dorella and Mansur (2007) reported the removal of 80% of aluminium with ammonium hydroxide. 20% of the cobalt in solution was co-precipitated with aluminium, making it a less favourable option for leach solution purification.

Chen *et al.* (2011) investigated the use of sodium sulphate for the removal of iron in the form of sodium jarosite according to equation 14 shown below. 99% of the iron in the sulphate leach solution was removed with the loss of less than 1% cobalt (Chen *et al.*, 2011).

$$Fe_2(SO_4)_3 + 12H_2O + Na_2SO_4 \rightarrow Na_2Fe_6(SO_4)_4(OH)_{12} + 6H_2SO_4 \quad [14]$$

The selective removal of Al, Cu and Fe with precipitation (with minimal Co and Ni losses) is pH dependent as confirmed by the data tabulated in Table 10 and Table 11. The experimental study by Badawy *et al.* in 2013 is another example that illustrates the high pH dependency. Badawy *et al.* (2013) reported negligible cobalt losses at pH values lower than 4.5 when sodium hydroxide was used to control the pH level. However, 27.5% of cobalt was lost at a pH of 5.5 and 80% of cobalt was lost at pH values between 6 and 6.5 (Badawy *et al.*, 2013).

Table 11: The pH values between which various metal hydroxides will precipitate (Zou *et al.*, 2013)

Metal Hydroxide	pH start	pH end
$Fe(OH)_3$	1.149	2.815
$Al(OH)_3$	-	4.49
$Cu(OH)_2$	-	6.65
$Ni(OH)_2$	5.156	8.869
$Co(OH)_2$	6.673	9.386
$Mn(OH)_2$	7.398	10.151
$Fe(OH)_2$	5.844	8.344

Solvent extraction is an alternative to precipitation allowing the selective extraction of impurity ions with minimal Co, Ni and Li losses. Refer to Table 12 below for the experimental conditions and results reported by various literature sources. Solvent extraction of impurities has only been done in sulfuric acid leach solutions as seen in Table 12. Thus, precipitation will possibly be the preferred option if leaching was done with hydrochloric or nitric acid.

Table 12:Solvent extraction for the removal of impurities

Reference	Leaching Media	Extractant	Diluent	O:A ratio	pH	Sta-ges	Extraction	Stripping Conditions
(Dutta *et al.*, 2018)	H_2SO_4	15 vol% LIX 84 IC	Kerosene	1:1	2	1	99.99% Cu	10% H_2SO_4 O:A=1:1
(Suzuki *et al.*, 2012)	H_2SO_4	10 vol% Acorga M5640	Kerosene	1:1	1.5-2	1	>98% Cu	3M H_2SO_4 98.7% stripping
(Chen, Xu, *et al.*, 2015)	H_2SO_4	10 vol% Mextral 5640H	Sulfonated kerosene	1:2	1.94	2	100% Cu	0.2M H_2SO_4 O:A=2:1
(Nan, Han and Zuo, 2005)	H_2SO_4	10 wt% Acorga M5640	Kerosene	1:1	1	1	97% Cu	2M H_2SO_4, O:A=1:1 2 stages
(Suzuki *et al.*, 2012)	H_2SO_4	10 vol% PC-88A	Kerosene	1:1	2.5-3	1	>98% Al	2M H_2SO_4 100% stripping
(Mantuano *et al.*, 2006)	H_2SO_4	0.3M Cyanex 272	Kerosene	1:1	2.5-3	1	100% Al	-
(Yang, Xu and He, 2017)	H_2SO_4	10 vol% D2EHPA	Sulfonated kerosene	1:2	2	-	Remaining Al, Fe, Cu and Ca	-
(Pranolo, Zhang and Cheng, 2010)	H_2SO_4	2 vol% Acorga M5640, 7 vol% Ionquest 801	Shellsol D70	1:2	4	3	100% Al, Fe and Cu	80 g/l H_2SO_4 O:A=1:1
(Nguyen *et al.*, 2014)	H_2SO_4	10 vol% D2EHPA	Kerosene	-	2.5	-	Al, Fe extraction	-

Roux *et al.* (2010) reported that the capital and operating expenses associated with solvent extraction will exceed that of precipitation. Depending on the pre-treatment process selected, the amount of

impurities in the system may be very low. The use of solvent extraction to recover small amounts of impurities that will not significantly influence product purities and the income, will not be economically feasible. If this is the case, precipitation for the removal of impurities will be more viable from a financial point of view.

2.3.2.4 Nickel recovery

In the past solvent extraction using acidic extractants has been the preferred option for the separation of cobalt and nickel in sulphate leach liquors. However, solvent extraction is only a suitable option if the nickel concentration in solution is low, else it becomes challenging to achieve acceptable separation factors (Sattar *et al.*, 2019). The separation of nickel and cobalt using solvent extraction is discussed in section 2.3.2.5 (b). Refer to Table 13 below for literature sources that used precipitation to recover nickel from solution.

Table 13: Nickel recovery with precipitation

Reference	Leaching Media	Precipitant	pH	Tempera-ture (℃)	Time	Ni recovery	Additional Information
(Wang, Lin and Wu, 2009)	HCl	DMG	9	-	10 min	>99%	Molar ratio of DMG: $[Ni(NH_3)_6]^{2+}$ =2:1
(Sattar *et al.*, 2019)	H_2SO_4	DMG	5	80	1 h	>99%	Molar ratio of DMG:Ni^{2+}=2:1
(Chen, Chen, *et al.*, 2015)	H_2SO_4	DMG	5	25	20 min	98.70%	Molar ratio of DMG:Ni^{2+}=2:1
(Chen and Ho, 2018)	H_2SO_4	DMG	9	25	30 min	99.5%	Molar ratio of DMG:Ni^{2+}=2:1
(Joulié, Laucournet and Billy, 2014)	HCl	NaOH	11	-	-	99.99%	96.36% Ni purity
(Nguyen *et al.*, 2014)	H_2SO_4	1M NaOH	8.5	-	-	-	96.7% Ni purity (1.33% Li co-precipitation)
(Chen, Xu, *et al.*, 2015)	H_2SO_4	2M NaOH	>8	-	-	99.1%	99.13% Ni purity
(Porvali *et al.*, 2019)	HCl	Na_2CO_3	8	50	-	97.1%	97.2% Co, 97.3% Mn co-precipitated
(Tanong *et al.*, 2017)	H_2SO_4	$NaCO_3$	10	25	10 min	100%	97% Ni purity

Dimethylglyoxime (DMG), with chemical formula $C_4H_8N_2O_2$, is the precipitation agent with the highest selectivity for nickel in leach solutions that contain manganese, cobalt and lithium. Wang, Lin and Wu (2009) investigated the use of Ni precipitation with DMG from a hydrochloric acid leach solution. Before DMG was added to the system, the pH was adjusted to 9 with the addition of a 28% NH_3 solution. The ammonia reacted with nickel ions in solution to produce the $[Ni(NH_3)_6]^{2+}$ complex that selectively reacted with DMG for 10 min to form a red solid complex. The red solid Ni-DMG complex was dissolved in a 4 M hydrochloric acid solution that enabled the regeneration of DMG as a white powder and transferred the nickel ions back into solution. Nickel hydroxide was finally recovered as a precipitate after the addition of 1 M NaOH until the pH reached a value of 11. Cobalt and lithium were not co-extracted during the described process, producing a nickel product with 97.43% purity (Wang, Lin and Wu, 2009).

Nickel recovery from sulphate leach solutions by DMG precipitation was investigated by Sattar *et al.* (2019) and Chen, Chen *et al.* (2015). The nickel in solution reacted with DMG according to equation 15 shown below (Sattar *et al.*, 2019). Chen, Chen *et al.* (2015) regenerated the DMG in 30 minutes at 25℃

using a 1 M hydrochloric acid solution and solid-to-liquid ratio of 0.1 g/ml. The regenerated DMG powder was recycled and re-used as nickel precipitant. A comparison of the precipitation performance between fresh and recycled DMG revealed a slight decrease in the precipitation efficiency of Ni from 98.7% to 97.6% (Chen, Chen, *et al.*, 2015).

$$(Ni^{2+})_{aq} + (2C_4H_8N_2O_2)_{aq} + (2OH^-)_{aq} \rightarrow [Ni - (C_4H_7N_2O_2)_2]_s + (2H_2O)_{aq} \qquad [15]$$

High nickel hydroxide recoveries are favoured at pH values greater than 8. At these pH values, the precipitation of cobalt, manganese and iron (Fe^{2+}) are also favoured (refer to Table 11). Thus, the use of sodium hydroxide for the recovery of a high purity nickel product should only be used if the Mn and Co have already been recovered from solution as seen in the work done by Joulié, Laucournet and Billy (2014) as well as Chen, Xu *et al.* (2015).

High nickel recoveries (97.1%) were reported after precipitation with sodium carbonate at a pH of 8 by Porvali *et al.* in 2019. However, 97.2% Co and 97.3% Mn co-precipitated with the nickel producing a mixed metal carbonate product. Tanong *et al.* (2017) also reported high nickel recoveries from a purified sulphate solution with sodium carbonate at a pH of 10. Thus, to produce a pure nickel carbonate product, Co and Mn should be recovered from the leach solution prior to the addition of sodium carbonate.

Nguyen *et al.* (2014) compared precipitation and solvent extraction for the recovery of nickel after Mn and Co have been recovered from the leach liquor. Over 99% Ni was extracted with only 0.01% Li co-extraction with a 5 vol% PC-88A organic phase at an equilibrium pH of 6. The stripped solution was used to produce a 99.8% pure nickel sulphate product. Precipitation using a 1 M NaOH solution to adjust the pH to 8.5, produced a nickel hydroxide product with 96.7% purity (1.33% Li co-precipitated). It was concluded that solvent extraction provides higher selectivity and higher purity products than precipitation which is the cheaper and simpler option (Nguyen *et al.*, 2014).

Electrowinning is an alternative method that can be used to recover nickel from solutions if cobalt has been recovered earlier in the process (Chagnes *et al.*, 2015). Lupi and Pasquali (2003) and Lupi, Pasquali and Dell'Era (2005) did experimental work on nickel electrowinning after cobalt was recovered by solvent extraction using Cyanex 272 in kerosene. Electrowinning was performed at 50℃, pH 3-3.2, with an electrolyte containing approximately 49.5 g/L Ni and 20 g/L H_3BO_3. The current density was 250 A/m^2. Less than 100 ppm Ni was left in solution after 80 minutes of electrolysis. The specific energy consumption was 2.96 kWh per kg of Ni deposit (Lupi and Pasquali, 2003; Lupi, Pasquali and Dell'Era, 2005). Cobalt can also be electrowon from a purified solution at 250 A/m^2, pH 4-4.2 and 50℃ (Lupi, Pasquali and Dell'Era, 2005; Wang *et al.*, 2019).

2.3.2.5 Cobalt recovery

a) Cobalt recovery by precipitation

Various precipitation agents have been used to recover cobalt from leach solutions. Refer to Table 14 below for a summary of the precipitation agents and conditions used in previous experimental studies.

Table 14: Cobalt recovery by precipitation

Reference	Leaching Media	Precipitant	pH	Co recovery	Product Purity	Additional Information
(Wang, Lin and Wu, 2009)	HCl	1M NaOH	11	>99%	96.94%	-
(Contestabile, Panero and Scrosati, 2001)	HCl	4M NaOH	6-8	100%	-	-
(Chen and Ho, 2018)	H_2SO_4	NaOH	11	>99%	>99.5%	-
(Chen, Chen, *et al.*, 2015)	H_2SO_4	0.5M $(NH_4)_2C_2O_4$	-	98.2%	97.47%	25°C, 30 min, 1.1 times stoichiometric requirement of $(NH_4)_2C_2O_4$
(Chen *et al.*, 2011)	HCl	$(NH_4)_2C_2O_4$	1.5	99%	99%	Molar ratio of $(NH_4)_2C_2O_4$:Co^{2+} = 1.15:1
(Nan, Han and Zuo, 2005)	H_2SO_4	$(NH_4)_2C_2O_4$	2	97%	99%	70°C, 3 times stoichiometric requirement of $(NH_4)_2C_2O_4$
(Porvali *et al.*, 2019)	HCl	Na_2CO_3	8	97.2%	-	50°C, 97.1% Ni and 97.3% Mn co-precipitation
(Barik, Prabaharan and Kumar, 2017)	HCl	Na_2CO_3	-	-	-	-
(Joulié, Laucournet and Billy, 2014)	HCl	NaClO	3	100%	90.25%	Molar ratio of $NaClO^-$:Co^{2+}=3
(Cai *et al.*, 2014)	H_2SO_4	Na_2S	4.24	99.7%	>99%	No Mn or Li co-precipitation

As stated previously, sodium hydroxide is a common additive used to control pH levels and metal hydroxide precipitation in systems. The pH ranges in which Co, Mn and Ni precipitate from solution overlap as seen in Table 11. Thus, the use of sodium hydroxide for the precipitation of a high purity cobalt product should only be used if the Mn and Ni have already been recovered from solution as seen in the work done by Wang, Lin and Wu (2009) and Contestabile, Panero and Scrosati (2001). The same conclusion can be made with regards to the use of sodium carbonate for selective cobalt recovery as seen in the work done by Porvali *et al.* (2019) and Barik, Prabaharan and Kumar (2017).

High cobalt recoveries can be achieved when ammonium oxalate is used as precipitation agent. The cobalt ions in solution react with ammonium oxalate according to equation 16 (Chen, Chen, *et al.*, 2015). Selective cobalt recovery producing a cobalt product with a purity greater than 97% is possible if only lithium, cobalt and small concentrations of impurities are present in solution.

$$Co^{2+}_{(aq)} + {C_2O_4^{2-}}_{(aq)} + 2H_2O \rightarrow CoC_2O_4.2H_2O_{(s)} \quad [16]$$

Joulié, Laucournet and Billy (2014) investigated the separation of nickel and cobalt with oxidative precipitation using sodium hypochlorite as oxidant. The selective recovery of these metals (in valence +2 state) is challenging because they precipitate from solutions within the same pH range. This can be explained by thermodynamic data that predict the co-precipitation of $Ni(OH)_2$ and $Co(OH)_2$ with solubility products (pKs) of 14.7 and 14.2 respectively. Selective precipitation will only be possible if Co^{2+} ions are oxidized to Co^{3+} ions which can react with NaOH to form $Co_2O_3.3H_2O$ (pKs=40.5) as product. The oxidation of cobalt with sodium hypochlorite is represented by equation 17. The $Co_2O_3.3H_2O$ product is formed at a pH of 3 according to equation 18. The nickel remaining in solution was recovered by the addition of sodium hydroxide until the pH reached 11 (Joulié, Laucournet and Billy, 2014).

$$2Co^{2+} + ClO^- + 2H_3O^+ \leftrightarrow 2Co^{3+} + Cl^- + 3H_2O \quad [17]$$

$$2Co^{3+} + 6OH^- \rightarrow Co_2O_3.3H_2O \quad [18]$$

b) Cobalt recovery by solvent extraction

Solvent extraction is a valuable technique used to separate cobalt from leach solutions to achieve high cobalt recoveries and to produce high purity cobalt products. Table 16 provides a summary of the experimental conditions used in previous work. Based on the literature sources evaluated, it was concluded that:

1. Solvent extraction is a popular strategy for the selective extraction of cobalt from sulfuric acid leach solutions. Limited work has been done on solvent extraction from hydrochloric acid leach solutions.
2. Cyanex 272 is the most popular organic extractant used for cobalt extraction. Kerosene is typically used as diluent.
3. Cobalt recoveries of greater than 90% are generally achieved in 1 or 2 stages if the pH value is between 3.5 and 5.5 and the O/A ratio is between 1 and 2.
4. High cobalt stripping efficiencies can be achieved with sulfuric acid solutions and high O/A ratios.

Small amounts of lithium or other metals can be co-extracted with cobalt as seen in Table 16. The purpose of solvent extraction is to produce a pure solution containing only cobalt after the organic phase has been stripped. Therefore, co-extracted species are typically removed by scrubbing the loaded organic phase with a scrubbing solution to wash the impurity ions back into the aqueous phase. Refer to Table 15 for the scrubbing conditions used in previous experimental work.

Table 15: Scrubbing conditions for the removal of lithium from loaded organic phase

Reference	Scrubbing agent	O:A ratio	Stages	Metals removed from organic phase
(Zhang *et al.*, 1998)	$CoCl_2$ and HCl solution containing 30 g/L Co	10:1	1	Li
(Swain *et al.*, 2007)	0.1M Na_2CO_3	3.8:1	3	Li
(Chen, Xu, *et al.*, 2015)	5 g/L Na_2CO_3	1:1	1	Li
(Nguyen *et al.*, 2014)	2 g/dm^3 $CoSO_4$ at pH=4.75	2:1	2	Ni, Li

Table 16: Solvent Extraction of Co from mineral acid leach solutions

Reference	Leaching Media	Extractant	Diluent	O:A ratio	pH	Sta-ges	Extraction	Stripping Conditions
(Zhang *et al.*, 1998)	HCl	0.9M PC-88A	Kerosene	0.85:1	6.7	1	99.99% Co, 13% Li	2M H_2SO_4, O:A=5:1, pH=0.8
(Fernandes, Afonso and Dutra, 2013)	HCl	10 vol% Alamine 336	Kerosene	1:1	-	2	93.6% Co, 2.8% Ni	-
(Ahn, J.W., Ahn, H.J., Son, S.H., Lee, 2012)	HCl	10 vol% Cyanex 272	Kerosene	1:1	4.5-5	1	-	0.1M HCl, O:A=1
(Porvali *et al.*, 2019)	HCl	20 vol% Cyanex 272,10 vol% TBP	Sulfonated kerosene	1:1	4	1	56.17% Co, 80.3% Mn, 3.15% Ni, 5.26% Li	-
(Dutta *et al.*, 2018)	H_2SO_4	20 vol% Cyanex 272	Kerosene	1:1	4.8	2	98% Co	10% H_2SO_4
(Sattar *et al.*, 2019)	H_2SO_4	0.64M Cyanex 272	Kerosene	1:1	5	2	Co	2M H_2SO_4 O:A=10:1
(Chen *et al.*, 2011)	H_2SO_4	25 wt% P507	Kerosene	1.5:1	3.5	1	95% Co, <5% Ni	3M H_2SO_4 O:A=4:1
(Kang *et al.*, 2010)	H_2SO_4	0.4M Cyanex 272	Kerosene	2:1	6	2	99.9% Co	2M H_2SO_4 O:A=11.7:1
(Suzuki *et al.*, 2012)	H_2SO_4	10 vol% PC-88A, 5 vol% TOA	Kerosene	1:1	5.5-6	1	>90% Co	3M H_2SO_4, >98% stripping
(Nan, Han and Zuo, 2005)	H_2SO_4	1M Cyanex 272	Kerosene	1:1	5.5	1	96% Co	2M H_2SO_4 O:A=1:1
(Pranolo, Zhang and Cheng, 2010)	H_2SO_4	15 vol% Cyanex 272	Shellsol D70	2:1	5.5-6	1	>90% Co	-
(Swain *et al.*, 2007)	H_2SO_4	0.5M (stage 1), 1.5M (stage 2) Cyanex 272, 5 vol% TBP	Kerosene	1.6:1, 1:1	5-5.35	2	100% Co	0.5M H_2SO_4 O:A=1:1
(Nguyen *et al.*, 2014)	H_2SO_4	0.56 mol/dm^3 PC-88A (60% saponified)	Kerosene	3:1	4.5	2	99.9% Co	0.2M H_2SO_4 O:A=1:1 99.9% stripping
(Chen, Xu, *et al.*, 2015)	H_2SO_4	20 vol% Mextral 272P	Sulfonated kerosene	1:1	4.5	1	97.8% Co, 0.72% Ni, 0.78% Li	0.1M H_2SO_4 O:A=2:1 99% stripping
(Chen *et al.*, 2011)	H_2SO_4	25 wt% P507	Kerosene	1.5:1	3.5	1	95% Co, <5% Ni, <5% Li	3M H_2SO_4 O:A=4:1
(Yang, Xu and He, 2017)	H_2SO_4	40 vol% D2EHPA	Sulfonated kerosene	1:1	3.5	3	100% Mn, 99% Co, 85% Ni, 30% Li	0.5M H_2SO_4
(Chen and Ho, 2018)	H_2SO_4	0.1M Cyanex 272	Kerosene	1.5:1	6	1	99.2% Co, 99.3% Mn, 3.3% Ni, 3% Li	0.1M H_2SO_4 O:A=2:1, 100% Co, Mn stripped
	H_2SO_4	0.2M Na-D2EHPA	Kerosene	1:1	2.95	1	85.14% Mn	0.05M H_2SO_4 O:A=2:1 100% stripping

After solvent extraction and stripping, a pure cobalt solution is produced. The cobalt can be recovered from solution using precipitation, electrowinning or evaporative crystallization. Precipitation of cobalt with the addition of ammonium oxalate (pH=1.5) recovered 99% of the cobalt in the strip liquor according to the results reported by Chen *et al.* (2011).

Dutta *et al.* (2018) investigated the recovery of cobalt from the strip liquor with evaporative crystallization and electrowinning. Evaporative crystallization produced a $CoSO_4$ product with a purity greater than 98%. Electrowinning at 60°C with a current density of 200 A/m^2, lead to the formation of 6 g cobalt metal on a single cathode with a current efficiency of 92% after 4 hours. The pH was controlled between 4 and 4.2 with the addition of sodium hydroxide. The cobalt concentration in the tank was controlled at 50 g/L Co with the addition of $CoSO_4$ salt (Dutta *et al.*, 2018).

Sattar *et al.* (2019) concentrated the cobalt in the pure stripping liquor by evaporation to produce pure $CoSO_4.xH_2O$ crystals. According to the chemical analyses performed, the crystals contained 20.54% cobalt. Zhang *et al.* (1998) proposed that cobalt in the strip liquor can be recovered by cobalt sulphate hexahydrate ($CoSO_4.6H_2O$) crystallization or electrowinning to obtain high-purity electrolytic cobalt.

2.3.2.6 Lithium recovery

Lithium is generally the last remaining metal in the original leach solution after the removal of impurities (Fe, Cu and Al) and the selective recovery of Mn, Ni and Co. Refer to Table 17 for a summary of previous experimental work done on lithium recovery by precipitation.

Table 17: Lithium recovery by precipitation

Reference	Leaching Media	Precipitant	Tempera-ture (°C)	Li recovery	Product Purity	Additional Information
(Wang, Lin and Wu, 2009)	HCl	Na_2CO_3	100	80%	96.97%	-
(Zhang *et al.*, 1998)	HCl	Na_2CO_3	100	80%	-	<0.07% Co co-precipitation
(Sattar *et al.*, 2019)	H_2SO_4	Na_2CO_3	90	99%	-	pH=12, 1 h, molar ratio of Na_2CO_3:Li^+=1.2:1
(Chen, Chen, *et al.*, 2015)	H_2SO_4	Na_2CO_3	95	81%	99.18%	-
(Nan, Han and Zuo, 2005)	H_2SO_4	Na_2CO_3	100	80%	-	0.96% Co, 0.001% Cu co-precipitation
(Chen and Ho, 2018)	H_2SO_4	Na_2CO_3	-	-	>99.5%	-
(Nguyen *et al.*, 2014)	H_2SO_4	Na_2CO_3	125	92%	-	<0.05% Ni co-precipitation
(Joulié, Laucournet and Billy, 2014)	HCl	Na_2CO_3 or Na_3PO_4	-	>80%	-	-
(Zou *et al.*, 2013)	H_2SO_4	Na_2CO_3	40	80%	-	-
(Yang, Xu and He, 2017)	H_2SO_4	0.5M Na_2CO_3	80	-	99.2%	-
(Huang *et al.*, 2016)	HCl	0.2M Na_3PO_4	90	93.68%	99.32%	pH=7
(Cai *et al.*, 2014)	HCl	Na_3PO_4	60	100%	-	pH=12.7
(Chen, Xu, *et al.*, 2015)	H_2SO_4	Na_3PO_4	-	96%	99.67%	-

Lithium can be recovered as a carbonate with the addition of Na_2CO_3 (equation 19) or a phosphate with the addition of Na_3PO_4 (equation 20). To maximize the recovery of lithium as a precipitate, the leach

solution can be concentrated by evaporation prior to the lithium precipitation step. Lithium carbonate precipitation is typically performed at higher temperatures (80-100°C) because the solubility of Li_2CO_3 in solutions is inversely proportional to temperature. For example, the solubility limit of Li_2CO_3 is 1.52 g/100g water at 0°C and 0.71 g/100g water at 100°C (Zhang *et al.*, 1998).

$$2Li^+_{(aq)} + {CO_3^{2-}}_{(aq)} \rightarrow {Li_2CO_3}_{(s)} \quad [19]$$

$$3Li^+_{(aq)} + {PO_4^{3-}}_{(aq)} \rightarrow {Li_3PO_4}_{(s)} \quad [20]$$

2.3.2.7 Reagent regeneration

After hydrochloric acid leaching, the metal recovery process may lead to large amounts of sodium chloride (NaCl) in the system especially if consecutive precipitation steps at different pH levels are used to recover Mn, Co and Ni from solution. Sodium chloride crystals (solubility limit of 35.8 g/100 g water) may precipitate from solution and negatively affect the purity of the metal products produced. Thus, it is critical to control the NaCl concentration in the leach solution throughout the process. Membrane electrolysis is a useful strategy that can be employed to control the amount of NaCl in solution while producing valuable products. The membrane cell operates with a saturated NaCl solution and dilute NaOH solution as inputs to produce a more concentrated NaOH solution, Cl_2 gas and H_2 gas. The gas products can be used to manufacture hydrochloric acid. The regenerated NaOH and HCl can be distributed to the process units requiring these reagents.

a) Membrane electrolysis

Membrane electrolysis is used in the chlor-alkali industry to produce sodium hydroxide, chlorine and hydrogen by electrolyzing near saturated NaCl brine. Globally, 76 000 000 tons of chlorine is produced annually of which more than 50% is produced by membrane electrolysis (Brinkmann *et al.*, 2014). Membrane electrolysis is an environmentally friendly process technology in comparison to the mercury and diaphragm cells that were used in the past (Nafion Ion Exchange Materials, 2016).

A membrane cell typically contains an ion exchange membrane that separates the anode and cathode chambers. The membranes used in membrane electrolysis are made from ion-exchange polymers that have perfluorinated cation exchange sites with carboxylic and sulfo groups (Nafion Ion Exchange Materials, 2016; Paidar, Fateev and Bouzek, 2016). Thus, these membranes will allow cations to pass through and will almost entirely reject anions and non-polar molecules. In brine electrolysis, the membrane will allow the sodium cations and water molecules to move from the anode compartment across the membrane into the cathode compartment where sodium hydroxide is produced.

Refer to Figure 4 for a schematic diagram illustrating the basic components and operation of a typical membrane cell. The anolyte fed to the anode chamber is a brine stream saturated in NaCl. A diluted NaOH solution is fed as catholyte to the cathode chamber. The properties of the feed and product streams and other operating conditions are summarized in Table 18.

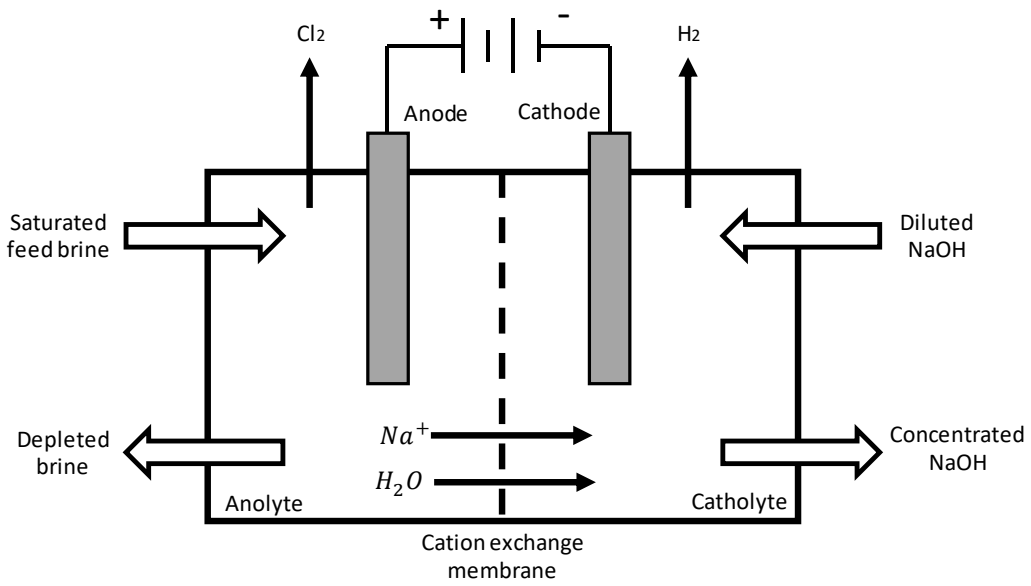

Figure 4: Schematic diagram of a typical membrane cell (adapted from Du *et al.* ,2018)

The oxidation of chlorine ions to produce chlorine gas is facilitated at the anode which is typically constructed of titanium coated with a RuO_2 or TiO_2 layer. A reduction reaction producing hydrogen gas take place at the cathode constructed of nickel-based materials (Paidar, Fateev and Bouzek, 2016). Refer to equations 21 and 22 for the oxidation and reduction reactions respectively. The overall cell reaction is shown in equation 23 (Du *et al.*, 2018).

$$2Cl^- \rightarrow Cl_2 + 2e^- \quad [21]$$

$$2H_2O + 2e^- \rightarrow H_2 + 2OH^- \quad [22]$$

$$2NaCl + 2H_2O \rightarrow 2NaOH + H_2 + Cl_2 \quad [23]$$

The energy consumed by the membrane cells, can be calculated by equation 24 (Du *et al.*, 2018) where $\dot{W}_{cell}$ is the energy consumption as work, I_{cell} is the electric current, U_{cell} is the cell voltage, F is Faraday's constant (96485 C/mol), $\Delta\dot{n}_{NaOH}$ is the change in the molar flowrate of NaOH over the membrane cell and η is the cathode current efficiency. Other literature sources reported that the energy consumption is 1950-2300 kWh/ton Cl_2 (Bommaraju *et al.*, 2000), approximately 1400 kWh/ton NaOH (Schneiders, Zimmermann and Henßen, 2001) and 2600-2860 kWh/ton Cl_2 (Brinkmann *et al.*, 2014).

$$\dot{W}_{cell} = U_{cell} I_{cell} = U_{cell} F \frac{\Delta\dot{n}_{NaOH}}{\eta} \quad [24]$$

Table 18: Membrane Cell Operating Conditions

Electrolyzer		**References**
Cell Voltage	<4.0 V	(Nafion Ion Exchange Materials, 2016)
	3.2 V	(Du *et al.*, 2018)
	3-4 V	(Paidar, Fateev and Bouzek, 2016)
	3.2-3.6 V	(Brinkmann *et al.*, 2014)
	3.74 V	(Abam Engineers Inc., 1980)
Current Density	1.5-6 kA/m^2	(Nafion Ion Exchange Materials, 2016)
	7000 A/m^2	(Paidar, Fateev and Bouzek, 2016)
	3.7-6 kA/m^2	(Brinkmann *et al.*, 2014)
	3.10 kA/m^2	(Abam Engineers Inc., 1980)
Membrane Size	0.2-5 m^2	(Brinkmann *et al.*, 2014)
	Width < 1.5 m Lengths < 4.5 m	(Nafion Ion Exchange Materials, 2016)
Membrane Lifetime	3-5 years	(Brinkmann *et al.*, 2014)
	2 years	(Abam Engineers Inc., 1980)
Anolyte Compartment		**References**
Temperature	80-90 ℃	(Nafion Ion Exchange Materials, 2016)
	88 ℃	(Du *et al.*, 2018)
Anolyte Pressure	1.09 bar	(Du *et al.*, 2018)
Anolyte pH	3	(Du *et al.*, 2018)
	>2	(Nafion Ion Exchange Materials, 2016)
	1-4.5	(Paidar, Fateev and Bouzek, 2016)
Inlet Concentration	310 g/L NaCl	(Bommaraju *et al.*, 2000; Moroz, 2016)
	290-310 g/L NaCl; 26 wt% NaCl	(Du *et al.*, 2018)
	305 g/L NaCl	(Abam Engineers Inc., 1980)
Outlet Concentration	230 g/L NaCl	(Moroz, 2016)
	220 g/L NaCl	(Abam Engineers Inc., 1980)
	20 wt% NaCl	(Du *et al.*, 2018)
Anolyte Strength in Compartment	200±30 g/L NaCl	(Nafion Ion Exchange Materials, 2016)
	180-240 g/dm^3	(Paidar, Fateev and Bouzek, 2016)
Anode Current Efficiency	96%	(Du *et al.*, 2018)
Catholyte Compartment		**References**
Temperature	88 ℃	(Du *et al.*, 2018)
	80-95 ℃	(Nafion Ion Exchange Materials, 2016; Paidar, Fateev and Bouzek, 2016)
Catholyte Pressure	1.05 bar	(Du *et al.*, 2018)
Catholyte pH	14	(Paidar, Fateev and Bouzek, 2016)
Inlet Concentration	30 wt% NaOH	(Brinkmann *et al.*, 2014; Du *et al.*, 2018)
Outlet Concentration	32-35 wt% NaOH	(Bommaraju *et al.*, 2000; Du *et al.*, 2018)
	32.5±2.5 wt% NaOH	(Nafion Ion Exchange Materials, 2016)
Cathode Current Efficiency	94%	(Du *et al.*, 2018)

b) Production of hydrochloric acid

The chlorine and hydrogen gases produced in the membrane cells can be used to manufacture hydrochloric acid. Refer to Figure 5 below for a simplified diagram of the production process of hydrochloric acid.

HCl gas is formed by the highly exothermic combustion reaction between hydrogen and chlorine gas (equation 25) that can lead to temperatures of up to 2000℃ (SGL Group, 2016). For optimal chlorine conversion, 5-10 vol% excess hydrogen gas should be fed to the furnace (Joseph, Koshy and Kallanickal, 2013; Moroz, 2016). The energy released due to the combustion reaction is 1667 kJ per mole HCl gas produced of which 40-60% can be recovered by generating steam as suggested by the SGL Group. 500-650 kg medium pressure steam (<10 barg) can be produced per ton of HCl gas that is formed in the combustion furnace utilizing the energy released by the combustion reaction (SGL Group, 2016).

$$H_{2(g)} + Cl_{2(g)} \rightarrow 2HCl_{(g)} + 1667\ kJ/mole \qquad [25]$$

The HCl gas is fed to an isothermal falling film absorber, where it is absorbed into demineralized water to produce 33 wt% hydrochloric acid. The absorption of HCl gas into water is also exothermic, releasing 2100 kJ of energy per kg of HCl absorbed (De Dietrich Process Systems, 2019). Cooling water is circulated through the absorber to remove the heat released due to absorption. High absorption efficiencies can only be achieved if the temperature is maintained below 40℃ (De Dietrich Process Systems, 2019). The unabsorbed gas is sent to a tail gas scrubber where the remaining HCl gas is scrubbed from the tail gas in counter-current flow to de-mineralized absorption water (Joseph, Koshy and Kallanickal, 2013).

Due to the high corrosivity of HCl, Diabon is used as construction material for both the HCl synthesis furnace and absorption units. Diabon is an impregnated graphite material which is resistant to hydrochloric acid with concentrations up to 38 wt% (SGL Carbon, 2018).

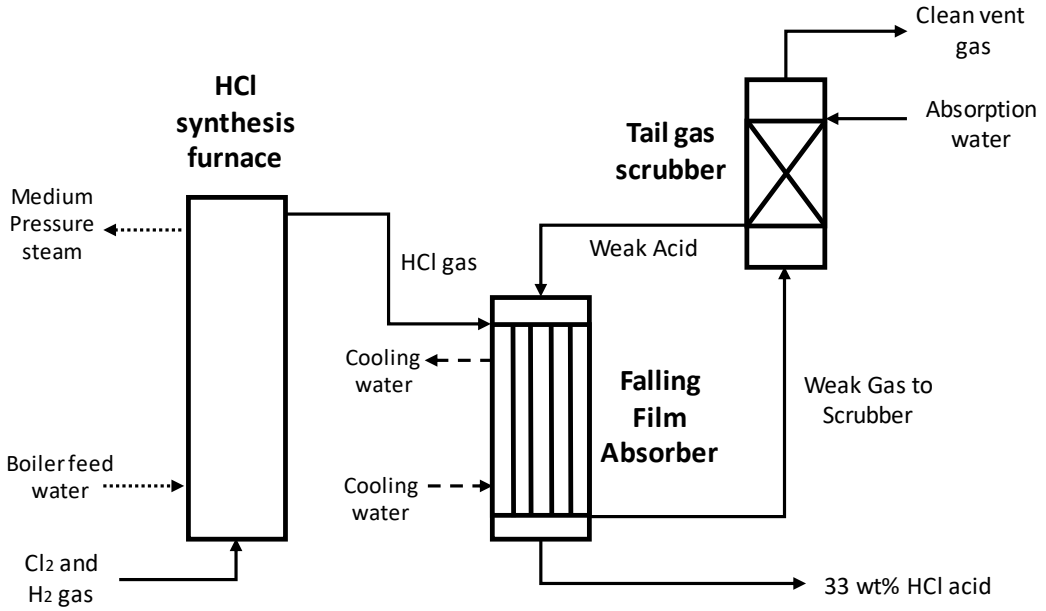

Figure 5: Simplified schematic of hydrochloric acid production unit (adapted from SGL Group, 2016)

2.3.3 Organic acid leaching process

2.3.3.1 Organic acid leaching

Various organic acids can be used as lixiviants for metal extraction from LIB waste. In a study done by Gao, Liu *et al.* (2018), a comparison between mineral (inorganic) acids and organic acids as leaching reagents were drawn. The inorganic acids provided the highest leaching efficiencies with low selectivity (with regards to impurities such as Al, Fe and Cu) at high solid-to-liquid ratios. High leaching selectivity and efficiencies were achieved with the organic acids.

The pKa values for various organic acids are tabulated in Table 19 below. The pKa value is a quantitative measure of the acidity of an acid. Strong acids have low pKa values. Based on the pKa_1 values, the strength of acidity increases in the following order: succinic acid, ascorbic acid, formic acid, DL-malic acid, citric acid, lactic acid, tartaric acid oxalic acid. Oxalic acid is not a suitable lixiviant due to the formation of cobalt oxalate precipitates (Musariri, 2019). Lactic acid dissociates to produce only one mole of hydrogen ions per mole of lactic acid, which will cause lower H^+ concentrations in leach solutions. Both tartaric and DL-malic acid are more expensive than citric acid and produce only two moles in comparison to the three moles of hydrogen ions produced per mole of citric acid (Musariri, 2019). Refer to Table 20 and Table 21 for the leaching conditions and the extent of metal extraction achieved with a variety of organic acids of which citric acid (Table 20) is the most widely used.

Table 19: pKa values for various organic acids (Serjeant and Dempsey, 1979)

Organic Acid	**pKa_1**	**pKa_2**	**pKa_3**
Citric acid	3.14	4.77	6.39
Ascorbic acid	4.10	11.79	15.89
DL-malic acid	3.4	5.11	-
Oxalic acid	1.23	4.19	-
Succinic acid	4.16	4.61	-
Tartaric acid	2.98	4.34	-
Formic acid	3.75	-	-
Lactic acid	3.08	-	-

Gao, Liu *et al.* (2018) concluded that the initial leaching speed is dependent on the hydrogen ion releasing capability and the initial concentration of hydrogen ions in the acidic leaching media. The total hydrogen ions (released and unreleased ions) in the leaching media will determine the overall metal recovery rate (Gao, Liu, *et al.*, 2018). Another study found that both the acid concentration and type of anion formed by the acid affected the leaching of cobalt (Li *et al.*, 2014).

For high leaching efficiencies, cobalt should be reduced to its lower oxidation state so that it can chelate with the anion. In the study done by Li *et al.* (2014), citric acid was shown to be one of the best chelating agents. This explains why citric acid is typically selected as organic leaching reagent. Further discussions in this section will primarily focus on citric acid leaching and the recovery of metals from citrate leach solutions.

Citric acid ($H_3C_6H_5O_7$) dissociates in three steps to produce three moles of hydrogen ions per mole of citric acid according to reactions 26 to 28 (Golmohammadzadeh, Rashchi and Vahidi, 2017). To simplify further references to the citric acid molecule, the $C_6H_5O_7^{3-}$ complex will be represented by *Cit* (thus H_3Cit represent the entire citric acid molecule).

$$H_3C_6H_5O_7 \leftrightarrow H_2C_6H_5O_7^- + H^+ \quad [26]$$

$$H_2C_6H_5O_7^- \leftrightarrow HC_6H_5O_7^{2-} + H^+ \quad [27]$$

$$HC_6H_5O_7^{2-} \leftrightarrow C_6H_5O_7^{3-} + H^+ \quad [28]$$

In the absence of a reductant, the overall leaching reaction of $LiCoO_2$ is shown in equation 29. $LiMn_2O_4$, $LiNiO_2$ and $LiCo_{0.33}Ni_{0.33}Mn_{0.33}O_2$ will react in a similar way. However, poor leaching efficiencies are obtained without the addition of a suitable reductant to reduce Co^{3+} and Mn^{4+} to Co^{2+} and Mn^{2+}. Gao, Liu *et al.* (2018) investigated the effect of the addition of a reductant on leaching efficiencies when using various leaching reagents. When using 1 M citric acid, an S/L ratio of 20 g/L at 80°C, the leaching efficiencies of cobalt and lithium increased from 50.78% and 74.80% to 99.21% and 99.46% respectively with the addition of 4 vol% hydrogen peroxide as reductant.

$$6H_3Cit + 6LiCoO_2 \rightarrow 2Li_3Cit + 2Co_3(Cit)_2 + 9H_2O + 1.5O_2 \quad [29]$$

Hydrogen peroxide is typically used as reductant in organic acid leaching systems to reduce Co^{3+} to Co^{2+} (refer to equations 4 and 5 in section 2.3.2.1). In the presence of hydrogen peroxide, citric acid will react with $LiCoO_2$ according to the set of reactions shown in equations 30 to 32 (Li, Ge, Wu, *et al.*, 2010). The balanced overall reaction is shown in equation 33. A fraction of the hydrogen peroxide will decompose to produce water and oxygen according to equation 34 (Golmohammadzadeh, Rashchi and Vahidi, 2017). Other reductants that have been tested experimentally are ascorbic acid (Nayaka *et al.*, 2015, 2019; G. P. Nayaka *et al.*, 2016a, 2016b; G.P. Nayaka *et al.*, 2016) and glucose (Chen *et al.*, 2016).

$$6H_3Cit + 2LiCoO_2 + H_2O_2 \rightarrow 2Li^+ + 2Co^{2+} + 6H_2Cit^- + 4H_2O + O_2 \quad [30]$$

$$6H_2Cit^- + 2LiCoO_2 + H_2O_2 \rightarrow 2Li^+ + 2Co^{2+} + 6HCit^{2-} + 4H_2O + O_2 \quad [31]$$

$$6HCit^{2-} + 2LiCoO_2 + H_2O_2 \rightarrow 2Li^+ + 2Co^{2+} + 6Cit^{3-} + 4H_2O + O_2 \quad [32]$$

$$6H_3Cit + 6LiCoO_2 + 3H_2O_2 \rightarrow 2Li_3Cit + 2Co_3(Cit)_2 + 12H_2O + 3O_2 \quad [33]$$

$$2H_2O_2 \rightarrow H_2O + O_2(g) \quad [34]$$

Although sources in the LIBs literature predict that the leaching of cathode materials in citric acid media will occur according to the leaching reactions in equations 26 to 34, some uncertainty exists regarding the release of hydrogen ions and the citrate metal complexes that will from at different pH levels. Citric acid is a tridentate ligand and exists as H_3Cit, H_2Cit^-, $HCit^{2-}$ and Cit^{3-} in the pH regions 1.75-3.0, 2.0-4.5, 3.5-5.5 and 4.0-8.0, respectively (Zelenin, 2007; Bastug, Göktürk and Sismanoglu, 2008; Pedada *et al.*, 2009). Thus, pH has a significant effect on the release of the citric acid hydrogen ions which will influence reaction stoichiometry. Additional research providing insight in reaction stoichiometry and the formation of citrate metal complexes may prove to be worthwhile.

Table 20: Citric acid leaching conditions and metal extraction efficiencies

Reference	Cathode Material Type	Acid Concentration	Tempera-ture (℃)	S/L ratio	Time	Reductant Concentration	Metal Extraction
(Musariri, 2019)	Mixed batteries	1.5 M citric acid	95	20 g/L	30 min	2 vol% H_2O_2	92% Co, 92% Li, 95% Ni
(Golmohammadzadeh, Rashchi and Vahidi, 2017)	Mixed batteries	2 M citric acid	60	30 g/L	2 h	1.25 vol% H_2O_2	92.53% Li, 81.50% Co
(Nayaka *et al.*, 2015)	$LiCoO_2$	100 mM citric acid	80	2 g/L	6 h	20mM Ascorbic acid	±100% Li, ±80% Co
(Chen, Luo, *et al.*, 2015)	$LiCoO_2$	2 M citric acid	70	50 g/L	80 min	0.6 g/g H_2O_2	98% Co, 99% Li
(dos Santos *et al.*, 2019)	$LiCoO_2$	1.25 M citric acid	90	-	30 min	1 vol% H_2O_2	-
(Li, Bian, Zhang, Guan, *et al.*, 2018)	$LiCoO_2$, $LiMn_2O_4$, $LiCo_{0.33}Ni_{0.33}Mn_{0.33}O_2$	0.5 M citric acid	90	20 g/L	60 min	1.5 vol% H_2O_2	99.1% Li, 99.8% Co, 98.7% Ni, 95.2% Mn
(Gao, Liu, *et al.*, 2018)	$LiCoO_2$	1 M citric acid	80	20 g/L	-	-	50.78% Co, 74.80% Li, 6.87% Al
	$LiCoO_2$	1 M citric acid	80	20 g/L	-	4 vol% H_2O_2	99.21% Co, 99.46% Li, 8.05% Al
(Fan *et al.*, 2016)	$LiCoO_2$	1.25 M citric acid	90	60 ml/g	35 min	1 vol% H_2O_2	98% Li, 90% Co
(Chen *et al.*, 2016)	$LiCo_{0.33}Ni_{0.33}Mn_{0.33}O_2$	1.5 M citric acid	80	20 g/L	2 h	0.5 g/g glucose	99% Li, 91% Ni, 92% Co, 94% Mn
(Li *et al.*, 2019)	$LiFePO_4$	20 g citric acid/g $LiFePO_4$	25	-	2 h	1 ml H_2O_2	99.35% Li, 3.86% Fe
(Li *et al.*, 2013)	$LiCoO_2$	1.25 M citric acid	90	20 g/L	30 min	1 vol% H_2O_2	±100% Li, >90% Co
(Li *et al.*, 2014)	$LiCoO_2$	2 M citric acid	60	25 g/L	5 h	0.55M H_2O_2	>96% Co, 100% Li
(Li, Ge, Wu, *et al.*, 2010)	$LiCoO_2$	1.25 M citric acid	90	20 g/L	30 min	1 vol% H_2O_2	>90% Co, 100% Li
(Zheng *et al.*, 2016)	$LiCoO_2$	*n*(citric acid): *n*($LiCoO_2$)=4	90	15 g/L	5 h	1 vol% H_2O_2	99.07% Co
(Chen and Zhou, 2014)	Mixed batteries	2 M citric acid	80	30 ml/g	90 min	2 vol% H_2O_2	97% Ni, 95% Co, 94% Mn, 99% Li
(Yao, Feng and Xi, 2015)	$LiCo_{0.33}Ni_{0.33}Mn_{0.33}O_2$	1 M citric acid	60	80 g/L	40 min	12 vol% H_2O_2	>98% total metals
(Yu *et al.*, 2019)	$LiCoO_2$	1 M citric acid	70	40 g/L	70 min	8% (V_{H2O2}/V_{H3Cit}) H_2O_2	99% leaching rate

Table 21: Leaching conditions and metal extraction efficiencies achieved for various organic acids

Reference	Cathode Material Type	Acid Concentration	Tempera-ture (℃)	S/L ratio	Time	Reductant Concentration	Metal Extraction
(Musariri, 2019)	Mixed batteries	1 M DL-malic acid	95	20 g/L	30 min	2 vol% H_2O_2	95% Co, 95% Li, 97% Ni
(Li, Ge, Chen, *et al.*, 2010)	Mixed batteries	1.5 M DL-malic acid	90	20 g/L	40 min	2 vol% H_2O_2	±100% Li, >90% Co
(Gao, Liu, *et al.*, 2018)	$LiCoO_2$	1 M DL-malic acid	80	20 g/L	-	-	34.86% Co, 62.30% Li, 6.93% Al
	$LiCoO_2$	1 M DL-malic acid	80	20 g/L	-	4 vol% H_2O_2	99.82% Co, 99.70% Li, 10.18% Al
(Li *et al.*, 2013)	$LiCoO_2$	1.5 M DL-malic acid	90	20 g/L	40 min	2 vol% H_2O_2	±100% Li, >90% Co
(Sun *et al.*, 2018)	$LiCo_{0.33}Ni_{0.33}Mn_{0.33}O_2$	1.2 M DL-malic acid	90	40 g/L	30 min	1 vol% H_2O_2	98.9% Li, 94.3% Co, 95.1% Ni, 96.4% Mn
(Nayaka *et al.*, 2019)	$LiCoO_2$	0.1 M nitrilotriacetic acid	80	2 g/L	6 h	0.02M ascorbic acid	75% Co, 96% Li
	$LiCoO_2$	0.1 M adipic acid	80	2 g/L	6 h	0.02M ascorbic acid	85% Co, 92% Li
(Li *et al.*, 2013)	$LiCoO_2$	1.5 M aspartic acid	90	10 g/L	2 h	4 vol% H_2O_2	60% Co, 60% Li
(G. P. Nayaka *et al.*, 2016a)	$LiCoO_2$	0.4 M tartaric acid	80	2 g/L	60 min	0.02M ascorbic acid	93% Co, 95% Li
(He, Sun, Mu, *et al.*, 2017)	Mixed batteries	2 M L-tartaric acid	70	17 g/L	30 min	4 vol% H_2O_2	98.6% Co, 99.1% Li, 99.3% Mn, 99.3% Ni
(Sun and Qiu, 2012)	CoO and $LiCoO_2$	1 M oxalate	80	50 g/L	2 h	5 vol% H_2O_2	98% Co
(Zeng, Li and Shen, 2015)	$LiCoO_2$	1M oxalic acid	95	15 g/L	150 min	-	97% Co, 98% Li
(G.P. Nayaka *et al.*, 2016)	$LiCoO_2$	1 M iminodiacetic acid	80	2 g/L	2 h	0.02M ascorbic acid	99% Co, 90% Li
(G.P. Nayaka *et al.*, 2016)	$LiCoO_2$	1 M maleic acid	80	2 g/L	2 h	0.02 M ascorbic acid	99% Co, 96% Li
(Li, Bian, Zhang, Xue, *et al.*, 2018)	$LiCo_{0.33}Ni_{0.33}Mn_{0.33}O_2$	2 M maleic acid	70	20 g/L	1 h	4 vol% H_2O_2	99.5% Li, 98.5% Co, 98.6% Ni, 98.2% Mn
(G. P. Nayaka *et al.*, 2016b)	$LiCoO_2$	0.5 M glycine	80	2 g/L	2 h	0.02 M ascorbic acid	91% Co

Reference	Cathode Material Type	Acid Concentration	Tempera-ture (℃)	S/L ratio	Time	Reductant Concentration	Metal Extraction
(Li *et al.*, 2015)	$LiCoO_2$	1.5 M succinic acid	70	15 g/L	40 min	4 vol% H_2O_2	100% Co, 96% Li
(Li *et al.*, 2012)	$LiCoO_2$	1.25 M ascorbic acid	70	25 g/L	20 min	-	94.8% Co, 98.5% Li
(Li *et al.*, 2017)	$LiCo_{0.33}Ni_{0.33}Mn_{0.33}O_2$	1.5 M lactic acid	70	20 g/L	20 min	0.5 vol% H_2O_2	97.7% Li, 98.2% Ni, 98.9% Co, 98.4% Mn
(Gao *et al.*, 2017)	$LiCo_{0.33}Ni_{0.33}Mn_{0.33}O_2$	2 M formic acid	60	50 g/L	20 min	6 vol% H_2O_2	>99% Co, Li, Mn, Ni
(Li, Bian, Zhang, Xue, *et al.*, 2018)	$LiCo_{0.33}Ni_{0.33}Mn_{0.33}O_2$	1 M acetic acid	70	20 g/L	1 h	6 vol% H_2O_2	98.8% Li, 97.9% Co, 97.9% Ni, 97.7% Mn
(Gao, Song, *et al.*, 2018)	$LiCo_{0.33}Ni_{0.33}Mn_{0.33}O_2$	3.5 M acetic acid	60	40 g/L	1 h	4 vol% H_2O_2	99.97% Li, 93.6% Co, 92.7% Ni, 96.3% Mn

2.3.3.2 Manganese recovery

Manganese can be recovered from citrate leach solutions by precipitation or solvent extraction directly after the leaching step or after the nickel and cobalt recovery steps. Manganese precipitation from citric acid systems is challenging due to the complex molecules that can be formed between manganese and citric acid (Chen, Zhou, *et al.*, 2015). Chen *et al.* (2016) removed manganese directly after leaching by adding potassium permanganate under the optimized conditions suggested by Wang, Lin and Wu (2009). Refer to Table 8 for these precipitation process conditions. All the manganese ions in solution was precipitated and recovered as MnO_2 or Mn_2O_3.

Musariri (2019) investigated the use of solvent extraction for manganese recovery directly after citric acid leaching. Thus, the leached cobalt and nickel were present in the aqueous phase that was mixed with a 10 vol% D2EHPA solution. Under the optimum conditions shown in Table 22, 92.77% Mn was recovered. However, 16.65% Li, 12.80% Co, 0.79% Ni, 3% Al and 9.20% Cu were co-extracted producing a Mn solution with a purity of approximately 93% after stripping. Ma *et al.* (2013) also extracted manganese with D2EHPA directly after leaching. High co-extraction of cobalt (18.8%) and nickel (18.2%) were reported. Scrubbing the co-extracted metal ions from the loaded organic can possibly increase the purity of the Mn solution produced.

Table 22: Solvent extraction of manganese from citrate leach solutions

Reference	Leaching Media	Extractant	Diluent	O:A ratio	pH	Sta-ges	Extraction	Stripping Conditions
(Musariri, 2019)	Citric acid	10 vol% D2EHPA	Kero-sene	5:1	2.5	1	92.77% Mn, 16.65% Li, 12.80% Co, 0.79% Ni, 3% Al, 9.20% Cu	0.5 M H_2SO_4 O:A=3:1
(Ma *et al.*, 2013)	Citric acid	30 vol% D2EHPA (65% saponified)	Kero-sene	2:1	1.5	1	92% Mn, 18.2% Ni, 18.8% Co, 73.7% Fe, 25.4% Cu	-
(Chen and Zhou, 2014)	Citric acid	20 vol% Na-D2EHPA (70-75% saponified), 5 vol% TBP	Kero-sene	2:1	4	1	98% Mn	0.2M H_2SO_4 O:A=1:1, 99% stripping
(Chen, Zhou, *et al.*, 2015)	Citric acid	20 vol% Na-D2EHPA (70-75% saponified)	Kero-sene	2:1	5	1	97% Mn	0.1M H_2SO_4 O:A=1:1, 99% stripping

Chen and Zhou (2014) and Chen, Zhou *et al.* (2015) recovered manganese from solution with solvent extraction after nickel and cobalt were selectively precipitated with DMG and ammonium oxalate respectively. Refer to Table 22 for the optimized extraction and stripping conditions. A small amount of lithium was co-extracted with manganese. A dilute sodium carbonate (5w/v% Na_2CO_3) solution was used to scrub the co-extracted lithium ions from the loaded organic phase before stripping with a 0.2 M sulphuric acid solution (Chen and Zhou, 2014; Chen, Zhou, *et al.*, 2015). After Li scrubbing and stripping, a pure Mn solution was produced from which a high purity Mn product can be precipitated as a hydroxide, carbonate or phosphate depending on the precipitant added.

The capital and operating costs associated with solvent extraction are typically higher than that associated with metal precipitation (Roux *et al.*, 2010). After stripping the metal species from the loaded

organic phase, an additional precipitation or electrowinning step will be required to recover the manganese ions from solution. The higher operating costs can primarily be attributed to the expensive extractant required for solvent extraction compared to relatively cheap precipitation agents such as sodium hydroxide. High product purities (and a higher potential income) should be weighed against the additional capital and operating expenses associated with solvent extraction before selecting a metal recovery mechanism for a large-scale facility.

2.3.3.3 Nickel recovery

Nickel is typically recovered from citrate leach solutions by precipitation. Musariri (2019) investigated the precipitation of a combined nickel and cobalt product using 0.5 M mono-sodium phosphate at 50°C. 91.87% of the nickel in solution was recovered. $Ni_3(PO_4)_2$ forms according to equation 35 and has a solubility constant of 4.74 x 10^{-32} at 25°C (Musariri, 2019).

$$3Ni^{2+} + 2PO_4^{3-} \rightarrow Ni_3(PO_4)_2 \quad [35]$$

High nickel recoveries can be achieved by using DMG as precipitant (Chen and Zhou, 2014; Chen, Zhou, *et al.*, 2015; Chen *et al.*, 2016). Refer to Table 23 for the optimized precipitation conditions and recoveries achieved. Nickel in citrate leach solutions reacts selectively with DMG to form a red Ni-DMG complex according to equation 36 (Chen *et al.*, 2016).

$$6C_4H_8N_2O_2 + Ni_3(Cit)_2 \rightarrow 3Ni(C_4H_7N_2O_2)_2 + 2H_3Cit \quad [36]$$

To regenerate the DMG as a white powder, Chen, Zhou *et al.* (2015) dissolved the red Ni-DMG complex in a 1 M hydrochloric acid solution. A $NiCl_2$ solution was produced from which nickel could be recovered as a hydroxide, carbonate or phosphate. The white powder was dissolved before it was re-used as nickel precipitant. The Ni precipitation performance of DMG decreased from 97.98% to 97.23% when regenerated DMG was used instead of fresh DMG.

Table 23: Selective nickel precipitation from citrate leach solutions

Reference	Leaching Media	Precipitant	pH	Ni recovery	Product Purity	Additional Information
(Musariri, 2019)	Citric acid	0.5M NaH_2PO4	13-14	91.87%	57 wt% Ni	50°C, 120 minutes
(Chen *et al.*, 2016)	Citric acid	0.2M DMG	-	98.5%	99.3%	Stoichiometric required amount of DMG fed, 25°C, 30 min, 300 rpm
(Chen and Zhou, 2014)	Citric acid	0.05M DMG	8	95%	98.46% Ni	Molar ratio Ni^{2+}:DMG = 0.5 25°C, 30 min, 300 rpm
(Chen, Zhou, *et al.*, 2015)	Citric acid	0.05M DMG	6	98%	-	Molar ratio Ni^{2+}:DMG = 0.5 25°C, 30 min, 300 rpm

Sodium hydroxide is generally not used as precipitant for cobalt or nickel in citric acid leach systems. Although the OH^- ion can act as a precipitant in mineral acid systems, both the OH^- ion and the citric acid molecule (H_2Cit^-, $HCit^{2-}$ and Cit^{3-}) work as complexing agents in citric acid systems (Chen, Zhou, *et al.*, 2015). This explains why metal hydroxide precipitates are not formed that easily with pH changes facilitated by the addition of NaOH to citric acid systems in comparison to mineral acid system (Ma *et al.*, 2013).

2.3.3.4 Cobalt recovery

Cobalt can be recovered from citrate leaching media by precipitation or solvent extraction. pH adjustments cannot be used to separate cobalt and manganese in citric acid leach solutions due to the complexing behaviour of the OH^- ion in citrate leach solutions. The oxalate ion ($C_2O_4^{-2}$) is typically used to facilitate selective cobalt precipitation when added to the system in the form of oxalic acid or ammonium oxalate (refer to Table 24). This is possible due to the weak chelation of the citric acid molecule with cobalt ions in comparison to manganese ions which can form complex molecules in the presence of citric acid (Chen, Zhou, *et al.*, 2015). Cobalt in the citrate leach solution reacts selectively with the oxalate ion to form $CoC_2O_4.2H_2O$ according to equation 37 (Chen *et al.*, 2016).

$$Co_3(Cit)_2 + 3C_2O_4^{2-} \rightarrow 3CoC_2O_4 + 2Cit^{3-} \quad [37]$$

When cobalt is selectively precipitated with ammonium oxalate before manganese have been removed from the leach solution, small amounts of manganese may co-precipitate as MnC_2O_4. A dilute oxalic acid solution (0.1 M) can be used as washing solution to remove the manganese from the cobalt precipitates (Chen and Zhou, 2014; Chen, Zhou, *et al.*, 2015).

Lithium may co-precipitate with cobalt according to equation 38 (Chen, Luo, *et al.*, 2015). However, the solubility product (pK_{sp}) of CoC_2O_4 is 7.2 in comparison to 1.9 for $Li_2C_2O_4$. The pK_{sp} values indicate that cobalt ions will preferentially precipitate before lithium ions if oxalate ions are added to the system. The high product purities shown in Table 24 confirms this.

$$2Li^+ + C_2O_4^{2-} \rightarrow Li_2C_2O_4 \quad [38]$$

Table 24: Selective cobalt precipitation from organic acid leach solutions

Reference	Leaching Media	Preci-pitant	pH	Co recovery	Product Purity	Additional Information
(Musariri, 2019)	Citric acid	0.5M NaH_2PO4	13-14	79.96%	42 wt% Co	50℃, 120 minutes
(Chen, Luo, *et al.*, 2015)	Citric acid	0.5M $H_2C_2O_4$	-	99%	99.3% Co	60℃, 30 minutes, 300 rpm Molar ratio $H_2C_2O_4$: Co^{2+} =1.05
(dos Santos *et al.*, 2019)	Citric acid	0.5M $H_2C_2O_4$	-	99.6%	-	Molar ratio $H_2C_2O_4$: Co^{2+} = 3:1
(Fan *et al.*, 2016)	Citric acid	$H_2C_2O_4$	-	99.5%	99.3% Co	Molar ratio $H_2C_2O_4$: Co^{2+} = 1.05 20 min
(Chen *et al.*, 2016)	Citric acid	0.5M $H_2C_2O_4$	-	96.8%	98.9%	1.2 times stoichiometric required amount of $H_2C_2O_4$ fed, 25℃, 30 min, 300 rpm
(Nayaka *et al.*, 2018)	Citric, tartaric, ascorbic acid	0.1M $H_2C_2O_4$	-	>99%	-	-
(Chen and Zhou, 2014)	Citric acid	0.5M $(NH_4)_2C_2O_4$	6	97%	96.47% Co, 1.07% Mn	25℃, 30 minutes, 300 rpm Molar ratio $C_2O_4^{2-}$: Co^{2+} =1.2
(Chen, Zhou, *et al.*, 2015)	Citric acid	$(NH_4)_2C_2O_4$	6	97%	-	55℃, 20 minutes, 300 rpm Molar ratio $C_2O_4^{2-}$: Co^{2+} =1.2

2.3.3.5 Lithium recovery

The final leach solution obtained after the recovery of Mn, Ni and Co usually contain lithium which can be recovered with phosphate or carbonate precipitation as seen in Table 25. Based on the literature

sources found and shown in Table 17 and Table 25, it was be concluded that carbonate precipitation is commonly used for lithium recovery from mineral acid leach solutions, whereas phosphate precipitation is used for lithium recovery form citrate leach solutions.

The solubilities of lithium phosphate and lithium carbonate are 0.039 g/100 ml water and 1.33 g/100 ml water respectively at 20℃ (Chen and Zhou, 2014). The solubilities indicate that higher lithium recoveries can be expected when using phosphate precipitation. Literature confirmed this expectation. Referring to Table 17, it can be concluded that lithium recoveries of approximately 80% can be expected with carbonate precipitation whereas recoveries of greater than 89% can be achieved with phosphate precipitation (Table 17 and Table 25).

Table 25: Lithium precipitation from citrate leach solutions

Reference	Leaching Media	Precipitant	Tempera-ture (℃)	Li recovery	Product Purity	Additional Information
(Musariri, 2019)	Citric acid	0.5M NaH_2PO4	80	77.20%	89 wt% Li	pH=13-14 120 minutes
(Chen, Luo, *et al.*, 2015)	Citric acid	0.5M H_3PO_4	60	93%	98.5%Li	30 minutes, 300 rpm Molar ratio H_3PO_4 : Li^+ =0.4
(Chen *et al.*, 2016)	Citric acid	0.5M H_3PO_4	25	92.7%	99.5%	Stoichiometric required amount of H_3PO_4 fed, 30 min, 300 rpm
(Fan *et al.*, 2016)	Citric acid	Na_3PO_4	-	90.2%	-	-
(Chen and Zhou, 2014)	Citric acid	0.5M Na_3PO_4	-	89%	99.7%	-
(Chen, Zhou, *et al.*, 2015)	Citric acid	0.5M Na_3PO_4	-	89%	-	-
(dos Santos *et al.*, 2019	Citric acid	Na_2CO_3	90	75%	-	-
(Li *et al.*, 2019)	Citric acid	Saturated Na_2CO_3	95	89.95%	-	Li concentration in feed = 20 g/L Li Ratio of volume Na_2CO_3 solution to Li containing solution = 0.2-0.3

Musariri (2019) used NaH_2PO_4 as precipitant and found that an increase in temperature, increased the extent of lithium phosphate precipitation. Precipitation at 50℃ yielded a lithium recovery of 4% which increased to 72% at 80℃. This can be explained by the possible decrease in the solubility of lithium phosphate with an increase in temperature. Musariri (2019) concluded that lithium can be separated from citrate leach solutions by using phosphate precipitation at different temperatures that affect the solubilities of various phosphate salts. Phosphate precipitation (directly after leaching) at two different temperature levels were tested to validate this conclusion. Precipitation at 50℃ recovered 3.53% Li whereas precipitation at 80℃ recovered 71.59% Li. Therefore, Co, Mn and Ni can be recovered at a temperature of 50 ℃ (96.65% Co, 99.45% Mn and 98.16% Ni extraction) where after Li can be recovered at 80℃ (Musariri, 2019).

Sodium phosphate and phosphoric acid can also be employed as Li precipitants. According to Chen *et al.* (2016), lithium cannot be precipitated by using carbonic acid (H_2CO_3) in a citric acid medium because the acidity of H_2CO_3 (pKa_1=6.38) is lower than that of citric acid (pKa_1=3.14). Phosphoric acid (pKa_1=2.12) has a stronger acidity and was proposed as appropriate alternative. Lithium remaining in the citrate leach solution reacts with phosphoric acid according to equation 39 (Chen *et al.*, 2016). An advantage of using

phosphoric acid to facilitate lithium precipitation is that citric acid (H_3Cit) is regenerated during the precipitation reaction (equation 39). The regenerated citric acid can be recycled to the leaching tank to reduce the amount of fresh acid required. Chen, Luo *et al.* (2015) and Chen *et al.* (2016) tested the leaching efficiency of the recycled acid in 5 consecutive cycles and concluded that the leaching performance will not be affected by recycling citric acid.

$$Li_3Cit + H_3PO_4 \rightarrow Li_3PO_4 + H_3Cit \quad [39]$$

2.4 Techno-economic considerations

Life-cycle analyses (LCA) evaluating the effect of LIB recycling on the overall cradle-to-grave impact of the batteries have been done (Notter *et al.*, 2010; Gaines *et al.*, 2011; Majeau-Bettez *et al.*, 2011; Dunn *et al.*, 2012; Hart, Curran and Davies, 2013; Ellingsen *et al.*, 2014). If the energy required to manufacture battery raw materials from virgin materials exceed the energy required to recycle these materials from spent LIBs, recycling becomes a viable option from an economic and environmental point of view (Dunn *et al.*, 2012). However, apart from energy requirement other LCA indicators may also affect decision-making. The following reported LCA results indicate that LIB recycling may have potential benefits:

1. Recycling LIBs may lead to a 50% reduction in the material production energy associated with batteries (Gaines *et al.*, 2011).
2. Direct recycling of $LiMn_2O_4$, aluminium and copper of LIBs in a closed-loop process can lower the energy required to produce raw materials by 48%. A 94% decrease in the production energy of $LiCoO_2$ was predicted, if the recycling conditions assumed for $LiMn_2O_4$ are valid for the recycling of $LiCoO_2$ as well (Dunn *et al.*, 2012).

CM Solutions did a study to investigate the techno-economic feasibility of a hydrometallurgical recycling facility in South Africa. Batteries were physically dismantled and roasted before leaching was done in two stages using hydrochloric acid as lixiviant. Their mass balance was based on the assumption that the facility will process 10 000 tons of LIB electrodes (13 600 ton raw batteries) annually which was calculated from the estimated LIB consumption rate in South Africa in 2020. The total capital expenditure for the facility was estimated as R 295 million in 2020 by using a factorial method. The monthly operating expenses and revenue were estimated as R 9.3 million and R 6.9 million respectively (Knights and Saloojee, 2015).

For the profitability analysis, cash flow values were discounted at a rate of 9% for 5 years resulting in a net present value (NPV) of R -440 million. The NPV indicated that the process will not be financially viable as a stand-alone process. Knights and Saloojee (2015) suggested that a levy or recycling fee should be charged to improve the economic feasibility of the proposed process. If a fee of R 8.12 per kg of LIBs (3% of the purchase cost of a new battery) is charged and used as additional income to the process, the facility could break even (NPV=0) after 5 years. A sensitivity analysis revealed that the profitability of the process is more sensitive to the operating costs than to the capital costs. Thus, it would make sense from a financial point of view to spend additional capital to decrease operating expenses (Knights and Saloojee, 2015).

From the literature review it is clear that there are many technically feasible processing options that could potentially be used to recover valuable metals from end-of-life LIBs. However, apart from the work done by Knights and Saloojee (2015), no information is available on the techno-economic feasibility of a LIB recycling facility in South Africa. Scope therefore exists for consideration of alternative flow sheet options to understand the technical and economic challenges associated with different recycling strategies. Therefore, this study aims to comprehensively compare the techno-economic feasibility of different flowsheets, taking the current status of the LIBs recycling in South Africa into account.

3 Mass and Energy Balances

3.1 Definition of system boundaries

The system boundaries used for mass and energy balance calculations are indicated with the dotted line in Figure 6 below. Raw batteries are fed to the process, thus the mechanical pre-treatment steps required to produce electrode material suitable for acid leaching are included. Waste treatment facilities are not included in mass and energy balance calculations. However, a waste disposal or treatment cost associated with each waste stream was considered in the economic analysis.

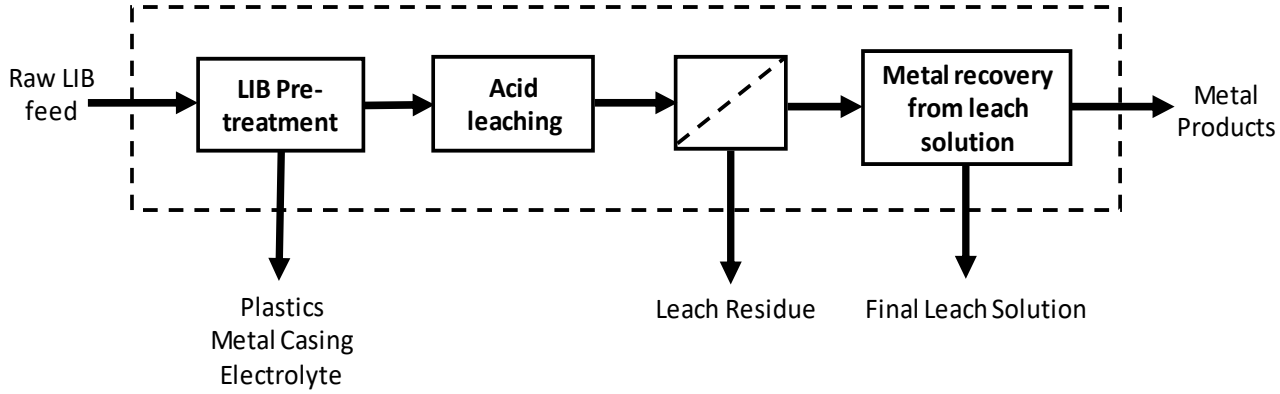

Figure 6: Schematic diagram illustrating the system boundaries

3.2 Lithium-ion battery feed

3.2.1 LIB processing capacity

The design LIB processing capacity for the recycling facilities was calculated based on the following recent statistics:

1. According to the e-Waste Association of South Africa (eWASA), each South African generate approximately 6.2 kg e-waste annually (Guy, 2017).
2. The South African population is estimated at 58.33 million inhabitants in 2019 (Statista, 2019).
3. Only 8% of the e-waste produced in South Africa is recycled (Kohler *et al.*, 2018).
4. According to a study done by Mintek for the Department of Science and Technology and the Council for Scientific and Industrial Research (CSIR), lithium-ion batteries contributed to 3% of the overall amount of e-waste recycled in South Africa (Lydall, Nyanjowa and James, 2017).
5. The facilities will operate 92% of the time, leaving time for maintenance activities (Turton *et al.*, 2012).

Based on the assumptions listed above, the LIB processing capacity was calculated as 868 ton of raw batteries per annum. Thus, the LIB feed rate to the processing facilities is 2.58 ton/day. Refer to Appendix B for sample calculations. These values compare well with the LIB waste production stated by other literature sources as seen in Table 26 below.

Table 26: Comparison of predicted LIB waste recycled in South Africa

Reference	E-waste/LIB waste (ton/yr)	Year	% e-waste recycled	% LIBs in recycled e-waste	LIB waste recycled (ton/yr)
(Guy, 2017; Statista, 2019)	361 646 (e-waste)	2019	8%	3%	868
(Kohler *et al.*, 2018)	324 520 (e-waste)	2017	8%	3%	779
(Guy, 2017)	360 000 (e-waste)	2019	8%	3%	864
(Knights and Saloojee, 2015)	13 600 (LIBs consumed)	2020	8%	-	1088

3.2.2 Feed stream composition

According to a study done by CM Solutions in 2015, lithium-ion batteries consist of approximately 4.92% plastics, 21.7% metal casing, 46.8% cathode material (aluminium electrode) and 27.1% anode material (graphite electrode) (Knights and Saloojee, 2015). However, the study did not include the electrolyte that contributes to 3.1% of the raw battery composition (Chagnes *et al.*, 2015). Thus, incorporating the electrolyte contribution, the bulk battery composition was calculated as shown in Table 27 below.

Table 27: Bulk battery composition used to calculate LIB feed composition

Battery Component	Composition (%)
Cathode	44.8
Anode	26.3
Plastics	4.8
Electrolyte	3.1
Metal Casing	21.0

Table 28 below shows the cathode material distribution expected based on the global battery market trends (Zou *et al.*, 2013; Chen, Xu, *et al.*, 2015). These values were used to determine the respective amounts of different battery types fed to the process.

Table 28: Cathode material distribution

Cathode Material Type	LIB Distribution (%)
$LiCoO_2$	37.2
$LiCo_{0.33}Ni_{0.33}Mn_{0.33}O_2$	29.0
$LiMn_2O_4$	21.4
$LiNiO_2$	7.2
$LiFePO_4$	5.2

Cathode materials typically contain copper, iron and aluminium which are considered as impurities in the feed material. It was assumed that the cathode material fed to the facilities contains approximately 11.14% aluminium (Chagnes *et al.*, 2015). The amounts of copper and iron present in the cathode material feed was assumed as an average calculated from multiple sources as shown in Table 29 below.

Table 29: Copper and iron impurities in cathode materials

Reference	Cu (Wt %)	Fe (Wt %)
(Sattar *et al.*, 2019)	0.004	0.05
(Meshram, Pandey and Mankhand, 2015)	0.005	0.06
(Musariri, 2019)	0.048	-
(Musariri, 2019)	0.088	-
(Hu *et al.*, 2017)	0.05	-
(Barik, Prabaharan and Kumar, 2016)	0.004	-
(Dutta *et al.*, 2018)	2.4	0.3
(Dorella and Mansur, 2007)	0.0	-
(Giuseppe Granata *et al.*, 2012)	6.0	-
(Ferreira *et al.*, 2009)	0.7	-
Average	0.85	0.04

The composition of the anode material was determined from the two literature sources shown in Table 30 below.

Table 30: Calculation of anode composition (wt%)

Reference	Al	Co	Li	Ni	Cu	Graphite
(Dorella and Mansur, 2007)	1.93	3.22	0.79	0.03	52.64	41.39
(Chagnes *et al.*, 2015)	0.054	0.047	0.5	0.00	40.7	58.69
Average	0.992	1.6335	0.645	0.015	46.67	50.04

The overall LIB feed composition was calculated by considering all the assumptions and literature sources stated above. The calculated values used in the mass and energy balances are tabulated in Table 31 below.

Table 31: Overall LIB feed composition

Component/Element	Composition (wt%)			
Plastics	4.8%			
Electrolyte	3.1%			
Metal Casing	21.0%			
Electrodes (Anode and cathode)	71.1%			
	Li	2.6%	P	0.4%
	Co	11.6%	O	13.3%
	Mn	7.3%	Al	5.3%
	Ni	4.0%	Cu	12.6%
	Fe	0.7%	Graphite	13.1%

3.3 Approach to solving mass balances

Mass balances were solved in Microsoft Excel by sequentially completing a mass balance around each unit operation starting from the LIB feed entering the pre-treatment section. The base value for the LIB feed rate was determined as 2.58 ton/day as discussed in section 3.2.1. The assumptions made with

regards to the process conditions and reactions taking place in each unit are discussed in section 3.5. An iterative approach as illustrated in Figure 7 was used to solve recycle streams. Elemental balances over units as well as an overall mass balance were performed to confirm that all mass that entered each process was accounted for and that all mass balances closed.

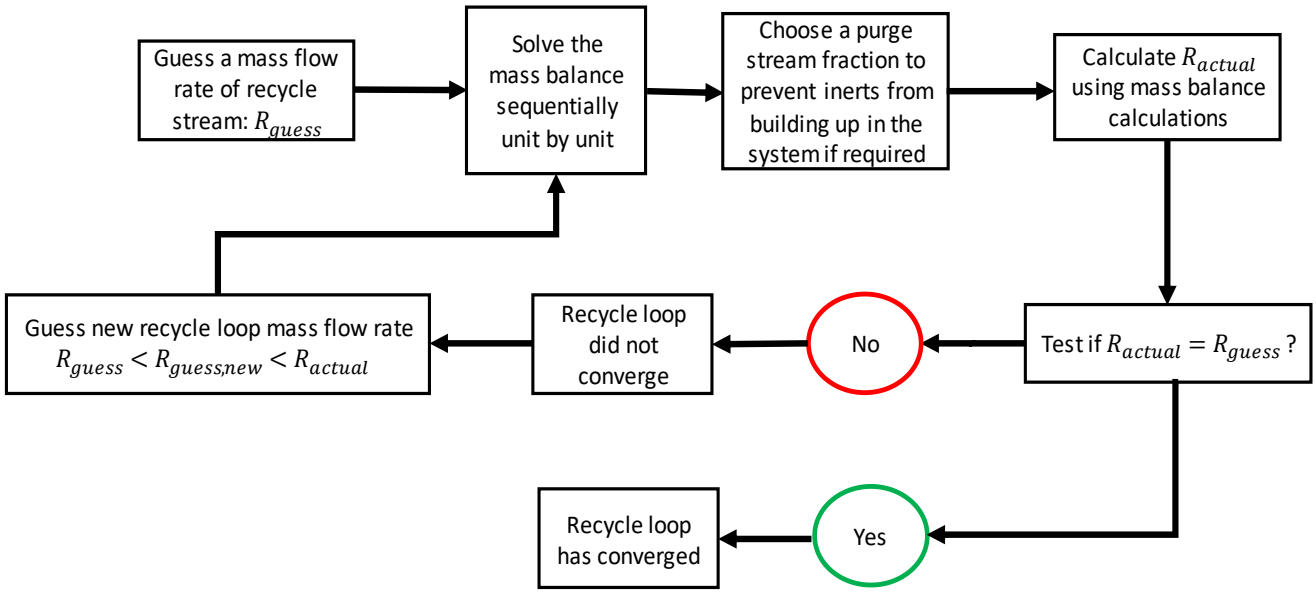

Figure 7: Iterative approach to solving recycle streams

3.4 LIB pre-treatment

The pre-treatment plant section consists of a discharging tank, cutting mill, 12 mm aperture screen, ultrasonic washing container, filter press, 2 dryers and a 2 mm aperture screen. The pre-treatment flowsheet is based on the process proposed by Jinhui Li, Shi *et al.* (2009). Refer to Figure 8 for a schematic representation of the proposed pre-treatment process.

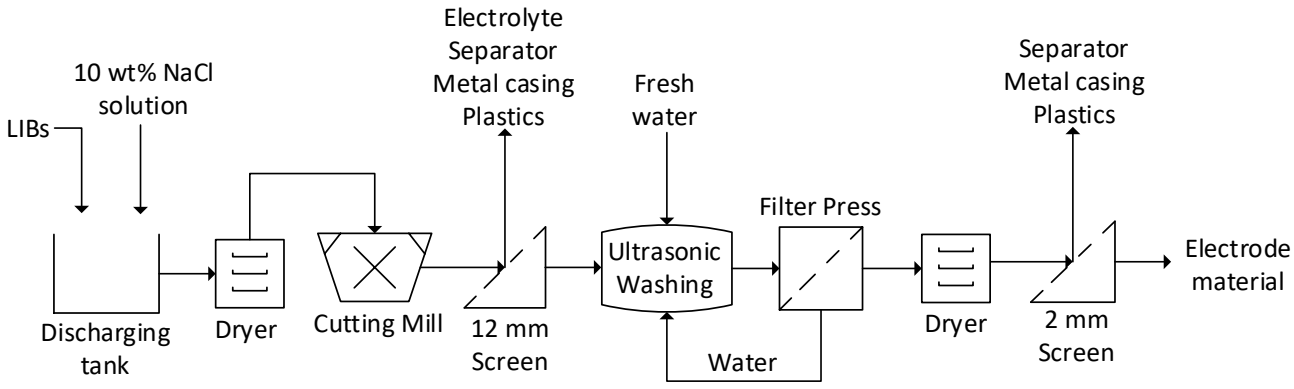

Figure 8: Schematic diagram of proposed pre-treatment process

Spent LIBs will be discharged in a salt solution to avoid potential dangers such as short circuiting and self-ignition. After discharging, the LIBs will be dried before being fed to the cutting mill (with a 12 mm screen) to crush and disintegrate the batteries. The underflow of the 12 mm screen will be treated in an ultrasonic washing container with agitation to enhance the separation of cathode material from the Al foils and anode material from the Cu foils respectively. A filter press will be used to remove the washing water

from the LIB material, prior to drying and final screening with a 2 mm aperture screen. The water obtained from the filter, will be recycled back to the ultrasonic washing container to reduce the amount of fresh water fed to the process. The following assumptions were made with regards to the pre-treatment section:

1. Batteries will be submerged in a 10 wt% NaCl solution for 6 hours to discharge them of their remaining capacity (Yao *et al.*, 2018).
2. The plastics (casing or separator), metal casing and electrolyte will be completely removed and discarded as waste in the pre-treatment section. It was assumed that 95% of these battery components will be removed after the cutting mill with the 12 mm aperture screen. The remaining 5% will be removed from the valuable electrode powder with the 2 mm aperture screen.
3. The ultrasonic washing container will be operated at room temperature, with a residence time of 30 minutes to ensure that optimal separation of the electrode materials from their respective foils can occur (Jinhui Li, Shi, *et al.*, 2009). An ultrasonic frequency of 40 kHz was selected as this is the frequency typically used in industrial applications (Ultrasonic Power Corporation, no date).
4. The mass flowrate of water fed to the ultrasonic washing tank should be more than twice the mass flowrate of the LIB material fed to the tank (Ultrasonic Power Corporation, no date). Thus, it was assumed that the mass flowrate of water will be 2.2 times greater than the LIB mass flowrate to the tank.
5. In the study done by Jinhui Li, Shi *et al.* (2009), the electrode powder obtained after pre-treatment using a 12 mm aperture screen, contained 0.3 wt% Cu, 0.8 wt% Al and 1.4 wt% Fe. Their pre-treatment feed contained 10 wt% Cu, 3 wt% Al and 19 wt% Fe respectively (Jinhui Li, Shi, *et al.*, 2009). Thus, a 97%, 73% and 93% reduction in the amounts of Cu, Al and Fe was observed. Similar reduction percentages were assumed for Cu, Al and Fe over the pre-treatment plant section.
6. 8% of the valuable electrode powder containing Li, Ni, Co and Mn will be lost during the pre-treatment section (Jinhui Li, Shi, *et al.*, 2009). For mass balance purposes, it was assumed that electrode material will leave the process with the residual plastic and metal casing discarded after the 2 mm screen.

3.5 Mineral acid process

Hydrochloric acid was selected as leaching reagent for the mineral acid process options. Three process alternatives were evaluated. The first two options produce similar products and have a similar sequence in which the various valuable metals are selectively recovered from the leach solution. The key difference is the inclusion of a membrane electrolysis and hydrochloric acid production system in the first option. In the third process option the metals are not selectively recovered as separate products; instead a mixed hydroxide product containing Ni, Co and Mn and a separate lithium product are produced. Assumptions made for mass and energy balance calculations are discussed in the sections below.

3.5.1 Mineral acid process option 1

The mineral acid process proposed is primarily based on the work done by Wang, Lin and Wu (2009). To regenerate hydrochloric acid and sodium hydroxide from sodium chloride salt produced during precipitation reactions, membrane cells and hydrochloric acid synthesis and absorption units were included prior to lithium recovery. The regeneration of these reagents will significantly decrease the raw material inputs to the process. Refer to Appendix A for the process flow diagram and stream table of mineral acid process option 1.

3.5.1.1 Hydrochloric acid leaching

Hydrochloric acid was selected as mineral acid lixiviant as it offers the highest leaching efficiency of valuable metals without the addition of a reductant (Gao, Liu, *et al.*, 2018). The following assumptions were made with regards to the hydrochloric acid leaching tank:

1. The process conditions selected (Wang, Lin and Wu, 2009) and metal extraction achieved in the leaching tank are summarized in Table 32 below. The extraction efficiencies used for Co, Li, Ni and Mn were reported by Wang, Lin and Wu (2009) when leaching was done with a cathode mixture of $LiCoO_2$, $LiMn_2O_4$ and $LiCo_{0.33}Ni_{0.33}Mn_{0.33}O_2$. It was assumed that the graphite in the anode material will not leach and will be discarded as part of the leach residue.
2. A 92% leaching efficiency was assumed for Fe, based on the results obtained by Huang *et al.* in 2016. Hydrochloric acid cannot selectively leach out the valuable metals thus, the leaching efficiency of both Al and Cu was assumed as 98% (Gao, Liu, *et al.*, 2018).

Table 32: Process conditions and metal extraction achieved in HCl leaching tank

Process Conditions	
HCl Concentration	4 mol/L
S/L	0.02 g/ml
Temp	80 ℃
Time	1 hour
Metal Extraction (%)	
Co	99.5
Li	99.8
Ni	99.9
Mn	99.8
Al	98.0
Fe	92.0
Cu	98.0
Carbon	0.0

3. Based on the metal extraction efficiencies tabulated in Table 32 an average leaching efficiency (refer to Table 33) for the respective cathode materials were calculated based on the molar ratio of the metals within each compound.

Table 33: Average leaching efficiencies for various cathode materials

Cathode Material	Average Leaching Efficiency
$LiCoO_2$	99.65%
$LiCo_{0.33}Ni_{0.33}Mn_{0.33}O_2$	99.27%
$LiMn_2O_4$	99.80%
$LiNiO_2$	99.85%
$LiFePO_4$	95.90%

4. The reactions that were considered for the leaching of the active cathode materials are listed in equations 40 to 44 below.

$$2LiCoO_2 + 6HCl \rightarrow 2CoCl_2 + 2LiCl + 3H_2O + \frac{1}{2}O_2 \quad [40]$$

$$4LiNiO_2 + 12HCl \rightarrow 4NiCl_2 + 4LiCl + 6H_2O + O_2 \quad [41]$$

$$4LiMn_2O_4 + 20HCl \rightarrow 8MnCl_2 + 4LiCl + 10H_2O + 3O_2 \quad [42]$$

$$12LiNi_{0.33}Co_{0.33}Mn_{0.33}O_2 + 36HCl \rightarrow 4CoCl_2 + 4NiCl_2 + 4MnCl_2 + 12LiCl + 18H_2O + 3O_2 \quad [43]$$

$$LiFePO_4 + 3HCl \rightarrow FeCl_2 + LiCl + H_3PO_4 \quad [44]$$

5. The small amounts of lithium, cobalt and nickel present in the anode material will react according to equations 45 to 47 listed below.

$$Li + HCl \rightarrow LiCl + \frac{1}{2}H_2 \quad [45]$$

$$Co + 2HCl \rightarrow CoCl_2 + H_2 \quad [46]$$

$$Ni + 2HCl \rightarrow NiCl_2 + H_2 \quad [47]$$

6. Copper, iron and aluminium were considered impurities in the system. These metals will be leached according to the reaction equations 48 to 51 listed below.

$$Fe + 2HCl \rightarrow FeCl_2 + H_2 \quad [48]$$

$$Fe + 3HCl \rightarrow FeCl_3 + \frac{3}{2}H_2 \quad [49]$$

$$2Cu + O_2 + 4HCl \rightarrow 2CuCl_2 + 2H_2O \quad [50]$$

$$2Al + 6HCl \rightarrow 2AlCl_3 + 3H_2 \quad [51]$$

7. The HCl solution fed to the leaching tank will be fed as a 33 wt% HCl solution produced in the HCl falling film absorber. Water evaporated in the forced circulation evaporator prior to the membrane cells, will be recycled to the leaching tank to minimize the additional heating required to ensure leaching operation at 80 ℃. The recycled water will contain a small fraction of ammonia that will be neutralised by hydrochloric acid according to equation 52 below.

$$NH_4OH + HCl \rightarrow NH_4Cl + H_2O \quad [52]$$

8. Although a fraction of the leach residue can be recycled to the leaching tank to maximize valuable metal recovery, recycling a large mass of residue will increase the liquid requirements and subsequently the tank volumes significantly. Without the recycle stream high leaching efficiencies (Table 33) are still obtainable. Therefore, the entire leach residue stream will be discarded as waste.
9. The 33 wt% HCl solution pumped from the intermediate HCl storage tank will be pre-heated in a shell-and-tube heat exchanger with the feed stream to the pH adjustment tank (pH=2). To ensure operation at 80 ℃, high pressure steam (254 ℃, 41 barg) will be utilised to provide the additional heat required.

3.5.1.2 Solid-Liquid separation

Filter presses will be used as solid-liquid separators after the respective reaction or precipitation steps. In a filter press, slurries or leach solutions are pressed in closed chambers to achieve the highest separation efficiency of all mechanical separation techniques (Welders Filtration Technology, no date). Filter pressing is the only solid-liquid separation technique that allow the combination of filtration, cake washing and cake drying in one machine (Welders Filtration Technology, no date). It was assumed that the filter cake produced have a low moisture content of 6-8% (Evoqua Water Technologies, 2014). For energy balance purposes it should be noted that a 15℃ temperature drop was assumed over filter presses with feed streams at temperatures above room temperature.

3.5.1.3 Manganese recovery

a) pH Adjustment with sodium hydroxide

Prior to manganese precipitation, the pH of the leach solution will be adjusted to 2 using sodium hydroxide solution. The following assumptions were made with regards to the pH adjustment step:

1. 32 wt% NaOH solution produced in the membrane cells will be fed to the agitated pH adjustment tank to neutralise the acidic solution coming from the HCl leaching tank. The flowrate of NaOH solution fed to the tank was adjusted to ensure that the pH of the solution leaving the tank will be 2. HCl and H_3PO_4 (formed as shown in equation 44) will be neutralised according to reaction equations 53 and 54 shown below.

$$HCl + NaOH \rightarrow NaCl + H_2O \quad [53]$$

$$H_3PO_4 + 3NaOH \rightarrow Na_3PO_4 + 3H_2O \quad [54]$$

2. pH calculations were based on equation 55 shown below. Phosphoric acid is present in very small amounts in the system. Therefore, the effect thereof on the system pH was considered negligible except in cases where the amount of acid is approximately the same as that of hydrochloric acid. This is a reasonable assumption as phosphoric acid is considered a weak acid that will not fully dissociate in aqueous solutions to produce hydrogen ions. The acid dissociation constants and pKa values tabulated in Table 34 confirms that phosphoric acid is a weak acid compared to HCl.

$$pH = -log[H^+] \quad [55]$$

Table 34: Dissociation constants and pKa values for acids at 25°C

Acid	pKa	Ka	Reference
HCl	$pKa = -6.3 << 1$	$Ka >> 1$	(Lumen, no date)
H_3PO_4	$pKa_1 = 2.16$ $pKa_2 = 7.21$ $pKa_3 = 12.32$	$Ka_1 = 6.9 \times 10^{-3}$ $Ka_2 = 6.2 \times 10^{-8}$ $Ka_3 = 4.8 \times 10^{-13}$	(Silberberg, 2013)

3. 13% of the manganese in the leach solution will react with NaOH to form $Mn(OH)_2$ precipitates (equation 56 below) at a pH of 2 according to the work done by Wang, Lin and Wu (2009).

$$MnCl_2 + 2NaOH \rightarrow 2NaCl + Mn(OH)_2 \quad [56]$$

4. Negligible amounts of Co, Ni, Li, Cu and Al will precipitate out at a pH level of 2 (Jinhui Li, Shi, *et al.*, 2009; Wang, Lin and Wu, 2009; Zou *et al.*, 2013).
5. 98% of iron in the Fe^{3+} oxidation state will react with NaOH to form $Fe(OH)_3$ precipitates (equation 57) at a pH of 2 (Jinhui Li, Shi, *et al.*, 2009; Zou *et al.*, 2013). Iron in the Fe^{2+} oxidation state can only be recovered from leach solutions at higher pH levels except if it is oxidized to the Fe^{3+} oxidation state (Zou *et al.*, 2013).

$$FeCl_3 + 3NaOH \rightarrow Fe(OH)_3 + 3NaCl \quad [57]$$

6. Aqueous ammonium chloride will react with NaOH to form ammonium hydroxide and sodium chloride salt (equation 58).

$$NH_4Cl + NaOH \rightarrow NH_4OH + NaCl \quad [58]$$

7. As stated previously, the leach solution stream fed to the pH adjustment tank will be cooled in a shell-and-tube heat exchanger with the 33 wt% HCl solution fed to the leaching tank. Cooling the feed solution will ensure that no cooling water will be required to cool the manganese precipitation tank to a temperature of 40-50℃ (Wang, Lin and Wu, 2009).

b) Manganese precipitation with potassium permanganate

The leach solution with a pH of 2 will be fed to an agitated tank that will facilitate the precipitation of manganese oxide. Potassium permanganate ($KMnO_4$) will be used as precipitation agent to selectively facilitate a redox reaction (equation 59 (Wang, Lin and Wu, 2009)) for the recovery of manganese from the leach solution. The operating conditions tabulated in Table 35 were selected based on the optimum conditions reported by Wang, Lin and Wu in 2009.

Table 35: Operating conditions for manganese precipitation (Wang, Lin and Wu, 2009)

Temperature	40-50 ℃
pH	2
Molar ratio of $KMnO_4$:Mn^{2+}	2
Mn recovered from solution	100%

$$3MnCl_2 + 2KMnO_4 + 2H_2O \rightarrow 5MnO_2 + 2KCl + 4HCl \quad [59]$$

Based on the high Mn product purities (>98%) reported by Huang *et al.* (2016), Sattar *et al.* (2019) and Wang, Lin and Wu (2009) and the low pH at which the Mn precipitation tank will operate, it was assumed that a negligible amount of Fe^{2+} will be oxidized by $KMnO_4$ to form $Fe(OH)_3$ precipitates. Hydrochloric acid and sodium phosphate in the feed stream react according to equations 60 and 61 shown below. It was assumed that the chlorine produced (reaction 60) is in the gas phase and can be fed to the HCl combustion furnace where gaseous HCl is produced.

$$2KMnO_4 + 16HCl \rightarrow 2KCl + 2MnCl_2 + 8H_2O + 5Cl_2 \quad [60]$$

$$Na_3PO_4 + 3HCl \rightarrow H_3PO_4 + 3NaCl \quad [61]$$

The manganese precipitates consisting of $Mn(OH)_2$ and MnO_2 present in the leach solution, will be recovered from solution with a filter press. Residual moisture in the filter cake will be removed with a dryer to produce a dry manganese product that can be sold.

3.5.1.4 Impurity removal

Iron, copper and aluminium are considered impurities in the system, which will negatively affect the purities of the products recovered if they are not removed at an early stage in the process. 32 wt% NaOH solution produced in the membrane cells will be fed to an agitated tank aiming to increase the pH to 4.5. HCl and H_3PO_4 are neutralized according to equations and 53 and 54 (refer to section 3.5.1.3).

A pH of 4.5 was selected to minimize the cobalt and nickel losses due to hydroxide precipitation (reactions 62 and 63). At a pH of 4.5, it was assumed that 2% cobalt and 1% nickel will be lost due to precipitation (Jinhui Li, Shi, *et al.*, 2009; Zou *et al.*, 2013). Lithium losses due to hydroxide precipitation is not a concern, because Li does not react with the hydroxide ion (Wang, Lin and Wu, 2009).

$$CoCl_2 + 2NaOH \rightarrow Co(OH)_2 + 2NaCl \quad [62]$$

$$NiCl_2 + 2NaOH \rightarrow Ni(OH)_2 + 2NaCl \quad [63]$$

At a pH of 4.5, all iron in the Fe^{3+} oxidation state will be separated from solution according to equation 57 (Jinhui Li, Shi, *et al.*, 2009; Zou *et al.*, 2013). Iron in the Fe^{2+} oxidation state will only start precipitating at a pH of 5.84 (Zou *et al.*, 2013). It was assumed that iron in the Fe^{2+} oxidation state, will be oxidized to Fe^{3+} by $KMnO_4$ according to equation 64 below (Puncochar, no date). The standard half-cell potentials (E_0) for the oxidation of Fe^{2+} to Fe^{3+} and the reduction of MnO_4^- to Mn^{2+} are 0.77 V and 1.49 V respectively (HyperPhysics, 2016). From the standard half-cell potentials a positive standard cell potential will be obtained ($E_{cell} = E_{reduction} - E_{oxidation}$), indicating a spontaneous reaction. Refer to equation 57 for the precipitation reaction of $FeCl_3$ with NaOH.

$$3FeCl_2 + KMnO_4 + 2H_2O \rightarrow Fe(OH)_3 + 2FeCl_3 + MnO_2 + KOH \quad [64]$$

According to the work done by Zou *et al.* in 2013, all aluminum will be separated from solution at a pH of 4.49. This was confirmed by the results obtained from Visual Minteq chemical speciation software. The amount of copper removed from the leach solution was assumed as 5% based on the experimental results obtained by Jinhui Li, Shi, *et al.* (2009). The reaction equations for the removal of Al and Cu is shown in equations 65 and 66 below.

$$AlCl_3 + 3NaOH \rightarrow Al(OH)_3 + 3NaCl \quad [65]$$

$$CuCl_2 + 2NaOH \rightarrow Cu(OH)_2 + 2NaCl \quad [66]$$

3.5.1.5 Nickel recovery

a) Ammonia addition

An ammonia solution (28 wt% NH_3) will be fed to an agitated tank prior to nickel precipitation to transform the Ni^{2+} in the leach solution to a $[Ni(NH_3)_6]^{2+}$ complex that can react with dimethylglyoxime ($C_4H_8N_2O_2$) to form a red solid complex (Wang, Lin and Wu, 2009). With the addition of ammonia, cobalt in solution is also transformed to a $[Co(NH_3)_6]^{2+}$ complex. It was assumed that 99.5% of both Ni and Co in solution will react to form their respective ammonia complexes according to equations 67 and 68.

$$NiCl_2 + 6NH_3 \rightarrow [Ni(NH_3)_6]Cl_2 \quad [67]$$

$$CoCl_2 + 6NH_3 \rightarrow [Co(NH_3)_6]Cl_2 \quad [68]$$

Ammonia is a weak base that does not fully dissociate in aqueous solutions to produce ammonium and hydroxide ions (equation 69). The base ionization constant of ammonia is expressed in equation 70 (Chemistry LibreTexts, no date) below and gives a quantitative indication of the extent of ammonia dissolution in water.

$$NH_{3\,(aq)} + H_2O_{(l)} \leftrightarrow NH_4^+{}_{(aq)} + OH^-_{(aq)} \quad [69]$$

$$K_b = \frac{[NH_4^+][OH^-]}{[NH_3]} = 1.8 \times 10^{-5} \quad at\ 25℃ \quad [70]$$

The amount of ammonia solution fed to the tank should be adjusted to ensure operation at pH 9, as this is the optimum operating conditions for the formation of the $[Ni(NH_3)_6]^{2+}$ complex (Wang, Lin and Wu, 2009). The following assumptions were made with regards to reactions with ammonium hydroxide:

1. The hydroxide ions in solution will neutralise acidic compounds such as HCl and H_3PO_4 (refer to equations 52 and 71).
2. According to Visual Minteq speciation software, approximately 50% of NaCl and KCl in the feed stream will react with NH_4OH as shown in equations 72 and 73.
3. The copper remaining in solution will be removed as a hydroxide precipitate (equation 74) at pH 9 (Zou *et al.*, 2013).

$$3NH_4OH + H_3PO_4 \rightarrow (NH_4)_3PO_4 + 3H_2O \quad [71]$$

$$NH_4OH + NaCl \rightarrow NaOH + NH_4Cl \quad [72]$$

$$NH_4OH + KCl \rightarrow KOH + NH_4Cl \quad [73]$$

$$2NH_4OH + CuCl_2 \rightarrow Cu(OH)_2 + 2NH_4Cl \quad [74]$$

Based on the product purities achieved in the study done by Wang, Lin and Wu (2009), it was assumed that none of the $KMnO_4$ will react with NH_4OH to form MnO_2 precipitates. The assumption is reasonable

as no manganese was present in the nickel powder (97.43% pure) produced in their study (Wang, Lin and Wu, 2009).

b) Ni-DMG precipitation

The leach solution, rich in the $[Ni(NH_3)_6]^{2+}$ complex, is transferred to an agitated tank that facilitates the formation of a red solid nickel complex. Dimethylglyoxime (DMG) was selected as precipitation reagent for the selective recovery of Ni (reaction 75). The tank will be operated at a pH of 9 and the molar ratio of DMG to $[Ni(NH_3)_6]^{2+}$ will be 2. These conditions were recommended as the optimum operating conditions for Ni-DMG precipitation by Wang, Lin and Wu (2009) and corresponds well with conditions reported by other sources (refer to Table 13 in section 2.3.2.4). The extraction of $[Ni(NH_3)_6]^{2+}$ was assumed as 99.5% (Wang, Lin and Wu, 2009).

$$[Ni(NH_3)_6]Cl_2 + 2C_4H_8N_2O_2 \rightarrow Ni(NH_3)_6(C_4H_7N_2O_2)_2 + 2HCl \quad [75]$$

c) DMG regeneration

The solid Ni-DMG complex is removed from the solution with a filter press and dissolved in hydrochloric acid to regenerate the DMG (white powder) and transfer the nickel ions back to the leach solution. The dissolution of the Ni-DMG complex in hydrochloric acid can be represented by equation 76 below. The tank will be operated at 25 °C with an HCl concentration of 1 mol/L and solid-to-liquid ratio (S/L) of 10 ml/g (Chen, Chen, *et al.*, 2015). It was assumed that 99.5% of the Ni-DMG complex will be dissolved.

$$Ni(NH_3)_6(C_4H_7N_2O_2)_2 + 2HCl \rightarrow [Ni(NH_3)_6]Cl_2 + 2C_4H_8N_2O_2 \quad [76]$$

The hydrochloric acid fed to the tank will be a fraction of the 33 wt% solution produced in the HCl falling film absorber. Additional water requirements will be met by recycling water from the evaporator prior to the membrane cells. Small amounts of other compounds will also react with HCl. Equations 52, 53 and 77 to 79 listed below were considered in the mass balance calculations:

$$KOH + HCl \rightarrow KCl + H_2O \quad [77]$$

$$Na_3PO_4 + 3HCl \rightarrow H_3PO_4 + 3NaCl \quad [78]$$

$$2HCl + Cu(OH)_2 \rightarrow CuCl_2 + 2H_2O \quad [79]$$

The DMG recovered after HCl dissolution is removed from solution with a filter press and recycled to the Ni-DMG precipitation tank to reduce the amount of fresh DMG required. A small fraction (5%) of the DMG recycle stream is purged to allow the introduction of fresh DMG to the system to enhance precipitation performance in the Ni-DMG precipitation tank.

d) Nickel hydroxide precipitation

The nickel in solution is finally recovered as a $Ni(OH)_2$ precipitates at pH 11 according to equation 80. 32 wt% NaOH produced in the membrane cells is fed to the agitated tank to ensure operation at a pH 11 (Wang, Lin and Wu, 2009).

$$Ni(NH_3)_6Cl_2 + 2NaOH + 6H_2O \rightarrow Ni(OH)_2 + 6(NH_3.H_2O) + 2NaCl \quad [80]$$

Other compounds will also react with NaOH. HCl and H_3PO_4 will be neutralized according to equations 53 and 54 (refer to section 3.5.1.3). Equations 81 to 84 listed below were also considered in the mass balance calculations.

$$Co(NH_3)_6Cl_2 + 2NaOH + 6H_2O \rightarrow Co(OH)_2 + 6(NH_3.H_2O) + 2NaCl \quad [81]$$

$$NH_4Cl + NaOH \rightarrow NH_4OH + NaCl \quad [82]$$

$$KCl + NaOH \rightarrow KOH + NaCl \quad [83]$$

$$CuCl_2 + 2NaOH \rightarrow Cu(OH)_2 + 2NaCl \quad [84]$$

The nickel hydroxide precipitate will be recovered with a filter press and dried before it is stored as saleable product. The remaining leach solution is fed to the mixing tank prior to the membrane electrolysis plant section.

3.5.1.6 Cobalt recovery

a) pH adjustment with hydrochloric acid

The Ni-DMG precipitates are recovered from solution with a filter press as discussed in the previous section. Thus, cobalt (present in the $[Co(NH_3)_6]^{2+}$ complex) is left in the leach solution. Cobalt will be recovered as a metal hydroxide precipitate with the addition of NaOH. However, the $[Co(NH_3)_6]^{2+}$ complex is a stable complex which influences hydroxide precipitation by causing partial dissolution of the hydroxide formed. To prevent hydroxide dissolution, hydrochloric acid is added to the system until a pH of 0 is reached (Wang, Lin and Wu, 2009). Refer to equations 52, 53, 77 and 78 for the neutralisation reactions of ammonium hydroxide, sodium hydroxide, potassium hydroxide and sodium phosphate. Other reactions that were considered in the pH adjustment step are listed below:

$$[Co(NH_3)_6]Cl_2 + 6HCl \rightarrow CoCl_2 + 6NH_4Cl \quad [85]$$

$$[Ni(NH_3)_6]Cl_2 + 6HCl \rightarrow NiCl_2 + 6NH_4Cl \quad [86]$$

The hydrochloric acid fed to the tank will be a 33 wt% solution of which a large fraction will be produced in the HCl production units. The remaining HCl requirements will be met by feeding fresh 33 wt% solution.

b) Cobalt hydroxide precipitation

Finally, the cobalt in solution can be recovered as a $Co(OH)_2$ precipitate at pH 11 (Wang, Lin and Wu, 2009). 32 wt% NaOH solution produced during membrane electrolysis will be fed to the agitated tank. The cobalt and small amount of nickel remaining in solution will react according to equations 87 and 88. Refer to equations 53, 54, 82, 83 and 84 for the reactions of NaOH with HCl, H_3PO_4, NH_4Cl, KCl and $CuCl_2$ respectively.

$$CoCl_2 + 2NaOH \rightarrow Co(OH)_2 + 2NaCl \quad [87]$$

$$NiCl_2 + 2NaOH \rightarrow Ni(OH)_2 + 2NaCl \quad [88]$$

The cobalt hydroxide precipitates will be recovered with a filter press and dried before it is stored as a saleable product. The remaining leach solution is fed to the mixing tank prior to the membrane electrolysis plant section.

3.5.1.7 Membrane electrolysis

Various process and recycle streams are combined in a mixing tank prior to membrane electrolysis. The membrane cells were included in the process to reduce the large amounts of NaCl in the process streams by facilitating the production of NaOH solution (and HCl in the HCl synthesis units) that could be recycled to various other units. Thus, the amount of fresh reagents required will be reduced.

The assumptions made with regards to the operation of the membrane cells are listed below.

1. The combined leach solution with a high NaCl concentration is fed to a forced circulation evaporator to further concentrate the NaCl in solution. The boiling point of the solution is dependent on the NaCl concentration in the solution. The fraction of water evaporated was adjusted until the NaCl concentration in the anolyte entering the membrane cells reached saturation at approximately 310 g/L NaCl (Bommaraju *et al.*, 2000; Moroz, 2016).
2. The feed to the evaporator will be pre-heated with the evaporated water produced in the NaCl crystallizer to reduce the amount of high-pressure steam (254℃, 41 barg) that will be required to facilitate the desired degree of evaporation.
3. To prevent unnecessary energy losses to the environment, the evaporated water will not be stored in an intermediate storage tank. It will be recycled directly to the leaching tank, Ni-DMG dissolution tank, lithium precipitation tank and membrane cells to reduce the heating and process water requirements at the respective units. The remaining water will leave the process as waste water.
4. The boiling point of ammonium hydroxide is 35.05℃. Thus, it was assumed that a fraction of the ammonium hydroxide entering the evaporator will evaporate with the water. The evaporated water contains 1.8 wt% ammonium hydroxide.
5. The anolyte entering the membrane cells should have a pH of between 1 and 4.5 (Paidar, Fateev and Bouzek, 2016). An anolyte pH of 3 was selected (Du *et al.*, 2018) because a pH of greater than 2 is suggested as optimum operating pH for Nafion membranes which are typically used in membrane electrolysis applications (Nafion Ion Exchange Materials, 2016).
6. The pH of the concentrated solution is adjusted with fresh 33 wt% HCl solution until the pH reaches a value of 3. Refer to equations 52 and 77 for the reactions of HCl with NH_4OH and KOH respectively. Other reactions that were considered are listed below:

$$Li_2CO_3 + 2HCl \rightarrow CO_2 + 2LiCl + H_2O \quad [89]$$

$$Na_2CO_3 + 2HCl \rightarrow CO_2 + 2NaCl + H_2O \quad [90]$$

7. The operating conditions for the membrane cells are summarized in Table 36. The membrane cell will operate at a cell voltage of 3.2 V (Du *et al.*, 2018).
8. The overall cell reaction considered in the mass balance is shown in equation 91 below. A side reaction, producing oxygen at the anode, is shown in equation 92. The hydrogen and chlorine gas

produced at the electrodes typically have a purity of greater than 99% (Paidar, Fateev and Bouzek, 2016). Thus, the fraction of water that reacted according to the side reaction (equation 92) was varied to give a chlorine gas purity of greater than 99%.

$$2H_2O + 2NaCl \rightarrow 2NaOH + H_{2(g)} + Cl_{2(g)} \quad [91]$$

$$2H_2O \rightarrow O_{2(g)} + 2H_{2(g)} \quad [92]$$

9. The NaCl depleted anolyte leaving the membrane cells typically have a NaCl concentration of 220-230 g/L (Abam Engineers Inc., 1980; Moroz, 2016). Thus, the percentage of NaCl that reacted (equation 91) was varied to ensure that the NaCl concentration in the outlet was approximately 230 g/L. To achieve the desired NaCl outlet concentration, 51% of the NaCl in the anolyte feed stream should be converted to NaOH according to equation 91.
10. To simplify the cell dynamics, it was assumed that the membranes will only allow sodium ions (Na^+) and water molecules to move from the anode chamber to the cathode chamber. If other cations pass through the membrane, it would be recirculated to the rest of the process as part of the 32 wt% NaOH produced in the cathodic chamber. Therefore, these compounds will not be lost but may lead to a larger component hold-up in the system.

Table 36: Membrane Cell Operating Conditions

Anolyte Compartment		**References**
Temperature	88 °C	(Nafion Ion Exchange Materials, 2016; Paidar, Fateev and Bouzek, 2016; Du *et al.*, 2018)
Anolyte Pressure	1.09 bar	(Du *et al.*, 2018)
Anolyte pH	3	(Nafion Ion Exchange Materials, 2016; Paidar, Fateev and Bouzek, 2016; Du *et al.*, 2018)
Inlet Concentration	305-310 g/L NaCl	(Abam Engineers Inc., 1980; Bommaraju *et al.*, 2000; Moroz, 2016)
Outlet Concentration	220-230 g/L NaCl	(Abam Engineers Inc., 1980; Moroz, 2016)
Anode Current Efficiency	96%	(Du *et al.*, 2018)
Catholyte Compartment		**References**
Temperature	88 °C	(Nafion Ion Exchange Materials, 2016; Paidar, Fateev and Bouzek, 2016; Du *et al.*, 2018)
Catholyte Pressure	1.05 bar	(Du *et al.*, 2018)
Catholyte pH	14	(Paidar, Fateev and Bouzek, 2016)
Inlet Concentration	30 wt% NaOH	(Du *et al.*, 2018)
Outlet Concentration	32 wt% NaOH	(Du *et al.*, 2018)
Cathode Current Efficiency	94%	(Du *et al.*, 2018)

11. To optimize the production of NaOH in the membrane cell, a fraction of the NaCl depleted solution leaving the anodic compartment is recycled back to the mixing tank prior to the membrane cells. A recycle fraction of 70% was selected to ensure that the anolyte is saturated in NaCl (305-310 g/L NaCl).
12. The 32 wt% NaOH solution produced in the membrane cells will be stored in an intermediate storage tank before it is distributed to the pH adjustment tank (pH=2) after HCl leaching, impurity removal

tank (pH=4.5), nickel precipitation tank (pH=11) and the cobalt precipitation tank (pH=11). A fraction of the 32 wt% NaOH product solution will be diluted with recycled water to produce the 30 wt% NaOH solution that is fed as catholyte to the membrane cells. The remaining product solution will be used to increase the pH of the NaCl depleted solution prior to lithium precipitation.

3.5.1.8 Hydrochloric acid production

Chlorine and hydrogen gas produced at the anodes and cathodes of the membrane cells will be used to produce a 33 wt% hydrochloric acid solution. Both gases are cooled with cooling water and fed to their respective hydrogen and chlorine gas demisters before entering the HCl gas synthesis unit (Moroz, 2016). The hydrochloric acid production system consists of a combustion furnace and a falling film absorber with a tail gas scrubber. The following assumptions were made with regards to these units:

1. The combustion furnace will facilitate the highly exothermic reaction between hydrogen gas (fuel) and chlorine gas (oxidant) according to equation 93 (Joseph, Koshy and Kallanickal, 2013).

$$Cl_{2(g)} + H_{2(g)} \rightarrow 2HCl_{(g)} + 1667\ kJ/mole \qquad [\ 93\ ]$$

2. To reduce the amount of free chlorine in the product acid (<10 w/w ppm Cl_2), the combustion chamber will operate with a hydrogen gas excess of 10 vol% (Joseph, Koshy and Kallanickal, 2013). Under these conditions, all of the chlorine will be combusted to produce HCl gas (Moroz, 2016). Additional fresh hydrogen gas will be fed to the combustion furnace to ensure operation with the desired excess of hydrogen gas. The feed to the falling film absorber typically contains 95% HCl gas and 5% hydrogen gas with inerts (O_2 produced in side reaction at the anode) (Moroz, 2016).
3. Fresh water at a temperature below 30 ℃ will be used as absorption water in the falling film absorber (Carbone Lorraine, no date). It was assumed that all of the HCl gas will be absorbed into the absorption water to produce a 33 wt% hydrochloric acid solution at 40 ℃ (Carbone Lorraine, no date).
4. The weak gas entering the tail gas scrubber typically contains 80-90% hydrogen gas with inerts (Moroz, 2016). A fraction of the excess hydrogen will also be absorbed into the water (Joseph, Koshy and Kallanickal, 2013). It was assumed that 20% of the unreacted hydrogen gas will be absorbed into the water.
5. The 33 wt% HCl acid produced will be stored in an intermediate storage tank before distribution to the HCl leaching, Ni-DMG dissolution and pH adjustment tanks (prior to cobalt precipitation and the membrane cells). Fresh 33 wt% HCl solution will be fed to the pH adjustment unit prior to the membrane cells to meet the remaining HCl requirements.
6. Both the combustion reaction and the absorption of HCl gas into water are exothermic (Joseph, Koshy and Kallanickal, 2013). A fraction of the energy will be removed by producing 650 kg of medium pressure steam (184 ℃, 10 barg) per ton of HCl produced (SGL Group, 2016). The 10 barg steam produced will be utilised to provide the heating required for the sodium carbonate make-up tank. Based on the HCl synthesis system (incorporating steam generation) designed by the SGL Group (2016), the remaining energy will be removed by circulating 84 m^3/h cooling water through

the system per ton of HCl produced. The cooling water fed will enter the unit at a temperature below 30 ℃ (Carbone Lorraine, no date).

3.5.1.9 Lithium recovery

a) pH Adjustment

The NaCl depleted anolyte leaving the membrane cells is acidic due to the pH adjustment with HCl in the anolyte feed stream. 32 wt% NaOH solution will be used to increase the pH to 13.5. The membrane cells do not produce enough 32 wt% NaOH to meet the entire NaOH requirement, thus additional fresh NaOH will be fed. A pH level of 13.5 was selected to ensure that the pH in the lithium precipitation tank will be approximately 12 (Sattar *et al.*, 2019). Refer to equations 53, 82 and 83 for the reactions of HCl, NH_4Cl and KCl with NaOH.

During the pH adjustment step, large amounts of NaCl form through the neutralization of HCl with NaOH. For this reason, the pH should be adjusted prior to evaporation and NaCl crystallization. The water fed to the system as part of the NaOH solution can be evaporated after pH adjustment to maximize the removal of NaCl and NH_4Cl from the system during crystallization. This will minimize lithium product contamination with NaCl and NH_4Cl.

b) NaCl Crystallization

To reduce NaCl, NH_4Cl and $KMnO_4$ contamination in the lithium product, water (and ammonium hydroxide in solution) will be evaporated in a forced circulation evaporator to facilitate crystallization of these compounds. The boiling point of the solution is dependent on the salt concentration of the solution. The feed to the crystallizer will be pre-heated with a fraction of the evaporated water produced in the evaporator prior to the membrane cells to reduce the amount of high-pressure steam (254℃, 41 barg) that will be required for evaporation in the crystallizer.

The solubility limits that dictate the formation of crystals were assumed as 39.7 g NaCl/ 100 g water (Mullin, 2001), 75.8 g NH_4Cl/ 100 g water (Mullin, 2001) and 25 g $KMnO_4$ /100 g water (Lide, 2005) at 100℃. The crystals will be removed from the remaining solution with a filter press. 20% of the crystals will be purged and the remaining fraction will be recycled to the mixing tank to increase the NaCl concentration in the anolyte fed to the membrane cells.

c) Lithium carbonate precipitation

After the removal of the NaCl, NH_4Cl and $KMnO_4$ crystals with a filter press, lithium can be recovered from the remaining purified solution. A saturated solution of sodium carbonate at 100 ℃ is fed to an agitated tank heated to 100 ℃ to recover lithium carbonate according to equation 94 (Wang, Lin and Wu, 2009). The molar ratio of lithium in the feed solution to sodium carbonate fed is 1.2:1 (Li^+:Na_2CO_3=1.2:1) (Sattar *et al.*, 2019).

$$2LiCl + Na_2CO_3 \rightarrow Li_2CO_3 + 2NaCl \qquad [\,94\,]$$

Theoretically lithium should be recovered completely but the experimental results reported in previous studies indicated that only 80% of lithium is recovered as Li_2CO_3 (Zhang *et al.*, 1998; Wang, Lin and Wu, 2009; Chen, Chen, *et al.*, 2015; Sattar *et al.*, 2019). Thus, it was assumed that approximately 80% of lithium in solution is recovered as Li_2CO_3 precipitates.

The amount of water required to make-up a saturated sodium carbonate solution was calculated by using the solubility limit of sodium carbonate at 100 ℃ as 45.5 g/100 g water (Wang, Lin and Wu, 2009). The water required to make up the saturated sodium carbonate solution will be recycled from the forced circulation evaporator prior to the membrane cell to minimize the steam heating requirements for the make-up tank. The additional heat required in the make-up tank will be supplied by the medium pressure steam (184℃, 10 barg) produced in the HCl synthesis unit. Additional heat required in the precipitation tank will be supplied by high pressure steam (254℃, 41 barg).

The amount of Li_2CO_3 precipitate recovered from solution were determined by the solubility limit of 0.71 g/100 g water at 100 ℃ (Wang, Lin and Wu, 2009). The major impurity in the lithium product is NaCl (due to reaction 95) with a solubility of 39.7 g/100 g water at 100℃. According to Visual Minteq speciation software, the KCl in the feed stream will react (equation 96 was considered).

$$2NH_4Cl + Na_2CO_3 \rightarrow 2NH_3 + CO_2 + 2NaCl + H_2O \quad [95]$$

$$KCl + NH_4OH \rightarrow NH_4Cl + KOH \quad [96]$$

The lithium carbonate product will be recovered from solution with a filter press and dried. 20% of the final leach solution will be purged. The remaining fraction will be recycled to the mixing tank prior to membrane electrolysis to maximize the recovery of lithium.

3.5.2 Mineral acid process option 2

The second mineral acid process is essentially the same as process option 1, except for the exclusion of the membrane cells and hydrochloric acid production units. Thus, fresh NaOH and HCl will be fed to all process units as required. Refer to Appendix A for the process flow diagram and stream table of mineral acid process option 2.

All mass balance assumptions stated for process option 1 (discussed in section 3.5.1) are valid for process option 2 unless stated otherwise. The following differences should be noted:

1. Fresh 33 wt% HCl solution will be pumped from a storage tank to the HCl leaching tank, Ni-DMG dissolution tank and to the pH adjustment tanks.
2. 50 wt% NaOH solution will be pumped from a make-up tank to the pH adjustment (pH=2), impurity removal, Ni precipitation and Co precipitation tanks respectively. Fresh NaOH crystals (>99% purity) will be dissolved in the water recycled from the forced circulation crystallizer. The evaporated water will be used for heating before being pumped to the NaOH make-up tank.
3. Evaporated water from the crystallizer will be used to pre-heat the 33 wt% HCl solution fed to the leaching tank and the feed stream to the Mn precipitation tank. A fraction of the high temperature

evaporated water will be fed to the leaching tank. Additional heating required to ensure leaching operation at 80℃ or Mn precipitation at 40℃ will be provided by high-pressure steam.

4. The remaining fraction of high temperature evaporated water will be used to pre-heat the feed stream to the NaCl crystallizer to minimize the high-pressure steam required to facilitate evaporation.
5. A fraction of the water and ammonium hydroxide in the feed stream to the crystallizer will be removed during evaporation. The evaporated water contains approximately 4.1 wt% ammonium hydroxide. The crystals (NaCl and NH_4Cl) formed in the crystallizer will not be recycled as in process option 1.
6. High pressure steam will be utilised to ensure that the sodium carbonate solution make-up tank and the Li precipitation tank operate at 100℃.
7. To prevent low Li_2CO_3 product purities, a small amount of dilution water is fed to the lithium precipitation tank to ensure that the minimal amount of NaCl precipitate out. Dilution water is fed so that the maximum amount of water can be evaporated to recover the largest amount of NaCl crystals without losing LiCl due to crystallization.

3.5.3 Mineral acid process option 3

Mineral acid process option 3 aims to produce only two products: a combined Mn, Ni and Co hydroxide product and a lithium carbonate product. These two products can be sold to battery manufacturers that combine the lithium and metal hydroxide products to manufacture the active cathode materials ($LiCo_{0.33}Ni_{0.33}Mn_{0.33}O_2$) used in LIBs through a high temperature solid-state reaction. According to the cost calculations done by Zou *et al.* (2013) the manufacturing cost of $LiCo_{0.33}Ni_{0.33}Mn_{0.33}O_2$ from virgin raw materials is 2.7 times greater per ton of cathode material than the manufacturing cost when recycled materials are used.

An advantage of this process option is that Co, Ni and Mn can be recycled and directly re-used in the battery manufacturing process without separating them from each other as done in options 1 and 2. This may reduce raw material, energy and labour requirements significantly. The proposed flowsheet is based on the process proposed by Zou *et al.* (2013.) Refer to Appendix A for the process flow diagram and stream table of mineral acid process option 3.

The following should be noted with regards to the mass and energy balances for process option 3:

1. A membrane cell and HCl synthesis unit are not present, thus fresh NaOH and HCl will be fed to all process units as required.
2. The assumptions made for the pre-treatment steps and HCl leaching of process option 1 apply to process option 3 as well. Evaporated water from the crystallizer will be used to pre-heat the 33 wt% HCl solution fed to the leaching tank. High pressure steam will be utilised to provide the heat necessary to operate the leaching tank at 80℃.
3. A 50 wt% NaOH solution will be pumped from a make-up tank to the impurity removal and metal hydroxide precipitation tanks respectively. Fresh NaOH crystals (>99% purity) will be dissolved in water recycled from the forced circulation crystallizer. The high temperature evaporated water will

be used to pre-heat the 33 wt% HCl solution and the crystallizer feed stream before being pumped to the NaOH make-up tank.

4. The impurity removal tank will facilitate the removal of all the Al (equation 65) and Fe in the Fe^{3+} oxidation state (equation 57). However, according to Visual Minteq speciation software, 10% of the manganese in the feed stream will be lost due to hydroxide precipitation (equation 56). The Co, Ni and Li losses are the same as assumed for process option 1.
5. Before precipitating the mixed hydroxide product, the molar concentration of Mn^{2+}: Co^{2+}: Ni^{2+} is adjusted to 1:1:1 by adding the required amounts of $MnCl_2$, $CoCl_2$ and $NiCl_2$ to an agitated tank with a residence time of 2 hours (Zou *et al.*, 2013).
6. After the metal ratio adjustment, 50 wt% NaOH solution will be used to increase the pH to 11. At a pH of 11, a mixture of $Co(OH)_2$, $Ni(OH)_2$ and $Mn(OH)_2$ could be fully co-precipitated (refer to equations 56, 62 and 63) (Zou *et al.*, 2013). The Fe, Al and Cu in solution will also be co-precipitated with the valuable metals as metal hydroxides (refer to equations 65 and 66). Fe in the Fe^{2+} oxidation state will be precipitated as $Fe(OH)_2$ according to equation 97 (Zou *et al.*, 2013).

$$FeCl_2 + 2NaOH \rightarrow Fe(OH)_2 + 2NaCl \qquad [97]$$

7. Mass balance assumptions with regards to the crystallizer and lithium precipitation in process option 1 and 2 are valid for option 3 as well.
8. High pressure steam will be utilised to facilitate evaporation in the NaCl crystallizer and to ensure that the sodium carbonate make-up tank and the Li precipitation tank operate at 100°C.

3.6 Organic acid process

The mass and energy balance assumptions made for the organic acid process options are discussed in the sections below. The pre-treatment steps and associated assumptions discussed in section 3.4 are valid for the organic acid process options as well.

3.6.1 Organic acid process option 1

The process proposed for the selective recovery of metals from the leach solution is based on the work done by Chen *et al.* (2016). Precipitation units with selective precipitants are used to recover the valuable metals from the citrate leach liquor. Refer to Appendix A for the process flow diagram and stream table of organic acid process option 1.

3.6.1.1 Citric acid leaching

Citric acid was selected as leaching reagent to selectively dissolve Co, Mn, Li, and Ni from the LIB electrode material. Hydrogen peroxide was chosen as reductant. The key assumptions made with regards to the leaching process are discussed below:

1. The process conditions selected, and metal extraction efficiencies achieved are based on the work done by Li, Bian, Zhang, Guan *et al.* (2018). Their study was done on a mixture of cathodic materials ($LiCoO_2$, $LiMn_2O_4$, $LiCo_{0.33}Ni_{0.33}Mn_{0.33}O_2$) and is therefore a suitable representation of the optimal

leaching conditions for the assumed LIB feed (refer to section 3.2). Refer to Table 37 for a summary of the operating conditions and leaching efficiencies. Average leaching efficiencies for $LiCoO_2$, $LiNiO_2$, $LiMn_2O_4$ and $LiCo_{0.33}Ni_{0.33}Mn_{0.33}O_2$ were calculated in a similar way as done for the HCl leaching process (refer to section 3.5.1.1).

Table 37: Citric acid leaching conditions and leaching efficiencies (Li, Bian, Zhang, Guan, *et al.*, 2018)

Process Conditions	Citric Acid Concentration	0.5 mol/L
	H_2O_2 Concentration	1.5 vol%
	S/L	20 g/L
	Temp	90 ℃
	Time	1 hour
Metal Extraction (%)	Co	99.80
	Li	99.10
	Ni	98.70
	Mn	95.20

2. The following leaching reactions were considered in the mass balance calculations (Chen *et al.*, 2016; Musariri, 2019):

$$6LiCoO_2 + 6H_3Cit + 3H_2O_2 \rightarrow 2Li_3Cit + 2Co_3(Cit)_2 + 12H_2O + 3O_2 \quad [98]$$

$$6LiNiO_2 + 6H_3Cit + 3H_2O_2 \rightarrow 2Li_3Cit + 2Ni_3(Cit)_2 + 12H_2O + 3O_2 \quad [99]$$

$$6LiMn_2O_4 + 10H_3Cit + H_2O_2 \rightarrow 2Li_3Cit + 4Mn_3(Cit)_2 + 16H_2O + 5O_2 \quad [100]$$

$$6LiNi_{0.33}Co_{0.33}Mn_{0.33}O_2 + 6H_3Cit + H_2O_2$$
$$\rightarrow 2Li_3Cit + \frac{2}{3}Ni_3(Cit)_2 + \frac{2}{3}Co_3(Cit)_2 + \frac{2}{3}Mn_3(Cit)_2 + 10H_2O + 2O_2 \quad [101]$$

3. The experimental work done by Li *et al.* (2019) investigated the dissolution of $LiFePO_4$ cathode material in a citric acid leaching media. The leaching reaction when hydrogen peroxide was added to the system is shown in equation 102 below (Li *et al.*, 2019). With the addition of hydrogen peroxide, only 3.86% Fe was dissolved at the optimal conditions although 99.35% of Li was leached. Thus, it was assumed that 3.86% of $LiFePO_4$ will react to produce Fe^{2+} ions in solution (equation 103) (Li *et al.*, 2019). To ensure 99.35% Li dissolution, it was assumed that 95.49% of $LiFePO_4$ reacted according to equation 102 to produce Li^+ ions in solution and $FePO_4$ precipitates that could be removed with a filter press after leaching.

$$2H_3Cit + 6LiFePO_4 + 3H_2O_2 \rightarrow 2Li_3Cit + 6FePO_4 + 6H_2O \quad [102]$$

$$3H_3Cit + 3LiFePO_4 \rightarrow Li_3Cit + Fe_3(Cit)_2 + 3H_3PO_4 \quad [103]$$

4. Cobalt, nickel and lithium present in the anode material will react according to equations 104 to 106 listed below.

$$3Co + 2H_3Cit + 3H_2O_2 \rightarrow Co_3(Cit)_2 + 6H_2O \quad [104]$$

$$3Ni + 2H_3Cit + 3H_2O_2 \rightarrow Ni_3(Cit)_2 + 6H_2O \quad [105]$$

$$3Li + H_3Cit + 2H_2O_2 \rightarrow Li_3Cit + \frac{7}{2}H_2O + \frac{1}{4}O_2 \quad [106]$$

5. The graphite in the anode material will not leach and thus it will be discarded as part of the leach residue. The aluminium, copper and iron impurities in the electrode material will react according to equations 107 to 109 listed below. The leaching efficiencies assumed for the impurity ions was 8.05% for aluminium (Gao, Liu, *et al.*, 2018), 3.86% for iron (Li *et al.*, 2019) and 95% for copper (Habbache *et al.*, 2009; Musariri, 2019).

$$Al + H_3Cit + 2H_2O_2 \rightarrow AlCit + \frac{7}{2}H_2O + \frac{1}{4}O_2 \quad [107]$$

$$3Cu + 2H_3Cit + 3H_2O_2 \rightarrow Cu_3(Cit)_2 + 6H_2O \quad [108]$$

$$3Fe + 2H_3Cit + 3H_2O_2 \rightarrow Fe_3(Cit)_2 + 6H_2O \quad [109]$$

6. Fresh 50 wt% H_2O_2 solution will be fed to the leaching tank. Excess hydrogen peroxide will decompose to produce water and oxygen according to equation 110 shown below.

$$2H_2O_2 \rightarrow 2H_2O + O_2 \quad [110]$$

7. The assumptions with regards to solid-liquid separation and filter press operation are discussed in section 3.5.1.2. Citric acid provides high leaching selectivity as limited amounts of Fe, Cu and Al are leached. Thus, the leach residue will not be recycled to prevent the undissolved impurities (Fe, Cu and Al) from re-entering the system and increasing the impurity concentrations throughout the process.
8. A fraction of the high temperature water evaporated prior to lithium precipitation will be recycled to the leaching tank. Recycling the heated water will significantly decrease the steam required to ensure that the leaching tank is maintained at 90℃. High pressure steam at 41 barg will be used to supply the residual heat required.

3.6.1.2 Manganese recovery

Chen *et al.* (2016) suggested selective manganese precipitation with potassium permanganate at a pH 2. After leaching (pH of $\pm$ 1.7) the pH was adjusted to pH 2 with the addition of 50 wt% NaOH solution. Citric acid and phosphoric acid (generated in reaction 103) present in the system will be neutralised according to equations 111 and 112 (Li *et al.*, 2019). It was assumed that all the phosphoric acid present in the system will be neutralised. The pH of the leach solution was calculated based on a correlation generated from data obtained from the Sensorex online pH calculator (Sensorex, no date).

$$H_3Cit + 3NaOH \rightarrow Na_3Cit + 3H_2O \quad [111]$$

$$H_3PO_4 + 3NaOH \rightarrow Na_3PO_4 + 3H_2O \quad [112]$$

After pH adjustment with NaOH, a 0.5 M $KMnO_4$ solution will be fed to the agitated tank facilitating the precipitation of MnO_2. The process conditions used are the same as the optimized conditions suggested by Wang *et al.* (2009). Refer to Table 35 in section 3.5.1.3 for these conditions. Manganese in solution (Mn_3Cit_2) will react according to equation 113. A fraction of the citric acid in solution will be oxidized by $KMnO_4$ to produce water and carbon dioxide according to equation 114 (ChemicalAid, no date). The

oxidation reaction will be limited by the excess amount of $KMnO_4$ present in the system. Manganese oxide precipitates are removed from the leach solution with a filter press.

$$Mn_3Cit_2 + 2KMnO_4 + 2H_2O \rightarrow 5MnO_2 + 2KH_2Cit \quad [113]$$

$$H_3Cit + 6KMnO_4 \rightarrow 6MnO_2 + 6CO_2 + 4H_2O + 3K_2O \quad [114]$$

3.6.1.3 Nickel recovery by selective precipitation

Various literature sources suggest selective nickel precipitation with dimethylglyoxime (DMG). The work done by Chen *et al.* (2015) reported that the optimum pH for Ni-DMG precipitation is 6. Thus, the solution pH was adjusted to 6 with 50 wt% NaOH solution prior to DMG addition. Citric acid and phosphoric acid are neutralised according to equations 111 and 112. The reactions between NaOH and K_2O, $KMnO_4$ and KH_2Cit are shown in equations 115 to 117 respectively. It was assumed that all phosphoric acid, K_2O and KH_2Cit will react. Based on the high purity nickel product (99.3% purity) reported by Chen *et al.* (2016), it was assumed that only a small fraction of $KMnO_4$ will react to produce MnO_2 precipitates.

$$K_2O + 2NaOH \rightarrow 2KOH + Na_2O \quad [115]$$

$$4KMnO_4 + 4NaOH \rightarrow 2Na_2O + 4MnO_2 + 4KOH + 3O_2 \quad [116]$$

$$KH_2Cit + 2NaOH \rightarrow KNa_2Cit + 2H_2O \quad [117]$$

With the addition of a 0.2M DMG solution, red Ni-DMG precipitates will form according to equation 118 (Chen *et al.*, 2016). A small fraction of cobalt (0.1%) will undergo a similar reaction to form a Co-DMG complex according to equation 119. An excess amount of 50 wt% NaOH solution will be fed to the pH adjustment tank to ensure that the citric acid produced (in reactions 118 and 119) and the recycled HCl can be neutralized to maintain an equilibrium pH of 6. At a molar feed ratio of DMG: Ni^{2+} of 2, 98.5% of nickel can be precipitated at room temperature (Chen *et al.*, 2016).

$$6C_4H_8N_2O_2 + Ni_3(Cit)_2 \rightarrow 3Ni(C_4H_7N_2O_2)_2 + 2H_3Cit \quad [118]$$

$$6C_4H_8N_2O_2 + Co_3(Cit)_2 \rightarrow 3Co(C_4H_7N_2O_2)_2 + 2H_3Cit \quad [119]$$

The red Ni-DMG complex is recovered from the leach solution with a filter press. The red precipitate will be dissolved in a 1 M HCl medium to produce a nickel rich solution and a white powder (DMG) according to equations 120 and 121. Fresh water and 33 wt% HCl solution will be fed continuously to the agitated tank to facilitate the dissolution reaction. A fraction of the white DMG powder is purged (5%) and the rest is recycled to reduce the amount of fresh DMG fed to the system.

$$Ni(C_4H_7N_2O_2)_2 + 2HCl \rightarrow 2C_4H_8N_2O_2 + NiCl_2 \quad [120]$$

$$Co(C_4H_7N_2O_2)_2 + 2HCl \rightarrow 2C_4H_8N_2O_2 + CoCl_2 \quad [121]$$

It was assumed that all MnO_2, Na_2O, K_2O and Na_3PO_4 will react with HCl according to equations 122 to 125. KOH and NaOH present in solution will be neutralized.

$$MnO_2 + 4HCl \rightarrow MnCl_2 + 2H_2O + Cl_2 \quad [122]$$

$$Na_2O + 2HCl \rightarrow 2NaCl + H_2O \quad [123]$$

$$K_2O + 2HCl \rightarrow 2KCl + H_2O \quad [124]$$

$$Na_3PO_4 + 3HCl \rightarrow H_3PO_4 + 3NaCl \quad [125]$$

Nickel hydroxide will be precipitated from the nickel rich solution with the addition of 50 wt% NaOH solution at pH 11 (equation 126). Cobalt and manganese present in solution will form hydroxide precipitates according to equations 127 and 128. Citric acid, phosphoric acid and hydrochloric acid will be neutralized by NaOH. The leach solution obtained after hydroxide precipitation and solid-liquid separation will be recycled to the oxalic acid make-up tank to reduce the fresh water requirements to the process.

$$NiCl_2 + 2NaOH \rightarrow Ni(OH)_2 + 2NaCl \quad [126]$$

$$CoCl_2 + 2NaOH \rightarrow Co(OH)_2 + 2NaCl \quad [127]$$

$$MnCl_2 + 2NaOH \rightarrow Mn(OH)_2 + 2NaCl \quad [128]$$

3.6.1.4 Cobalt recovery

Chen *et al.* (2016) proposed the selective precipitation of cobalt with the addition of a 0.5 M oxalic acid solution. At a molar feed ratio of $C_2O_4^{2-}$: Co^{2+} of 1.2, 97% of cobalt can be precipitated at room temperature according to equation 129 (Chen *et al.*, 2016). It was assumed that the NaOH remaining in solution will react with citric acid (equation 111) and oxalic acid (equation 130).

$$Co_3(Cit)_2 + 3H_2C_2O_4 \rightarrow 3CoC_2O_4 + 2H_3Cit \quad [129]$$

$$H_2C_2O_4 + 2NaOH \rightarrow Na_2C_2O_4 + 2H_2O \quad [130]$$

Based on the cobalt product purities of 98.9% and 96.47% reported by Chen *et al.* (2016) and Chen and Zhou (2014), it was assumed that that small amounts of the impurity ions present in solution will precipitate out according to equations 131 to 133.

$$2AlCit + 3H_2C_2O_4 \rightarrow Al_2(C_2O_4)_3 + 2H_3Cit \quad [131]$$

$$Cu_3(Cit)_2 + 3H_2C_2O_4 \rightarrow 3CuC_2O_4 + 2H_3Cit \quad [132]$$

$$Fe_3(Cit)_2 + 3H_2C_2O_4 \rightarrow 3FeC_2O_4 + 2H_3Cit \quad [133]$$

3.6.1.5 Lithium recovery

To increase the lithium concentration in solution, a fraction of water will be evaporated prior to lithium precipitation. The amount of water evaporated was varied to ensure that trisodium citrate (Na_3Cit) with a solubility limit of 42.5 g/100 g water at 25°C remain in solution (PubChem, 2017).

A fraction of the evaporated water will be fed to the leaching tank operating at 90°C. The remaining water will be used to pre-heat the feed to the evaporator with a shell-and-tube heat exchanger. After pre-heating the evaporator feed stream, the water will be pumped to the NaOH and $KMnO_4$ make-up tanks respectively to reduce the water requirements and waste water treatment costs of the facility.

Phosphoric acid (0.5 M solution) was used as precipitant to recover the lithium as a phosphate from the concentrated leach solution. At a molar feed ratio of Li_3PO_4: H_3PO_4 of 1, 92.7% of lithium can be precipitated at room temperature according to equation 134 (Chen *et al.*, 2016). The lithium phosphate in solution forms precipitates until it reaches its solubility limit of 0.039 g/100 g water. Based on the lithium product purities of 99.5% and 99.07% reported by Chen *et al.* (2016) and Chen and Zhou (2014), respectively, it was assumed that that negligible amounts of the other metals present in solution will precipitate out.

$$Li_3Cit + H_3PO_4 \rightarrow Li_3PO_4 + H_3Cit \quad [134]$$

Musariri (2019) concluded that lithium precipitation is highly temperature dependent and recommended lithium phosphate precipitation at 80℃. Thus, 80℃ was selected as precipitation temperature. The leach solution exiting the evaporator has a temperature of approximately 100℃. The additional heat required will be supplied by high pressure steam.

Chen *et al.* (2016) did not explicitly mention controlling the pH at a specific value during cobalt or lithium precipitation. pH control with a NaOH solution in the cobalt and lithium precipitation tanks was investigated to understand the effect thereof on the project profitability and to give a more conservative estimation of the viability of the process option (refer to section 5.7.2). The pH in the cobalt precipitation tank was controlled to 6 by neutralizing excess oxalic acid and the citric acid produced during cobalt oxalate precipitation (equation 129). The lithium precipitation tank pH was maintained at 13-14 by neutralizing excess phosphoric acid and the citric acid produced during the precipitation reaction (equation 134). The addition of NaOH solution to the system will increase the cost of raw materials and potentially the capital costs (larger tanks will be required).

3.6.2 Organic acid process option 2

The second organic acid process is based on the work done by Chen and Zhou (2014) and Chen *et al.* (2015). Refer to Appendix A for the process flow diagram and stream table of organic acid process option 2. Precipitation units with selective precipitants are used to recover nickel and cobalt before manganese is recovered with solvent extraction to produce a pure manganese solution. Lithium is recovered from the final leach solution by precipitation. Thus, the sequence of metal recovery and the manganese recovery mechanism (precipitation vs. solvent extraction) are the major differences between organic acid process options 1 and 2.

3.6.2.1 Nickel recovery

The citric acid leaching tank will operate under the conditions and assumptions discussed in section 3.6.1.1. After citric acid leaching, the pH is adjusted to 6 with a 50 wt% NaOH solution before nickel is recovered by DMG precipitation. Reactions 111 and 112 were considered for the neutralization of citric and phosphoric acid. Excess 50 wt% NaOH solution will be fed to the pH adjustment tank to ensure the neutralization of citric and hydrochloric acid present in the DMG recycle stream.

The Ni-DMG precipitation and DMG regeneration process will operate as discussed in section 3.6.1.3. However, all reactions involving $KMnO_4$ or products formed during the Mn precipitation step in option 1 can be ignored. Refer to equations 118 and 119 for the nickel precipitation and cobalt co-precipitation reactions. At this stage in the process, manganese has not been recovered from solution. Therefore, small amounts of manganese will also co-precipitate according to equation 135. Equation 136 show the HCl dissolution of Mn-DMG precipitates to regenerate DMG and equation 137 show the formation reaction of $Mn(OH)_2$ precipitates with the addition of NaOH. Chen and Zhou (2014) reported that Co and Mn co-precipitates contributed 0.37 wt% and 0.21 wt% to the final nickel product with a purity of 98.46%. Thus, the extent of Co and Mn co-precipitation were dictated by these values to achieve a Ni product with a similar purity.

$$Mn_3(Cit)_2 + 6C_4H_8N_2O_2 \rightarrow 3Mn(C_4H_7N_2O_2)_2 + 2H_3Cit \quad [\ 135\ ]$$

$$Mn(C_4H_7N_2O_2)_2 + 2HCl \rightarrow MnCl_2 + 2C_4H_8N_2O_2 \quad [\ 136\ ]$$

$$MnCl_2 + 2NaOH \rightarrow Mn(OH)_2 + 2NaCl \quad [\ 137\ ]$$

3.6.2.2 Cobalt recovery

A 0.5 M ammonium oxalate solution will be used to facilitate the selective precipitation of cobalt from the leach solution at a pH of 6. According to the work done by Chen and Zhou (2014), 97% of cobalt can be recovered as cobalt oxalate (equation 138) at a molar feed ratio of $C_2O_4^{2-}$: Co^{2+} of 1.2. Approximately 8% of the manganese in solution will co-precipitate according to equation 139 (Chen and Zhou, 2014). Based on the product composition reported by Chen and Zhou (2014), it was assumed that negligible nickel co-precipitation will occur.

$$Co_3(Cit)_2 + 3(NH_4)_2C_2O_4 \rightarrow 3CoC_2O_4 + 2(NH_4)_3Cit \quad [\ 138\ ]$$

$$Mn_3(Cit)_2 + 3(NH_4)_2C_2O_4 \rightarrow 3MnC_2O_4 + 2(NH_4)_3Cit \quad [\ 139\ ]$$

Chen and Zhou (2014) reported a cobalt product purity of 96.47% (with 1.07 wt% Mn and 2.47 wt% other impurities). Based on their work, it was assumed that Fe, Cu and Al in solution will react with ammonium oxalate (equations 140 to 142) to contribute to a maximum of 2.47 wt% of the final cobalt product.

$$Fe_3(Cit)_2 + 3(NH_4)_2C_2O_4 \rightarrow 3FeC_2O_4 + 2(NH_4)_3Cit \quad [\ 140\ ]$$

$$Cu_3(Cit)_2 + 3(NH_4)_2C_2O_4 \rightarrow 3CuC_2O_4 + 2(NH_4)_3Cit \quad [\ 141\ ]$$

$$2AlCit + 3(NH_4)_2C_2O_4 \rightarrow Al_2(C_2O_4)_3 + 2(NH_4)_3Cit \quad [\ 142\ ]$$

A filter press will be used to remove the solid precipitates from the leach solution. To reduce the effect of the co-precipitated manganese (MnC_2O_4) on the final cobalt product purity, a dilute solution of oxalic acid (0.01 M) is used to dissolve the MnC_2O_4 in the cobalt product. It was assumed that only the manganese oxalate precipitates will be dissolved in the oxalic acid solution. A filter press recovers the cobalt product from the oxalic acid solution after MnC_2O_4 dissolution. A fraction of the oxalic acid solution obtained from the filter press is recycled to reduce fresh reagent requirements to the dissolution tank. 10% of the solution was purged to prevent build-up of MnC_2O_4 in the system.

3.6.2.3 Solvent extraction of manganese

Manganese will be recovered from the leach solution by solvent extraction after cobalt precipitation. The solvent extraction principle is based on a cation exchange reaction with the aim of transferring specific metal ions from the aqueous to the organic phase. A general cation exchange reaction is shown in equation 143 where M^{n+} is the metal to be extracted and AH is the organic extractant (Musariri, 2019).

$$M^{n+}_{(aq)} + nAH_{(org)} \leftrightarrow MA_{n\,(org)} + nH^{+}_{(aq)} \quad [\,143\,]$$

D2EHPA (di-(2-ethylhexyl) phosphoric acid) diluted in kerosene was selected as organic extractant based on the literature sources shown in Table 22 in section 2.3.3.2. D2EHPA is an acidic extractant (represented by HA in the equations) that is typically saponified prior to metal extraction. The saponified form of an extractant is usually the sodium or ammonia salt of the extractant (Musariri, 2019). A 50 wt% NaOH solution was selected as saponification agent that will react with D2EHPA according to equation 144 (Chen, Zhou, *et al.*, 2015). Saponification reduces the amount of sodium hydroxide or ammonium hydroxide required to control the pH in the solvent extraction system.

$$NaOH + \frac{1}{2}(HA)_{2\,(org)} \rightarrow NaA_{(org)} + H_2O \quad [\,144\,]$$

The operating conditions selected for the solvent extraction system are tabulated in Table 38 below. The balanced extraction reactions for manganese and lithium when 75% of the extractant is saponified can be represented by equations 145 and 146 (Kang *et al.*, 2010). The optimal equilibrium pH in the solvent extraction system is 5 and was calculated based on the pH of the aqueous phase (Chen, Zhou, *et al.*, 2015). A 50 wt% NaOH solution will be fed to the extraction system to neutralize the citric acid produced during manganese and lithium extraction (equation 145 and 146). Refer to equation 111 for the neutralization reaction of citric acid with NaOH.

$$4Mn_3(Cit)_2 + 9NaA_{(org)} + 3HA_{(org)} \rightarrow 6MnA_{2\,(org)} + 3Na_3Cit + H_3Cit \quad [\,145\,]$$

$$4Li_3Cit + 9NaA_{(org)} + 3HA_{(org)} \rightarrow 12LiA_{(org)} + 3Na_3Cit + H_3Cit \quad [\,146\,]$$

Table 38: Solvent extraction operating conditions (Chen and Zhou, 2014; Chen, Zhou, *et al.*, 2015)

Organic extractant	20 vol% D2EHPA in kerosene (75% saponified)
O:A ratio	2:1
Equilibrium pH	5
Extraction time	300 seconds
Mn extraction	97% in 1 stage
Li co-extraction	2% in 1 stage

It was assumed that 0.5 vol% of the organic extractant will be lost due to evaporation. The organic losses were estimated based on solvent extraction plant data and reflect the worst case scenario (Jergensen, 1999). Organic losses due to entrainment in the leach solution (aqueous phase) and stripping liquor (sulfuric acid solution) were not considered in mass balance calculations. Fresh D2EHPA and kerosene is saponified (75%) in the saponification tank before being fed to the solvent extraction circuit to maintain an O:A ratio of 2:1.

The co-extracted lithium is scrubbed from the Mn-loaded organic phase with a 5 w/v% solution of sodium carbonate in 1 scrubbing stage (Chen and Zhou, 2014; Chen, Xu, *et al.*, 2015; Chen, Zhou, *et al.*, 2015). The scrubbing reaction in which the lithium ions is transferred from the loaded organic to the aqueous phase (scrub solution) is shown in equation 147. An O:A ratio of 1 was selected for the scrubbing system (Chen, Xu, *et al.*, 2015). It was assumed that none of the extracted manganese will be washed into the scrub solution.

$$2LiA_{(org)} + Na_2CO_3 \rightarrow 2NaA_{(org)} + Li_2CO_3 \quad [147]$$

The fraction of co-extracted lithium scrubbed from the loaded organic was determined by the concentration (mg/L) ratio of manganese to lithium in the pure Mn solution obtained after stripping. Chen and Zhou (2014) reported concentrations of 4895.6 mg/L Mn and 15.8 mg/L Li in the pure Mn solution. 95% of the scrub solution will be recycled to reduce the amount of fresh Na_2CO_3 solution fed to the process. The remaining 5% of the scrub solution will be mixed with the Mn-depleted leach solution that is fed to the evaporator.

Manganese and the remaining lithium are stripped from the Mn-loaded organic extractant with a sulphuric acid solution according to equations 148 and 149. It was assumed that 99% stripping can be achieved in a single stripping stage with a 0.1 M sulphuric acid solution, an O:A ratio of 1:1 and stripping time of 300 seconds (Chen, Zhou, *et al.*, 2015). The stripping liquor will consist of concentrated sulphuric acid (98 wt%) diluted with water. The stripped regenerated D2EHPA is in its acidic form (HA) and is pumped to the saponification tank where it is saponified before being re-used for Mn extraction.

$$MnA_{2\,(org)} + H_2SO_4 \rightarrow MnSO_4 + 2HA_{(org)} \quad [148]$$

$$2LiA_{(org)} + H_2SO_4 \rightarrow Li_2SO_4 + 2HA_{(org)} \quad [149]$$

After stripping a pure manganese solution is obtained from which manganese can be recovered by precipitation, electrowinning or evaporative crystallization. Manganese precipitation with NaOH was selected as recovery mechanism due to the high energy requirements associated with both electrowinning and evaporative crystallisation. A 50 wt% NaOH solution was used to increase the pH to 11. It was assumed that all of the Mn in solution will be precipitated as manganese hydroxide at pH 11 (Zou *et al.*, 2013). The reactions considered are shown in equations 150 and 151 below.

$$MnSO_4 + 2NaOH \rightarrow Na_2SO_4 + Mn(OH)_2 \quad [150]$$

$$H_2SO_4 + 2NaOH \rightarrow Na_2SO_4 + 2H_2O \quad [151]$$

3.6.2.4 Lithium recovery

The Mn-depleted solution is fed to an evaporator to concentrate the solution with the aim of maximizing lithium recovery. The extent of lithium concentration achieved by evaporation is limited by the solubility limit of trisodium citrate (42.5 g/100 g water at 25℃). Trisodium citrate can potentially precipitate and negatively affect the lithium product purity.

A fraction of the evaporated water will be fed to the leaching tank operating at 90°C. The remaining water will be used to pre-heat the feed to the evaporator with a shell-and-tube heat exchanger. After pre-heating the evaporator feed stream, the water will be pumped to the NaOH make-up, DMG make-up and Ni-DMG dissolution tanks respectively to reduce the water requirements and waste water treatment costs of the facility. The heated leach solution will be fed to a lithium precipitation tank that operates at 80°C (Musariri, 2019).

A 0.5 M sodium phosphate solution is used to facilitate lithium precipitation to recover 89% of lithium as a phosphate according to equation 152 (Chen and Zhou, 2014; Chen, Zhou, *et al.*, 2015). The sodium phosphate solution will be fed in stoichiometric quantities (molar ratio Li_3Cit:Na_3PO_4 = 1:1) (Chen *et al.*, 2016). The Li_3PO_4 solubility limit of 0.039 g/100 g water at 25°C was used to calculate the mass of solid Li_3PO_4 that precipitates from solution.

$$Li_3Cit + Na_3PO_4 \rightarrow Li_3PO_4 + Na_3Cit \quad [\,152\,]$$

3.6.3 Organic acid process option 3

The third organic acid process is based on the work done by Musariri (2019). After citric acid leaching, two phosphate precipitation steps at different temperatures are used to recover a mixed phosphate product (Co, Ni and Mn) and a lithium phosphate product. The aim is to produce products that could be sold to battery manufactures similar to mineral acid process option 3 (refer to section 3.5.3). Refer to Appendix A for the process flow diagram and stream table of organic acid process option 3.

The mass balance calculations were based on the following assumptions:

1. The citric acid leaching tank will operate under the conditions and assumptions discussed in section 3.6.1.1. The water evaporated prior to lithium precipitation will not be enough to meet the leaching water requirements. Thus, fresh water at room temperature will be fed to meet the additional water requirements.
2. After citric acid leaching, the pH is adjusted to 13 with a 50 wt% NaOH solution before Ni, Co and Mn are recovered by phosphate precipitation at 50°C (Musariri, 2019). Reactions 111 and 112 were considered for the neutralization of citric and phosphoric acid.
3. In mineral acid process option 3, the ratio of Mn:Ni:Co was adjusted to 1:1:1 prior to precipitation. The metal ratio adjustment step was excluded in this process as no literature sources were found that employed this step in a citrate leach media. This will influence the operating costs and revenue estimated for OA-3. A lower income from Mn and Ni products can therefore be expected when compared to MA-3.
4. A mixed metal product containing primarily Co, Ni and Mn is precipitated at 50°C for 2 hours in a tank with a 0.5 M NaH_2PO_4 concentration (Musariri, 2019). Heating requirements are met with high pressure steam. The reactions that were considered are shown in equations 153 to 158.

$$2NaH_2PO_4 + Co_3(Cit)_2 \rightarrow Co_3(PO_4)_2 + 2NaH_2Cit \quad [\,153\,]$$

$$2NaH_2PO_4 + Ni_3(Cit)_2 \rightarrow Ni_3(PO_4)_2 + 2NaH_2Cit \quad [\,154\,]$$

$$2NaH_2PO_4 + Mn_3(Cit)_2 \rightarrow Mn_3(PO_4)_2 + 2NaH_2Cit \quad [155]$$

$$NaH_2PO_4 + Li_3Cit \rightarrow Li_3PO_4 + NaH_2Cit \quad [156]$$

$$NaH_2PO_4 + AlCit \rightarrow AlPO_4 + NaH_2Cit \quad [157]$$

$$2NaH_2PO_4 + Cu_3(Cit)_2 \rightarrow Cu_3(PO_4)_2 + 2NaH_2Cit \quad [158]$$

5. After the first precipitation step, the leach solution containing primarily lithium is concentrated by evaporating a fraction of water. The heat required for evaporation will be supplied by high pressure steam (41 barg).
6. A lithium phosphate product is precipitated from the concentrated leach solution at 80℃ (Musariri, 2019). The process conditions and reactions are similar to that occurring in the mixed product precipitation tank.
7. The metal extraction efficiencies reported by Musariri (2019) are tabulated in Table 39. These values were used as the assumed extraction percentages for mass balance purposes.

Table 39: Average metal extraction percentages achieved during phosphate precipitation at 50℃ and 80℃ as reported by Musariri (2019)

Metal	**Phosphate precipitation at 50℃**	**Phosphate precipitation at 80℃ after precipitation at 50℃**
Co	96.65	97.04
Ni	98.16	98.95
Mn	99.45	98.65
Li	3.53	71.59
Al	97.76	73.35
Cu	45.90	29.41

8. The pH in both precipitation tanks will be maintained at pH 13-14 by feeding 50 wt% NaOH solution to neutralize the NaH_2Cit that forms during precipitation reactions (equations 153 to 158) and the unreacted NaH_2PO_4. Due to the amphoteric nature of the $H_2PO_4^-$ ion (Monterey Peninsula College, no date), it was assumed that enough NaOH will be fed to neutralize all of the unreacted NaH_2PO_4. Equations 159 and 160 were used as neutralization reactions in mass balance calculations.

$$NaH_2Cit + 2NaOH \rightarrow Na_3Cit + 2H_2O \quad [159]$$

$$NaH_2PO_4 + 2NaOH \rightarrow Na_3PO_4 + 2H_2O \quad [160]$$

4 Process Economics

4.1 Equipment selection, design and sizing

The basic design, sizing calculations and assumptions used to estimate the purchased equipment cost of each facility are discussed in the sections below. Refer to Appendix D for details regarding the design conditions and materials of construction of each unit.

4.1.1 Storage vessels

The following assumptions were made with regards to the design and sizing of storage vessels:

1. The volumes of the feed, waste, product and intermediate storage tanks were calculated with equation 161 shown below.

$$Volume\ (m^3) = Volumetric\ feed\ rate(\frac{m^3}{hr}) \times Residence\ time(hr) \qquad [\ 161\ ]$$

2. The LIB feed, hydrogen peroxide, phosphoric acid, sulfuric acid, D2EHPA, kerosene storage tanks and all hoppers (NaCl, $KMnO_4$, DMG, Na_3PO_4, NaH_2PO_4 oxalic acid, ammonium oxalate, Na_2CO_3) except if mentioned otherwise have a residence time of 1 month. It was assumed that fresh NaOH crystals, citric acid, 33 wt% HCl solution and 28% ammonia solution can be delivered to the facility every 1-2 weeks.
3. Intermediate storage tanks have a residence time of 2 hours to provide buffering capacity and reduce control errors propagating through the system.
4. Storage tanks for solid waste such as leach residues, metal hydroxides, DMG or salts have a residence time of 1 month.
5. The wet powder products obtained from filter presses contain 6-8% moisture. The wet powders are transported to intermediate storage tanks with a residence time of 1 week. Wet and dry powders will be transported with specialised powder handling equipment (Dec Group, 2019). A single dryer will be used to dry each product stream once a week. All dried powder product storage tanks have a residence time of 1 month.
6. For solid phase feed, waste or product streams, an average stream density was calculated based on the mass fractions of the various solid components in the feed stream to the tank. Stream densities were used to convert mass flowrates to volumetric flowrates (equation 162).

$$Volumetric\ flow\ rate\ \left(\frac{L}{hr}\right) = \frac{Mass\ flow\ rate\ (\frac{kg}{hr})}{Average\ density\ (\frac{kg}{L})} \qquad [\ 162\ ]$$

7. A 10% safety or over design factor was assumed for all storage tanks.

4.1.2 Agitated tanks and mixing vessels

The following assumptions were made with regards to the design and sizing of agitated process vessels:

1. The volume of each agitated vessel was calculated with equation 161.

2. Average stream densities of the feed streams to the various tanks were used to convert mass flow rates to volumetric flow rates (equation 162).
3. Tanks that facilitate pH adjustments with the addition of an acid or base were sized based on the number of pH units by which the feed stream should be adjusted. If the pH of the feed stream should be altered with more than 2 pH units, the pH adjustment system was designed as 2 tanks in series. The first tank facilitates a rough pH adjustment and the second tank facilitates fine tuning to the desired pH level (Goel, Flora and Chen, 2005).
4. Based on the residence times typically required for small pH adjustments, it was assumed that a residence time of 10 minutes will be allowed for each pH unit adjustment (Goel, Flora and Chen, 2005).
5. A 10% safety or over design factor was assumed for all agitated tanks.
6. The power requirements of each agitation motor were calculated based on data obtained from the product manual of a supplier in the mining industry (Xinhai Mineral Processing EPC, no date a). The data was used to plot the power requirements (kW) as a function of the effective volumes of agitation tanks. The straight line obtained from the plot was used to estimate the agitation power required in each of the designed tanks.
7. The physical tank geometry was manipulated to ensure that the height to diameter ratio is as close as possible to 1 as this is the suggested ratio to achieve optimal mixing in vessels (Dynamix Agitators, 2015).

4.1.3 Heat exchangers and evaporators

Forced circulation evaporators were selected to facilitate evaporation due to their suitability in systems where crystallization or surface fouling may occur during evaporation (Sinott, 2005). Floating head shell-and-tube heat exchangers were selected due to their suitability in systems that should be able to tolerate fouling and corrosion. These heat exchangers can operate at high temperature and pressure and can be cleaned easily (shell side and tube side) when the tube bundle is pulled out (Tico, 2019). Heat exchangers and evaporators were designed and sized based on the following assumptions:

1. The amount of heat ($\dot{Q}$) that will be required to increase the temperature of a process stream or tank is dependent on the mass flow rate ($\dot{m}$) and specific heat capacity (C_p) of that stream, and the desired temperature difference (ΔT) as seen in equation 163 (Cengel, 2003).

$$\dot{Q} = \dot{m} C_p \Delta T \qquad [\ 163\ ]$$

2. The heat capacity of water at different temperatures was calculated with a correlation obtained from NIST. The heat capacity of leach solutions consisting of mainly water was assumed as equal to the heat capacity of water at the specified temperature. Due to a lack of information regarding the heat capacities of certain components at different temperatures, it was assumed that the heat capacities of components other than water are not temperature dependent.
3. Shell-and-tube heat exchangers and evaporators were sized based on the heat transfer area required to ensure that the desired amount of heat is transferred. The heat transfer area (A) was calculated

by using equations 164 and 165 where U is overall heat transfer coefficient and ΔT_{lm} is the log-mean temperature difference (Sinott, 2005).

$$\dot{Q} = UA\Delta T_{lm} \quad [164]$$

$$\Delta T_{lm} = \frac{\Delta T_1 - \Delta T_2}{ln\left(\frac{\Delta T_1}{\Delta T_2}\right)} \quad [165]$$

4. The overall heat transfer coefficient suggested for evaporators using steam to evaporate water is 1500-6000 W/m^2.K (The Engineering Toolbox, no date). An average value of 3750 W/m^2.K was assumed as the overall heat transfer coefficient for the evaporators. High pressure steam at 254°C and 41 barg will be used to provide the heat required for evaporation.
5. The overall heat transfer coefficient suggested for shell-and-tube heat exchangers where no phase change occur is 900-2500 W/m^2.K (The Engineering Toolbox, no date). An average value of 1700 W/m^2.K was assumed as the overall heat transfer coefficient for the heat exchangers.
6. Perfect mixing was assumed for agitated vessels. Thus, the temperature of the outlet stream is equal to that of vessel content.
7. Heat will be lost to the environment primarily by convective heat transfer from the surfaces of process and intermediate storage tanks that do not operate at room temperature. Heat transfer by convection can be determined by equation 166 where h is the convection heat transfer coefficient, A is the surface area, T_s is the surface temperature of the tank and T_∞ is the temperature sufficiently far from the surface (Cengel, 2003). It was assumed that the surface temperature is equal to the temperature of the fluid in the tank and that T_∞ is 25°C. The convective heat transfer coefficient of air is typically 10-100 W/m^2.K and was assumed as 55 W/m^2.K (Engineers Edge, 2000).

$$\dot{Q} = hA(T_s - T_\infty) \quad [166]$$

8. The convective heat lost in pipelines was considered for the high temperature evaporated water that is distributed to different units in each facility. Equation 166 was used for the calculation where A was assumed as the outer surface area of the pipelines from which heat can be lost.

4.1.4 Other equipment

The following assumptions apply to the sizing of equipment pieces not discussed in the previous sections:

1. The cutting mill, vibrating screens and dryers were sized according to their feed rate capacity. Each product powder will be stored in an intermediate storage tank prior to drying. A single dryer will be used in batch operation for all the product powders (1 day per week allocated for drying each product). Thus, the dryer was sized based on the product produced at the highest rate (largest mass of powder that should be dried).
2. Filter presses were sized based on product data sheet obtained from Xinhai Mineral Processing EPC. The filter area (m^2) required was plotted as a function of the filter press capacity (ton/hour). A straight-line relationship was observed and used to calculate the filter area required for each filter press (Xinhai Mineral Processing EPC, no date b).

3. The membrane cells were not physically sized due to direct cost escalation based on work done by Abam Engineers in 1980. The size of the HCl combustion chamber was calculated with equation 161 assuming a residence time of 10 seconds and 10% over-design or safety factor.
4. The falling film absorber product specification sheet of Goel (2019) was used to determine the absorption surface area, number of tubes and absorber height required to produce the desired mass flow rate of hydrochloric acid (Goel, 2019).
5. The column diameter (D_c) of the tail gas tower was calculated with equations 167 and 168 where $\hat{u}_v$ is the maximum allowable vapour velocity (m/s), $\hat{V}_v$ is the vapour mass flow rate (kg/s) and ρ_L and ρ_v is the liquid and vapour densities (kg/m^3) respectively. A plate spacing (l_t) of 0.5 m was assumed as initial estimate (Sinott, 2005). The height of the tower was estimated with equation 169 assuming a packing height of zero (Barbour, Oommen and Shareef, 1995). The tower height and diameter were used to approximate the volume of the tail gas tower.

$$\hat{u}_v = (-0.171 l_t^2 + 0.27 l_t - 0.047)\left[\frac{\rho_L - \rho_v}{\rho_v}\right]^{\frac{1}{2}} \quad [167]$$

$$D_c = \sqrt{4\frac{\hat{V}_v}{\pi \rho_v \hat{u}_v}} \quad [168]$$

$$H_{tower} = 1.02 D_c + 2.81 + 1.40 H_{pack} \quad [169]$$

6. The solvent extraction circuit consists of a single extraction, scrubbing and stripping stage as discussed in section 3.6.2.3. A mixer-settler was sized for each of these stages. A mixing time of 5 minutes were used as residence time for the mixer compartment of each mixer-settler (Chen and Zhou, 2014). A settling time of 15 minutes were allowed for phase disengagement in the settler compartment (Arroyo, Fernández-Pereira and Bermejo, 2015). The volumes of the respective mixing and settling compartments were calculated with equation 161. The volumetric flowrate substituted into equation 161 is the sum of the aqueous and organic phase flowrates to a mixer-settler.

4.2 Capital cost estimations

4.2.1 Purchased equipment cost

The purchased equipment cost of each unit was calculated by scaling known values to ensure that it can withstand operation at the design conditions. The base equipment costs (C_p^0) of most units were calculated with equation 170 (Turton *et al.*, 2012), where A is the equipment cost parameter used to scale the equipment cost and K_1, K_2 and K_3 are sizing constants obtained from Turton *et al.* (2012). The equipment cost parameter (A) is generally related to either the size of the unit or the processing capacity thereof.

$$log_{10} C_p^0 = K_1 + K_2 \, log_{10}(A) + K_3 [log_{10}(A)]^2 \quad [170]$$

The base equipment cost (C_p^0) represents the cost of a unit at base conditions which is defined as ambient temperature, atmospheric pressure and carbon steel as material of construction. The purchased equipment cost was calculated by adjusting the base equipment cost with correction factors if more

expensive materials of construction (F_M) will be used or if the unit should be able to operate at higher temperatures (F_T) or pressures (F_P) as shown in equation 171 (Van Wyk, 2014). Refer to Table 40 for typical values of these correction factors.

$$Purchased\ Equipment\ Cost = C_p^0 \times F_M \times F_P \times F_T \quad [171]$$

Table 40: Typical correction factors for materials and temperature (Smith, 2005; Turton *et al.*, 2012)

Material	F_M	Temperature (℃)	F_T
Carbon steel	1.0	0 – 100	1.0
Stainless Steel 316	1.8	100 – 300	1.6
Nickel (Monel)	3.6	300 – 500	2.1
Hastelloy C	5.8		

For the hydrochloric acid facilities, materials with high corrosion resistance should be used due to the high corrosivity of hydrochloric acid. Materials such as graphite, titanium and Hastelloy C are suitable materials but are very expensive (Totton Pumps, 2008; Turton *et al.*, 2012). However, rubber lined steel is a suitable and cheaper alternative material of construction (PolyCorp, no date). When a steel tank is lined with rubber, a cheaper steel than stainless steel 316 can be used. No information regarding the cost of rubber lined steel in comparison to carbon steel was found. For rubber lined steel, a conservative material correction factor of 1.8 was assumed which is the same as the correction factor used for stainless steel 316.

Diabon, which is an impregnated graphite material was selected as material of construction for the hydrochloric acid production units (combustion furnace, falling film absorber and tail gas tower). Based on average prices for stainless steel 316 and graphite obtained from Alibaba, a material correction factor of 5 was calculated for graphite. Diabon (impregnated graphite) will be more expensive than pure graphite. Thus, a conservative material correction factor of 5.8 was assumed for Diabon. Stainless steel 316 is resistant to citric acid thus, a material correction factor of 1.8 was assumed for all units in the citric acid process options (Totton Pumps, 2008).

All units except the HCl combustion furnace will operate at temperatures below 100℃. Thus, the temperature correction factors of all units were assumed as 1 (Van Wyk, 2014). A temperature correction factor of 2.1 was assumed for the impregnated graphite HCl production units that can withstand temperatures up to 430℃ (Moroz, 2016). Typically the gases in the HCl combustion chamber is cooled to 300℃ (SGL Group, 2016). Pressure factors were calculated with equation 172 where P is the operating pressure in bar and K_1, K_2 and K_3 are constants (Turton *et al.*, 2012).

$$log_{10} F_p^0 = K_1 + K_2\, log_{10}(P) + K_3[log_{10}(P)]^2 \quad [172]$$

If the equipment cost for a unit with a different size or capacity than the design value was available, equation 173 was used to correct for the difference in size. Various literature sources were used to find the cost exponents (n) for units (Peters, Timmerhaus and West, 2003; El-Halwagi, 2011; Turton *et al.*, 2012). If a specific cost exponent value could not be found, the six-tenths rule was used and the cost exponent was assumed as 0.6 (Turton *et al.*, 2012). Equation 174 was used to correct known cost values

from the past to present day cost values. The Chemical Engineering Plant Cost Index (CEPCI) was used as scaling index to update cost values (Turton *et al.*, 2012).

$$C_A = C_B \times \left(\frac{S_A}{S_B}\right)^n \quad [\ 173\ ]$$

$$C_2 = C_1 \times \frac{CEPCI_2}{CEPCI_1} \quad [\ 174\ ]$$

The capital cost of all units was calculated based on the scaling principles discussed above except those mentioned below:

1. The cost of the vibrating screens, ultrasonic washing tank and dryers were obtained from the Alibaba website (www.alibaba.com).
2. A quotation received from Retsch was used as purchased equipment cost for the cutting mill.
3. The Matches website (www.matche.com) was used to determine the base cost of shell-and-tube heat exchangers with different heat transfer areas.
4. The capital cost associated with the membrane cells was scaled from previous design data published by Abam Engineers (1980). The production capacity of the facility was scaled from 544 ton/day chlorine to the design capacity with the six-tenths rule.
5. The falling film absorber was costed based on its absorption surface area whereas the tail gas tower was costed based on the tower volume.
6. The mixer settlers in the solvent-extraction circuit were costed based on equipment costs reported in previous work (Arroyo, Fernández-Pereira and Bermejo, 2015).

4.2.2 Total capital investment

The total capital investment of each process option was evaluated with the major equipment cost ratio method suggested by Turton *et al.* (2012) and Peter, Timmerhaus and West (2003). Each cost contribution factor is expressed as a percentage of the delivered equipment cost. The delivered equipment cost was calculated by incorporating a 10% delivery allowance (Peters, Timmerhaus and West, 2003).

Refer to Table 41 for the capital cost breakdown and cost contribution factors for a facility processing both solids and fluids. These factors were used in CAPEX calculations. The working capital was estimated as 15% of the fixed capital investment and will be used to start-up the processing facility and cover expenses in the first few months of operation (Peters, Timmerhaus and West, 2003; Smith, 2005; Turton *et al.*, 2012). Refer to Appendix D for the detailed capital cost breakdown of each process option.

It was assumed that the piping cost factor in Table 41 includes the costs related to pumps, conveyors or other transport systems. The cost of land was assumed as included in the buildings and yard improvements cost factors. The service facilities cost factor includes costs associated with steam generation and distribution, water supply and cooling, water treatment and distribution, electric substations and electricity distribution, process and sanitary waste disposal, communications, fire-protection systems and safety installations (Peters, Timmerhaus and West, 2003).

It was assumed that the scaled capital cost of the membrane cells included the costs associated with equipment installation, piping, instrumentation, controls and electrical systems. However, costs associated with utilities, offsites and other indirect costs were not included (Abam Engineers Inc., 1980). The membrane cells capital cost was shown as a separate entry in the CAPEX calculations and were included in the calculation of costs related to buildings, yard improvements, service facilities and the indirect costs.

Table 41: Capital cost estimation for a solid-fluid processing plant (Peters, Timmerhaus and West, 2003)

Cost Component	**% of Delivered Equipment Cost**
Direct Costs	
Delivered Equipment Cost	100%
Purchased Equipment Installation	39%
Instrumentation and controls	26%
Piping (Installed)	31%
Electrical Systems (Installed)	10%
Buildings	29%
Yard Improvements	12%
Service Facilities	55%
Indirect Costs	
Engineering and supervision	32%
Construction and Expenses	34%
Legal Expenses	4%
Contractor's fee	19%
Contingency	37%
Fixed Capital Investment (FCI)	Direct + Indirect Costs
Working Capital (WC)	15%
Total Capital Investment	FCI + Working Capital

4.3 Operating cost estimations

The ratio method recommended by various literature sources was used to estimate the annual direct, fixed and general operating costs associated with each of the process options. The cost factors or ratios used in the OPEX estimation were obtained from Turton *et al.* (2012) and are tabulated in Table 42. For comparison and validation purposes, the cost contribution ranges from Peters, Timmerhaus and West (2003) are also shown in Table 42.

The cost contributions of patents and royalties as well as research and development were neglected from OPEX calculations. Using the cost factors from Turton *et al.* (2012) shown in Table 42, equations 175 to 179 were developed and used to calculate the total operating cost (C_{TOC}) of each flowsheet alternative. The sections below discuss the correlations used and assumptions made for the calculation of depreciation, raw materials, waste treatment, utilities and operating labour costs.

$$Direct\ Operating\ Costs = C_{RM} + C_{WT} + C_{UT} + 1.33C_{OL} + 0.069FCI \qquad [\ 175\ ]$$

$$Fixed\ Operating\ Costs = 0.708C_{OL} + 0.068FCI + Depreciation \quad [176]$$

$$General\ Operating\ Costs = 0.177C_{OL} + 0.009FCI + 0.11C_{TOC} \quad [177]$$

$$C_{TOC} = Direct\ Operating\ Costs + Fixed\ Operating\ Costs + General\ Operating\ Costs \quad [178]$$

$$C_{TOC} = \frac{C_{RM}+C_{WT}+C_{UT}+2.215C_{OL}+0.146FCI+Depreciation}{0.89} \quad [179]$$

Table 42: Cost factors used in OPEX calculations (Peters, Timmerhaus and West, 2003; Turton *et al.*, 2012)

Cost Component	Cost factor (Turton *et al.*, 2012)	Cost Contribution (Peters, Timmerhaus and West, 2003)
Direct Operating Costs		
Raw Materials (C_{RM})	1 C_{RM}	10-80% C_{TOC}
Waste treatment (C_{WT})	1 C_{WT}	-
Utilities (C_{UT})	1 C_{UT}	10-20% C_{TOC}
Operating labour (C_{OL})	1 C_{OL}	10-20% C_{TOC}
Direct Supervisory and Labour	0.18 C_{OL}	10-20% C_{OL}
Maintenance and Repairs	0.06 FCI	2-10% FCI
Operating Supplies	0.009 FCI	10-20% of maintenance or 0.5-1% FCI
Laboratory Charges	0.15 C_{OL}	10-20% C_{OL}
Patents and Royalties	0.03 C_{TOC}	0-6% C_{TOC}
Fixed Operating Costs		
Depreciation	-	-
Local Taxes and Insurance	0.032 FCI	1.4-5% FCI
Plant Overhead Costs	0.708 C_{OL} 0.036 FCI	50-70% C_{OL}or 5-15% C_{TOC}
General Operating Expenses		
Administration Costs	0.177 C_{OL} 0.009 FCI	20% of operating labour, supervision and maintenance or 2-5% C_{TOC}
Distribution and Selling Costs	0.11 C_{TOC}	2-20% C_{TOC}
Research and Development	0.05 C_{TOC}	2-5% of total sales
Total Operating Cost (C_{TOC})		**Direct + Fixed + General Operating Expenses**

4.3.1 Cost of raw materials

The raw material requirements were determined based on data obtained from the mass and energy balances completed for each flowsheet option. The cost associated with each raw material was calculated using the required mass flowrate (kg/hr), the number of annual operating hours (h) and the price of the raw material (US $/ton). Refer to Table 43 for the raw material prices used in these calculations. The prices reported in Table 43 are an average of 3-6 prices obtained from the Alibaba, Kemcore and OK Chem websites.

The price of LIB waste was not found in literature. Fisher *et al.* (2006) estimated that the LIB collection cost for waste quantities greater than 1 tonne would be £ 75/tonne in the period 2006 to 2030. It was

assumed that LIB collection companies will make a profit of 100%, thus selling the collected waste to recycling companies at £ 150/tonne ($ 195/tonne).

Table 43: Raw material costs

Raw Material	Formula	Purity (%)	Cost (US $/tonne)	Reference
LIB waste	-	-	195	Fisher *et al.* (2006)
Hydrochloric Acid	HCl	33	185	Alibaba (2019)
Process water	H_2O	100	1.41	Stellenbosch Municipality (2018)
Citric acid	$H_3C_6H_5O_7$	>99	719	Alibaba (2019)
Hydrogen Peroxide	H_2O_2	50	614	Alibaba (2019), Kemcore (2019)
Sodium Hydroxide	NaOH	99	508	Alibaba (2019)
	NaOH	32	275	Alibaba (2019)
Potassium Permanganate	$KMnO_4$	>99	2 300	Kemcore (2019)
Dimethylglyoxime	$C_4H_8N_2O_2$	>99	36 500	Alibaba (2019)
Ammonia	NH_3	28	310	Alibaba (2019)
Sodium Chloride	NaCl	>99	95	Alibaba (2019)
Ammonium oxalate	$(NH_4)_2C_2O_4$	>99	1 531	Alibaba (2019)
Oxalic acid	$H_2C_2O_4$	>99	726	Alibaba (2019), Kemcore (2019)
Sodium Carbonate	Na_2CO_3	>99	178	Alibaba (2019)
Phosphoric acid	H_3PO_4	85	761	Alibaba (2019)
Sodium phosphate	Na_3PO_4	>99	373	Alibaba (2019)
Mono-sodium phosphate	NaH_2PO_4	>99	1 019	OKCHEM (2019)
D2EHPA	$C_{16}H_{35}O_4P$	-	4 600	Kemcore (2019)
Kerosene	-	-	286	Alibaba (2019)
Sulphuric acid	H_2SO_4	98	275	Kemcore (2019)
Manganese chloride	$MnCl_2$	98-99	2 050	Alibaba (2019)
Nickel chloride	$NiCl_2$	98-99	4 317	Alibaba (2019)
Hydrogen	H_2	100	13 990	California Fuel Cell Partnership (no date)

4.3.2 Waste treatment cost

Waste streams generated in each process option were classified as solid or liquid waste to calculate a waste treatment or disposal cost based on the correlation shown in equation 180 where $C_{S,U}$ is the waste treatment cost, a and b are cost coefficients and $C_{S,f}$ is the fuel price in $/GJ (Ulrich and Vasudevan, 2004). A CEPCI value of 601.55 for 2018 was used in calculations as the index for 2019 is not published yet. For a conservative estimation the average fuel price of heating oil over the last ten years (2009-2019) of 15.5 $/GJ was used (index mundi, no date; Clarke, 2015).

$$C_{S,U} = a(CEPCI) + b(C_{S,f}) \quad [180]$$

For the disposal cost associated with the treatment of toxic or hazardous solid waste (e.g. the battery waste, leach residue or metal hydroxides (impurity stream)), the value assumed for a was 2 x 10^{-3} and b was assumed as zero (Ulrich and Vasudevan, 2004). When these values are substituted into equation 180, the solid waste disposal cost was determined as $ 1203/tonne waste.

A disadvantage of hydrometallurgical facilities is the production of large volumes of waste water or chemically hazardous solutions. Tertiary waste water treatment costs (including filtration, activated sludge and chemical processing steps) associated with the liquid waste produced in each facility was estimated with equation 180. The value of a was estimated with equation 181 where q is the waste water flowrate in m^3/s and b is equal to 0.1 (Ulrich and Vasudevan, 2004).

$$a = 0.0005 + 1 \times 10^{-4} q^{-0.6} \qquad [\ 181\ ]$$

The pure NaCl or NaCl/NH_4Cl streams produced in the mineral acid process options were not considered waste streams. Pure NaCl streams were treated as product streams that can be sold to chlor-alkali industries such as NCP Chlorchem, Straits, Mondi or Sasol Polymers in South Africa (C11 Chlor-alkali, 2010). Combined NaCl/NH_4Cl streams were not treated as an income due to the additional sublimation step that will be required to further purify the stream to produce pure NaCl. Thus, zero cost was associated with these streams.

Carbon dioxide gas formed during precipitation reactions was treated as a gas waste stream. A wet scrubber would typically be operated to remove carbon dioxide from the gas streams before emission into the atmosphere. According to the US Environmental Protection Agency, the annualized cost of treating gas waste streams was $ 110 to $ 550 per metric ton of pollutant in 2002 (United States Environmental Protection Agency, 2003). Thus, an average gas waste treatment cost of $ 330 per ton of carbon dioxide gas was assumed and scaled to a present-day operating cost using an inflation rate of 6%.

4.3.3 Utility costs

Costs related to electricity, steam and cooling water requirements were considered as utility costs. The cost of electricity was assumed as R 1.07/kWh (BusinessTech, 2019). The following assumptions were made with regards to the electricity consumption of various unit operations:

1. According to the product specification sheet supplied by Retsch, the cutting mill has an electricity requirement of 3 kW (Retsch, 2019).
2. Typically, the power requirement for ultrasonic washing is 15.9-22.5 watts per litre for tanks with a volume of 23-114 litres (Ultrasonic Power Corporation, no date). A power requirement of 22.5 watts per litre was assumed.
3. The filter presses consume 42.5 kWh per tonne of dewatered solids produced (Huber Technology, no date).
4. The energy consumption in the product dryers were assumed as 2400 kJ/kg of water or moisture removed (Kemp, 2014).

5. The typical energy consumption by membrane cells is 1950-2300 kWh/tonne Cl_2 produced (Bommaraju *et al.*, 2000). Thus, it was assumed that the membrane cells consume 2125 kWh/tonne Cl_2 produced.
6. The electricity consumption due to the agitation of process vessels was calculated based on the assumptions discussed in section 4.1.2.
7. It was assumed that all other electricity requirements were included in the general plant electricity contribution which was assumed as 10% of the total equipment electricity consumption.

Steam requirements for process heating were calculated from the information obtained from energy balances. Heat integration between different units reduced the amount of steam required for heating. The cost of steam was calculated by assuming that natural gas would be the fuel burned to supply energy to boilers. Thus, the cost of natural gas determined the cost of steam production in the boilers. Natural gas have an energy content of approximately 38 400 kJ/m^3 and combustion efficiency of 85.7% (US Department of Energy, 2012). According to a SASOL gas application document the maximum natural gas price between July 2017 and September 2018 was R 104.13/ GJ for class 4 gas consumers consuming between 40 000 and 400 000 GJ/annum (Khoele, 2017). Thus, a natural gas price of $ 7.50/ GJ was used to calculate the cost of steam with equation 182.

It was assumed that the boiler feed water will have a temperature of 23.5℃. The energy required to generate 41 barg high-pressure steam from boiler feed water with a temperature of 23.5℃ is 1159 Btu per pound (2696 kJ/kg) of saturated steam produced (US Department of Energy, 2012).

$$Steam\ cost\left(\frac{\$}{kg}\right) = Boiler\ energy\ requirements\left(\frac{kJ}{kg}\right) \times Fuel\ cost\left(\frac{\$}{GJ}\right) \times \frac{1\ GJ}{10^6\ kJ} \qquad [\ 182\ ]$$

Cooling water requirements were also determined from energy balances. The cost of cooling water ($/m^3) was calculated with equation 180. The value of a is calculated with equation 183 where q is the cooling water flowrate in m^3/s and b is 0.003 (Ulrich and Vasudevan, 2004).

$$a = 0.00007 + 2.5 \times 10^{-5} q^{-1} \qquad [\ 183\ ]$$

4.3.4 Operating labour costs

Operating labour costs were calculated by estimating the number of operators required per shift for each piece of equipment on the respective facilities. Refer to Table 44 below for the labour requirements estimated by Peters, Timmerhaus and West (2003). For equipment not mentioned in Table 44, it was assumed that 1 operator will be required per unit per shift. For each operator required per shift, 4.5 operators should be hired as shown in equation 184 (Turton *et al.*, 2012). The annual salary earned by plant operators were assumed as $ 13 184 based on the average salary proposed by 3 sources (Kasibiz, 2015; Career Junction, 2018; indeed, 2019).

$$C_{OL} = 4.5 N_{OL} \times Operator\ Salary/annum \qquad [\ 184\ ]$$

Table 44: Typical labour requirements for process equipment (Peters, Timmerhaus and West, 2003)

Process Equipment	Workers/unit/shift
Blowers and compressors	0.15
Crystallizer	0.16
Rotary dryer	0.5
Evaporator	0.25
Plate and Frame Filter Press	1
Heat Exchangers	0.1
Process Vessels, Towers	0.35
Auxiliary Pumps	0.35
Continuous reactor	0.5

4.3.5 Depreciation

Depreciation is not written off on the total capital investment that consist of the both the fixed capital and working capital as shown in equation 185 below. The value of land cannot be depreciated. Secondly, because working capital is recovered at the end of the project lifetime, it cannot be depreciated (Turton *et al.*, 2012).

$$Total\ Capital\ Investment = Fixed\ Capital + Working\ Capital \quad [\ 185\ ]$$

The salvage value of a chemical plant is the value of the fixed capital investment (excluding land) evaluated at the end of the project's lifetime and was assumed as 10% of the initial fixed capital investment (Towler and Sinnott, 2013). The depreciable capital (D) is expressed as shown in equation 186 where FCI_L is the fixed capital investment excluding land and S is the salvage value of the plant. Using the straight-line depreciation method over an assumed equipment lifetime of 10 years the annual depreciation was calculated with equation 187 (Turton *et al.*, 2012).

$$D = FCI_L - S \quad [\ 186\ ]$$

$$d_k^{SL} = \frac{FCI_L - S}{n} \quad [\ 187\ ]$$

4.4 Annual revenue

The annual revenue is a function of the metal recoveries in each flowsheet option, the product purities and the assumed product prices. Refer to Table 45 for the assumed product values which were calculated as an average of 4-6 price values obtained from the respective source. Impurities such as Fe, Cu, Al and NaCl in product streams will result in less valuable selling products. To incorporate penalties for impurities in the products, the assumed selling prices were multiplied with the product purity. Due to the great amount of uncertainty that resides within the assumed metal prices, the effect of fluctuations in the revenue was investigated in the sensitivity analysis (refer to Chapter 6).

No information was found with regards to the prices of $Mn(OH)_2$, $Mn_3(PO_4)_2$, $Co_3(PO_4)_2$, and $Ni_3(PO_4)_2$. The selling prices of these products were calculated from the known prices of MnO_2, $Co(OH)_2$, CoC_2O_4 and $Ni(OH)_2$. Each base price was adjusted by multiplying with the mass fraction of the valuable metal in

the compound with the unknown price and dividing by the mass fraction of the valuable metal in the known base price. Refer to Table 72 in Appendix B for the mass fractions of the valuable metals in each product and for sample calculations with regards to the price calculations. An average price was calculated for the combined hydroxide and phosphate products. This was done by incorporating the mass fraction contributions of the Mn, Co and Ni compounds respectively.

Table 45: Prices assumed for various product streams

Metal	Product	Purity (%)	Price ($/kg)	Reference
Lithium	Li_2CO_3	99%	16.8	Alibaba (2019)
	Li_3PO_4	99.9%	15.4	Alibaba (2019)
Cobalt	$Co(OH)_2$	>95%	55.1	Alibaba (2019)
	CoC_2O_4	99%	50.6	Alibaba (2019)
	$Co_3(PO_4)_2$	-	51.4	Calculated based on $Co(OH)_2$, CoC_2O_4 prices
Manganese	MnO_2	99%	42.6	Alibaba (2019)
	$Mn(OH)_2$	-	41.7	Calculated based on MnO_2 price
	$Mn_3(PO_4)_2$	-	31.3	Calculated based on MnO_2 price
Nickel	$Ni(OH)_2$	99%	39.5	Alibaba (2019)
	$Ni_3(PO_4)_2$	-	30.0	Calculated based on $Ni(OH)_2$ price
Salt	NaCl	>99%	0.095	Alibaba (2019)

If additional purification steps are added to enhance the purity of the products manufactured, products can be sold as high purity laboratory products. Laboratory products are sold at exceptionally high prices due to the small volumes in which they are packaged, sold and distributed. The average price per kg of high purity laboratory product was calculated based on the selling prices of companies such as Sigma-Aldrich, Alfa Aesar, TCI Chemical and Strem Chemicals (*ChemicalBook*, 2019; City Chemical LLC, 2019). Refer to Table 46 for a summary of laboratory product selling prices. Adding process steps for product purification and packaging, will however increase the CAPEX and OPEX of the processes.

Table 46: High purity laboratory product prices (*ChemicalBook*, 2019; City Chemical LLC, 2019)

Metal	Product	Purity	Price ($/kg)
Lithium	Li_2CO_3	>98%	791
	Li_3PO_4	98%	315
Cobalt	$Co(OH)_2$	97%-99.9%	461
	CoC_2O_4	99.9%	1310
	$Co_3(PO_4)_2$	-	1378
Manganese	MnO_2	90%-99.9%	219
Nickel	$Ni(OH)_2$	-	251

4.5 Profitability analysis

Using the calculated CAPEX, OPEX and revenue, the cumulative cash flow over a project lifetime of 20 years was evaluated for each flowsheet option. The cumulative cash flow position of a project at a

given moment in time is defined as the Net Present Value (NPV) and is calculated with equation 188 (Turton *et al.*, 2012). An NPV of greater than zero indicates that the project is profitable.

$$NPV = \sum_{n=1}^{n=project\ life} \frac{Estimated\ net\ cash\ flow\ in\ year\ n}{(1+r)^n} \quad [\ 188\ ]$$

The NPV calculations were based on the following assumptions:

1. The construction phase of the facility will take 2 years. 50% of the fixed capital investment will be paid out in the first construction year and the remainder in the second.
2. Working capital will be paid out at the end of the second construction year.
3. Plant operation will start in year 3 in which only 85% of the annual income is expected. From year 4 onwards the total revenue was considered.
4. A taxation rate of 28% was used to calculate the annual profit after tax (SARS, no date).
5. An annual internal discount rate of 15% was used (Van Wyk, 2014). This is conservative when compared to the discount rate of 9% used in the economic analysis done by CM Solutions (Knights and Saloojee, 2015).
6. The working capital and salvage value is fully recoverable at the end of the project lifetime (year 20) (Van Wyk, 2014).
7. The discounted annual cash flow was calculated by using equations 189 to 191 (Turton *et al.*, 2012).

$$Profit\ before\ tax = Revenue - Expenses = R - COM_d - d \quad [\ 189\ ]$$

$$After\ tax\ cash\ flow = Net\ Profit + Depreciation = (R - COM_d - d)(1 - t) + d \quad [\ 190\ ]$$

$$Annual\ discounted\ cash\ flow = \frac{Estimated\ net\ cash\ flow\ in\ year\ n}{(1+r)^n} \quad [\ 191\ ]$$

The Present Value Ratio (PVR) is an economic indicator that quantifies the financial return received from the initial fixed capital investment. The PVR is calculated with equation 192 and measures the overall gain in project value as a function of the fixed capital initially invested. A value of greater than 1 indicates profitable operation (Turton *et al.*, 2012; Van Wyk, 2014).

$$PVR = \frac{Present\ Value\ of\ all\ positive\ cash\ flows}{Present\ Value\ of\ all\ negative\ cash\ flows} = 1 + \frac{NPV}{FCI} \quad [\ 192\ ]$$

The discounted cash flow rate of return (DCFROR) is defined as the interest rate at which annual cash flows should be discounted to ensure that the NPV at the end of the project lifetime is zero. A DCFROR greater than the internal discount rate (minimum rate of return acceptable for capital investment) indicates profitable operation.

The period needed (after start-up) to recover the initial fixed capital investment when all the annual cash flows are discounted are termed the discounted payback period (DPBP). The shortest possible payback period is desirable from a financial point of view (Turton *et al.*, 2012).

5 Economic Analysis and Process Comparison

The results of the economic analysis of the evaluated process options are compared in the sections that follow. For discussion purposes, the results presented in Chapter 5 will refer to the process options proposed in Chapter 3 according to the labels tabulated in Table 47 below. Mineral acid process options are referred to as MA-1, MA-2 and MA-3 whereas organic acid processes are referred to as OA-1, OA-2 and OA-3. Refer to the appendices for the results or sample calculations relevant to each section.

Table 47: Flowsheet options and key process characteristics

Process Option	Key Process Characteristics
MA-1	Hydrochloric acid leaching, membrane electrolysis, Mn, Ni, Co, Li precipitation
MA-2	Hydrochloric acid leaching, Mn, Ni, Co, Li precipitation
MA-3	Hydrochloric acid leaching, combined Mn, Ni, Co hydroxide precipitation
OA-1	Citric acid leaching, Mn, Ni, Co, Li precipitation
OA-2	Citric acid leaching, Ni, Co, Li precipitation, Mn solvent extraction
OA-3	Citric acid leaching, combined Mn, Ni, Co phosphate precipitation

5.1 Metal recovery

The Mn, Ni, Co and Li recoveries achieved in the six flowsheet options investigated are compared in Figure 9 below. It was assumed that 8% of the valuable metals are lost during the pre-treatment plant section. This explains why all metal recoveries are below 90% except for Ni in MA-3. The investigation of alternative pre-treatment strategies to minimize these losses may be worthwhile.

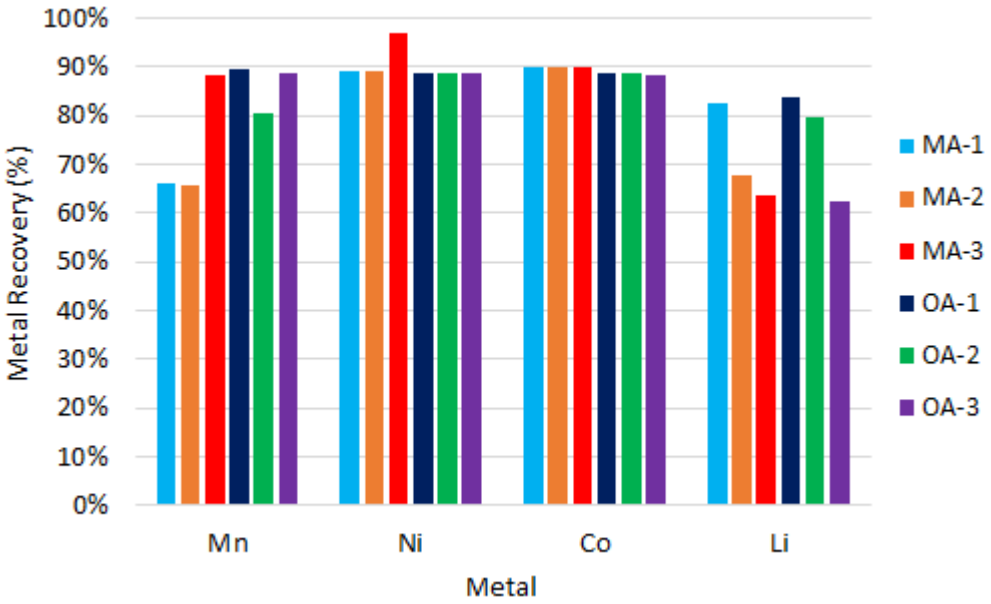

Figure 9: Comparison of valuable metal recoveries achieved in process options

The lower manganese recoveries of MA-1 (66.1%) and MA-2 (65.5%) were calculated by incorporating the addition of excess $KMnO_4$ to facilitate MnO_2 precipitation. No $KMnO_4$ was added in MA-3 explaining the higher Mn recovery of 88.3%. The addition of 9 kg/hr $MnCl_2$ prior to the combined hydroxide precipitation step in MA-3 also contributed to the higher Mn recovery reported. Although excess $KMnO_4$

was added to the system in OA-1, the Mn recovery was improved by the oxidation of a fraction of the citric acid to produce additional MnO_2 precipitates (refer to equation 114). The lower Mn recovery of 80.4% achieved in OA-2 can be ascribed to Mn losses and co-precipitation during the nickel and cobalt recovery steps preceding Mn solvent extraction. Thus, it can be concluded that the sequence in which metals are selectively recovered from leach solutions may have a notable effect on metal recovery, product purity and ultimately the revenue. The high Mn recovery reported by Musariri (2019) after phosphate precipitation at pH 13 explains the Mn recovery of 88.7% in OA-3.

Similar nickel (88.6% - 89.2%) and cobalt (88.3% - 89.9%) recoveries are achieved in all process options. Due to the addition of $NiCl_2$ to ensure a Mn:Ni:Co ratio of 1:1:1 in MA-3, the high nickel recovery of 96.7% observed for MA-3 makes sense.

In general, lithium recoveries are lower than that of the other valuable metals due to the solubility limits of Li_2CO_3 (0.71 g/100 g water) and Li_3PO_4 (0.039 g/100 g water) that dictates the precipitation of these compounds. The lower solubility limit of Li_3PO_4 ensures higher Li recovery with phosphate precipitation (~89%) compared to carbonate precipitation (80%). This explains the high Li recoveries obtained in OA-1 (83.9%) and OA-2 (79.4%). The lower Li recovery in OA-2 compared to OA-1 makes sense due to the Li co-extraction that occurs during Mn solvent extraction in OA-2. The low Li recovery (71.59%) assumed over the lithium phosphate precipitation step in OA-3 (Musariri, 2019) explains the low overall Li recovery (62.6%) of OA-3.

In all mineral acid processes, an evaporative crystallizer is present prior to lithium precipitation to remove excess NaCl that prevents lithium product contamination. In MA-1, the large NaCl crystal recycle stream (only 20% is purged) to the membrane cells allows unreacted LiCl back into the process and increases the overall Li recovery to 82.5%. Large amounts of LiCl are lost in the NaCl crystal stream leaving the system prior to Li precipitation in MA-2 and MA-3 resulting in lower Li recoveries of 67.7% and 63.7% respectively.

5.2 Product purity

The purities of the products produced in the processes that selectively extract each valuable metal are compared in Figure 10 below. From Figure 10 it can be observed that Mn and Ni products produced in the organic acid processes have higher purities compared to the mineral acid processes. This was expected since citric acid leaches with higher selectivity than hydrochloric acid resulting in less impurity ions (Fe, Cu and Al) in the leach solution. Thus, the co-precipitation of Fe, Cu and Al during Mn and Ni recovery has a smaller effect on the product purities in OA-1 and OA-2. Solvent extraction is used for the selective recovery of Mn in OA-2, resulting in the highest Mn product purity of 99.9% after co-extracted lithium is scrubbed from the loaded organic phase. The purity of the nickel hydroxide precipitated in OA-1 (98.9%) and OA-2 (98.7%) are notably higher than that of MA-1 (90.2%) and MA-2 (89.6%) primarily because of the Cu co-precipitation occurring in the mineral acid processes.

Similar cobalt product purities are achieved in MA-1 (98.3%), MA-2 (97.8%) and OA-1 (97.8%). Mn solvent extraction as third recovery step in OA-2 allows for the co-precipitation of manganese oxalate with the

cobalt oxalate resulting in a lower Co product purity (96.4%). From Figure 10 it is clear that similar lithium product purities can be expected for process options MA-2 (97.2%), OA-1 (97.9%) and OA-2 (97.7%). The slightly lower lithium product purity of MA-2 can be explained by NaCl crystallisation during the lithium carbonate precipitation step. The high Li product purity achieved in MA-1 (99.4%) is primarily due to the membrane cells and NaCl crystallizer in MA-1 that reduces the NaCl concentration prior to Li precipitation. Thus, less NaCl crystallizes out to contaminate the lithium product stream. The main contaminant co-precipitating with lithium phosphate in OA-1 and OA-2 is trisodium citrate (Na_3Cit). The mass fraction of trisodium citrate in the final lithium product is 1.5% and 1.9% in OA-1 and OA-2 respectively.

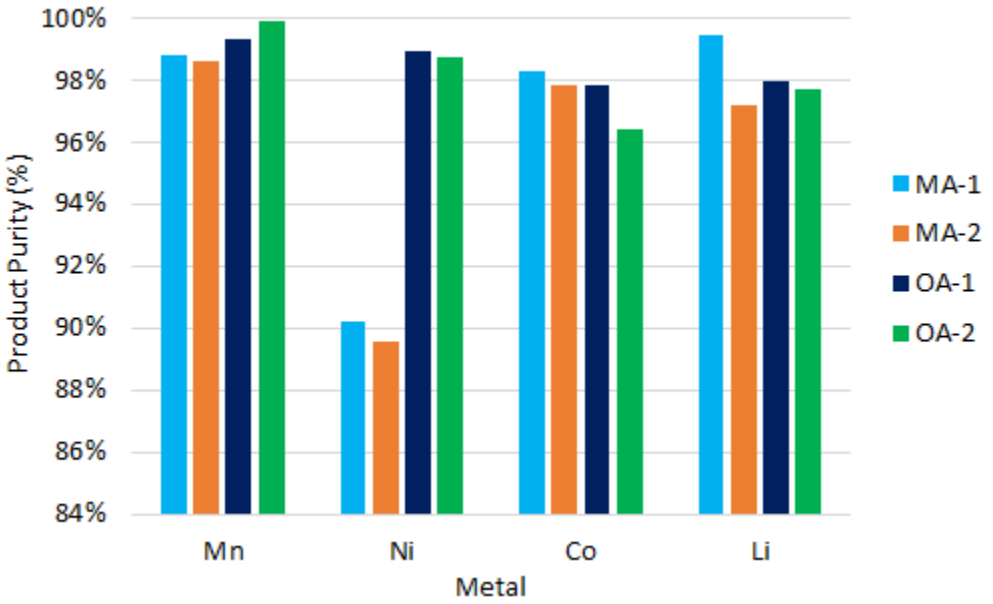

Figure 10: Product purities of process options producing selective products

MA-3 and OA-3 aim to produce a combined Mn, Ni and Co product by simultaneously precipitating these metals in single precipitation stage. The calculated product purities are presented in Table 48 below. The lower product purities of OA-3 are a result of the higher levels of co-precipitation assumed based on the experimental work done by Musariri (2019).

Table 48: Product purities of process options producing a combined Ni, Mn, Co product

Product	MA-3	OA-3
Combined Mn, Ni, Co product	96.0%	95.7%
Li product	97.1%	86.9%

5.3 Revenue

The metal recoveries and product purities of the various flowsheet alternatives have a direct influence on the expected annual revenue of each facility. Refer to Figure 11 below for a comparison of the revenue distribution of the process options. The general trend observed in Figure 11 is that the Co and Mn products are the primary contributors to the income earned in all process options. Thus, the investigation of possible strategies to minimize Co and Mn losses and maximize product purities may have a notable

effect on the process revenue and project profitability. Cobalt contributes to between 37.4% (MA-3) and 61.8% (OA-2) of the annual revenue. This makes sense as cobalt is the metal with the highest intrinsic value compared to nickel, manganese and lithium (refer to Table 45 in section 4.4).

Although similar cobalt recoveries are achieved in all process options (refer to Figure 9), the estimated income obtained from cobalt products are lower for the mineral acid processes compared to the organic acid processes. This is because cobalt is produced as $Co(OH)_2$ (92.95 g/mol) which is a smaller and lighter compound compared to CoC_2O_4 (146.95 g/mol) and $Co_2(PO_4)_2$ (366.74 g/mol) in the organic acid processes. Thus, the cobalt product income is affected by the production rate (ton/yr) of the cobalt oxalate product which is almost 1.6 times greater than the production rate of cobalt hydroxide (e.g. 145 ton/yr $Co(OH)_2$ in MA-1 compared to 230 ton/yr CoC_2O_4 in OA-2).

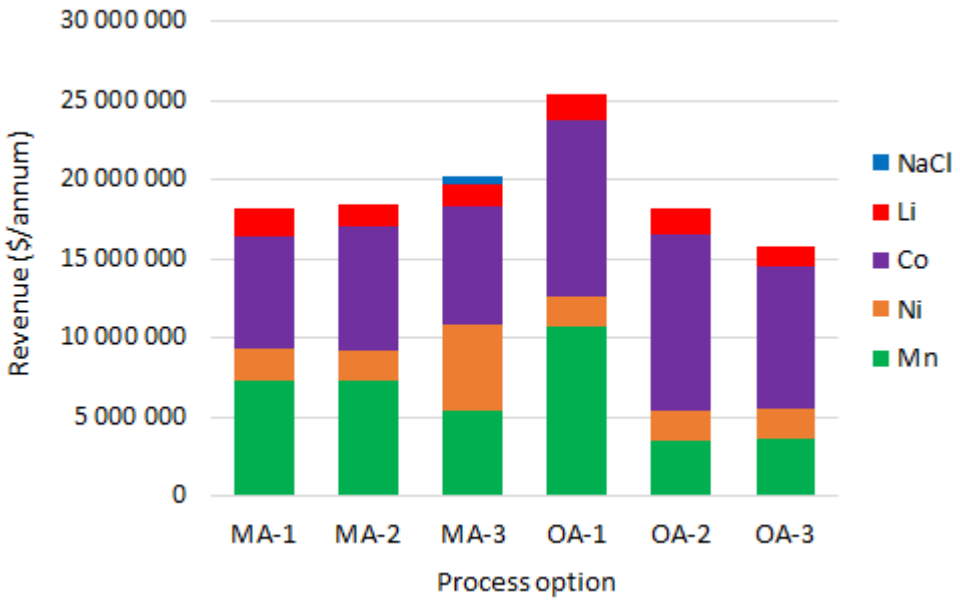

Figure 11: Comparison of revenue distribution

Income earned from manganese products contributes to between 18.9% (OA-2) and 41.9% (OA-1) of the total revenue. The large Mn income contribution in OA-1 can be ascribed to the partial oxidation of citric acid with $KMnO_4$ producing additional MnO_2 precipitates (equation 114) that increase the MnO_2 production rate to 252 ton/yr. The low Mn income obtained in OA-2 and OA-3 makes sense as no additional Mn containing compounds are fed to these processes whereas either $KMnO_4$ or $MnCl_2$ are fed to the other processes. The metal ratio adjustment step in MA-3 led to additional Mn and Ni income that were not included in OA-3. For comparison purposes, the effect of excluding the metal ratio adjustment step on the profitability criteria of MA-3 was evaluated. These results are presented and discussed in section 5.7.1.

The income gained from selling nickel products, ranges between 7.6% and 11.8% of the total income. However, with the addition of $NiCl_2$ in MA-3, the nickel income contribution improved to 26.7% of the total income. Due to the lower intrinsic value of lithium and the lower overall Li recoveries, Li contributes to only 6.5% (MA-3) to 9.3% (MA-1) of the annual revenue. The pure NaCl stream produced in MA-3 are sold as a product that contributes to 2.4% of the annual income of MA-3.

The maximum theoretical revenue (refer to Table 49) of each process option was calculated based on the combined metal content of the feed LIBs and process additives such as $KMnO_4$, $MnCl_2$ and $NiCl_2$. For the calculation it was assumed that 100% of the valuable metals fed to each process are recovered to pure saleable products costed according to the prices tabulated in Table 45.

Table 49: Comparison of the actual revenue to the maximum theoretical revenue (values in $/kg LIB)

Process Option	MA-1	MA-2	MA-3	OA-1	OA-2	OA-3
Maximum theoretical revenue	27.7	27.7	26.5	33.1	24.3	22.1
Actual revenue	20.9	21.8	23.2	29.3	20.9	18.2
Actual revenue as a percentage of the maximum theoretical revenue (%)	75.4%	76.7%	87.5%	88.6%	85.9%	82.3%

The actual revenue reported as a percentage of the theoretical revenue is the lowest for MA-1 (75.4%) and MA-2 (76.7%) due to the large fraction of $KMnO_4$ that are fed in excess to these process systems. As mentioned earlier, a fraction of the excess $KMnO_4$ are oxidized in OA-1 to produce Mn precipitates which account for the higher revenue percentage of 88.6%. The process simplicity associated with the combined metal hydroxide precipitation step in MA-3 (when compared to MA-1 and MA-2) minimizes the metal losses throughout the process. This allows the flowsheet to earn 87.5% of its maximum theoretical revenue.

No metal containing reagents are fed to either OA-2 or OA-3 which justifies their high revenue percentages. If a metal containing reagent is fed in excess, some of the unused reagent will be discarded which subsequently decreases the revenue percentage. Although OA-3 has very little process complexity compared to the other organic acid flowsheet options, it still has a lower reported revenue percentage (82.3%). This makes sense when the higher levels of co-precipitation (product contamination) assumed for OA-3 is considered.

5.4 Capital cost

Capital costs associated with each LIB recycling facility were estimated based on the delivered equipment cost as discussed in section 4.2.2. Refer to Appendix D for a more detailed breakdown of the estimated delivered equipment cost and the total fixed capital investment of each process option. Figure 12 compares the purchased equipment cost (excluding membrane cells) of the evaluated LIB recycling options.

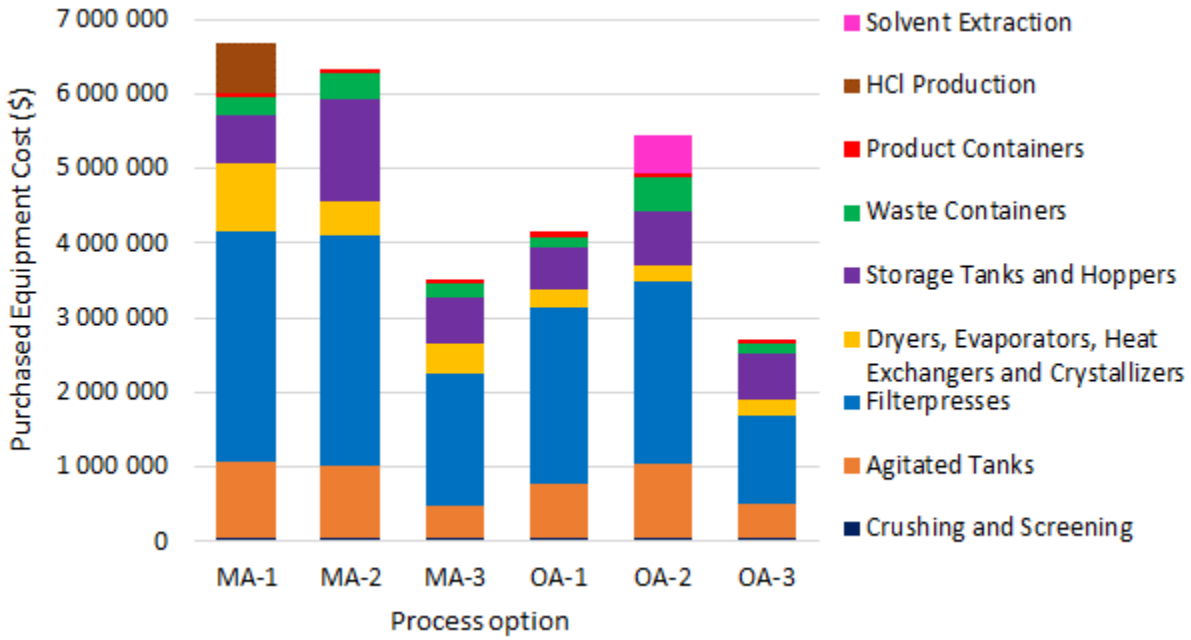

Figure 12: Comparison of purchased equipment cost

By studying Figure 12, the following key differences between the processes were observed:

1. The storage tank cost of MA-2 notably exceeds that of MA-1 as well as all other process options. This is primarily due to the large 33 wt% hydrochloric acid storage tank in MA-2 required to hold fresh acid for at least a week. Due to the continuous regeneration of 33 wt% hydrochloric acid in MA-1, an intermediate HCl storage tank (2 hour residence time) and a small storage tank with fresh HCl feed would be sufficient in MA-1.
2. The estimated waste container cost of MA-2 is higher than that of MA-1 due to the large NaCl crystal stream leaving the system in MA-2. In MA-1 only 20% of the NaCl crystal stream is purged. The remaining fraction (80%) is recycled to ensure NaCl saturation in the feed stream to the membrane cells that will enhance the production of NaOH.
3. The costs associated with waste containers are higher for OA-2 when compared to OA-1 and OA-3. This can be explained by the additional liquid waste streams produced through the dissolution of MnC_2O_4 to purify the cobalt product and the waste solution generated after Mn precipitation from the Mn rich electrolyte.
4. The cost associated with evaporators is the highest in MA-1 since the process requires an additional evaporator prior to the membrane cells to concentrate the stream to NaCl saturation. No evaporative crystallizers are present in the organic acid processes.
5. The cost of agitated tanks in MA-1, MA-2 and OA-2 are higher than that of OA-1 that produces similar products. The pH adjustment tanks and addition of large volumes ammonia solution are the primary reasons explaining the high tank cost in MA-1 and MA-2. The high agitated tank cost of OA-2 can be ascribed to the additional oxalic acid, scrubbing solution and D2EHPA make-up tanks and the manganese oxalate dissolution tank.
6. The primary reason for the difference in the purchased equipment cost of MA-3 compared to OA-3 is the presence of the agitated metal ratio adjustment tank, NaCl crystallizer and subsequent filter

press in MA-3. Detailed sizing and costing of the filter presses are recommended as it is the major cost contributor to the purchased equipment cost and may notably affect the accuracy of the CAPEX estimations. The work done by Knights and Saloojee (2015) confirmed that filter presses will be the main capital expense concerning the purchased equipment. Filter press expenses contributed to approximately 50% of their delivered equipment cost.

Figure 13 compares the direct capital expenditure of the 6 flowsheet options that were evaluated. The direct capital cost of MA-1 is remarkably higher than the costs estimated for any of the other flowsheet alternatives. The reason for this is the incorporation of the membrane electrolysis and hydrochloric acid production units to regenerate NaOH and HCl from the salt (NaCl) present in the system. The estimated cost of the membrane cells was not included in the delivered equipment cost as indicated in the legend of Figure 13. A high amount of uncertainty resides within the assumed capital cost associated with the membrane cells due to the lack of recent costing information. Detailed sizing and costing of the membrane electrolysis system is recommended to improve the accuracy of the CAPEX estimation of MA-1.

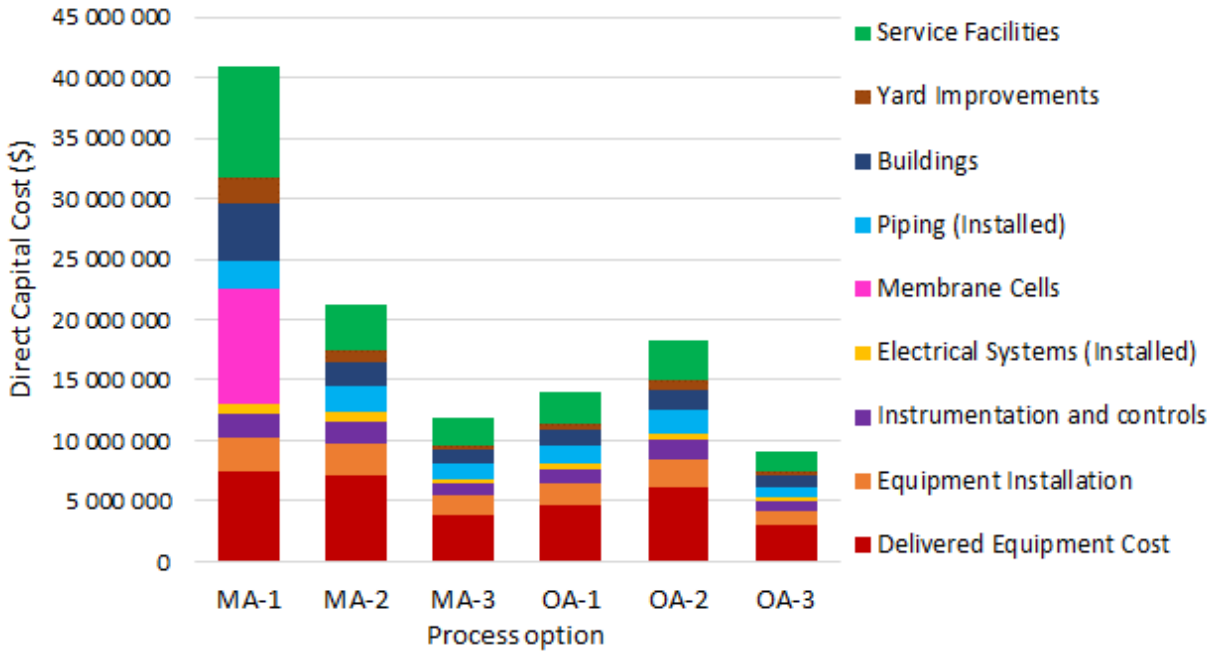

Figure 13: Direct capital expenditure of processing facilities

Figure 14 compares the overall capital cost of the evaluated process options. Although the total direct and indirect capital cost of the various processes differ, the capital cost distribution of all process options (except MA-1) are similar since the capital cost components were calculated as functions of the delivered equipment cost. Refer to section 4.2.2 for a breakdown of all the factors included in the indirect capital costs and to Appendix D (Table 89) for the calculated values. The high CAPEX of MA-1 (refer to Figure 14) will make it exceptionally difficult to operate the facility profitably even if operating costs are minimized and an annual profit is made.

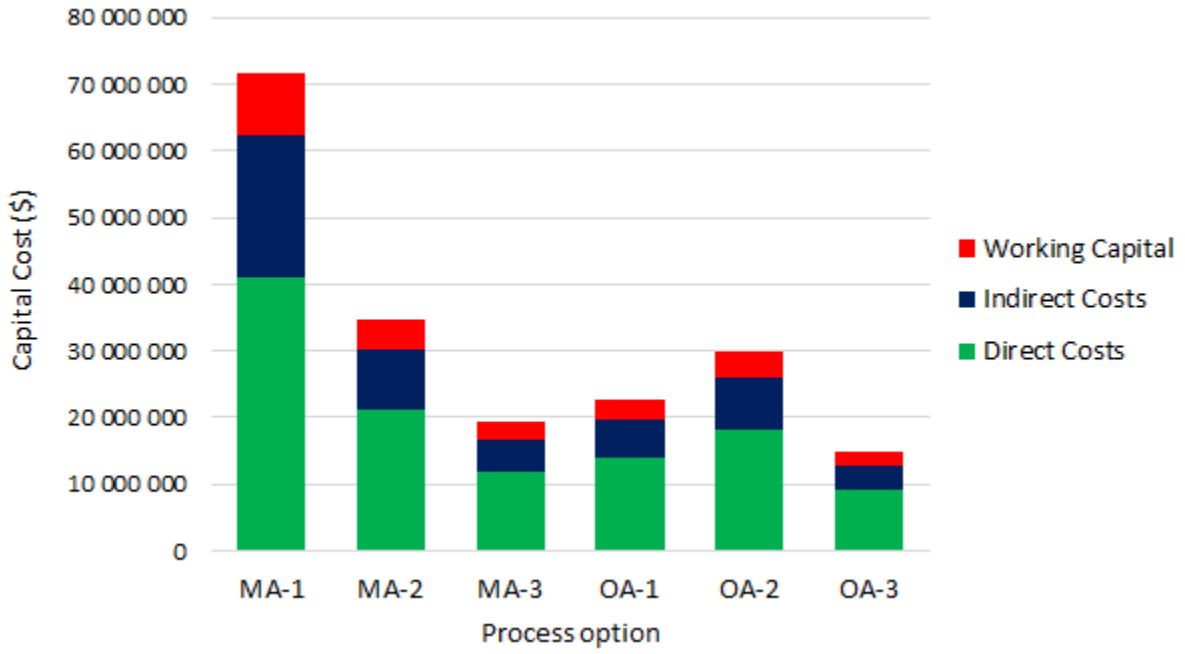

Figure 14: Comparison of capital cost distribution of processing facilities

CM Solutions estimated the CAPEX of a LIB recycling facility with a feed capacity of 13 600 ton/yr as R 295 million ($ 20.8 million at an exchange rate of R 14.20 to $ 1 (*Exchange-Rates.org*, 2019)) in the year 2020 (Knights and Saloojee, 2015). Their estimated CAPEX was calculated by multiplying the delivered equipment cost ($ 6.59 million) with a Lang factor of 3.15. For the purpose of comparison with the current study, the delivered equipment cost reported by Knights and Saloojee (2015) was used to recalculate the CAPEX for their plant using the factor-based method discussed in section 4.2.2; this approach estimated the CAPEX at $ 32.5 million, which was used in further costs comparisons. The capital cost per kilogram of processed LIBs reported in Table 50 was calculated based on an operational facility lifetime of 18 years.

Table 50: Comparison of estimated CAPEX values with CM Solutions CAPEX predictions

Process	CM Solutions	MA-1	MA-2	MA-3	OA-1	OA-2	OA-3
CAPEX (million US $)	32.5	71.6	34.7	19.2	22.8	29.8	14.8
CAPEX (US $/kg LIB processed)	0.13	4.59	2.22	1.23	1.46	1.91	0.95

The CAPEX values that were estimated for processes investigated in this project ($ 14.8 - $ 71.6 million) are in the same order of magnitude as the CAPEX projected by CM Solutions. However, the LIB feed capacity of the designed facilities was only 868 ton/yr. Thus, it can be concluded that the CAPEX estimations are very conservative when compared to the work done by CM Solutions. It should be noted that their proposed process did not aim to selectively recover each of the valuable metals as done in MA-1, MA-2, OA-1 and OA-2. Instead, the process aimed to recover a lithium product (Li_2CO_3) and a combined metal hydroxide product.

5.5 Operating cost

The annual operating expenses (OPEX) for each facility were estimated according to the guidelines suggested by Peters, Timmerhaus and West (2003) as discussed in section 4.3. Refer to Appendix E for a detailed breakdown of the various cost components (e.g. raw materials) contributing to the overall OPEX of each LIB recycling facility. The direct operating expenses of the 6 flowsheet options are compared in Figure 15 below.

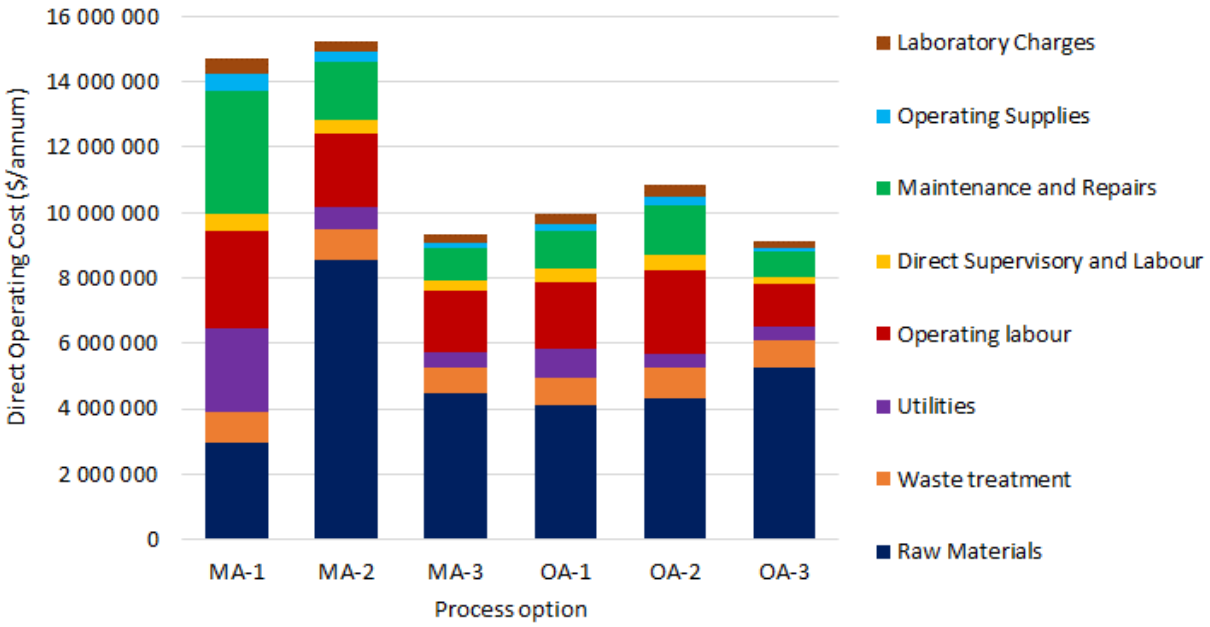

Figure 15: Direct operating cost of evaluated process options

Raw material requirements are the major cost contributor to the overall OPEX (22%-38% of OPEX) in all process options except MA-1 (9.5% of OPEX). The cost of spent LIBs was assumed to be $ 195/t based on the assumptions discussed in section 4.3.1. With an annual feed capacity of 868 tonnes, the LIBs cost will amount to $ 169 250 per annum which contributes between 2.0% (MA-2) and 5.7% (MA-1) to the total raw material cost. To improve the accuracy of the spent LIBs cost estimation, correspondence with companies that collect and handle e-waste such as eWASA, Cape E-waste or Desco is recommended.

NaOH and HCl are the raw materials required in the largest quantities for the mineral acid processes due to the large pH changes required between tanks (e.g. pH increase from 0 to 11 before Co precipitation in MA-1 and MA-2). The 28% ammonia solution added prior to Ni-DMG precipitation in MA-1 and MA-2 contributes to 33% and 12% of the raw material costs in MA-1 and MA-2 respectively. The low raw material cost of MA-1 ($ 3.41/kg LIB feed) can be ascribed to the membrane cells and hydrochloric acid synthesis units that regenerate most of the NaOH and HCl required for process operation. Thus, the raw material cost of MA-1 is 65.3% lower than that of MA-2 due to the NaOH cost and HCl cost decreasing with 93.5% and 87.3% respectively. Together, NaOH and HCl contribute to 80% of the raw material cost in MA-3.

Citric acid, hydrogen peroxide and sodium hydroxide are the main raw material expenses in the organic acid processes. The estimated raw material cost of OA-3 ($ 6.08/kg LIB feed) exceeds that of OA-1 ($ 4.76/kg LIB feed) and OA-2 ($ 4.96/kg LIB feed) although the process has only two metal recovery steps compared to the higher process complexity observed in OA-1 and OA-2. Mono-sodium phosphate (NaH_2PO_4) was selected as phosphate precipitant for both precipitation steps in OA-3 as suggested in the work done by Musariri (2019). However, mono-sodium phosphate ($ 1019/ton) is expensive compared to sodium phosphate ($ 373/ton) or phosphoric acid ($ 761/ton) which are typically used to facilitate phosphate precipitation from citrate leach solutions (refer to Table 25 in section 2.3.3). The high NaH_2PO_4 cost and the large amounts of NaOH required to neutralise the leach solution to pH 13 are the primary reasons for the high raw material cost in OA-3.

Utility costs were estimated based on the electricity, steam and cooling water requirements in each process. The utility costs of MA-1 are remarkably higher than that of any of the other process options and contribute to 8.3% of the total OPEX. The electricity consumption of the membrane cells (37.6% of utility cost), the cooling water required for cooling the HCl falling film absorber and the gases produced during membrane electrolysis (22.4% of utility cost) and the high steam requirements for the operation of two evaporators explain the high utility cost. The utility cost associated with OA-1 is the highest of the three organic acid process options due to the cooling water required to cool down the Mn precipitation tank to a temperature of 40-50℃. The utility cost of OA-3 is higher than that of OA-2 due to the additional high-pressure steam required to operate the Mn, Co and Ni precipitation tank at 50℃ as specified by Musariri (2019).

With regards to the other direct operating expenses, the following was noted:

1. The waste treatment costs for the facilities are very similar as illustrated in Figure 15. OA-2 have the highest waste treatment cost due to the additional liquid waste streams produced during MnC_2O_4 dissolution in a dilute oxalic acid solution and Mn precipitation from the Mn rich electrolyte.
2. The operating labour cost of MA-1 and OA-2 are the highest due to the additional process complexity that is added with the membrane electrolysis, hydrochloric acid production and solvent extraction sub-processes respectively.
3. Maintenance and repairs as well as operating supplies were calculated as functions of the fixed capital investment. Thus, it makes sense that these cost contributions are notably higher for MA-1 based on the results and discussion presented in section 5.4.
4. Although MA-1 have the lowest raw material cost, the utility, operating labour and fixed capital investment are higher than that of the other processes increasing the OPEX to $ 35.9/kg LIB processed.

The distribution of the direct, fixed and general operating costs is illustrated in Figure 16. Both fixed and general operating expenses are dependent on the fixed capital investment and operating labour costs. The contribution of the direct operating costs to the overall OPEX ranged between 47.2% (MA-1) and 65.4% (OA-3). Fixed operating costs contributed to between 21.2% (OA-3) and 38.3% (MA-1) of the total

OPEX. General operating costs contribute to between 13.5% (OA-3) and 14.5% (MA-1 and OA-2) of the total OPEX.

The overall OPEX of MA-3 ($ 17.8/kg LIB feed) is 10.8% higher than the OPEX of OA-3 ($ 16.09/kg LIB feed) although similar product streams are produced. Despite the differences in the distribution of the direct operating expenses of MA-3 and OA-3, the total direct expenses are similar (refer to Figure 15). Therefore, the higher OPEX of MA-3 can be explained by the higher CAPEX of MA-3 affecting the fixed and general operating expenses as seen in Figure 16.

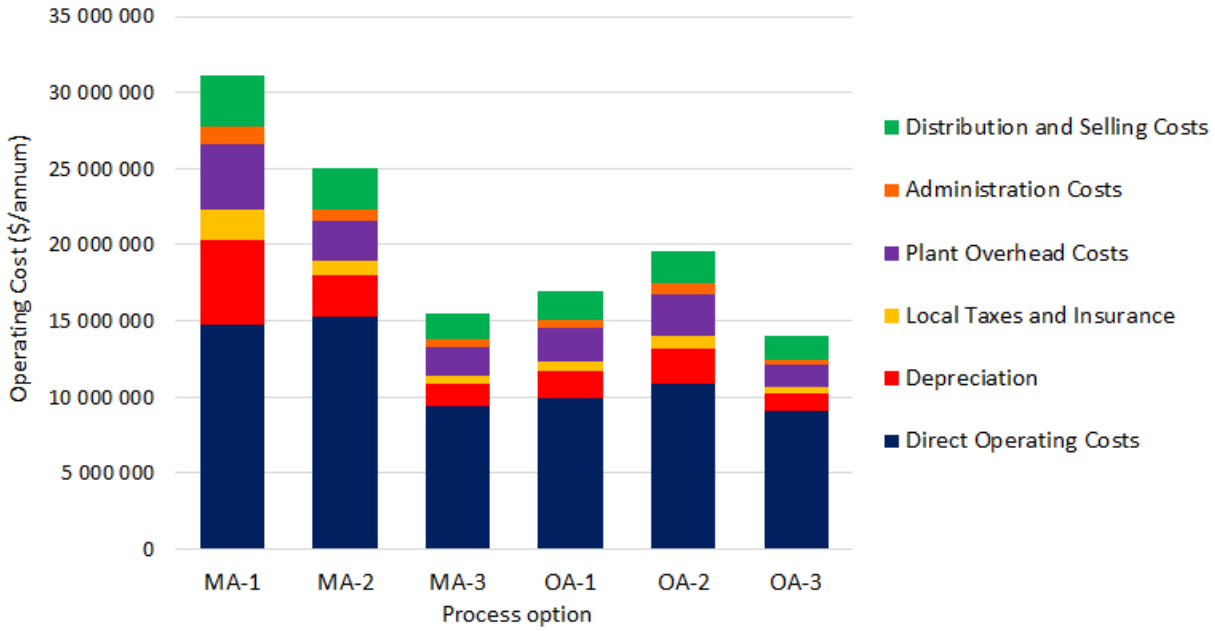

Figure 16: Direct, fixed and general operating expenses of the proposed process options

The OPEX estimated by Knights and Saloojee (2015) is an order of magnitude smaller than the corresponding values estimated for each of the proposed flowsheets. Only the cost of electricity, labour and raw materials were incorporated in their estimation of the OPEX whereas waste treatment, maintenance, taxes, administration and various other operating expenses were included in OPEX projections done in this study.

5.6 Project profitability

A project will only be profitable in its lifetime if the annual profit made is sufficient to pay back the initial fixed capital investment. Refer to Table 51 for the profit or loss made per kilogram of LIBs recycled in each facility. Annually MA-1, MA-2 and OA-2 will make a loss as the OPEX exceed the annual income. Therefore, profitable operation will only be possible with MA-3, OA-1 and OA-3 depending on the magnitude of the fixed capital investment that should be recovered within the project lifetime.

Table 51: Annual revenue, OPEX and profit before tax per kilogram of LIBs processed (values in $/kg LIB)

Process Option	MA-1	MA-2	MA-3	OA-1	OA-2	OA-3
Revenue	20.9	21.8	23.2	29.3	20.9	18.2
OPEX (including depreciation)	35.9	28.8	17.8	19.5	22.6	16.1
Profit (before tax)	-15.0	-7.6	5.4	9.8	-1.7	2.1

The project profitability of each LIB recycling facility was evaluated over a project lifetime of 20 years. Refer to Appendix F for the profitability analysis of each process option. The cumulative NPV of each process option is shown in Figure 17. Based on the graph, it was concluded that only OA-1 and MA-3 can be operated profitably as their cumulative NPV are greater than zero. The NPV of MA-1, MA-2 and OA-2 are negative as expected (based on Table 51), confirming that profitable operation will not be possible. Despite the annual loss made in OA-2, the cumulative NPV of OA-2 increases slightly after year 3 which seems contradicting. This trend is observed because depreciation is a tax-deductible expense but does not represent actual negative cash flow (refer to equation 189 and 190 in section 4.5). After tax calculations, the depreciation subtraction is reversed (equation 190) which results in a small positive cash flow in OA-2.

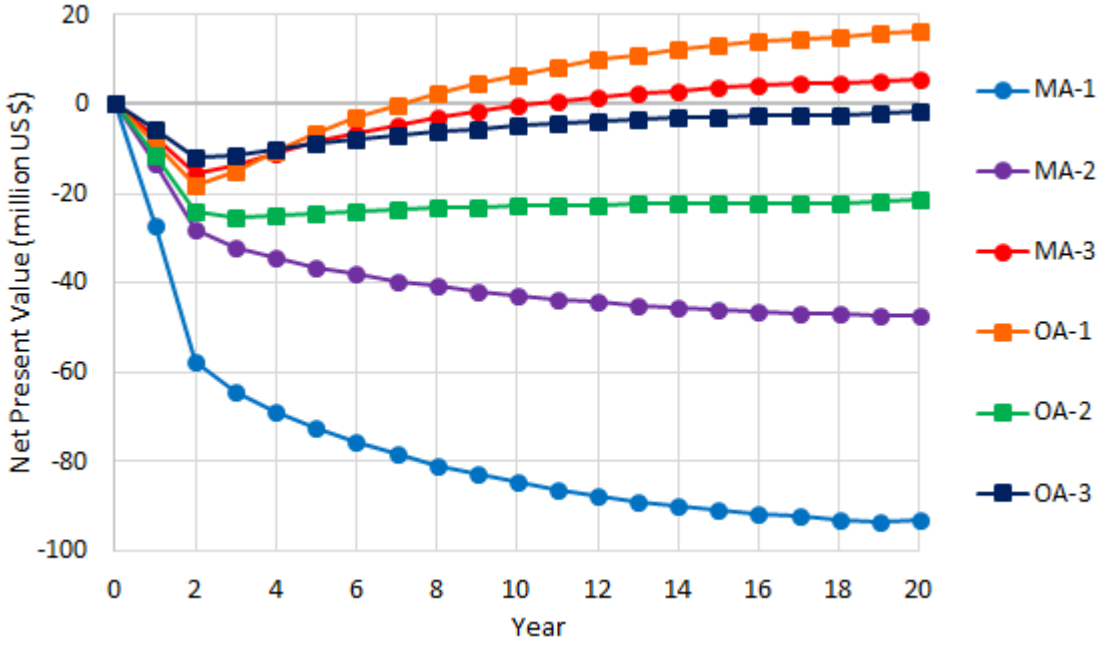

Figure 17: Net Present Value of mineral acid and organic acid process options

Although an annual profit is expected in OA-3 (refer to Table 51), it will be not be adequate to pay back the initial fixed capital investment as illustrated in Figure 17. Decreasing the CAPEX or OPEX or increasing the revenue of OA-3, to increase the annual profit margin may allow profitable operation. It should be noted that the estimated CAPEX of the organic acid processes are conservative as cheaper construction materials such as plastics (polypropylene, PVDF, PVC, PTFE etc.) will be suitable for these processes (Totton Pumps, 2008). The OPEX can be decreased by using a cheaper alternative precipitation agent instead of NaH_2PO_4 (refer to section 5.7.3).

Both the CAPEX ($ 0.95 vs. $ 1.23 per kg LIB feed) and OPEX ($ 16.1 vs. $ 17.8 per kg LIB feed) of OA-3 are lower than that of MA-3. Thus, the low income earned from OA-3 is the primary factor influencing its economic feasibility. The revenue of OA-3 producing a combined phosphate product, is 28.0% lower than the revenue of MA-3 producing a combined hydroxide product. This is because additional nickel and manganese salts are added to the system in MA-3 and a saleable NaCl product is produced in MA-3 increasing the revenue slightly. A high amount of uncertainty resides within the low combined phosphate product selling price. OA-3 will be able to break even (NPV=0) if the combined product could be sold at a price of $ 40 760/ton which is 3.65% higher than the estimated price ($ 39 324/ton). To achieve NPVs similar to that of MA-3 and OA-1, the combined phosphate product should be sold at approximately $ 45 450 and $ 54 370 per ton of phosphate product respectively.

Based on Figure 17 it can be concluded that MA-3 will be the preferred mineral acid process option whereas OA-1 will be the preferred organic acid process option. MA-3 is the most viable mineral acid process option primarily because of its reduced process complexity that resulted in a lower CAPEX and OPEX while still achieving high metal recoveries and product purities. Although the CAPEX and OPEX of OA-1 exceed that of OA-3, the high annual revenue and subsequent profit margin allow OA-3 to be the preferred organic acid process option.

The process proposed by Knights and Saloojee (2015) in the study conducted by CM Solutions was not financially viable (NPV = R -440 million). Consequently, they recommended that a levy or recycling fee should be charged to make the process self-sustaining. A recycling fee of R 8.12/kg LIBs processed allowed a break-even scenario when future cash flows were discounted at a rate of 9% over a project lifetime of 5 years. For comparison purposes, the NPV and recycling levy of the CM Solutions process were recalculated over an operational lifetime of 18 years based on the assumptions discussed in section 4.5. The NPV was determined as $ -35.68 million which is comparable to the NPVs of the evaluated processes.

Table 52 below compares the recycling fees required to return the NPV to zero (for processes with negative NPV) when discount rates of 9% and 15% are used. Compared to the fee proposed by CM Solutions, the recycling fee of MA-1, MA-2 and OA-2 are very high. Using an internal discount rate of 9%, no recycling fee will be required for OA-3 as an NPV of $ 3.7 million is projected. The influence of the internal discount rate can be evaluated by comparing calculated recycling levies when using a 9% and 15% discount rate. When using a 9% discount rate instead of 15%, the recycling levy decreased with 25.2%, 23.9% and 41.0% for MA-1, MA-2 and OA-2 respectively. Therefore, the internal discount rate has a notable influence on project profitability and should be chosen carefully.

Table 52: Minimum levy or recycling fee ($/kg LIB feed) required to break even

Process	CM Solutions	MA-1	MA-2	OA-2	OA-3
15% discount rate	0.74	27.01	13.62	6.85	0.61
9% discount rate	0.54	20.25	10.36	4.04	0.00

4 economic indicators were used to compare the profitability of the two profitable process options. The DCFROR, PVR, DPBP and NPV of MA-3 and OA-1 are summarized in Table 53 below. Both flowsheet

options have a PVR greater than 1 and DCFROR values that exceed 15% (internal discount rate) confirming the economic feasibility of these options.

Table 53: Economic indicators of the profitable flowsheet options

Economic indicator	MA-3	OA-1
Discounted Cash Flow Rate of Return (DCFROR)	20.69%	28.15%
Present Value Ratio (PVR)	1.34	1.83
Discounted Payback Period (DPBP) (years)	6.75	4.28
Net Present Value (NPV)	$ 5 687 787	$ 16 439 761

Despite the higher CAPEX and OPEX of OA-1 ($ 1.5 and $ 19.5 per kg LIB feed) compared to the CAPEX and OPEX of MA-3 ($ 1.2 and $ 17.8 per kg LIB feed), all calculated profitability criteria indicate higher economic feasibility with OA-1. This can be explained by the higher revenue earned ($ 29.3 vs. 23.2 per kg LIB feed) due to the higher value products produced in OA-1 compared to the combined Co, Mn, and Ni product produced in MA-3. The minimum annual revenue to return a NPV of zero over the project lifetime was calculated for both MA-3 and OA-1. MA-3 will break even if a minimum of 91.3% of the planned income is received whereas OA-1 requires only 80.2% of the planned income to return a NPV of zero. Therefore, the profitability of OA-1 is more robust to fluctuations in the revenue that may occur due to changing market conditions, metal price fluctuations or penalties paid for impurities in product streams.

Based on the economic indicators presented in Table 53, it can be concluded that OA-1 will be the techno-economically more favourable option for recovering valuable metals from end-of-life LIBs in South Africa. However, the choice between a mineral acid and organic acid leaching reagent is dependent on the type of products that should be produced by a LIB recycling facility. If the facility aims to selectively recover valuable metals in separate product streams, citric acid will be the more viable option. If a combined metal product suitable for cathode material regeneration should be produced, a hydrochloric acid based flowsheet will be a suitable option.

5.7 Evaluation of alternative operating conditions

5.7.1 Exclusion of metal ratio adjustment step in MA-3

As stated in section 5.3, the addition of $NiCl_2$ and $MnCl_2$ to adjust the Mn:Ni:Co ratio to 1:1:1 in MA-3 allowed the process to be more profitable when compared to OA-3 even though similar metal recoveries were achieved. To directly compare these processes, the metal ratio adjustment step in MA-3 was excluded and the profitability was re-evaluated.

The influence of excluding the metal ratio adjustment process step in MA-3 can be observed in Figure 18. The CAPEX and OPEX of MA-3 decreased with 3.9% and 7.7%, respectively, with the exclusion of the agitated metal ratio adjustment tank and metal chloride salt addition. However, the revenue decreased with 28.9% explaining the significant decrease seen in the NPV of MA-3. Similar metal recoveries are achieved but the production rate of the hydroxide product decreased with 32.8%. The feed to the

precipitation tank contains similar amounts of impurities (Fe and Cu) which co-precipitated with the hydroxide product at pH 11 in both cases. Similar impurity precipitation efficiencies combined with a lower production rate resulted in a lower hydroxide product purity (94.1% vs. 96.0%). Due to the lower production rate and lower product purity, only 83.1% (compared to 87.5% for MA-3) of the maximum theoretical revenue can be expected. The maximum theoretical revenue decreased with 25.1% with the exclusion of the ratio adjustment step.

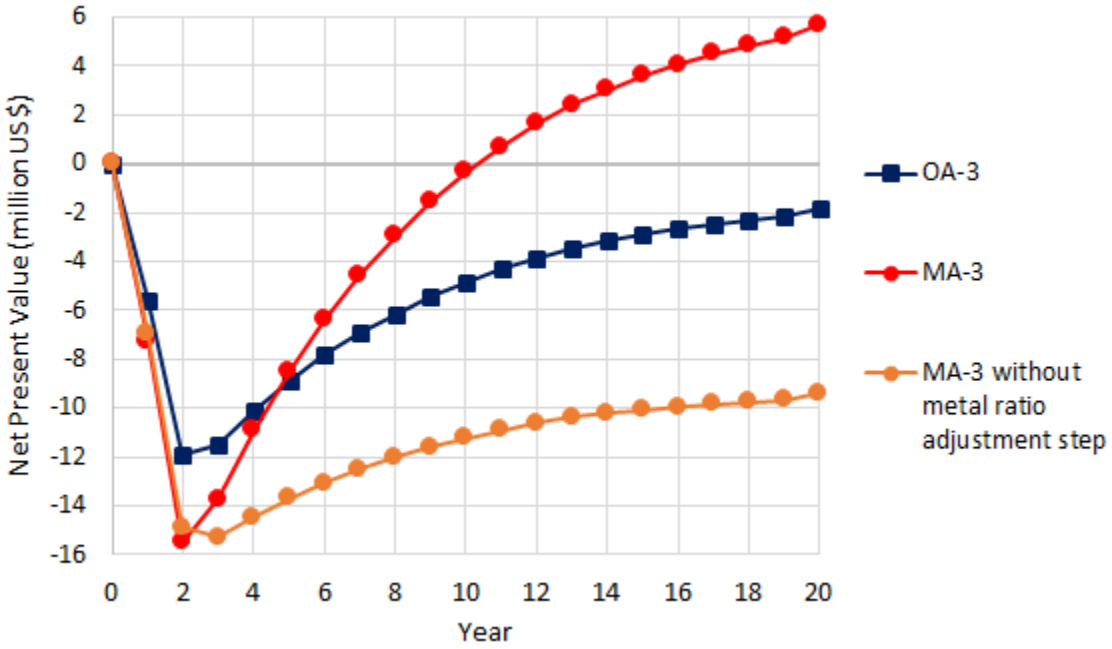

Figure 18: Comparison of NPV of OA-3 and MA-3 with and without the metal ratio adjustment step

Based on Figure 18, it can be concluded that MA-3 will only be more profitable than OA-3 if additional metal containing compounds are fed to the system. Investigation of low-cost metal additives that could be used to adjust the metal ratio in citrate systems may be worthwhile when considering the significant effect observed in Figure 18.

5.7.2 pH control in OA-1

As mentioned in section 3.6.1.5, no pH control was implemented for the cobalt or lithium precipitation tanks in organic acid process option 1. Similar process conditions as discussed in section 3.6.1 were used to complete mass and energy balances for OA-1 while implementing pH control at the cobalt precipitation tank (pH=6) and lithium precipitation tank (pH=13-14).

Raw material costs increased with 3.3% due to the additional sodium hydroxide required to neutralize excess oxalic and citric acid in solution. This gave rise to a higher OPEX which resulted in the NPV decreasing with 3%. Despite the implementation of pH control and the observed decrease in the NPV, OA-1 will still be the most profitable flowsheet option when compared with the other evaluated alternatives. The effect of pH control on the economic indicators of OA-1 are summarized in Table 54.

Table 54: Effect of pH control on the profitability of OA-1

Economic indicator	OA-1 (without pH control)	OA-1 (with pH control)
Discounted Cash Flow Rate of Return (DCFROR)	28.15%	27.70%
Present Value Ratio (PVR)	1.83	1.80
Discounted Payback Period (DPBP) (years)	4.28	4.38
Net Present Value (NPV)	$ 16 439 761	$ 15 947 976

5.7.3 Alternative precipitation agent in OA-3

As mentioned in section 5.5, mono-sodium phosphate used as precipitation agent in OA-3 can be substituted with sodium phosphate or phosphoric acid to improve the financial feasibility of the process. To investigate the effect of the precipitation agent on the profitability criteria, mono-sodium phosphate was substituted with sodium phosphate. The assumptions made for mass and energy balance calculations were the same as discussed in section 3.6.3 except for the use of Na_3PO_4 instead of NaH_2PO_4 as precipitation agent. The effect of substituting NaH_2PO_4 with Na_3PO_4 on the raw material cost, OPEX, CAPEX and revenue are summarized in Table 55.

Table 55: Effect of using an alternative precipitant in OA-3 on cost indicators

OA-3 Precipitant	NaH_2PO_4	Na_3PO_4
Raw Materials	$ 5 280 804	$ 3 473 445
OPEX	$ 13 966 237	$ 11 848 414
CAPEX	$ 14 778 114	$ 14 533 951
Revenue	$ 15 755 830	$ 15 808 600

The use of Na_3PO_4 instead of NaH_2PO_4 has the largest effect on the raw material cost and subsequently the OPEX. Raw material costs decreased with 34.2% whereas the overall OPEX decreased with 15.2%. This makes sense as NaH_2PO_4 ($ 1019/ton) is expensive compared to Na_3PO_4 ($ 373/ton) and large amounts of NaOH are required to neutralize the excess NaH_2PO_4 to maintain precipitation tanks at pH 13-14. Small changes in the CAPEX (-1.7%) and revenue (+0.3%) were also observed.

The observed decrease in the OPEX has a net positive effect on the profitability of the process as seen in Figure 19 below. The NPV increased from $ -1.82 million to $ 5.64 million when Na_3PO_4 was used as precipitant. The notable difference between the NPVs provides an indication of the high sensitivity of the project profitability to changes in the OPEX. Despite the higher CAPEX and OPEX, the NPV of MA-3 ($ 5.69 million) is slightly higher than the NPV returned by the alternative OA-3 option using Na_3PO_4 as precipitant.

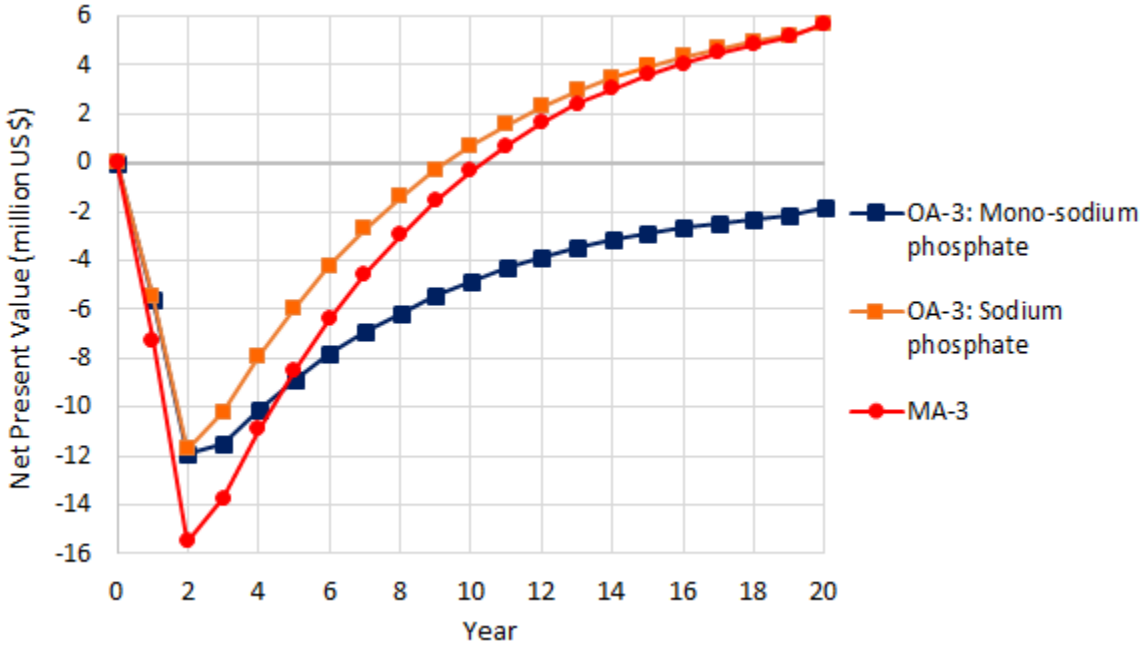

Figure 19: Comparison of NPV of alternative process option with original processes (MA-3 and OA-3)

The economic indicators of the three process options compared in Figure 19 are tabulated in Table 56. The unprofitable operation of OA-3 (using NaH_2PO_4 as precipitant) is verified by the PVR of 0.86 which is smaller than 1 and the DCFROR of 12.47% which is smaller than the internal discount rate of 15%. The PVR, DCFROR and DPBP of OA-3 (using Na_3PO_4) indicate better financial feasibility compared to MA-3 even though the NPV of MA-3 is greater than the NPV of OA-3 (using Na_3PO_4) which seems contradicting. This makes sense when the CAPEX ($ 1.23 vs. $ 0.93 per kg LIB feed), OPEX ($ 17.8 vs. $ 13.7 per kg LIB feed) and revenue ($ 23.2 vs. $ 18.2 per kg LIB feed) of MA-3 is compared with that of OA-3 (using Na_3PO_4).

Table 56: Comparison of economic indicators of MA-3 and OA-3 with alternative process option

Economic indicator	**MA-3**	**OA-3 (NaH_2PO_4)**	**OA-3 (Na_3PO_4)**
Discounted Cash Flow Rate of Return (DCFROR)	20.69%	12.47%	22.35%
Present Value Ratio (PVR)	1.34	0.86	1.45
Discounted Payback Period (DPBP) (years)	6.75	-	5.99
Net Present Value (NPV)	$ 5 687 787	$ -1 815 757	$ 5 636 094

The NPV and CAPEX of MA-3 is 0.92% and 32.3% higher than that of OA-3 (using Na_3PO_4), justifying the lower PVR and DCFROR values of MA-3. Thus, a smaller relative return on the initial fixed capital investment should be expected with MA-3. MA-3 will also require a longer period to recover the fixed capital investment even though the profit margin of MA-3 is higher. Based on the economic analysis done, it was concluded that profitable operation of OA-3 might be possible using Na_3PO_4 as precipitant. Therefore, both organic acids and mineral acids can potentially be used to recover valuable metals from end-of-life LIBs to produce a combined Ni, Co and Mn product. Experimental work to assess the viability of combined Ni, Co and Mn phosphate precipitation with sodium phosphate is recommended.

6 Sensitivity Analysis

The mass balance and economic models used to estimate the profitability of the process facilities were based on various assumptions and correlations as discussed in Chapters 3 and 4. Thus, uncertainty resides within the estimated economic indicators. The aim of the sensitivity analysis was to investigate the effect of changing market and operating conditions on the profitability criteria and to quantify the risk involved with investing capital in the LIB recycling project.

Based on the results presented and discussed in Chapter 5, it was concluded that OA-1 will be the techno-economically most favourable flowsheet option for valuable metal recovery from LIB waste. Thus, the sensitivity analysis was performed on OA-1 only.

6.1 Effect of individual variables

Before the effect of multi-variable interaction on the NPV could be assessed, the sensitivity (S) of the NPV to variation in individual variables were determined with equation 193 (Turton *et al.*, 2012). The sensitivity of the NPV to each variable was calculated by varying the specific variable from its base value while keeping all other variables constant. Therefore, interaction between parameters and the possible effect thereof on the profitability was not considered in this section.

$$S_1 \approx \left[\frac{\Delta NPV}{\Delta x_1}\right]_{x_2, x_3, \ldots x_n} \quad [\ 193\ ]$$

Due to the straight-line relationships observed between the NPV and the changes in variables, linear regression was used to determine the slope of each curve. The slope of each straight line equals the NPV sensitivity to fluctuations in each variable (according to equation 193).

6.1.1 Capital cost

Changes in the fixed capital investment (FCI), working capital and salvage value will directly influence the total CAPEX of the project and subsequently the NPV and other financial indicators. These CAPEX contributors were varied independently from each other while keeping the other 2 factors at their respective base values. The outcome is graphically presented in Figure 20. In general, increasing the capital costs will have a negative effect on the NPV as seen in the response curves of the FCI and working capital. The salvage value of the facility will have the opposite effect as an increase in the salvage value will result in an increase in the NPV.

When comparing the slopes of the three straight-line graphs in Figure 20, it is clear that fluctuations in the FCI have a remarkably greater effect on the NPV than similar fluctuations in the working capital or salvage value. This makes sense as the FCI accounts for all purchased equipment, installation, instrumentation, buildings as well as indirect capital costs. For a 1% increase in the fixed capital investment a decrease in the NPV of $ 256 240 can be expected. Similarly, a decrease of $ 20 636 and an increase of $ 694 can be anticipated if the working capital and salvage value are increased with 1% respectively. Thus, it can be concluded that the profitability of OA-3 are relatively robust to fluctuations in the working capital and salvage value.

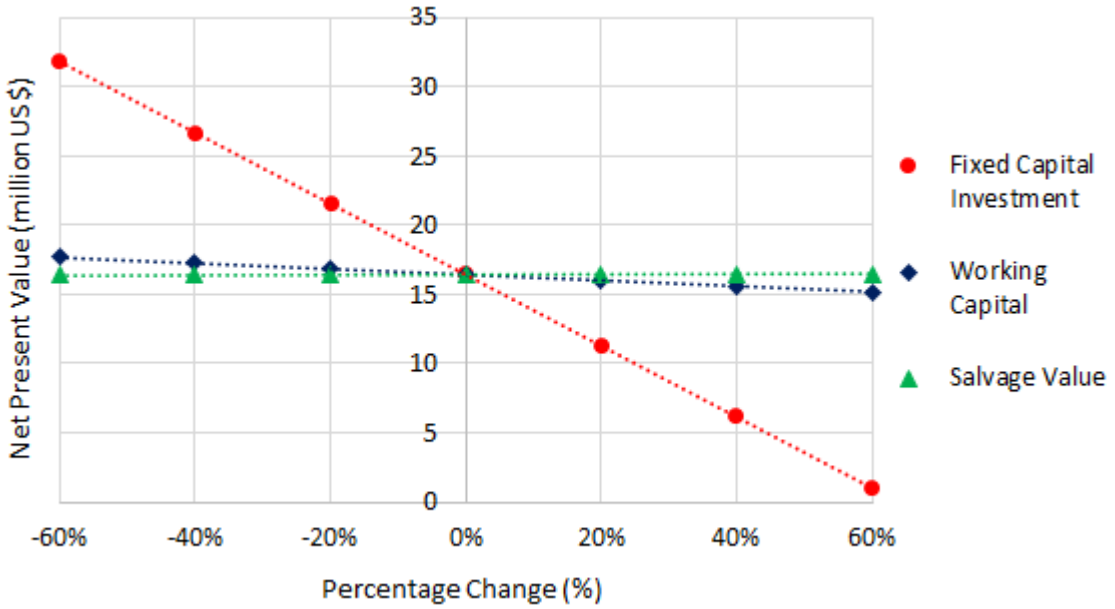

Figure 20: Sensitivity of the NPV to fluctuations in FCI, salvage value and working capital

Fluctuations in the overall CAPEX caused the Present Value Ratio (PVR) to deviate from its base value of 1.83 as illustrated in Figure 21. This makes sense as the PVR is calculated as a function of the initial fixed capital investment and the NPV. A straight-line relationship was not observed. According to the graph, a 60% increase in the CAPEX will return a PVR of approximately 1 corresponding to a break-even scenario. A 60% increase in the CAPEX is highly unlikely when one considers the relatively low CAPEX estimated by CM Solutions for a facility with a much higher feed rate (refer to section 5.4) and the contingency of 37% of the delivered equipment cost that was included in the original CAPEX projections.

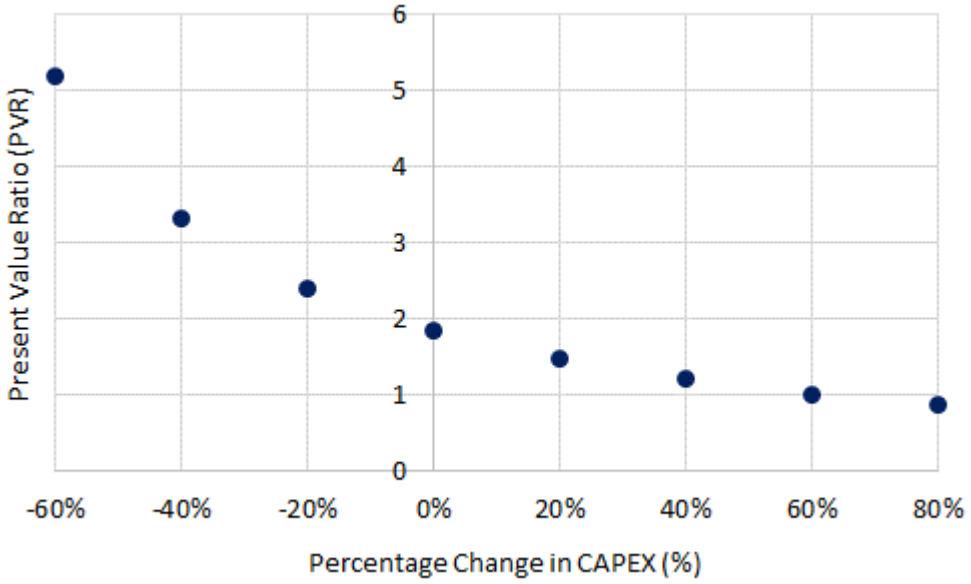

Figure 21: Present Value Ratio as a function of fluctuations in the CAPEX from its estimated value

6.1.2 Operating cost

Operating cost estimations were calculated as a function of the raw material, operating labour, waste treatment and utility costs. Uncertainty in these cost factors would influence the accuracy of the overall OPEX. The sensitivity of the NPV to changes in these operating costs is graphically presented in Figure 22 below. The negative slopes of the graphs depict the expected inverse proportionality between the operating costs and the profitability of the recycling facility.

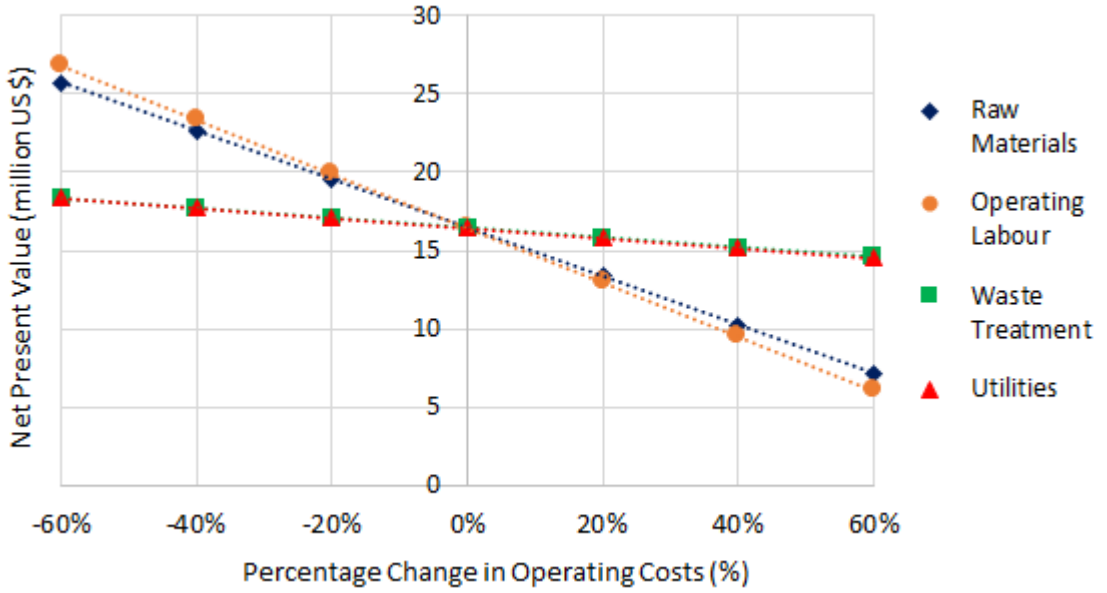

Figure 22: Sensitivity of the NPV to fluctuations in operating costs

The profitability of the proposed process is more robust to changes in waste treatment and utility costs compared to raw materials and operating labour as depicted by the slopes of the linear graphs in Figure 22. This is because raw materials and operating labour contributes to 24.4% and 12.2% of the OPEX compared to 5.0% and 4.9% for utilities and waste treatment respectively. A 1% decrease in the waste treatment and utility cost will result in a $ 31 417 and $ 31 776 increase in the NPV respectively.

Although operating labour contributes to a smaller fraction of the total OPEX compared to raw materials, the project profitability is more sensitive to changes in the operating labour. This is because the direct supervisory, laboratory charges and other operating expenses were calculated as functions of the operating labour cost. The NPV will be increased with approximately $ 154 850 compared to $ 172 700 if the raw materials and operating labour cost are 1% less than the original estimates.

Efforts to minimize operating costs should focus on raw materials and operating labour requirements. Raw material costs could be decreased by using cheaper alternative reagents or decreasing the excess amount of reagents fed to units. However, laboratory work will be required to test if similar metal recoveries will be attainable with alternative reagents or concentrations. Operating labour costs could be decreased by improving the level of automation and energy-efficiency of equipment. Additional capital will be required to make these improvements.

6.1.3 *Metal selling prices*

The feed composition, metal selling prices, metal recoveries and product purities are the key factors influencing the process revenue. Figure 23 below illustrates the sensitivity of the project profitability to changes in the selling prices of the 4 metal products produced in OA-1.

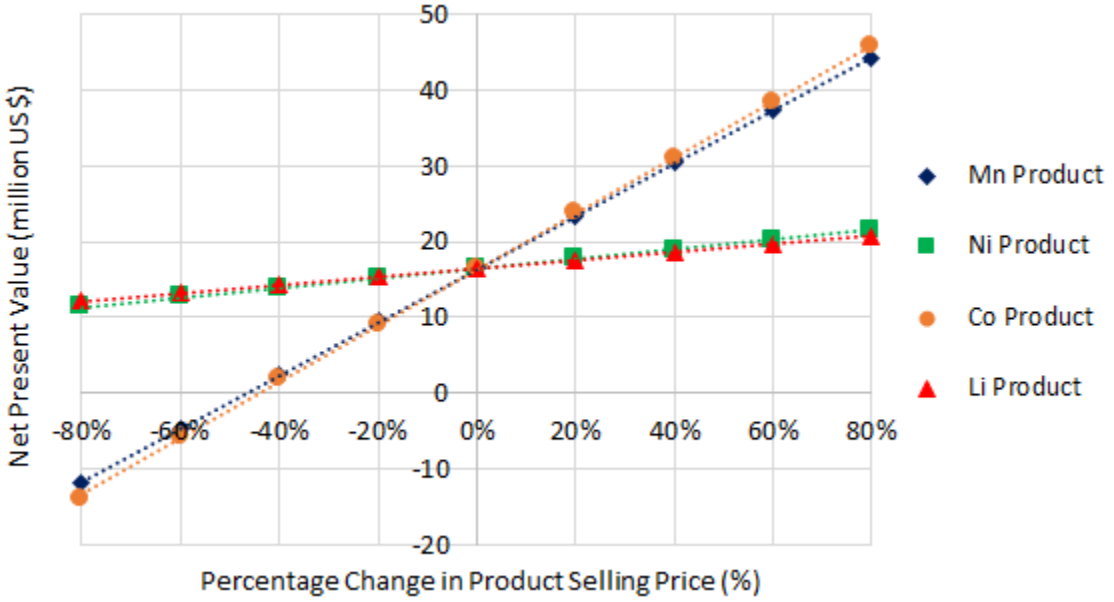

Figure 23: Sensitivity of the NPV to fluctuations in metal product selling prices

The project profitability is more robust to fluctuations in the selling prices of the nickel and lithium products ($Ni(OH)_2$ and Li_3PO_4 powders) compared to the selling prices of the cobalt and manganese products (CoC_2O_4 and MnO_2 powders), as depicted in Figure 23. This makes sense as 44.1% of the annual revenue is earned from cobalt, 41.9% from manganese, 7.6% from nickel and 6.5% from lithium. An 1% increase in the nickel and lithium selling prices will result in a $ 63 152 and $ 53 755 increase in the projected NPV respectively. For a 1% increase in the cobalt and manganese product selling prices, the NPV will correspondingly increase with $ 369 800 and $ 350 060.

A high amount of uncertainty resides within the assumed product selling prices due to the global market fluctuations observed in pure metal prices. Historical price fluctuations were considered in the Monte Carlo simulations discussed in section 6.2. The penalties that will be paid for impurities in the products is another factor contributing to possible inaccuracies in the estimation of the annual revenue that will be earned. Market research focussing on the prices that potential customers will be willing to pay for products should be undertaken to improve the accuracy of the selling prices used in the economic analysis. This will also provide an indication of how impurities in the product will influence the price that customers will realistically pay for products.

Investing additional capital to expand the recycling facility to enable the production of high purity laboratory quality products may positively affect the profitability of the project. The laboratory product prices demanded by companies such as Sigma Aldrich and Alfa Aeser are on average an order of magnitude greater than the assumed selling prices obtained from Alibaba.com (refer to Table 45 and

Table 46). The annual revenue increased from $ 25.5 to $ 391.0 million when the laboratory product prices were used instead of the assumed Alibaba prices (CAPEX and OPEX at base values).

However, a detailed process design and economic analysis that investigate the effect of the additional capital and operating costs required to produce high purity products is recommended to determine if it will be financially feasible. Market research and analysis should be conducted to understand the demand for different types of products (e.g. battery grade products, high purity lab products, combined metal products for cathode material regeneration) within a South African context. Opportunities for export should also be explored if the local demand for specific products does not indicate long-term financial feasibility.

6.1.4 Feed capacity

Economy of scale is a widely accepted concept stating that production or operation on a larger scale generally becomes more economical. Economy of scale was considered in the sensitivity analysis to determine what the LIB feed capacity of the smallest possible recycling facility should be for the proposed project to return an NPV of zero over the project lifetime of 20 years. Mass and energy balance calculations were redone for every LIB feed rate investigated and used to determine a new NPV corresponding to that specific feed capacity. The relationship between the NPV and the annual LIB feed capacity is depicted in Figure 24 below.

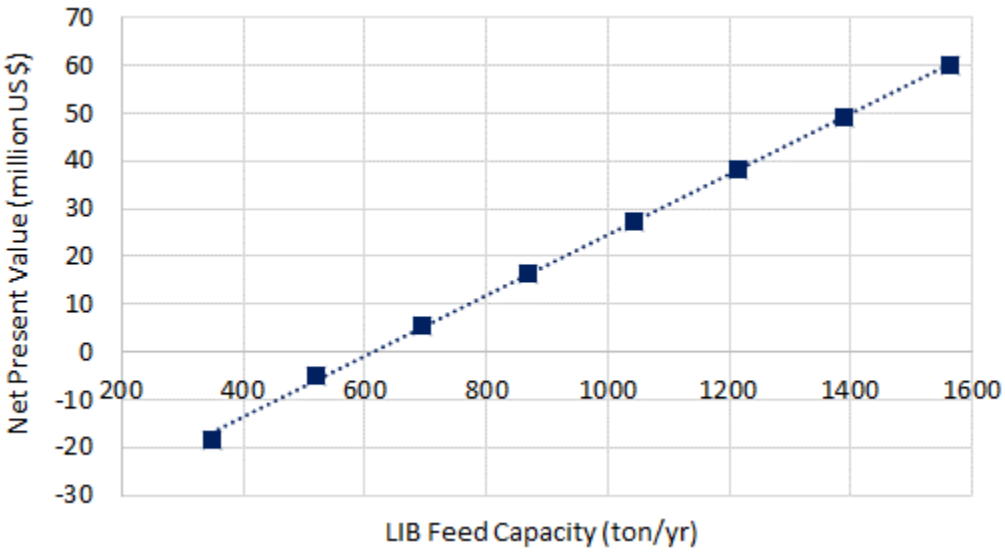

Figure 24: Net Present Value as a function of the annual LIB feed capacity

Based on the straight-line relationship observed in Figure 24, a LIB feed capacity of 615 ton per year will be the minimum requirement to allow a break-even scenario. This corresponds to a decrease of 29.1% from the assumed base feed capacity of 868 ton LIB waste per year. Thus, for a 1% increase in the feed capacity, the NPV will increase with approximately $ 552 440. Compared to the fixed capital investment, the NPV is 2.2 times more sensitive to the feed capacity. The observation makes sense as the feed capacity has a notable influence on the CAPEX, OPEX and revenue and is therefore a crucial factor to consider when making financial projections concerning any chemical processing facility.

The chances of profitably operating a LIB recycling facility in South Africa will increase if the facility could be designed for operation at a higher feed capacity. Therefore, detailed market analysis concerning the production and lifetime of LIBs and the collection and recycling rates of spent LIBs in South Africa is recommended to improve the accuracy of the LIB feed capacity approximations used in this study.

Although an annual increase of 10% in South African e-waste was predicted (Knights and Saloojee, 2015), only 8-12% of e-waste are currently recycled with the balance being landfilled. Recycling e-waste locally instead of exporting the waste could potentially provide 25 jobs per 1000 tonnes of handled waste and could therefore have a positive socio-economic impact on South Africa (Naidoo, 2017). Growing South Africa's e-waste recycling sector will give rise to opportunities for the development of and investment in innovative new technologies. The following strategies or approaches to improve the availability of LIB waste in South Africa should be explored:

1. Legislation directing the collection and recycling of LIB waste should be implemented. The directive can be similar to the "Battery Directive" implemented by the European Union in 2006 prescribing a minimum battery collection rate of 25% in 2012 and of 45% in 2016. Furthermore, a recycling efficiency of 50% (by weight) should be achieved (Georgi-Maschler *et al.*, 2012; Knights and Saloojee, 2015).
2. A compulsory "take-back" system where consumers will be allowed to take any end-of-life products back to its suppliers should be implemented as soon as legally possible (Baloyi, no date). If the public actively participates in taking spent LIBs back to suppliers, these companies will collect LIBs that could be sent to a local recycling facility.
3. The general public should be educated regarding the recycling of LIBs and encouraged to separate their electronic waste from domestic refuse at household level. Companies collecting their end-of-life LIBs should receive incentives or pay fines to encourage the collection and recycling of LIB waste.
4. Companies that are currently collecting and exporting spent LIBs should be consulted to determine if they would be willing to partner with a local LIB recycling facility rather than exporting their waste.
5. Currently not a single LIB recycling facility is located on the African continent and end-of-life LIBs are either exported or landfilled. Therefore, importing LIB waste from nearby African countries should also be considered.

The future adoption of electric vehicles (EVs) in South Africa is an important factor to account for when designing a LIB recycling facility. Various sources predict a rising demand and growth in the EV market while others do not see EVs as a suitable alternative for fuel-based vehicles in the near future. Market research concerning the electric vehicle market is recommended as it may notably affect the feed capacity and feed composition to the proposed LIB recycling facility.

Knights and Saloojee (2015) recommended charging a recycling fee or levy on every battery that is sold. The levy could fall under the "Extended Producer Responsibility" framework in the Waste Act. The collected money could be used to advance the LIB recycling industry. To shift the South African vehicle market towards EV sales, the levy could alternatively be charged on the purchase of fossil-fuels or as license fee for fossil-fuel vehicles. Implementing the levy could motivate the public towards increased

environmental responsibility and the adoption of electric vehicles. However, the levy will only be collected while there is an adequate demand in the fossil fuel vehicle market (Knights and Saloojee, 2015).

Although growth in the South African EV market is expected by various experts, some sources are pessimistic about the feasibility of EVs in the near future. South Africa's unstable electricity supply and the increasing pressure on the electricity grid are the main reasons. Electric vehicles are designed to be an environmentally friendly alternative reducing the amount of greenhouse gases released by fuel-based vehicles. However, South Africa's electricity is generated by the combustion of coal (non-renewable fossil fuel), implying that the use of EVs will not decrease the country's carbon footprint. Using solar energy to power EV charging stations may be an environmentally friendly option worth investigating in the future.

6.1.5 Feed composition

To investigate the effect of the cathode material feed composition, the mass fraction of each cathode type in the feed was changed with certain percentages above and below its base mass fraction (refer to Table 28). The other 4 cathode types were increased or decreased proportionally to ensure that sum of the mass fractions equals 1. Thus, the feed composition could not be varied independently for each cathode type. The results are graphically presented in Figure 25. The cathode materials were abbreviated as LFP ($LiFePO_4$), LCO ($LiCoO_2$), NMC ($LiNi_{0.33}Mn_{0.33}Co_{0.33}O_2$), LMO ($LiMn_2O_4$) and LNO ($LiNiO_2$) as seen in the legend of Figure 25.

Based on Figure 25, it is clear that LCO have the greatest effect on the project profitability causing the NPV to increase with $ 107 440 with every 1% increase in the mass fraction of LCO in the feed cathode material. This was expected as cobalt is the main source of income and metal with the highest intrinsic value (refer sections 5.3 and 6.1.3). If the mass fraction of LFP, LNO, NMC or LMO in the feed increase, the mass fraction of LCO will proportionally decrease which will have a negative effect on the profitability explaining the negative slopes associated with LFP, LNO, NMC and LMO.

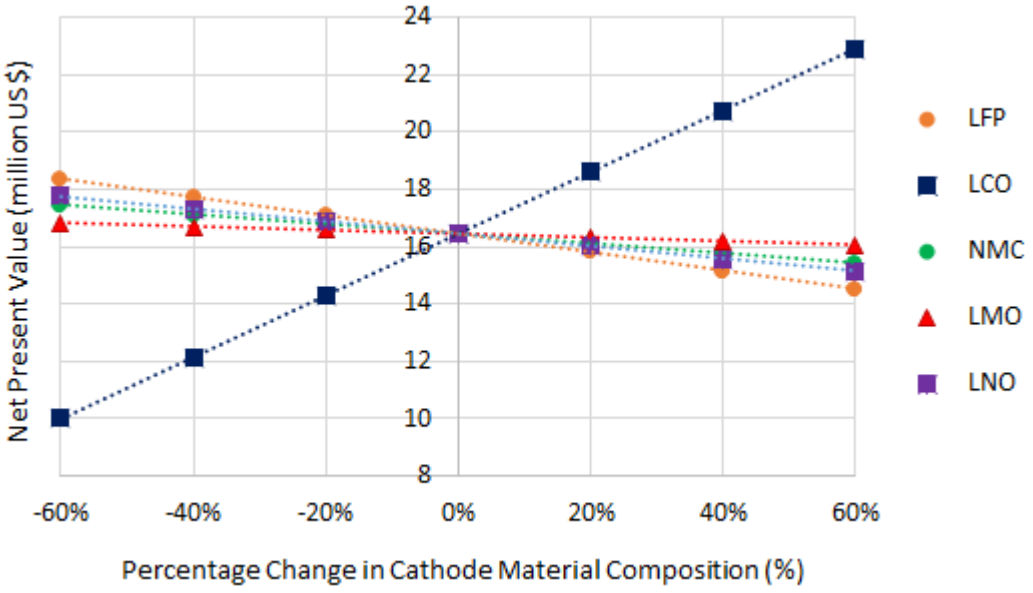

Figure 25: Sensitivity of the NPV to fluctuations in cathode feed material composition

Although $LiCoO_2$ (LCO) is simple to manufacture and has better performance in voltage stability, capacity, reversibility and charging efficiency compared to the other cathode materials, cobalt is very expensive and is also known for its volatile price, toxicity and geopolitical instability (Zou *et al.*, 2013; Croy and Claxton, 2019). Thus, the expected future market trend is a decline in the production of $LiCoO_2$ to produce cheaper alternative cathode types.

$LiFePO_4$ (LFP) is a non-layered cathode material that has been mainly used by Chinese EV manufacturers. Although LFP is the cheapest cathode material for EV applications, it is expected to be phased out and replaced by layered cathode chemistries with higher energy densities. A similar trend is expected for LMO cathode materials (Olivetti *et al.*, 2017).

$LiNi_{0.33}Mn_{0.33}Co_{0.33}O_2$ is cheaper than $LiCoO_2$ and have greater performance and safety compared to $LiFePO_4$, $LiNiO_2$ and $LiMn_2O_4$ (Zou *et al.*, 2013). Therefore, global cathode markets are shifting towards nickel-manganese-cobalt (NMC) batteries especially for the electric vehicle industry. To improve the cost efficiency of NMC batteries, the typical Ni:Co:Mn ratio of 1:1:1 will be shifted to higher nickel ratios such as 6:2:2 and 8:1:1 in the future (Jaffe, 2017; Croy and Claxton, 2019; Roskill, 2019). For example, Olivetti *et al.* (2017) estimated that the electric vehicle cathode market share will be 50% NMC-6:2:2, 35% NMC-1:1:1 and 15% NMC-8:1:1 in 2025. The tendency towards higher nickel ratios in cathode chemistries will also bring its challenges. As the amount of nickel increases the management of the overall stability and safety of the batteries become more difficult. The development of layered-layered-spinel (LLS) Mn-rich cathodes consisting of approximately 50% or more Mn and less than 35% Ni may prove to be a competitive alternative for low cost, safe, high-energy batteries (Croy and Claxton, 2019).

According to projections made, the global LIB recycling market share could be worth $ 2.2 billion by 2022 (Olivetti *et al.*, 2017). However, the economic incentive for recycling LIBs will be influenced by the future cathode chemistries of electric vehicles. The observed decline in the manufacturing and use of $LiCoO_2$ as cathode material in LIBs will negatively affect the financial feasibility of the recycling processes. Therefore, research regarding the market share of the various cathode material types in South Africa should be conducted.

6.1.6 Pre-treatment losses

According to Jinhui Li, Shi *et al.* (2009), 8% of the valuable electrode material in the LIB feed are lost during the proposed mechanical pre-treatment steps (refer to section 3.4). Therefore, maximum metal recoveries of 92% are attainable over the entire flowsheet. Metal recoveries have a direct impact on the process revenue and subsequently the project profitability. Refer to Figure 26 for a graphical presentation of the inversely proportional relationship between the NPV and pre-treatment losses. The NPV of the project decreases with $ 646 750 if the pre-treatment losses increase with 1%. Extrapolating the graph in Figure 26, the project will reach a break-even situation (NPV=0) if 33.4% of the valuable electrode material is lost during pre-treatment.

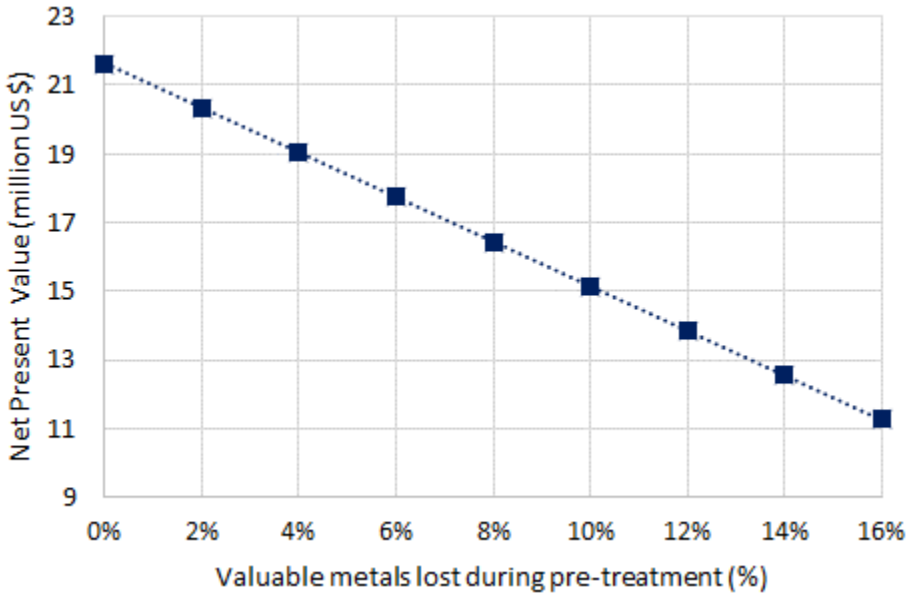

Figure 26: Effect of pre-treatment losses on process profitability

To improve metal recoveries and in turn process revenues, an alternative pre-treatment method can be implemented to reduce the loss of valuable cathode materials during the pre-treatment phase. Physically dismantling LIBs may reduce pre-treatment losses and is a viable alternative option in a South African context. Physical battery dismantling can potentially provide jobs for many South Africans that are currently unemployed. However, the additional labour cost should be weighed against the expected increase in revenue to determine the financial feasibility of physical dismantling as pre-treatment method.

Designing batteries with recycling and dismantling in mind will improve the efficiency and feasibility of using physical dismantling in the pre-treatment phase (Gaines, 2014). An advantage of using physical dismantling rather than crushing or milling is that the different material fractions (e.g. plastics, steel, paper and electrodes) can be kept separate without additional separation steps. Anode and cathode material can be separated prior to leaching, thus reducing the amount of carbon, copper and other impurities that enter the leaching tank. This will have a positive effect on the product purities.

Another alternative may be to outsource the pre-treatment of the raw LIBs to another recycling company and to buy the dismantled battery cathodes as a raw material. Economic analyses focussing on the financial feasibility of various pre-treatment methods will provide useful information that may guide final decision-making.

6.1.7 Concluding remarks

To conclude the individual variable sensitivity analysis presented and discussed in section 6.1, the sensitivity of the NPV to the overall CAPEX, OPEX, revenue and feed capacity were compared. Figure 27 is a graphical representation of the sensitivity of the profitability to the mentioned parameters.

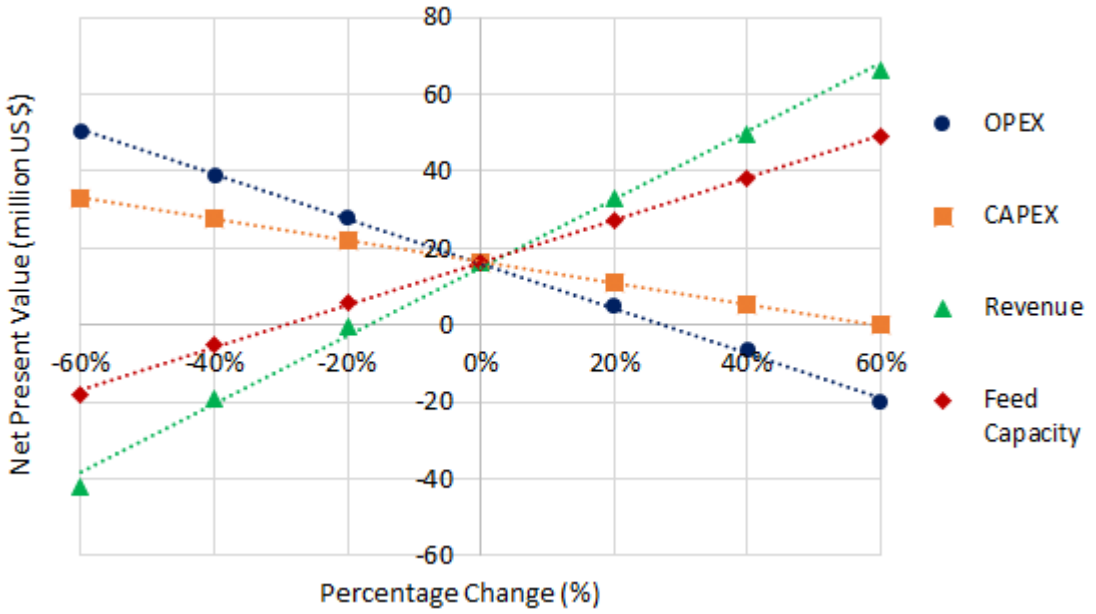

Figure 27: Comparison of the effect of OPEX, CAPEX, revenue and feed capacity on the NPV

After linear regression was applied to each set of data points, the NPV sensitivities were calculated as shown in Table 57 below. The results obtained compare well with the sensitivity analysis performed in the study by CM Solutions as they also found that the profitability will be more robust to changes in the CAPEX than similar fluctuations in the OPEX (Knights and Saloojee, 2015). The NPV is 2.1 times more sensitive to fluctuations in the OPEX compared to the CAPEX. Thus, investing additional capital to allow the minimization of operating costs may improve the chances of profitable operation.

Table 57: NPV sensitivity to key parameters

Parameter	CAPEX	OPEX	Revenue	Feed Capacity
Sensitivity (million USD per 1% increase in respective variable)	-0.2765	-0.5807	0.8860	0.5524

The financial feasibility of the LIB recycling facility is most sensitive to the revenue with the OPEX and feed capacity following. Therefore, optimization efforts should focus on increasing the revenue and feed capacity while decreasing the OPEX. The accuracy of profitability estimations could be improved by concentrating on eliminating uncertainties in the projection of the revenue, OPEX and feed capacity.

6.2 Monte Carlo simulation

6.2.1 Assumptions and input specifications

The Monte Carlo method is a probabilistic approach to quantifying risk associated with projects by investigating the effect of multi-variable interaction on the profitability criteria of a project. The simulations provide an indication of how robust the project profitability is to the random interaction of various parameters. The Monte Carlo technique is based on the principle of selecting probability distributions for all variables, repeatedly sampling random values from the chosen distributions and using

them in a model, function or correlation to calculate the value of an output parameter (e.g. the NPV in this case).

17 process or costing parameters in which uncertainty resides, were identified as variables for the Monte Carlo simulations. Triangular probability distributions with an estimated maximum, minimum and mode value were assigned to each variable in the simulation. Triangular probability distributions give a more realistic distribution of possible outcomes as it is a good model for skewed distributions. The base case values which were calculated based on the assumptions and correlations discussed in Chapters 3 and 4 were assumed as the mode values in each triangular probability distribution. The minimum and maximum bounds were expressed as percentages of the base case values. Minimum and maximum bounds for CAPEX and OPEX related variables were based on the ranges suggested by Turton *et al.* (2012) and are tabulated in Table 58 below.

Table 58: Minimum and maximum bounds for CAPEX and OPEX variables (Turton *et al.*, 2012)

Variable	Minimum	Maximum
Fixed Capital Investment	-20%	+30%
Working Capital	-20%	+50%
Salvage Value	-100%	+10%
Raw Materials	-10%	+10%
Operating Labour	-10%	+10%
Utilities	-10%	+10%
Waste Treatment	-10%	+10%

Three input maximum and minimum combinations were evaluated for the selling prices of the various metals. The various minimum and maximum combinations are summarized in Table 59. Refer to Appendix B for sample calculations of how the Shanghai Metals Market and pure metal price fluctuation limits were determined. The pure metal price fluctuation limits were used based on the assumption that the selling price of metal products (CoC_2O_4, MnO_2, $Ni(OH)_2$ and Li_3PO_4) will be directly influenced by the market price of the pure metals (Co, Ni, Mn, and Li).

Table 59: Metal product selling price input specifications for Monte Carlo simulations

Input Specification	Shanghai Metals Market		Turton *et al.* (2012)		Pure Metal Price Fluctuations	
Variable	Minimum	Maximum	Minimum	Maximum	Minimum	Maximum
MnO_2 Selling Price	-47%	+0%	-20%	+5%	-38%	+59%
$Ni(OH)_2$ Selling Price	-58%	+0%	-20%	+5%	-42%	+58%
CoC_2O_4 Selling Price	-69%	+0%	-20%	+5%	-38%	+97%
Li_3PO_4 Selling Price	-28%	+0%	-20%	+5%	-34%	+88%

A base case LIB feed capacity of 868 ton/year was assumed based on the assumptions discussed in section 3.2.1. The LIB feed predicted based on the South African State of Waste Report published in 2018 is 779 ton/yr which is approximately 10% below the base case value (refer to Table 26 in section 3.2.1) (Kohler *et al.*, 2018). Maximum bounds of both 25% and 50% above the base feed capacity were

evaluated based on recycling rates of 10% and 12% instead of the assumed base case recycling rate of 8% (Guy, 2017; Stats SA, 2018).

Uncertainty resides within the amount of valuable electrode material that will be lost during the pre-treatment process. Allowance for 6-10% losses (corresponding to $\pm$ 25% from the base value of 8%) of the valuable material was incorporated in the simulations.

Refer to Table 28 (section 3.2.1) for the assumed cathode material distribution in the feed. The minimum and maximum bounds for $LiNi_{0.33}Mn_{0.33}Co_{0.33}O_2$, $LiFePO_4$, $LiNiO_2$ and $LiMn_2O_4$ were specified as -5%, +20% based on the observed and predicted market trends (refer to section 6.1.5), advantages and disadvantages (refer to Table 2 in section 2.1) previously discussed. The $LiCoO_2$ contribution in the feed was not randomly generated (by sampling from a specified triangular distribution) as it was calculated by subtracting the other cathode material contributions from 1. This ensured that the total of the cathode mass fractions always equaled 1 regardless of the random values generated for the other 4 cathode types. Thus, the $LiCoO_2$ contribution to the cathode feed material randomly varied between 24.6 wt% and 40.3 wt% (corresponding to -33.8%, +8.4% bounds) depending on the random values generated for each of the other cathode types.

Based on the effect of individual parameters on the NPV, the total change in the NPV when changes in multiple variables occur at the same time was predicted with equation 194 (Turton *et al.*, 2012). The NPV sensitivity to fluctuations in individual variables ($S_1, S_2 \ldots . S_n$) was defined as the change in the NPV value (ΔNPV) per percentage change in the respective variable from its base value (Δx). Due to the straight-line relationships observed between the NPV and the changes in variables (refer to section 6.1), linear regression was employed, and the NPV sensitivity to individual variables was assumed constant. The individual variable sensitivities used in the Monte Carlo simulations are tabulated in Table 60 below.

$$\Delta NPV = S_1\Delta x_1 + S_2\Delta x_2 + S_3\Delta x_3 + \ \ldots \ + S_n\Delta x_n \qquad [\ 194\ ]$$

For simulation purposes, only the sensitivity to the $LiCoO_2$ to content of the cathode was incorporated in calculating the change in the NPV (ΔNPV). This was done based on the three reasons listed below:

1. The NPV is more sensitive to fluctuations in the amount of $LiCoO_2$ in the feed compared to fluctuations in the other cathode material types as seen in Figure 25 (refer to section 6.1.4) and Table 60.
2. Individual sensitivities were calculated by increasing or decreasing a specific cathode type while changing the other 4 cathode types proportionally to ensure that the sum of the cathode mass fractions equals 1. If the sensitivity of all the cathode types are included in the simulation, the predicted simulation NPVs will be penalised or improved more than once leading to inaccurate NPV projections.
3. The statement mentioned in point 2 was tested by comparing the results of 2 simulations. The NPVs predicted by a Monte Carlo simulation incorporating all the cathode type sensitivities were compared with the actual NPVs calculated in the original mass balance and economic analysis model. An average error of 2.88% was calculated. When only the $LiCoO_2$ sensitivity was considered, an average error of 0.41% was obtained.

Table 60: Sensitivity of NPV to changes in individual variables (million USD/100% change in variable)

Variable		Sensitivity (S)
CAPEX	Fixed Capital Investment	-25.624
	Working Capital	-2.0636
	Salvage Value	0.0694
OPEX	Raw Materials	-15.485
	Operating Labour	-17.27
	Utilities	-3.1776
	Waste Treatment	-3.1417
Revenue	Mn Product Selling price	35.006
	Ni Product Selling price	6.3152
	Co Product Selling price	36.98
	Li Product Selling price	5.3755
Feed Conditions	Feed Capacity	55.244
	% $LiCoO_2$ in cathode feed material	10.744
	% $LiNi_{0.33}Mn_{0.33}Co_{0.33}O_2$ in cathode feed material	-1.6838
	% $LiMn_2O_4$ in cathode feed material	-0.6221
	% LiNiO2 in cathode feed material	-2.1789
	% $LiFePO_4$ in cathode feed material	-3.2111
Operating Conditions	Pre-treatment Losses	-5.174

The coefficient of variation (CV) was calculated with equation 195 and is simply defined as the ratio of the standard deviation to the mean. The CV provides an indication of the financial risk per unit earnings. Therefore, optimizing the financial feasibility (NPV) of a process will focus on minimizing the coefficient of variation (Okagbue, Edeki and Opanuga, 2014).

$$Coefficient\ of\ Variation = \frac{Standard\ deviation}{Mean} \quad [\ 195\ ]$$

The standard error of the mean was calculated by dividing the output (NPV) standard deviation (S) by the square root of the number of iterations (n) completed. The margin of error associated with the average NPV was calculated by multiplying the standard error with the appropriate Z-value as shown in equation 196. A 95% confidence interval corresponding to a Z-value of 1.96 was used in error calculations.

$$Margin\ of\ Error = \frac{Z \times S}{\sqrt{n}} \quad [\ 196\ ]$$

6.2.2 Monte Carlo simulation results

Six Monte Carlo simulations with 100 000 iterations each were completed in XLStat to investigate the effect of different input specifications on the profitability predictions. Two maximum bounds for the feed capacity (+25% and +50%) and three metal selling price minimum and maximum combinations (refer to Table 59) were evaluated. The different input specification combinations and summarized results are tabulated in Table 61. For comparison purposes the error in simulation results was expressed as a percentage of the average NPV for each simulation.

Table 61: Input specifications and summarized results of Monte Carlo simulations

Monte Carlo Simulation		**Simulation 1**		**Simulation 2**		**Simulation 3**		**Simulation 4**		**Simulation 5**		**Simulation 6**	
Selling price reference in Table 59		Shanghai Metals Market				Turton *et al.* (2012)				Pure Metal Price Fluctuations			
100000 iterations		Min	Max	Min	Max	Min	Max	Min	Max	Min	Max	Min	Max
Inputs	Feed Capacity	-10%	25%	-10%	50%	-10%	25%	-10%	50%	-10%	25%	-10%	50%
	MnO_2 Selling Price	-47%	0%	-47%	0%	-20%	5%	-20%	5%	-38%	59%	-38%	59%
	$Ni(OH)_2$ Selling Price	-58%	0%	-58%	0%	-20%	5%	-20%	5%	-42%	58%	-42%	58%
	CoC_2O_4 Selling Price	-69%	0%	-69%	0%	-20%	5%	-20%	5%	-38%	97%	-38%	97%
	Li_3PO_4 Selling Price	-28%	0%	-28%	0%	-20%	5%	-20%	5%	-34%	88%	-34%	88%
Outputs	Average NPV	$1 579 251		$6 139 859		$13 030 026		$17 633 641		$28 241 357		$32 844 996	
	Probability of NPV>0	58.45%		71.90%		98.90%		99.52%		98.90%		99.36%	
	Standard deviation	$8 777 099		$10 579 109		$5 728 376		$8 299 640		$13 681 866		$14 978 290	
	Coefficient of Variation	5.558		1.723		0.440		0.471		0.484		0.456	
	Skewness	-0.198		0.037		0.083		0.319		0.208		0.210	
	Minimum	-$32 806 994		-$33 005 440		-$7 317 974		-$8 096 514		-$17 494 637		-$13 113 643	
	Maximum	$30 605 490		$42 786 196		$34 114 220		$46 332 565		$81 247 138		$95 395 037	
	Range	$63 412 484		$75 791 636		$41 432 193		$54 429 079		$98 741 776		$108 508 681	
	Standard error of the mean	$27 756		$33 454		$18 115		$26 246		$43 266		$47 366	
	Error Margin	$54 401		$65 570		$35 505		$51 442		$84 802		$92 837	
	Error (%)	3.44%		1.07%		0.27%		0.29%		0.30%		0.28%	

The cumulative probability curves for the simulations are compared in Figure 28. The curves indicated with solid lines had the +25% maximum feed capacity bound whereas the dotted line curves had the +50% maximum feed capacity bound.

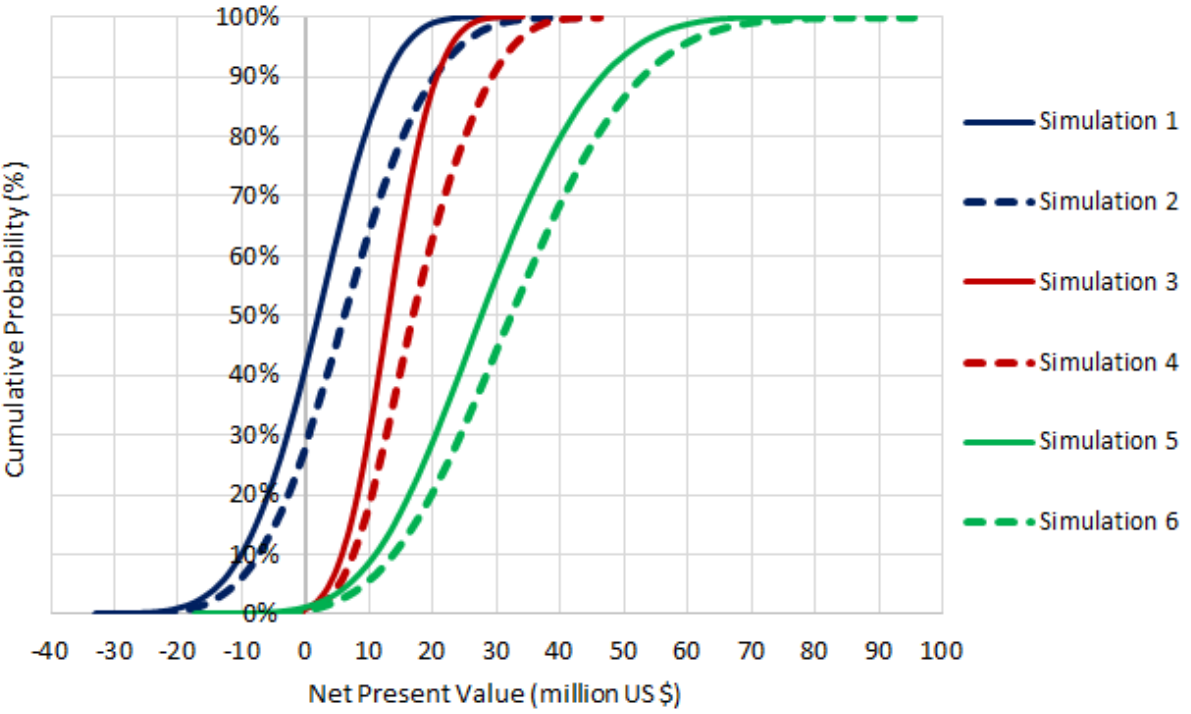

Figure 28: Comparison of cumulative probability curves of Monte Carlo simulations

The following observations were made from the Monte Carlo simulation results shown in Table 61 and Figure 28:

1. The selling price input specifications have a more notable effect on the simulation results compared to the feed capacity. This is expected as the NPV is very sensitive to changes in the revenue which is primarily a function of the selling prices (refer to sections 6.1.3 and 6.1.7).
2. Regardless of the random fluctuations in variables, all simulations indicated that profitable operation of the proposed LIB recycling facility will be more likely than unprofitable operation. The likelihood of profitable operation ranged between 58.45% (simulation 1) and 99.52% (simulation 4) depending on the input specifications to the simulation.
3. In all cases the probability of an NPV greater than zero increased when the higher feed capacity bound (+50%) was incorporated. An increase in the feed capacity maximum bound from 25% to 50% caused an average increase of $ 4.6 million in the NPV if the same selling price input bounds were used.
4. In all simulations the NPV range and standard deviation increased when the feed capacity maximum bound was increased from 25% to 50%. This makes sense as the feed capacity was randomly generated within a wider range of values giving rise to more uncertainty (larger standard deviation and margin of error) in the NPV outputs.
5. The skewness observed in the curves is a result of the triangular probability distributions assigned to all the input variables. The output data of all simulations except simulation 1 are positively skewed

(skewness > 0) indicating that the probability of obtaining NPVs larger than the predicted average is greater than obtaining NPVs below the predicted average.

6. Simulation 1 has the largest coefficient of variation (CV) indicating the highest risk per unit financial gain (NPV). Simulation 3 has the lowest CV of 0.440. This implies that there is a 44% chance of the NPV deviating from the predicted average NPV.
7. Errors in the simulation results ranged between 0.27% and 3.44% of the average NPV. The large errors in simulations 1 and 2 can be explained by the relatively large standard deviations and low average NPVs. To reduce the errors, additional iterations will be required or narrower input bounds on variables should be defined.

Simulations 1 and 2 using the Shanghai Metals Market prices as minimum selling price bounds provided the most conservative results as the selling prices were not allowed to fluctuate to values above the base case selling prices (Alibaba prices). The average NPV increased with $ 4.56 million when the feed capacity maximum bound was increased from 25% to 50%. The probability of achieving an NPV greater than zero improved from 58.45% to 71.90% correspondingly.

Simulations 3 and 4 showed the smallest range in NPVs which clarifies why the associated cumulative probability curves are the steepest (Figure 28). This is because the Turton *et al.* (2012) input specifications (-20%, +5%) are in a narrower range when compared to the input bounds of the other 4 simulations. The NPV results of simulations 5 and 6 have the largest ranges, therefore a wider distribution of NPVs are expected. The observed trend is confirmed by Figure 29 which compares the distribution of NPVs for three simulations with the same feed capacity input bounds (-10%, +25%). Refer to Appendix G for supporting data and histograms presenting the data illustrated in Figure 28 and Figure 29.

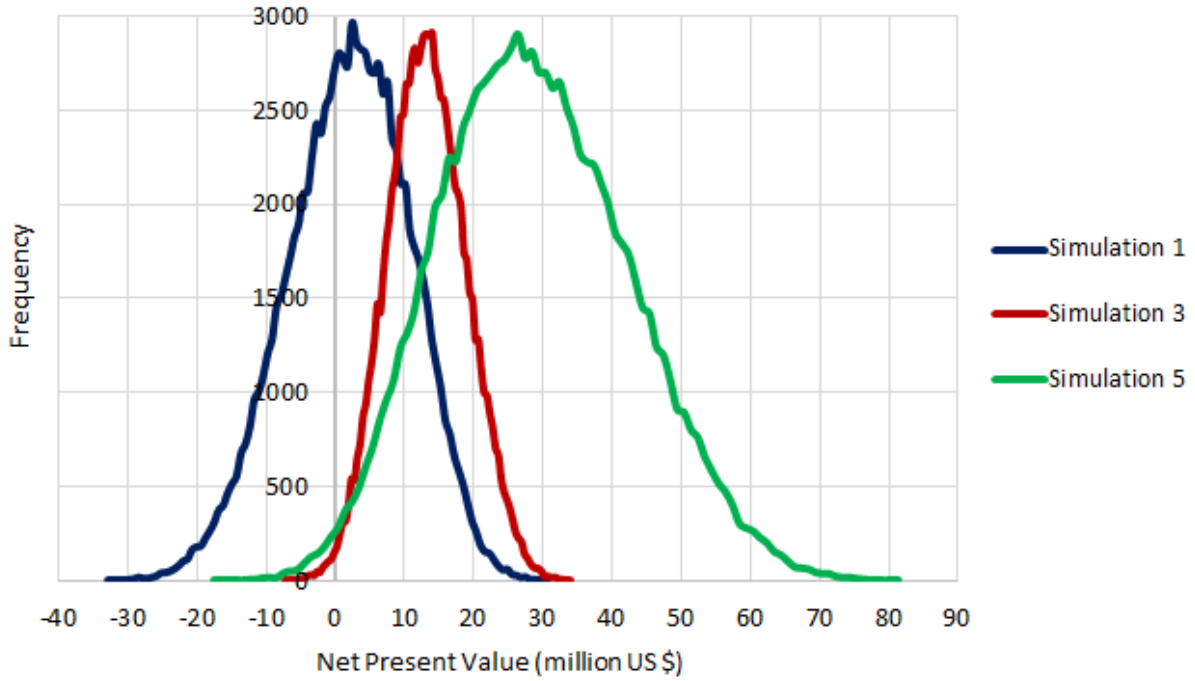

Figure 29: Effect of selling price input bounds on the resulting NPV distribution

7 Conclusions and Recommendations

The study aimed to investigate the techno-economic feasibility of various hydrometallurgical flowsheet options for the recovery of manganese, cobalt, nickel and lithium from end-of-life lithium-ion batteries in a South African context. The proposed processes consisted of three main steps: pre-treatment of the raw LIB waste to expose the valuable cathode material, leaching the valuable metals from the electrode material using a suitable lixiviant and finally recovering the metals selectively from the leach solution. Three process options using a mineral acid as lixiviant and three options using an organic acid as lixiviant were investigated and compared. The conclusions and recommendations concerning each of the objectives set in section 1.2 are presented below. Refer to Table 47 for the abbreviated process names of the six evaluated options.

7.1 Objective 1: Review of LIB processing options

A detailed literature study was done to gain understanding of hydrometallurgical processes and the unit operations typically used for the mechanical pre-treatment and leaching of LIBs as well as the recovery of metals from the resulting leach solutions. The literature review presented in Chapter 2 provided insight in previous work done in the field of LIB recycling. Before mass and energy balances could be completed, information regarding the LIB waste generation and recycling rates were required to calculate the design feed capacity of a LIB recycling facility in South Africa. From the literature review and LIB recycling assessment, the following conclusions were made:

1. Hydrochloric acid and sulphuric acid are the mineral acid lixiviants typically employed to achieve high leaching efficiencies of valuable metals. Current commercial hydrometallurgical facilities are using these mineral acids in their processes (e.g. Recupyl process).
2. Currently no commercial LIB recycling facilities are using organic acids to facilitate leaching. The leaching abilities of various organic acids have been investigated experimentally, showing extraction efficiencies similar to that achieved with mineral acids. The organic acid that has been tested most extensively is citric acid.
3. Selective precipitation and solvent extraction are the techniques generally used to recover valuable metals from leach solutions. A trend was observed in the sequence in which metals are selectively recovered starting with Mn, followed by Ni and Co and lastly Li.
4. The flowsheet complexity is highly dependent on the type of products that should be produced and the purity requirements thereof. The LIB recycling facility can aim to produce high purity laboratory products by selectively recovering each metal or a combined metal product that could be used in the manufacturing of new cathode materials by precipitating metals from the leach solution in a single step.
5. Based on an e-waste recycling rate of 8%, the design feed capacity of a LIB recycling facility should be 868 tonnes of raw LIB waste per year.

Based on the literature review and LIBs recycling assessment, the following can be recommended:

1. Further experimental work providing insight in the stability of metal citrate complexes that form at specific pH levels should be done as this affect the citric acid reaction stoichiometry, process performance of subsequent solvent extraction or precipitation steps and the amount of citric acid consumed which will consequently have cost implications.
2. Due to the uncertainty in the feed rate and the small volume of LIB waste available for recycling in South Africa, the feasibility of operating the facility as a batch process instead of a continuous process should be investigated. A batch process will allow more flexibility in the feed capacity which is uncertain at this stage.
3. Limited work has been done to investigate the techno-economic feasibility of LIB recycling opportunities in South Africa. Correspondence with key stakeholders such as electronic waste collectors, regulatory bodies, primary metal producers and local manufacturing industries could provide valuable insight and reveal opportunities in the LIB recycling sector. Basic techniques such as SWOT and PESTLE analyses should be used to investigate the current industry and need for LIB recycling in South Africa.
4. A detailed market analysis concentrating on the type of metal products that will have the highest local demand or export opportunities may provide information that will assist in the decision-making process regarding the process design. The local demand and value of different products should be compared and evaluated extensively as it will directly impact the profitability of the process.

7.2 Objective 2: Flowsheet development and mass and energy balances

Based on the information obtained during the literature study, system boundaries were defined and various flowsheets were developed. The assumptions on which these flowsheets and subsequent calculations are based are presented in Chapter 3. Alternative flowsheet options used different leaching reagents (HCl or citric acid), process conditions, metal recovery steps or aimed to produce different products. Mass and energy balances were performed for the six flowsheet options. Based on the results, the following was concluded:

1. Approximately 8% of the valuable electrode material is lost during the pre-treatment steps. This has a negative effect on the overall metal recoveries.
2. Similar cobalt (88.3%-89.9%) and nickel (88.6%-89.2% apart from 96.7% in MA-3) recoveries are achieved in all the evaluated flowsheets. The manganese recoveries ranged between 66.1% in MA-1 and 89.6% in OA-1. The lithium recoveries are generally the lowest (62.6%-83.9%) because it is highly dependent on the solubility of the lithium salts in solution and lithium is the final metal recovered from solution.
3. Products will be produced and sold as dried powders. The product purities of the processes aiming to produce 4 pure products ranged between 96.4% and 98.3% for Co, 89.6% and 98.9% for Ni, 98.7% and 99.9% for Mn and 97.1% and 99.4% for Li.

4. MA-3 and OA-3 aimed to produce a combined metal product and a lithium product. The product purities achieved with MA-3 and OA-3 were 96.0% and 95.7% for the combined products and 97.1% and 86.9% for the lithium products respectively.

The mass and energy balances were based on assumptions (discussed in Chapter 3) that should be re-evaluated or even retested experimentally to improve the accuracy of the results. Uncertainty resides within various assumptions such as the feed composition, pre-treatment losses, reaction stoichiometry and kinetics, system pH, salt solubilities and how recycle loops will affect the interaction between unit operations. Advanced chemical speciation software can be used to predict the composition of leach solutions under various conditions. However, speciation software is typically built on the principle of Gibbs free energy minimization and predict the system composition at equilibrium conditions which will rarely be achieved in practice. To improve accuracy or future research the following recommendations can be made:

1. Most of the mass and energy balance assumptions were based on experimental conditions and results which were obtained under ideal optimized conditions (especially for the citric acid process). The likelihood of continuously operating a large-scale facility at these idealized laboratory conditions is small. To make the results more reliable, the effect of scale-up and fluctuating process conditions should be considered. The best way to improve and validate the accuracy of the mass and energy balance results will be through pilot plant studies which will also allow further process development by exposing potential technical challenges, unit-to-unit interactions and system dynamics.
2. To improve the sustainability of the processes, additional strategies to employ heat integration and recycle streams should be investigated to minimize raw material and energy inputs to the process. Waste streams with varying levels of toxicity are produced in the processes. The treatment and environmental impact of these waste streams should be considered in detail.
3. To improve the overall recoveries achieved, an alternative pre-treatment method should be considered. Physically dismantling the batteries may be a viable alternative option which can provide jobs for many unemployed citizens of South Africa. However, economic analyses incorporating the additional labour cost and income will ultimately determine the pre-treatment method selected.
4. Separation techniques to recover the electrolyte, plastics, steel casing and graphite as separate fractions should be evaluated. Selling these waste fractions to other recycling industries may improve the financial feasibility of the processes.

7.3 Objective 3: Economic analysis and process comparison

The information obtained from the mass and energy balances were used to size the major equipment units in each facility. Various correlations and high-level costing methods were used to calculate the CAPEX, OPEX and revenue of the processes (refer to Chapter 4). The profitability of the 6 facilities were evaluated over a project lifetime of 20 years and compared using 4 economic indicators namely the NPV, DCFROR, DPBP and PVR. An internal discount rate of 15% was used in the economic analyses. The results

are presented and discussed in Chapter 5. Based on the economic analysis and profitability criteria, the following conclusions were made:

1. In general, the CAPEX of the mineral acid processes exceeds that of the organic acid process options producing the similar products. The CAPEX of MA-1 is very high ($ 4.59/kg of LIBs treated) in comparison to the other options due to the additional costs ($ 9.49 million) associated with the membrane cells. MA-3 and OA-3 producing only two product streams, have the least process steps and subsequent complexity allowing the lowest CAPEX of $ 1.23 and $ 0.95 per kg LIB treated respectively.
2. The OPEX of the mineral acid processes are higher than that of the citric acid processes producing similar products. In all process options (except MA-1) raw material costs are the major contributor to the OPEX (22.0%-37.8% of OPEX). Although MA-1 have the lowest raw material requirements (due to the membrane cells) it have the highest OPEX ($ 35.9 per kg LIB feed) due to the high utility costs, labour and maintenance required for the membrane cell operation. OA-3 has the lowest OPEX of $ 13.97 million per annum.
3. Cobalt is the primary source of income in all process options contributing to between 37.4% (MA-3) and 61.8% (OA-2) of the annual revenue. The highest revenue is earned in OA-1 ($ 29.32/kg LIB feed) due to the higher MnO_2 production rate. OA-3 producing only two phosphate products has the lowest annual revenue of $ 15.76 million which can be ascribed to the lower estimated value of phosphate products containing smaller fractions of the valuable metals compared to the hydroxide products.
4. A negative NPV and PVR smaller than 1 was calculated for MA-1, MA-2, OA-2 and OA-3 and indicated that these flowsheet options will not be feasible from a financial point of view. However, a recycling levy of $ 0.61 per kg of LIB feed will allow a break-even scenario for OA-3.
5. The estimated NPV for MA-3 is $ 5.69 million indicating that the process will be economically self-sustainable. However, OA-1 is the techno-economically more feasible option for LIB recycling in a South African context. The facility has an estimated CAPEX of $ 22.76 million, OPEX of $ 16.95 million per year and revenue of $ 25.45 million per year resulting in an NPV of $ 16.44 million after 20 years. The PVR of 1.83 and DCFROR of 28.15% also indicate that profitable operation will be possible. The initial fixed capital investment will be recovered in the first 4 years and 4 months of operation.
6. Excluding the metal ratio adjustment step in MA-3, will lead to a decrease of 28.9% in the revenue of MA-3. The lowered revenue was the primary reason for the observed decrease in the NPV from $ 5.69 million to $ -9.38 million. Therefore, without the metal ratio adjustment step, OA-3 is more profitable than MA-3.
7. The NPV of OA-3 improved from $ -1.82 million to $ 5.64 million when the precipitant NaH_2PO_4 was substituted with the cheaper precipitant Na_3PO_4. Using Na_3PO_4 instead of NaH_2PO_4 decreased the raw material costs with 34.2% and consequently the calculated profitability criteria are very similar to that of MA-3. Thus, both the HCl and citric acid processes may allow profitable operation if the processes aim to produce a combined Mn, Ni and Co product.

To improve the validity of the economic analysis or advance research in this field, the following recommendations could be made:

1. The CAPEX was calculated as a function of the purchased equipment cost. Thus, validity of the CAPEX estimations can be improved by designing units in detail, reconsidering the materials of construction and obtaining present-day quotes from companies manufacturing these units.
2. A high level of uncertainty resides within the CAPEX and OPEX estimated for the membrane cells and the hydrochloric acid production units in MA-1. Research regarding the operation, energy requirements, cost of membrane cells and the possible application thereof in the LIB recycling industry may be worthwhile considering the 65.2% decrease in raw material costs with the inclusion of the membrane cells in MA-1.
3. Investigation of low-cost metal additives that could be used to adjust the metal ratio in citrate systems may be worthwhile considering the big influence on the revenue observed for MA-3.
4. The use of Na_3PO_4 as precipitant to produce a combined metal phosphate and a lithium phosphate product should be investigated experimentally as a high-level techno-economic assessment indicated that it would be financially viable.
5. Fluctuations in pure metal market prices and the uncertain demand for the products produced, make it difficult to accurately estimate the annual income. Market research to identify export opportunities and potential local customers and the prices that they will be willing to pay may provide valuable information regarding the economic feasibility of the projects.
6. The relationship between impurities in products and the product value should be reconsidered. The option of investing additional capital to purify products further to produce high purity laboratory products should be evaluated from a techno-economic point of view.
7. The techno-economic assessment indicated that citric acid may be a suitable alternative leaching reagent for mineral acids in hydrometallurgical LIB recycling processes. However, the environmental impact of organic acid based processes has not been considered. A detailed life-cycle assessment to compare the potential environmental impact of hydrochloric acid based and citric acid based processes is recommended.

7.4 Objective 4: Sensitivity analysis

Organic acid process option 1 was selected as the techno-economically most favourable option based on the economic analysis presented in Chapter 5. Consequently, a sensitivity analysis was performed to quantify how robust the profitability of OA-1 would be if changes in market and operating conditions occur randomly. The sensitivity analysis presented in Chapter 6 evaluated the effect of individual variables and multi-variable interaction on the profitability criteria of OA-1. The Monte Carlo simulations predicted the NPV for 100 000 scenarios incorporating fluctuations in 17 variables that could affect the profitability. Triangular probability distributions were assigned to each variable. The results of the sensitivity analysis lead to the following conclusions:

1. The profitability of the project is most sensitive to the feed capacity, selling prices of the cobalt and manganese product and the fixed capital investment. Increasing each of these parameters with 1%

will cause an increase of $ 552 440, increase of $ 369 800, increase of $ 350 060 and decrease of $ 256 240 in the NPV respectively.

2. A LIB feed capacity of 615 ton/year will be the minimum design feed capacity that will return an NPV of zero.
3. Because cobalt is the primary source of income, the $LiCoO_2$ contribution to the feed cathode material affects the profitability of the project to a greater extent than the other 4 cathode types. The global decline in the use of $LiCoO_2$ and market shift towards less expensive cathode types will therefore negatively affect the economic feasibility of a LIBs recycling facility.
4. The effects of the overall CAPEX, OPEX, revenue and feed capacity on the project profitability were compared. It was concluded that the NPV is more sensitive to the revenue and OPEX. Thus, investing additional capital to minimize operating costs may improve the chances of profitable operation.
5. The six simulations proved that the output NPVs predicted by Monte Carlo simulations is highly dependent on the mode and minimum and maximum bounds of the input variables. The chances of profitable operation ranged between 58.45% and 99.52% depending on the input specifications.
6. The feed capacity of the facility has a significant effect on profitability. Increasing the feed capacity maximum bound from 25% to 50% resulted in an average increase of $ 4.6 million in the NPV.
7. The Monte Carlo simulations proved that profitable operation of the facility will be possible regardless of randomly changing market and operating conditions. Even the most conservative simulation, indicated a 58.45% probability of profitable operation.

The conclusions regarding the sensitivity analysis gave rise to the following recommendations:

1. Assumptions concerning the parameters influencing the profitability the most (feed capacity, selling prices and fixed capital investment) should be reconsidered. Detailed process design, equipment sizing and costing of the proposed facility to increase the confidence in projected estimations will encourage stakeholders to invest capital in the project.
2. The availability of LIB waste will ultimately determine the design feed capacity of a local recycling facility. Strategies to improve the availability of waste should be evaluated. These strategies may include enforcing legislation that direct the collection and recycling of spent LIBs, educating the public, granting companies incentives depending on their co-operation with regards to LIBs collection, partnering with companies currently exporting collected LIBs and assessing import opportunities from nearby African countries.
3. Market trends regarding electric vehicle usage in South Africa should be studied as many conflicting opinions regarding the prospect of electric vehicles exist. Electric vehicles may pose new opportunities for development as well as challenges for the country.
4. The market share of the various cathode chemistries in South Africa should be studied as they may differ from global market shares which are primarily influenced by the economies of developed countries.

8 References

Abam Engineers Inc. (1980) 'Final Report on Process Engineering and Economic Evaluations of Diaphragm and Membrane Chloride Cell Technologies'. Available at: https://www.osti.gov/servlets/purl/6540048/.

Ahn, J.W., Ahn, H.J., Son, S.H., Lee, K. W. (2012) 'Solvent extraction of Ni and Li from sulfate leach liquor of the cathode active materials of spent Li-ion batteries by PC88A', *Journal of the Korean Institute of Resources Recycling*, 21(6), pp. 58–64.

Alibaba (2019) *Alibaba.com*. Available at: https://www.alibaba.com/ (Accessed: 3 May 2019).

Arroyo, F., Fernández-Pereira, C. and Bermejo, P. (2015) 'Demonstration Plant Equipment Design and Scale-Up from Pilot Plant of a Leaching and Solvent Extraction Process', *Minerals*, 5(2), pp. 298–313. doi: 10.3390/min5020298.

Badawy, S. M., Nayl, A. A., El Khashab, R. A., El-Khateeb, M. A. (2013) 'Cobalt separation from waste mobile phone batteries using selective precipitation and chelating resin', *Journal of Material Cycles and Waste Management*, 16(4), pp. 739–746. doi: 10.1007/s10163-013-0213-y.

Baloyi, C. (no date) *Management of Spent Dry Cell Batteries in South Africa*. Available at: http://sawic.environment.gov.za/documents/6529.pdf.

Barbour, W., Oommen, R. and Shareef, G. S. (1995) *Wet scrubbers for acid gas*. Available at: https://www3.epa.gov/ttn/ecas/docs/cs5-2ch1.pdf.

Barik, S. P., Prabaharan, G. and Kumar, B. (2016) 'An innovative approach to recover the metal values from spent lithium-ion batteries', *Waste Management*. Elsevier Ltd, 51, pp. 222–226. doi: 10.1016/j.wasman.2015.11.004.

Barik, S. P., Prabaharan, G. and Kumar, L. (2017) 'Leaching and separation of Co and Mn from electrode materials of spent lithium-ion batteries using hydrochloric acid: Laboratory and pilot scale study', *Journal of Cleaner Production*. Elsevier Ltd, 147, pp. 37–43. doi: 10.1016/j.jclepro.2017.01.095.

Bastug, A. S., Göktürk, S. and Sismanoglu, T. (2008) '1:1 Binary complexes of citric acid with some metal ions: Stability and thermodynamic parameters', *Asian Journal of Chemistry*, 20(2), pp. 1269–1278. doi: 10.1515/REVIC.2007.27.1.53.

Bommaraju, T. V., Luke, B., O'Brien, T. F., Blackburn, M. C. (2000) *Kirk-Othmer Encyclopedia of Chemical Technology*. 5th edn. John Wiley & Sons, Inc.

Brinkmann, T., Santonja, G. G., Schorcht, F., Roudier, S., Sancho, L. D. (2014) *Best Available Techniques*

(BAT) Reference Document for the Production of Chlor-alkali, *European Commission*. doi: 10.2791/13138.

BusinessTech (2019) *South Africa's petrol and electricity prices vs the world*. Available at: https://businesstech.co.za/news/energy/306592/south-africas-petrol-and-electricity-prices-vs-the-world/ (Accessed: 28 March 2019).

C11 Chlor-alkali (2010) *The South African Chlor-Alkali Industry*. Available at: https://vula.uct.ac.za/access/content/group/9eafe770-4c41-4742-a414-0df36366abe6/Chem Ind Resource Pack/html/learner-sheets/C/LS_C11.pdf (Accessed: 16 March 2019).

Cai, G., Fung, K. Y., Ng, K. M. (2014) 'Process development for the recycle of spent lithium ion batteries by chemical precipitation', *Industrial and Engineering Chemistry Research*, 53(47), pp. 18245–18259. doi: 10.1021/ie5025326.

California Fuel Cell Partnership (no date) *Cost to refill*. Available at: https://cafcp.org/content/cost-refill (Accessed: 28 March 2019).

Cape E-Waste Recyclers (no date) *Electronic Waste*. Available at: http://capee-waste.co.za/ (Accessed: 15 April 2019).

Carbone Lorraine (no date) *CARBONE LORRAINE's Hydrochloric Acid Synthesis Units*. Available at: https://www.mersen.us/products/anticorrosion-equipment/process-technologies/hcl-sintaclor (Accessed: 27 March 2019).

Career Junction (2018) *South Africa's Latest Salary Review*. Available at: https://www.careerjunction.co.za/marketing/salarysurvey (Accessed: 3 May 2019).

Castillo, S., Ansart, F., Laberty-Robert, C., Portal, J. (2002) 'Advances in the recovering of spent lithium battery compounds', *Journal of Power Sources*, 112(1), pp. 247–254. doi: 10.1016/S0378-7753(02)00361-0.

Cengel, Y. A. (2003) *Heat Transfer - A Practical Approach*. 2nd edn. Boston: McGraw-Hill. Available at: http://web.a.ebscohost.com/bsi/detail/detail?vid=4&sid=255d93e3-d360-45ca-a768-9a8bd96ae785%40sessionmgr4007&hid=4209&bdata=JnNpdGU9YnNpLWxpdmU%3D#AN=111093111&db=bth.

Chagnes, A., Barboux, P., Lorente, D., Christmann, P., Ekberg, C., Petranikova, M. (2015) *Lithium Process Chemistry - Resources, Extraction, Batteries and Recycling*. Edited by A. Chagnes and J. Swiatowska. Elsevier.

Chase, M. W. (1998) *Water | NIST Chemistry Webbok, SRD 69*, *J. Phys. Chem. Ref. Data, Monograph 9*.

Available at: https://webbook.nist.gov/cgi/cbook.cgi?ID=C7732185&Type=JANAFL&Plot=on (Accessed: 15 June 2019).

ChemicalAid (no date) *Chemical Equation Balancer | KMnO4+C6H8O7=MnO2+CO2+H2O+K2O*. Available at: https://en.intl.chemicalaid.com/tools/equationbalancer.php?equation=KMnO4+%2B+C6H8O7+%3D+MnO2+%2B+CO2+%2B+H2O+%2B+K2O (Accessed: 23 April 2019).

ChemicalBook (2019). Available at: https://www.chemicalbook.com/ (Accessed: 6 May 2019).

Chemistry LibreTexts (no date) *Acid Strength and the Acid Dissociation Constant (Ka)*. Available at: https://chem.libretexts.org/Bookshelves/General_Chemistry/Map%3A_A_Molecular_Approach_(Tro)/16%3A_Acids_and_Bases/16.04%3A_Acid_Strength_and_the_Acid_Dissociation_Constant_(Ka) (Accessed: 25 March 2019).

Chen, L., Tang, X., Zhang, Y., Li, L., Zeng, Z., Zhang, Y. (2011) 'Process for the recovery of cobalt oxalate from spent lithium-ion batteries', *Hydrometallurgy*. Elsevier B.V., 108(1–2), pp. 80–86. doi: 10.1016/j.hydromet.2011.02.010.

Chen, W.-S. and Ho, H.-J. (2018) 'Recovery of Valuable Metals from Lithium-Ion Batteries NMC Cathode Waste Materials by Hydrometallurgical Methods', *Metals*, 8(5), p. 321. doi: 10.3390/met8050321.

Chen, X., Chen, Y., Zhou, T., Liu, D., Hu, H., Fan, S. (2015) 'Hydrometallurgical recovery of metal values from sulfuric acid leaching liquor of spent lithium-ion batteries', *Waste Management*. Elsevier Ltd, 38(1), pp. 349–356. doi: 10.1016/j.wasman.2014.12.023.

Chen, X., Zhou, T., Kong, J., Fang, H., Chen, Y. (2015) 'Separation and recovery of metal values from leach liquor of waste lithium nickel cobalt manganese oxide based cathodes', *Separation and Purification Technology*. Elsevier B.V., 141, pp. 76–83. doi: 10.1016/j.seppur.2014.11.039.

Chen, X., Xu, B., Zhou, T., Liu, D., Hu, H., Fan, S. (2015) 'Separation and recovery of metal values from leaching liquor of mixed-type of spent lithium-ion batteries', *Separation and Purification Technology*. Elsevier B.V., 144, pp. 197–205. doi: 10.1016/j.seppur.2015.02.006.

Chen, X., Luo, C., Zhang, J., Kong, J., Zhou, T. (2015) 'Sustainable Recovery of Metals from Spent Lithium-Ion Batteries: A Green Process', *ACS Sustainable Chemistry and Engineering*, 3(12), pp. 3104–3113. doi: 10.1021/acssuschemeng.5b01000.

Chen, X., Fan, B., Xu, L., Zhou, T., Kong, J. (2016) 'An atom-economic process for the recovery of high value-added metals from spent lithium-ion batteries', *Journal of Cleaner Production*. Elsevier

Ltd, 112, pp. 3562–3570. doi: 10.1016/j.jclepro.2015.10.132.

Chen, X. and Zhou, T. (2014) 'Hydrometallurgical process for the recovery of metal values from spent lithium-ion batteries in citric acid media', *Waste Management and Research*, 32(11), pp. 1083–1093. doi: 10.1177/0734242X14557380.

City Chemical LLC (2019) *Cobalt Phosphate CAS No. 13455-36-2*. Available at: https://www.citychemical.com/cobalt-phosphate.html (Accessed: 4 June 2019).

Clarke, D. (2015) *Energy cost calculator*. Available at: https://ramblingsdc.net/EnCalcs.html#Calculate_cost_of_energy_from_oil (Accessed: 3 May 2019).

Contestabile, M., Panero, S. and Scrosati, B. (2001) 'Laboratory-scale lithium-ion battery recycling process', *Journal of Power Sources*, 92(1–2), pp. 65–69. doi: 10.1016/S0378-7753(00)00523-1.

Croy, J. R. and Claxton, C. M. (2019) *The road ahead for lithium-ion batteries*, *ESI Africa - Africa's Power Journal*. Available at: https://www.esi-africa.com/industry-sectors/future-energy/the-road-ahead-for-lithium-ion-batteries/ (Accessed: 14 June 2019).

Dec Group (2019) *Powder Handling Excellence*. Available at: https://www.dec-group.net/fileadmin/products/DEC_PRODUCTS_EN_4.pdf (Accessed: 20 June 2019).

Dewulf, J., Van der Vorst, G., Dentruck, K., Van Langenhove, H., Ghyoot, W., Tytgat, J., Vandeputte, K. (2010) 'Recycling rechargeable lithium ion batteries: Critical analysis of natural resource savings', *Resources, Conservation and Recycling*, 54(4), pp. 229–234. doi: 10.1016/j.resconrec.2009.08.004.

De Dietrich Process Systems (2019) *Absorption of Hydrochloric Acid (HCL) Treatment System*. Available at: https://www.dedietrich.com/en/solutions-and-products/mineral-acid-treatment/hydrochloric-acid-treatment/absorption-hcl (Accessed: 25 March 2019).

Dorella, G. and Mansur, M. B. (2007) 'A study of the separation of cobalt from spent Li-ion battery residues', *Journal of Power Sources*, 170(1), pp. 210–215. doi: 10.1016/j.jpowsour.2007.04.025.

Du, F., Warsinger, W. M., Urmi, T. I., Thiel, G. P., Kumar, A., Lienhard, J. H. (2018) 'Sodium Hydroxide Production from Seawater Desalination Brine: Process Design and Energy Efficiency', *Environmental Science and Technology*. American Chemical Society, 52(10), pp. 5949–5958. doi: 10.1021/acs.est.8b01195.

Dunn, J. B., Gaines, L., Sullivan, J., Wang, M. Q. (2012) 'Impact of recycling on cradle-to-gate energy

consumption and greenhouse gas emissions of automotive lithium-ion batteries', *Environmental Science and Technology*, 46(22), pp. 12704–12710. doi: 10.1021/es302420z.

Dutta, D., Kumari, A., Panda, R., Jha, S., Gupta, D., Goel, S., Jha, M. K. (2018) 'Close loop separation process for the recovery of Co, Cu, Mn, Fe and Li from spent lithium-ion batteries', *Separation and Purification Technology*. Elsevier, 200(December 2017), pp. 327–334. doi: 10.1016/j.seppur.2018.02.022.

Dynamix Agitators (2015) *Mixing 101: Optimal Tank Design*. Available at: https://www.dynamixinc.com/optimal-tank-design (Accessed: 15 April 2019).

El-Halwagi, M. M. (2011) *Sustainable Design Through Process Integration*. Elsevier.

Electropaedia (no date) *Battery and Energy Technologies*. Available at: https://www.mpoweruk.com/chemistries.htm (Accessed: 12 April 2019).

Ellingsen, L. A. W., Majeau-Bettez, G., Singh, B., Srivastava, A. K., Valoen, L. O., Stromman, A. H. (2014) 'Life Cycle Assessment of a Lithium-Ion Battery Vehicle Pack', *Journal of Industrial Ecology*, 18(1), pp. 113–124. doi: 10.1111/jiec.12072.

Engineers Edge (2000) *Overall Heat Transfer Coefficient Table Charts and Equation*. Available at: https://www.engineersedge.com/thermodynamics/overall_heat_transfer-table.htm (Accessed: 15 April 2019).

Evoqua Water Technologies (2014) *Filter Press Technology - High Performance Dewatering Applocations For Mining*. Available at: https://integralpx.com/wp-content/uploads/evoqua_brochure_filter_press_technology.pdf (Accessed: 3 March 2019).

Exchange-Rates.org (2019). Available at: https://www.exchange-rates.org/history/ZAR/USD/G/M (Accessed: 3 June 2019).

Fan, B., Chen, X., Zhou, T., Zhang, J., Xu, B. (2016) 'A sustainable process for the recovery of valuable metals from spent lithium-ion batteries', *Waste Management and Research*, 34(5), pp. 474–481. doi: 10.1177/0734242X16634454.

Fernandes, A., Afonso, J. C. and Dutra, A. J. B. (2013) 'Separation of nickel(II), cobalt(II) and lanthanides from spent Ni-MH batteries by hydrochloric acid leaching, solvent extraction and precipitation', *Hydrometallurgy*. Elsevier B.V., 133, pp. 37–43. doi: 10.1016/j.hydromet.2012.11.017.

Ferreira, D. A., Prados, L. M. Z., Majuste, D., Mansur, M. B. (2009) 'Hydrometallurgical separation of aluminium, cobalt, copper and lithium from spent Li-ion batteries', *Journal of Power Sources*,

187(1), pp. 238–246. doi: 10.1016/j.jpowsour.2008.10.077.

Fisher, K., Wallen, E., Laenen, P. P., Collins, M. (2006) *Battery waste management life cycle assessment*. Available at: http://www.lcm2007.ethz.ch/paper/424.pdf.

Gaines, L., Sullivan, J., Burnham, A. (2011) 'Life-Cycle Analysis for Lithium-Ion Battery Production and Recycling', in *90th Annual Meeting of the Transportation Research Board*. Washington DC. Available at: https://www.researchgate.net/publication/265158823.

Gaines, L. (2014) 'The future of automotive lithium-ion battery recycling: Charting a sustainable course', *Sustainable Materials and Technologies*. Elsevier B.V., 1, pp. 2–7. doi: 10.1016/j.susmat.2014.10.001.

Gao, W., Zhang, X., Zheng, X., Lin, X., Cao, H., Zhang, Y., Sun, Z. (2017) 'Lithium Carbonate Recovery from Cathode Scrap of Spent Lithium-Ion Battery: A Closed-Loop Process', *Environmental Science and Technology*, 51(3), pp. 1662–1669. doi: 10.1021/acs.est.6b03320.

Gao, W., Liu, C., Cao, H., Zheng, X., Lin, X., Wang, H., Zhang, Y., Sun, Z. (2018) 'Comprehensive evaluation on effective leaching of critical metals from spent lithium-ion batteries', *Waste Management*. Elsevier Ltd, 75(2018), pp. 477–485. doi: 10.1016/j.wasman.2018.02.023.

Gao, W., Song, J., Cao, H. Lin, X., Zhang, X., Zheng, X., Zhang, Y. Sun, Z. (2018) 'Selective recovery of valuable metals from spent lithium-ion batteries – Process development and kinetics evaluation', *Journal of Cleaner Production*. Elsevier Ltd, 178, pp. 833–845. doi: 10.1016/j.jclepro.2018.01.040.

Georgi-Maschler, T., Friedrich, B., Weyhe, R., Heegn, H., Rutz, M. (2012) 'Development of a recycling process for Li-ion batteries', *Journal of Power Sources*. Elsevier B.V., 207, pp. 173–182. doi: 10.1016/j.jpowsour.2012.01.152.

Goel (2019) *Falling Film Absorber*. Available at: https://www.goelscientific.com/SubProduct/Industrial_Glassware/Technical_Packages/Falling_Film_Absorber (Accessed: 8 May 2019).

Goel, R. K., Flora, J. R. V. and Chen, J. P. (2005) 'Flow Equalization and Neutralization', *Physicochemical Treatment Processes*, 3. doi: 10.1385/1-59259-820-x:021.

Golmohammadzadeh, R., Rashchi, F. and Vahidi, E. (2017) 'Recovery of lithium and cobalt from spent lithium-ion batteries using organic acids: Process optimization and kinetic aspects', *Waste Management*. Elsevier Ltd, 64, pp. 244–254. doi: 10.1016/j.wasman.2017.03.037.

Granata, Giuseppe, Moscardini, E., Pagnanelli, F., Trabucco, F., Toro, L. (2012) 'Product recovery from Li-

ion battery wastes coming from an industrial pre-treatment plant: Lab scale tests and process simulations', *Journal of Power Sources*. Elsevier B.V., 206, pp. 393–401. doi: 10.1016/j.jpowsour.2012.01.115.

Granata, G., Pagnanelli, F., Moscardini, E., Takacova, Z., Havlik, T., Toro, L. (2012) 'Simultaneous recycling of nickel metal hydride, lithium ion and primary lithium batteries: Accomplishment of European Guidelines by optimizing mechanical pre-treatment and solvent extraction operations', *Journal of Power Sources*. Elsevier B.V, 212, pp. 205–211. doi: 10.1016/j.jpowsour.2012.04.016.

Guo, Y., Li, F., Zhu, H., Li, G., Huang, J., He, W. (2016) 'Leaching lithium from the anode electrode materials of spent lithium-ion batteries by hydrochloric acid (HCl)', *Waste Management*. Elsevier Ltd, 51, pp. 227–233. doi: 10.1016/j.wasman.2015.11.036.

Guy, J. (2017) *E-waste: the fastest growing form of garbage | eNCA*. Available at: https://www.enca.com/weather/e-waste-the-fastest-growing-form-of-garbage (Accessed: 18 March 2019).

Habbache, N., Alane, N., Djerad, S., Tifouti, L. (2009) 'Leaching of copper oxide with different acid solutions', *Chemical Engineering Journal*, 152, pp. 503–508. doi: 10.1016/j.cej.2009.05.020.

Hart, K., Curran, M. A. and Davies, C. (2013) *Application of Life-Cycle Assessment to Nanoscale Technology: Lithium-ion Batteries for Electric Vehicles*, *United States Environmental Protection Agency*. doi: 10.1038/nchem.2085.

He, L. P., Sun, S. Y., Song, X. F., Yu, J. G. (2015) 'Recovery of cathode materials and Al from spent lithium-ion batteries by ultrasonic cleaning', *Waste Management*, 46, pp. 523–528. doi: 10.1016/j.wasman.2015.08.035.

He, L. P., Sun, S. Y., Song, X. F., Yu, J. G. (2017) 'Leaching process for recovering valuable metals from the LiNi1/3Co1/3Mn1/3O2cathode of lithium-ion batteries', *Waste Management*, 64, pp. 171–181. doi: 10.1016/j.wasman.2017.02.011.

He, L. P., Sun, S. Y., Mu, Y. Y., Song, X. F., Yu, J. G. (2017) 'Recovery of Lithium, Nickel, Cobalt, and Manganese from Spent Lithium-Ion Batteries Using l -Tartaric Acid as a Leachant', *ACS Sustainable Chemistry and Engineering*, 5(1), pp. 714–721. doi: 10.1021/acssuschemeng.6b02056.

He, L. P., Sun, S. Y. and Yu, J. G. (2018) 'Performance of LiNi1/3Co1/3Mn1/3O2 prepared from spent lithium-ion batteries by a carbonate co-precipitation method', *Ceramics International*, 44(1), pp. 351–357. doi: 10.1016/j.ceramint.2017.09.180.

Hu, J., Li, H., Chen, Y., Wang, C. (2017) 'A promising approach for the recovery of high value-added metals from spent lithium-ion batteries', *Journal of Power Sources*. Elsevier B.V, 351, pp. 192–199. doi: 10.1016/j.jpowsour.2017.03.093.

Huang, Y., Han, G., Liu, J., Chai, W., Wang, W., Yang, S., Su, S. (2016) 'A stepwise recovery of metals from hybrid cathodes of spent Li-ion batteries with leaching-flotation-precipitation process', *Journal of Power Sources*. Elsevier B.V, 325, pp. 555–564. doi: 10.1016/j.jpowsour.2016.06.072.

Huber Technology (no date) *Sludge Dewatering*. Available at: https://www.huber.de/solutions/energy-efficiency/sludge-treatment/dewatering.html (Accessed: 3 May 2019).

HyperPhysics (2016) *Table of Standard Electrode Potentials in Aqueous Solution at 25C*. Available at: http://hyperphysics.phy-astr.gsu.edu/hbase/Tables/electpot.html (Accessed: 9 May 2019).

indeed (2019) *Plant Operator Salaries in South Africa*. Available at: https://www.indeed.co.za/salaries/Plant-Operator-Salaries (Accessed: 3 May 2019).

index mundi (no date) *Heating Oil Daily Price*. Available at: https://www.indexmundi.com/commodities/?commodity=heating-oil&months=120 (Accessed: 3 May 2019).

Investing.com (2019) *Stock Market Quotes & Financial News*. Available at: https://www.investing.com/ (Accessed: 25 May 2019).

Jaffe, S. (2017) 'Vulnerable Links in the Lithium-Ion Battery Supply Chain', *Joule*. Elsevier Inc., 1(2), pp. 225–228. doi: 10.1016/j.joule.2017.09.021.

Jergensen, G. V. (1999) *Copper Leaching, Solvent Extraction, and Electrowinning Technology*. Society for Mining, Metallurgy and Exploration Inc. (SME).

Jha, M. K., Kumari, A., Jha, A. K., Kumar, V., Hait, J., Pandey, B. D. (2013) 'Recovery of lithium and cobalt from waste lithium ion batteries of mobile phone', *Waste Management*. Elsevier Ltd, 33(9), pp. 1890–1897. doi: 10.1016/j.wasman.2013.05.008.

Joo, S. H., Shin, S. M., Shin, D., Oh, C., Wang, J. P. (2015) 'Extractive separation studies of manganese from spent lithium battery leachate using mixture of PC88A and Versatic 10 acid in kerosene', *Hydrometallurgy*. Elsevier B.V., 156, pp. 136–141. doi: 10.1016/j.hydromet.2015.06.002.

Joseph, G., Koshy, J. and Kallanickal, P. M. (2013) 'A study of hydrochloric acid synthesis process in a chlor-alkaly industry', *Certified International Journal of Engineering Science and Innovative Technology (IJESIT)*, 2(2). Available at: http://www.ijesit.com/Volume 2/Issue

2/IJESIT201302_17.pdf.

Joulié, M., Laucournet, R. and Billy, E. (2014) 'Hydrometallurgical process for the recovery of high value metals from spent lithium nickel cobalt aluminum oxide based lithium-ion batteries', *Journal of Power Sources*. Elsevier B.V, 247, pp. 551–555. doi: 10.1016/j.jpowsour.2013.08.128.

Kang, J., Senanayake, G., Sohn, J., Shin, S. M. (2010) 'Recovery of cobalt sulfate from spent lithium ion batteries by reductive leaching and solvent extraction with Cyanex 272', *Hydrometallurgy*. Elsevier B.V., 100(3–4), pp. 168–171. doi: 10.1016/j.hydromet.2009.10.010.

Kasibiz (2015) *South African Salaries: How much people earn*. Available at: https://kasibiz.co.za/?p=8385 (Accessed: 3 May 2019).

Kemcore (2019) *Mining Chemicals and Services From Kemcore*. Available at: https://www.kemcore.com/ (Accessed: 3 May 2019).

Kemp, I. C. (2014) 'Fundamentals of Energy Analysis of Dryers', *Modern Drying Technology*, 4, pp. 1–45. doi: 10.1002/9783527631728.ch21.

Khoele, G. (2017) *SASOl Gas application for approval of maximum gas prices in terms of section 21(1)(p) and approval of distinguishing features in terms of section 22(1) of the Gas Act, 2001 (ACT NO.48 of 2001) for the period 1 July 2017 to 30 September 2018*. Available at: http://www.nersa.org.za/Admin/Document/Editor/file/Piped Gas/Consultations/Document/Sasol Gas Application For Approval of Maximum Gas Prices.pdf.

Knights, B. D. H. and Saloojee, F. (2015) *Lithium battery recycling - Green Economy Research Report No.1*. Development Bank of Southern Africa, Midrand. Available at: https://waste-management-world.com/a/1-the-lithium-battery-recycling-challenge.

Kohler, N., Van Niekerk, M., Manchidi, D., Nemakhavhani, L., Meyer, S., Steyn, G., Els, R. (2018) 'South Africa State of Waste Report'. Available at: http://sawic.environment.gov.za/documents/8641.pdf.

Lee, C. K. and Rhee, K.-I. (2002) 'Preparation of LiCoO2 from spent lithium-ion batteries', *Journal of Power Sources*. Elsevier, 109(1), pp. 17–21. doi: 10.1016/S0378-7753(02)00037-X.

Lee, C. K. and Rhee, K.-I. (2003) 'Reductive leaching of cathodic active materials from lithium ion battery wastes', *Hydrometallurgy*. Elsevier, 68(1–3), pp. 5–10. doi: 10.1016/S0304-386X(02)00167-6.

Li, Jinhui, Shi, P., Wang, Z., Chen, Y., Changm C. C. (2009) 'A combined recovery process of metals in spent lithium-ion batteries', *Chemosphere*. Elsevier Ltd, 77(8), pp. 1132–1136. doi: 10.1016/j.chemosphere.2009.08.040.

Li, Jiangang, Zhao, R., He, X., Liu, H. (2009) 'Preparation of LiCoO2cathode materials from spent lithium-ion batteries', *Ionics*, 15(1), pp. 111–113. doi: 10.1007/s11581-008-0238-8.

Li, Jinhui, Li, X., Hu, Q., Wang, Z., Zheng, J., Wu, L., Zhang, L. (2009) 'Study of extraction and purification of Ni, Co and Mn from spent battery material', *Hydrometallurgy*. Elsevier B.V., 99(1–2), pp. 7–12. doi: 10.1016/j.hydromet.2009.05.018.

Li, L., Ge, J., Chen, R., Wu, F., Chen, S., Zhang, X. (2010) 'Environmental friendly leaching reagent for cobalt and lithium recovery from spent lithium-ion batteries', *Waste Management*, 30(12), pp. 2615–2621. doi: 10.1016/j.wasman.2010.08.008.

Li, L., Ge, J., Wu, F., Chen, R., Chen, S., Wu, B. (2010) 'Recovery of cobalt and lithium from spent lithium ion batteries using organic citric acid as leachant', *Journal of Hazardous Materials*, 176(1–3), pp. 288–293. doi: 10.1016/j.jhazmat.2009.11.026.

Li, L., Lu, J., Ren, Y., Zhang, X. X., Chen, R. J., Wu, F., Amine, K. (2012) 'Ascorbic-acid-assisted recovery of cobalt and lithium from spent Li-ion batteries', *Journal of Power Sources*. Elsevier B.V, 218, pp. 21–27. doi: 10.1016/j.jpowsour.2012.06.068.

Li, L., Dunn, J. B., Zhang, X. X., Gaines, L., Chen, R. J., Wu, F., Amine, K. (2013) 'Recovery of metals from spent lithium-ion batteries with organic acids as leaching reagents and environmental assessment', *Journal of Power Sources*, 233, pp. 180–189. doi: 10.1016/j.jpowsour.2012.12.089.

Li, L., Zhai, L., Zhang, X., Lu, J., Chen, R., Wu, F., Amine, K. (2014) 'Recovery of valuable metals from spent lithium-ion batteries by ultrasonic-assisted leaching process', *Journal of Power Sources*, 262, pp. 380–385. doi: 10.1016/j.jpowsour.2014.04.013.

Li, L., Qu, W., Zhang, X., Lu, J., Chen, R., Wu, F., Amine, K. (2015) 'Succinic acid-based leaching system: A sustainable process for recovery of valuable metals from spent Li-ion batteries', *Journal of Power Sources*, 282, pp. 544–551. doi: 10.1016/j.jpowsour.2015.02.073.

Li, L., Fan, E., Guan, Y., Zhang, X., Xue, Q., Wei, L., Wu, F., Chen, R. (2017) 'Sustainable Recovery of Cathode Materials from Spent Lithium-Ion Batteries Using Lactic Acid Leaching System', *ACS Sustainable Chemistry and Engineering*, 5(6), pp. 5224–5233. doi: 10.1021/acssuschemeng.7b00571.

Li, L., Bian, Y., Zhang, X., Xue, Q., Fan, E., Wu, F., Chen, R. (2018) 'Economical recycling process for spent lithium-ion batteries and macro- and micro-scale mechanistic study', *Journal of Power Sources*, 377(August 2017), pp. 70–79. doi: 10.1016/j.jpowsour.2017.12.006.

Li, L., Bian, Y., Zhang, X., Guan, Y., Fan, E., Wu, F., Chen, R. (2018) 'Process for recycling mixed-cathode materials from spent lithium-ion batteries and kinetics of leaching', *Waste Management*, 71, pp. 362–371. doi: 10.1016/j.wasman.2017.10.028.

Li, L., Bian, Y., Zhang, X., Yao, Y., Xue, Q., Fan, E., Wu, F., Chen, R. (2019) 'A green and effective room-temperature recycling process of LiFePO4 cathode materials for lithium-ion batteries', *Waste Management*, 85, pp. 437–444. doi: 10.1016/j.wasman.2019.01.012.

Lide, D. (2005) *CRC Handbook of Chemistry and Physics*. 91st edn, *CRC Handbook of Chemistry and Physics*. 91st edn. Available at: papers2://publication/uuid/55E853FE-9E62-4EEC-97D7-AFAB12AA3361.

Lumen (no date) *Strength of Acids*. Available at: https://courses.lumenlearning.com/boundless-chemistry/chapter/strength-of-acids/ (Accessed: 25 March 2019).

Lupi, C. and Pasquali, M. (2003) 'Electrolytic nickel recovery from lithium-ion batteries', *Minerals Engineering*, 16(6), pp. 537–542. doi: 10.1016/S0892-6875(03)00080-3.

Lupi, C., Pasquali, M. and Dell'Era, A. (2005) 'Nickel and cobalt recycling from lithium-ion batteries by electrochemical processes', *Waste Management*, 25(2 SPEC. ISS.), pp. 215–220. doi: 10.1016/j.wasman.2004.12.012.

Lv, W., Wang, Z., Cao, H., Sun, Y., Zhang, Y., Sun, Z. (2018) 'A Critical Review and Analysis on the Recycling of Spent Lithium-Ion Batteries', *ACS Sustainable Chemistry and Engineering*, 6(2), pp. 1504–1521. doi: 10.1021/acssuschemeng.7b03811.

Lydall, M., Nyanjowa, W. and James, Y. (2017) 'Mapping South Africa ' s Waste Electrical and Electronic Equipment (WEEE) Dismantling , Pre-Processing and Processing Technology Landscape Waste Research Development and Mapping South Africa ' s Waste Electrical and Electronic Equipment (WEEE) Dismant', (March), pp. 1–91.

Ma, L., Nie, Z., Xi, X., Han, X. (2013) 'Cobalt recovery from cobalt-bearing waste in sulphuric and citric acid systems', *Hydrometallurgy*. Elsevier B.V., 136(x), pp. 1–7. doi: 10.1016/j.hydromet.2013.01.016.

Majeau-Bettez, G., Hawkins, T. R. and Strømman, A. H. (2011) 'Life Cycle Environmental Assessment of Li-iion and Nickel Metal Hydride Batteries for Plug-in Hybrid and Battery Electric Vehicles', *Environmental Science and Technology*, 45(10), pp. 4548–4554. doi: 10.1021/es103607c.

Mantuano, D. P., Dorella, G., Elias, R. C. A., Mansur, M. B. (2006) 'Analysis of a hydrometallurgical route to recover base metals from spent rechargeable batteries by liquid-liquid extraction with

Cyanex 272', *Journal of Power Sources*, 159(2), pp. 1510–1518. doi: 10.1016/j.jpowsour.2005.12.056.

Meshram, P., Pandey, B. D. and Mankhand, T. R. (2015) 'Recovery of valuable metals from cathodic active material of spent lithium ion batteries: Leaching and kinetic aspects', *Waste Management*. Elsevier Ltd, 45, pp. 306–313. doi: 10.1016/j.wasman.2015.05.027.

Metalary (2019) *Metalary - Latest and Historical Metal Prices*. Available at: https://www.metalary.com/ (Accessed: 25 May 2019).

Monterey Peninsula College (no date) *Brønsted-Lowry Acids and Bases Acid and Base Definitions*. Available at: http://www.mpcfaculty.net/mark_bishop/Bronsted_Lowry.pdf (Accessed: 2 May 2019).

Moroz, W. W. (2016) *HCl Synthesis Units With Enhanced Safety Features*. Available at: http://clorosur.org/seminar2016/presentation/17/12-HCL.pdf (Accessed: 27 March 2019).

Mullin, J. W. (2001) *Crystallization*. 4th Editio. Elsevier.

Musariri, B. (2019) *Development of an environmentally friendly lithium-ion battery recycling process*. Stellenbosch University.

Nafion Ion Exchange Materials (2016) *General Information on Nafion ™ Membrane for Electrolysis*. Available at: https://www.chemours.com/Nafion/en_US/assets/downloads/nafion-membrane-electrolysis-product-information.pdf (Accessed: 26 March 2019).

Naidoo, R. (2017) *Why SA is losing out on full e-waste recycling potential | Infrastructure news*. Available at: http://infrastructurenews.co.za/2017/05/04/why-sa-is-losing-out-on-full-e-waste-recycling-potential/ (Accessed: 6 June 2019).

Nan, J., Han, D., Yang, M., Cui, M. (2005) 'Dismantling, Recovery, and Reuse of Spent Nickel–Metal Hydride Batteries', *Journal of The Electrochemical Society*, 153(1), p. A101. doi: 10.1149/1.2133721.

Nan, J., Han, D. and Zuo, X. (2005) 'Recovery of metal values from spent lithium-ion batteries with chemical deposition and solvent extraction', *Journal of Power Sources*, 152, pp. 278–284. doi: 10.1016/j.jpowsour.2005.03.134.

Nayaka, G. P., Manjanna, J., Pai, K. V., Vadavi, R., Keny, S. J., Tripathi, V. S. (2015) 'Recovery of valuable metal ions from the spent lithium-ion battery using aqueous mixture of mild organic acids as alternative to mineral acids', *Hydrometallurgy*. Elsevier B.V., 151, pp. 73–77. doi: 10.1016/j.hydromet.2014.11.006.

Nayaka, G. P., Pai, K. V., Santhosh, G., Manjanna, J. (2016a) 'Dissolution of cathode active material of spent Li-ion batteries using tartaric acid and ascorbic acid mixture to recover Co', *Hydrometallurgy*, 161, pp. 54–57. doi: 10.1016/j.hydromet.2016.01.026.

Nayaka, G. P., Pai, K. V., Santhosh, G., Manjanna, J. (2016b) 'Recovery of cobalt as cobalt oxalate from spent lithium ion batteries by using glycine as leaching agent', *Journal of Environmental Chemical Engineering*. Elsevier B.V., 4(2), pp. 2378–2383. doi: 10.1016/j.jece.2016.04.016.

Nayaka, G.P., Pai, K. V., Manjanna, J., Keny, S. J. (2016) 'Use of mild organic acid reagents to recover the Co and Li from spent Li-ion batteries', *Waste Management*. Elsevier Ltd, 51, pp. 234–238. doi: 10.1016/j.wasman.2015.12.008.

Nayaka, G. P., Zhang, Y., Dong, P., Wang, D., Pai, K. V., Manjanna, J., Santhosh, G., Duan, J., Zhou, Z., Xiao, J. (2018) 'Effective and environmentally friendly recycling process designed for LiCoO2 cathode powders of spent Li-ion batteries using mixture of mild organic acids', *Waste Management*. Elsevier Ltd, 78, pp. 51–57. doi: 10.1016/j.wasman.2018.05.030.

Nayaka, G. P., Zhang, Y., Dong, P., Wang, D., Zhou, Z., Duan, J., Li, X., Lin, Y., Meng, Q., Pai, K. V., Manjanna, J., Santhosh, G. (2019) 'An environmental friendly attempt to recycle the spent Li-ion battery cathode through organic acid leaching', *Journal of Environmental Chemical Engineering*. Elsevier, 7(1), p. 102854. doi: 10.1016/j.jece.2018.102854.

Nguyen, V. T., Lee, J., Jeong, J., Kim, B. S., Pandey, B. D. (2014) 'Selective recovery of cobalt, nickel and lithium from sulfate leachate of cathode scrap of Li-ion batteries using liquid-liquid extraction', *Metals and Materials International*, 20(2), pp. 357–365. doi: 10.1007/s12540-014-1016-y.

Notter, D., Gauch, M., Widmer, R., Wager, P., Stamp, A., Zah, R., Althaus, H. J. (2010) 'Contribution of Li-Ion Batteries to the Environmental Impact of Electric Vehicles', *Environmental Science and Technology*, 44(17), pp. 6550–6556.

Okagbue, H. I., Edeki, S. O. and Opanuga, A. A. (2014) 'A Monte Carlo Simulation Approach in Assessing Risk and Uncertainty Involved in Estimating the Expected Earnings of an Organization : A Case Study in Nigeria', *American Journal of Computational and Applied Mathematicccs*, 4(5), pp. 161–166. doi: 10.5923/j.ajcam.20140405.02.

OKCHEM (2019) *Global B2B Platform for Chemical Raw Materials*. Available at: https://www.okchem.com/ (Accessed: 3 May 2019).

Olivetti, E. A., Ceder, G., Gaustad, G. G., Fu, X. (2017) 'Lithium-Ion Battery Supply Chain Considerations: Analysis of Potential Bottlenecks in Critical Metals', *Joule*. Elsevier Inc., 1(2), pp. 229–243. doi:

10.1016/j.joule.2017.08.019.

Paidar, M., Fateev, V. and Bouzek, K. (2016) 'Membrane electrolysis—History, current status and perspective', *Electrochimica Acta*. Elsevier Ltd, 209, pp. 737–756. doi: 10.1016/j.electacta.2016.05.209.

Paulino, J. F., Busnardo, N. G. and Afonso, J. C. (2008) 'Recovery of valuable elements from spent Li-batteries', *Journal of Hazardous Materials*, 150(3), pp. 843–849. doi: 10.1016/j.jhazmat.2007.10.048.

Pedada, S. R., Bathalu, S., Vasa, S. S. R., Charla, K. S., Gollapalli, N. R. (2009) 'Micellar effect on metal-ligand complexes of Co(II), Ni(II), Cu(II) and Zn(II) with citric acid', *Bulletin of the Chemical Society of Ethiopia*, 23(3), pp. 347–358. doi: 10.4314/bcse.v23i3.47659.

Peng, C., Hamuyuni, J., Wilson, B. P., Lundstrom, M. (2018) 'Selective reductive leaching of cobalt and lithium from industrially crushed waste Li-ion batteries in sulfuric acid system', *Waste Management*. Elsevier Ltd, 76, pp. 582–590. doi: 10.1016/j.wasman.2018.02.052.

Peters, M. S., Timmerhaus, K. D. and West, R. E. (2003) *Plant design and economics for chemical engineers*. 5th edn. Boston: McGraw-Hill.

Petranikova, M., Miskufova, A., Havlik, T., Forsen, O., Pehkonen, A. (2011) 'Cobalt Recovery From Spent Portable Lithium Accumulators', *Acta Metallurgica Slovaca*, 17(2), pp. 106–115.

PolyCorp (no date) *Rubber Lining Material Selection*. Available at: http://www.poly-corp.com/assets/file/resource/Polycorp-Protective-Linings--Rubber-Linings-Material-Selection-V5.pdf (Accessed: 16 April 2019).

Porvali, A., Aaltonen, M., Ojanen, S., Velazquez-Martinez, O., Eronen, E., Liu, F., Wilson, B. P., Serna-Guerrero, R., Lundstrom, M. (2019) 'Mechanical and hydrometallurgical processes in HCl media for the recycling of valuable metals from Li-ion battery waste', *Resources, Conservation & Recycling*. Elsevier, In Press(November 2018), pp. 257–266. doi: 10.1016/j.resconrec.2018.11.023.

Pranolo, Y., Zhang, W. and Cheng, C. Y. (2010) 'Recovery of metals from spent lithium-ion battery leach solutions with a mixed solvent extractant system', *Hydrometallurgy*. Elsevier B.V., 102(1–4), pp. 37–42. doi: 10.1016/j.hydromet.2010.01.007.

PubChem (2017) *Sodium Citrate*, *U.S. National Library of Medicine - National Center for Biotechnology Information*. Available at: http://www.ilo.org/dyn/icsc/showcard.display?p_version=2&p_card_id=1218 (Accessed: 20

June 2019).

Puncochar, M. (no date) *Chemical Equations online!* Available at: http://chemequations.com/en/?k=1&s=FeCl2+%2B+KMnO4+%2B+H2O+%3D+Fe%28OH%293+%2B+FeCl3+%2B+MnO2+%2B+KOH&ref=search (Accessed: 2 May 2019).

Retsch (2019) *Cutting Mill SM 400 XL*. Available at: https://www.retsch.com/products/milling/cutting-mills/sm-400/function-features/ (Accessed: 6 May 2019).

Roskill (2019) *Lithium-ion Batteries Outlook to 2028 — Market Report*. Available at: https://roskill.com/market-report/lithium-ion-batteries/ (Accessed: 20 May 2019).

Roux, L. M., Minnaar, E., Cilliers, P. J., Bellino, M., Dye, R. (2010) 'Comparison of solvent extraction and selective percipitation for the purification of cobalt electrolytes at the Luilu refinery , DRC', *The South Africa Institute of Mining and Metallurgy*, (1), pp. 343–364. Available at: https://www.saimm.co.za/Conferences/BM2007/343-364_leRoux.pdf.

Sakultung, S., Pruksathorn, K. and Hunson, M. (2007) 'Simultaneous recovery of valuable metals from spent mobile phone battery by an acid leaching process', *Korean J. Chem. Eng.*, 24(2), pp. 272–277. doi: 10.4212/cjhp.v69i4.1581.

dos Santos, C. S., Alves, J. C., da Silva, S. P., Sita, L. E., da Silva, P. R. C., de Almeida, L. C., Scarminio, J. (2019) 'A closed-loop process to recover Li and Co compounds and to resynthesize LiCoO2 from spent mobile phone batteries', *Journal of Hazardous Materials*. Elsevier, 362(September), pp. 458–466. doi: 10.1016/j.jhazmat.2018.09.039.

SARS (no date) *Companies, Trusts and Small Business Corporations (SBC)*. Available at: https://www.sars.gov.za/Tax-Rates/Income-Tax/Pages/Companies-Trusts-and-Small-Business-Corporations.aspx (Accessed: 6 May 2019).

Sattar, R., Ilyas, S., Bhatti, H. N., Ghaffar, A. (2019) 'Resource recovery of critically-rare metals by hydrometallurgical recycling of spent lithium ion batteries', *Separation and Purification Technology*, 209(August 2018), pp. 725–733. doi: 10.1016/j.seppur.2018.09.019.

Schneiders, K., Zimmermann, A. and Henßen, G. (2001) *Membrane electrolysis - innovation for the chlor-alkali industry*. Available at: https://www.researchgate.net/publication/295822120_Membrane_electrolysis_-_Innovation_for_the_chlor-alkali_industry.

Sensorex (no date) *pH Calculator | Calculate pH of a Solution*. Available at: https://sensorex.com/ph-calculator/ (Accessed: 23 April 2019).

Serjeant, E. P. and Dempsey, B. (1979) *Ionisation Constants of Organic Acids in Aqueous Solution*. Pergamon.

SGL Carbon (2018) *The Resistants- Our process technology for corrosive applications*. Available at: https://www.sglcarbon.com/en/markets-solutions/material/diabon/ (Accessed: 5 April 2019).

SGL Group (2016) *SGL Group's outstanding expertise – HCl synthesis units with steam generation*. Available at: http://clorosur.org/seminar2016/presentation/17/11-SGL.pdf (Accessed: 27 March 2019).

Shanghai Metals Market (2019) *Copper,Aluminum,Lead,Zinc,Nickel,Tin,Steel Prices Charts*. Available at: https://www.metal.com/ (Accessed: 25 March 2019).

Shin, S. M., Kim, N. H., Sohan, J. S., Yang, D. H., Kim, Y. H. (2005) 'Development of a metal recovery process from Li-ion battery wastes', *Hydrometallurgy*, 79(3–4), pp. 172–181. doi: 10.1016/j.hydromet.2005.06.004.

Shuva, M. A. H. and Kurny, A. (2013) 'Hydrometallurgical Recovery of Value Metals from Spent Lithium Ion Batteries', *American Journal of Materials Engineering and Technology*, 1(1), pp. 8–12. doi: 10.12691/materials-1-1-2.

Silberberg, M. (2013) 'Appendix C: Dissociation Constants and pKa Values for Acids at 25°C', in *Principles of General Chemistry*. Available at: https://2012books.lardbucket.org/books/principles-of-general-chemistry-v1.0/s31-appendix-c-dissociation-consta.html (Accessed: 25 March 2019).

Sinott, R. K. (2005) *Coulson & Richardson's Chemical Engineering Design*. 4th edn. Elsevier.

Skoog, D. A. and West, D. M. (1982) *Fundamentals of Analytical Chemistry*. 4th edn. New York: Cengage Learning.

Smith, R. (2005) *Chemical Process Design and Integration*, *John Wiley & Sons, Ltd*. doi: 10.1529/biophysj.107.124164.

Sohn, J. S., Shin, S. M., Yang, D. H., Kim, S. K., Lee, C. K. (2006) 'Comparison of two acidic leaching processes for selecting the effective recycle process of spent lithium ion battery', *Geosystem Engineering*, 9(1), pp. 1–6. doi: 10.1080/12269328.2006.10541246.

Statista (2019) *South Africa - total population 2012-2022*. Available at: https://www.statista.com/statistics/578867/total-population-of-south-africa/ (Accessed: 18 March 2019).

Stats SA (2018) *Only 10% of waste recycled in South Africa | Statistics South Africa*. Available at: http://www.statssa.gov.za/?p=11527 (Accessed: 28 May 2019).

Stellenbosch Municipality (2018) *Stellenbosch Municipality Tariffs 2018/2019*. Available at: https://www.stellenbosch.gov.za/afr/dokumente/verslae/quarterly-fin-reports/5895-final-draft-tariff-proposals-20182019/file.

Sun, C., Xu, L., Chen, X., Qiu, T., Zhou, T. (2018) 'Sustainable recovery of valuable metals from spent lithium-ion batteries using DL-malic acid: Leaching and kinetics aspect', *Waste Management and Research*, 36(2), pp. 113–120. doi: 10.1177/0734242X17744273.

Sun, L. and Qiu, K. (2011) 'Vacuum pyrolysis and hydrometallurgical process for the recovery of valuable metals from spent lithium-ion batteries', *Journal of Hazardous Materials*. Elsevier B.V., 194, pp. 378–384. doi: 10.1016/j.jhazmat.2011.07.114.

Sun, L. and Qiu, K. (2012) 'Organic oxalate as leachant and precipitant for the recovery of valuable metals from spent lithium-ion batteries', *Waste Management*. Elsevier Ltd, 32(8), pp. 1575–1582. doi: 10.1016/j.wasman.2012.03.027.

Suzuki, T., Nakamura, T., Inoue, Y., Niinae, M., Shibata, J. (2012) 'A hydrometallurgical process for the separation of aluminum, cobalt, copper and lithium in acidic sulfate media', *Separation and Purification Technology*. Elsevier B.V., 98, pp. 396–401. doi: 10.1016/j.seppur.2012.06.034.

Swain, B., Jeong, J., Lee, J., Lee, G. H., Sohn, J. S. (2007) 'Hydrometallurgical process for recovery of cobalt from waste cathodic active material generated during manufacturing of lithium ion batteries', *Journal of Power Sources*, 167(2), pp. 536–544. doi: 10.1016/j.jpowsour.2007.02.046.

Takacova, Z., Havlik, T., Kukurugya, F., Orac, D. (2016) 'Cobalt and lithium recovery from active mass of spent Li-ion batteries: Theoretical and experimental approach', *Hydrometallurgy*. Elsevier B.V., 163, pp. 9–17. doi: 10.1016/j.hydromet.2016.03.007.

Tanong, K., Tran, L. H., Mercier, G., Blais, J. F. (2017) 'Recovery of Zn (II), Mn (II), Cd (II) and Ni (II) from the unsorted spent batteries using solvent extraction, electrodeposition and precipitation methods', *Journal of Cleaner Production*. Elsevier Ltd, 148, pp. 233–244. doi: 10.1016/j.jclepro.2017.01.158.

The Engineering Toolbox (no date) *Overall Heat Transfer Coefficient*. Available at: https://www.engineeringtoolbox.com/overall-heat-transfer-coefficient-d_434.html (Accessed: 15 April 2019).

Tico (2019) *Floating Head Heat Exchanger*. Available at: http://www.ansonindustry.com/pressure-vessel/floating-head-heat-exchanger.html (Accessed: 8 May 2019).

Totton Pumps (2008) *Chemical compatibility chart*. Available at: http://www.saltech.co.il/_uploads/dbsattachedfiles/chemical.pdf (Accessed: 22 April 2019).

Towler, G. and Sinnott, R. K. (2013) *Chemical Engineering Design: Principles, Practice and Economics of Plant and Process Design*. 2nd edn. Oxford, UK: Elsevier. Available at: http://uniquebec.info/materialsapp/Y14REGULATION/CHEMICAL/41/41BOOKS/ChemicalEngineeringDesignPrinciplesSecondEdition.pdf.

Turton, R., Bailie, R. C., Whiting, W. B., Shaeiwitz, J. A., Bhattacharyya, D. (2012) *Analysis, Synthesis and Design of Chemical Processes*. 4th edn. Pearson Education Inc.

Ulrich, G. D. and Vasudevan, P. T. (2004) 'Chemical engineering process design and economics, a practical guide', *Chemical Engineering*, 113(4), pp. 66–69.

Ultrasonic Power Corporation (no date) *Ultrasonic Cleaning Technical Information*. Available at: https://www.upcorp.com/technical-information.html (Accessed: 13 February 2019).

United States Environmental Protection Agency (2003) 'Air Pollution Control Technology Fact Sheet', pp. 1–6. Available at: http://infohouse.p2ric.org/ref/50/49195.pdf.

US Department of Energy (2012) *Benchmark the Fuel Cost of Steam Generation*, *Energy Efficiency and Renewable Energy*. doi: DOE/GO-102012-3391.

Wang, R. C., Lin, Y. C. and Wu, S. H. (2009) 'A novel recovery process of metal values from the cathode active materials of the lithium-ion secondary batteries', *Hydrometallurgy*. Elsevier B.V., 99(3–4), pp. 194–201. doi: 10.1016/j.hydromet.2009.08.005.

Wang, W. Y., Yen, C. H., Lin, J. L., Xu, R. B. (2019) 'Recovery of high-purity metallic cobalt from lithium nickel manganese cobalt oxide (NMC)-type Li-ion battery', *Journal of Material Cycles and Waste Management*. Springer Japan, 21(2), pp. 300–307. doi: 10.1007/s10163-018-0790-x.

Welders Filtration Technology (no date) *The filter press: filtration with the highest separation efficiency*. Available at: https://www.wft.be/en/filter-presses/ (Accessed: 24 March 2019).

Van Wyk, A. P. (2014) *Flowsheet development and comparison for the recovery of precious metals from cyanide leach solutions*. Stellenbosch University. Available at: http://scholar.sun.ac.za/handle/10019.1/86302 (Accessed: 5 March 2019).

Xinhai Mineral Processing EPC (no date a) *High Efficiency Agitation Tank*. Available at: http://www.xinhaimining.com/product/agitator/high-efficiency-agitation-tank#bbb (Accessed: 15 April 2019).

Xinhai Mineral Processing EPC (no date b) *Press Filter*. Available at:

http://www.xinhaimining.com/product/dewater/press-filter (Accessed: 15 April 2019).

Yang, Y., Xu, S. and He, Y. (2017) 'Lithium recycling and cathode material regeneration from acid leach liquor of spent lithium-ion battery via facile co-extraction and co-precipitation processes', *Waste Management*. Elsevier Ltd, 64, pp. 219–227. doi: 10.1016/j.wasman.2017.03.018.

Yao, L., Yao, H., Xi, G., Feng, Y. (2016) 'Recycling and synthesis of LiNi1/3Co1/3Mn1/3O2from waste lithium ion batteries using d,l-malic acid', *RSC Advances*. Royal Society of Chemistry, 6(22), pp. 17947–17954. doi: 10.1039/c5ra25079j.

Yao, L., Feng, Y. and Xi, G. (2015) ' A new method for the synthesis of LiNi 1/3 Co 1/3 Mn 1/3 O 2 from waste lithium ion batteries ', *RSC Advances*. Royal Society of Chemistry, 5(55), pp. 44107–44114. doi: 10.1039/c4ra16390g.

Yao, Y., Zhu, M., Zhao, Z., Tong, B., Fan, Y., Hua, Z. (2018) 'Hydrometallurgical Processes for Recycling Spent Lithium-Ion Batteries: A Critical Review', *ACS Sustainable Chemistry and Engineering*. American Chemical Society, 6(11), pp. 13611–13627. doi: 10.1021/acssuschemeng.8b03545.

Yu, M., Zhang, Z., Xue, F., Yang, B., Guo, G., Qiu, J. (2019) 'A more simple and efficient process for recovery of cobalt and lithium from spent lithium-ion batteries with citric acid', *Separation and Purification Technology*. Elsevier, 215(October 2018), pp. 398–402. doi: 10.1016/j.seppur.2019.01.027.

Zelenin, O. Y. (2007) 'Interaction of the Ni2+ ion with citric acid in an aqueous solution', *Russian Journal of Coordination Chemistry*, 33(5), pp. 346–350. doi: 10.1134/s1070328407050065.

Zeng, X., Li, J. and Shen, B. (2015) 'Novel approach to recover cobalt and lithium from spent lithium-ion battery using oxalic acid', *Journal of Hazardous Materials*. Elsevier B.V., 295(2015), pp. 112–118. doi: 10.1016/j.jhazmat.2015.02.064.

Zeng, X., Li, J. and Singh, N. (2014) 'Recycling of spent lithium-ion battery: A critical review', *Critical Reviews in Environmental Science and Technology*, 44(10), pp. 1129–1165. doi: 10.1080/10643389.2013.763578.

Zhang, P., Yokoyama, T., Itabashi, O., Suzuki, T. M., Inoue, K. (1998) 'Hydrometallurgical process for recovery of metal values from spent lithium-ion secondary batteries', 47, pp. 2–3. doi: 10.1016/S0304-386X(97)00050-9.

Zhang, T., He, Y., Ge, L., Fu, R., Zhang, X., Huang, Y. (2013) 'Characteristics of wet and dry crushing methods in the recycling process of spent lithium-ion batteries', *Journal of Power Sources*. Elsevier B.V, 240, pp. 766–771. doi: 10.1016/j.jpowsour.2013.05.009.

Zhang, T., He, Y., Wang, F., Ge, L., Zhu, X., Li, H. (2014) 'Chemical and process mineralogical characterizations of spent lithium-ion batteries: An approach by multi-analytical techniques', *Waste Management*. Elsevier Ltd, 34(6), pp. 1051–1058. doi: 10.1016/j.wasman.2014.01.002.

Zhang, W., Xu, C., He, W., Li, G. Huang, J. (2018) 'A review on management of spent lithium ion batteries and strategy for resource recycling of all components from them', *Waste Management and Research*, 36(2), pp. 99–112. doi: 10.1177/0734242X17744655.

Zheng, X., Zhu, Z., Lin, X., Zhang, Y., He, Y., Cao, H., Sun, Z. (2018) 'A Mini-Review on Metal Recycling from Spent Lithium Ion Batteries', *Engineering*, 4(3), pp. 361–370. doi: 10.1016/j.eng.2018.05.018.

Zheng, Y., Long, H. L., Zhou, L., Wu, Z. S., Zhou, X., You, L., Yang, Y., Liu, J. W. (2016) 'Leaching procedure and kinetic studies of cobalt in cathode materials from spent lithium ion batteries using organic citric acid as leachant', *International Journal of Environmental Research*, 10(1), pp. 159–168.

Zou, H., Gratz, E., Apelian, D., Wang, Y. (2013) 'A novel method to recycle mixed cathode materials for lithium ion batteries', *Green Chemistry*, 15(5), pp. 1183–1191. doi: 10.1039/c3gc40182k.

Appendix A -

Process Flow Diagrams and Stream Tables

Process Flow Diagram of Mineral Acid Process Option 1 (MA-1)

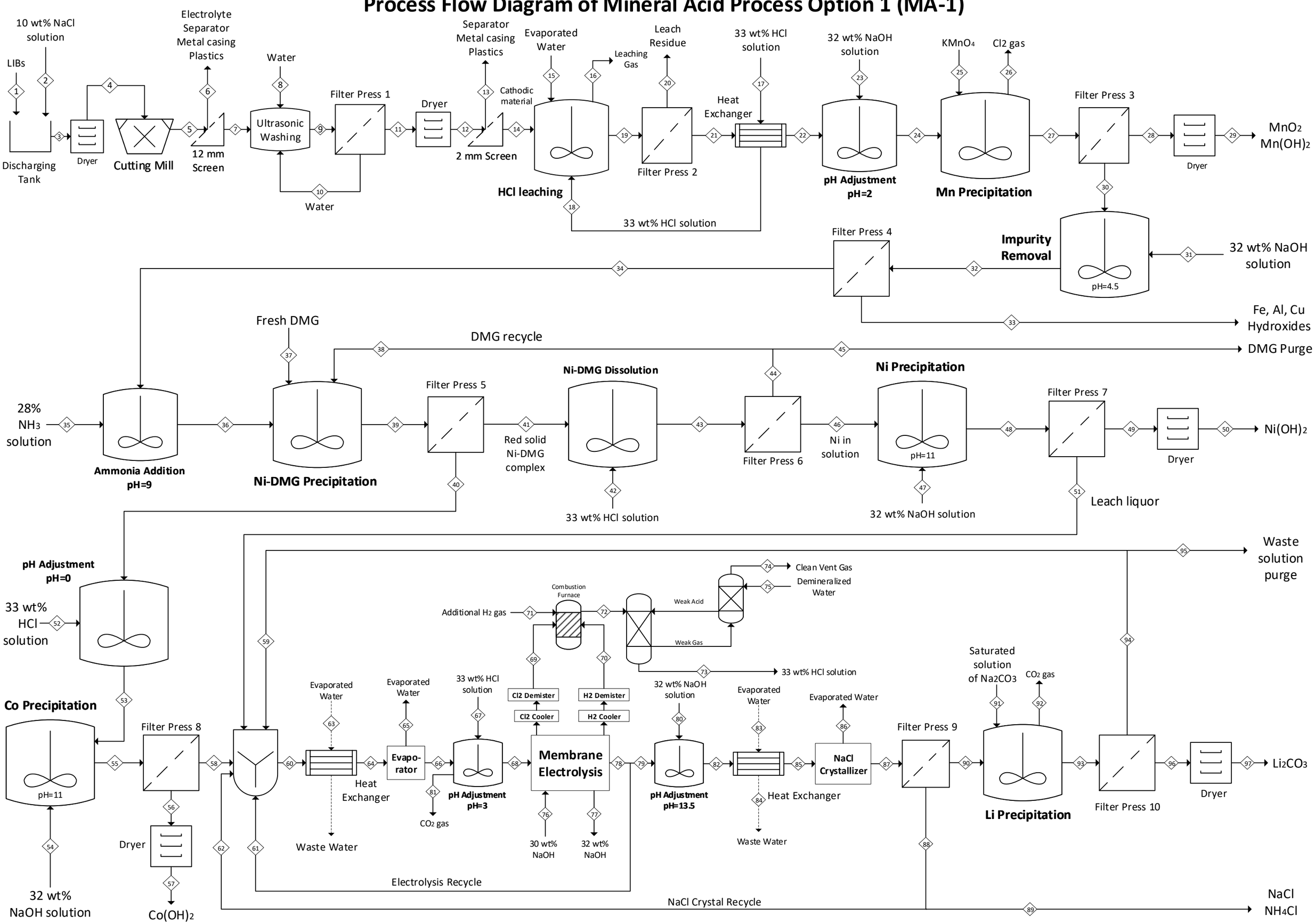

Table 62: Stream table for MA-1 (kg/hr)

Component	1	2	3	4	5	6	7	8	9	10	11	12	13	14	15	16	17	18	19	20
Total	107.70	161.49	123.85	107.70	107.70	29.76	77.94	4.97	249.41	166.49	82.92	77.94	23.33	54.61	1878.81	3.56	1206.67	1206.67	3136.52	14.54
Plastics	5.13		5.13	5.13	5.13	4.88	0.26		0.26		0.26	0.26	0.26	0.00						
Electrolyte	3.37		3.37	3.37	3.37	3.37	0.00		0.00		0.00	0.00	0.00	0.00						
Metal Casing	22.64		22.64	22.64	22.64	21.51	1.13		1.13		1.13	1.13	1.13	0.00						
$LiCoO_2$	15.80		15.80	15.80	15.80		15.80		15.80		15.80	15.80	1.26	14.54					0.051	0.051
$LiNi_{0,33}Co_{0,33}Mn_{0,33}O_2$	12.32		12.32	12.32	12.32		12.32		12.32		12.32	12.32	0.99	11.33					0.083	0.083
$LiMn_2O_4$	9.09		9.09	9.09	9.09		9.09		9.09		9.09	9.09	0.73	8.36					0.017	0.017
$LiNiO_2$	3.06		3.06	3.06	3.06		3.06		3.06		3.06	3.06	0.24	2.81					0.004	0.004
$LiFePO_4$	2.21		2.21	2.21	2.21		2.21		2.21		2.21	2.21	0.18	2.03					0.083	0.083
Al	5.66		5.66	5.66	5.66		5.66		5.66		5.66	5.66	4.15	1.51					0.030	0.030
Cu	13.60		13.60	13.60	13.60		13.60		13.60		13.60	13.60	13.19	0.41					0.008	0.008
Fe	0.02		0.02	0.02	0.02		0.02		0.02		0.02	0.02	0.02	0.00					0.000	0.000
Co	0.46		0.46	0.46	0.46		0.46		0.46		0.46	0.46	0.04	0.42					0.002	0.002
Li	0.18		0.18	0.18	0.18		0.18		0.18		0.18	0.18	0.01	0.17					0.000	0.000
Ni	0.00		0.00	0.00	0.00		0.00		0.00		0.00	0.00	0.00	0.00					0.000	0.000
Carbon	14.15		14.15	14.15	14.15		14.15		14.15		14.15	14.15	1.13	13.02					13.02	13.016
NaCl		16.15	1.61																	
H_2O		145.34	14.53					4.97	171.47	166.49	4.97				1845.48		808.47	808.47	2681.20	1.072
HCl																	398.20	398.20	313.81	0.126
LiCl																			15.94	0.006
$CoCl_2$																			25.20	0.010
$NiCl_2$																			8.78	0.004
$MnCl_2$																			16.51	0.007
$FeCl_2$																			1.57	0.001
$FeCl_3$																			0.00	0.000
$AlCl_3$																			7.31	0.003
CuCl																			0.00	0.000
$CuCl_2$																			0.85	0.000
H_3PO_4																			1.21	0.000
O_2																3.35				
H_2																0.21				
NH_4OH															33.34					
NH_4Cl																			50.86	0.02

Component	21	22	23	24	25	26	27	28	29	30	31	32	33	34	35	36	37	38	39	40
Total	3121.98	3121.98	1192.52	4314.50	36.06	4.85	4345.80	23.09	23.09	4322.71								16.08	4736.86	4733.69
HCl	313.69	313.69		1.34			0.02	0.00		0.02		0.00	0.00	0.00		0.00		0.02	4.84	4.83
H_2O	2680.13	2680.13	810.92	3646.07			3646.07	1.46		3644.61	23.91	3669.05	0.37	3668.68	284.34	3863.66		1.12	3864.78	3862.85
LiCl	15.93	15.93		15.93			15.93	0.01	0.01	15.93		15.93	0.00	15.93		15.93		0.00	15.93	15.92
$CoCl_2$	25.19	25.19		25.19			25.19	0.01	0.01	25.18		24.67	0.00	24.67		0.12		0.00	0.12	0.12
$NiCl_2$	8.77	8.77		8.77			8.77	0.00	0.00	8.77		8.68	0.00	8.68		0.04		0.00	0.04	0.04
$MnCl_2$	16.50	16.50		14.36			0.00	0.00	0.00	0.00										
$FeCl_2$	1.57	1.57		1.57			1.57	0.00	0.00	1.56		0.00		0.00						
$FeCl_3$	0.00	0.00		0.00			0.00	0.00	0.00	0.00		0.00		0.00						
$AlCl_3$	7.31	7.31		7.31			7.31	0.00	0.00	7.31		0.00		0.00						
CuCl	0.00	0.00		0.00			0.00	0.00	0.00	0.00		0.00		0.00						
$CuCl_2$	0.85	0.85		0.85			0.85	0.00	0.00	0.85		0.80	0.00	0.80				0.00	0.00	0.00
H_3PO_4	1.21	1.21		0.02			1.21	0.00	0.00	1.21								0.00	0.00	0.00
NaCl				555.41			557.53	0.22	0.22	557.31		571.58	0.06	571.52		285.76		0.00	285.76	285.62
$Mn(OH)_2$				1.52			1.52	1.52	1.52	0.00										
$Fe(OH)_3$				0.00			0.00	0.00	0.00	0.00		1.32	1.32	0.00						
NaOH			381.61	0.00							11.25	0.00		0.00		195.59			195.59	195.50
Na_3PO_4				1.98								2.02	0.00	2.02		2.02			2.02	2.02
NH_4Cl	50.84	50.84		2.54			2.54	0.00	0.00	2.54		0.13	0.00	0.13		265.38		0.03	265.41	265.27
NH_4OH				31.65			31.65	0.01	0.01	31.63		33.21		33.21		33.21			33.21	33.20
$KMnO_4$					36.06		17.31	0.01	0.01	17.30		16.65	0.00	16.65		16.65		0.00	16.65	16.64
Cl_2 gas						4.85								0.00						
KCl							8.50	0.00	0.00	8.50		8.50	0.00	8.50		4.25		0.00	4.25	4.25
MnO_2							19.84	19.84	19.84	0.00		0.36	0.36	0.00						
Drying Loss									1.46	0.00										
$Fe(OH)_2$												0.00	0.00	0.00						
$Cu(OH)_2$												0.03	0.03	0.00		0.58			0.58	0.00
$Al(OH)_3$												4.27	4.27	0.00						
$Co(OH)_2$												0.38	0.38	0.00						
$Ni(OH)_2$												0.06	0.06	0.00						
KOH												0.23	0.00	0.23		3.43			3.43	3.43
NH_3															110.58			0.00	0.00	0.00
$Ni(NH_3)_6Cl_2$																15.45		0.07	0.14	0.14
$Co(NH_3)_6Cl_2$																43.86		0.00	43.86	43.84
DMG																	0.78	14.84	0.22	
Ni-DMG																		0.12	26.06	

Component	41	42	43	44	45	46	47	48	49	50	51	52	53	54	55	56	57	58	59	60
Total	3.17	272.62	306.40	16.92	0.85	289.47	50.11	339.59	7.71	7.75	331.88	971.95	5705.64	732.43	6438.07	19.03	19.03	6419.04	167.79	12781.64
HCl	0.00	14.76	4.67	0.02	0.00	4.65		0.00	0.00		0.00	320.74	67.80		0.00	0.00		0.00		0.20
H_2O	1.93	257.86	262.29	1.18	0.06	261.11	34.08	292.50	0.88		291.62	651.21	4620.30	498.05	5215.99	1.04		5214.95	82.78	8646.72
LiCl	0.01		0.01	0.00	0.00	0.01		0.01	0.00	0.00	0.01		15.92		15.92	0.00	0.00	15.91	1.98	73.04
$CoCl_2$	0.00		0.00	0.00	0.00	0.00		0.00	0.00	0.00	0.00		24.66							0.00
$NiCl_2$	0.00		0.00	0.00	0.00	0.00		0.00	0.00	0.00	0.00		0.12							
$CuCl_2$	0.00		0.80	0.00	0.00	0.80							0.00							
H_3PO_4	0.00		0.00	0.00	0.00	0.00							1.21							
NaCl	0.14		0.29	0.00	0.00	0.29		23.71	0.07	0.07	23.64		573.40		913.66	0.18	0.18	913.48	32.25	2372.28
NaOH	0.10						16.04							234.38						
Na_3PO_4	0.00							0.00	0.00	0.00	0.00				2.02	0.00	0.00	2.02	6.46	33.67
NH_4Cl	0.13		6.44	0.03	0.00	6.41							376.78		188.39	0.04	0.04	188.35	5.41	1062.51
NH_4OH	0.02							13.90	0.04	0.04	13.86								1.51	156.19
$KMnO_4$	0.01		0.01	0.00	0.00	0.01		0.01	0.00	0.00	0.01		16.64		16.64	0.00	0.00	16.64	4.17	278.63
Cl_2 gas																				
KCl	0.00		0.89	0.00	0.00	0.89		0.18	0.00	0.00	0.18		8.81		4.40	0.00	0.00	4.40	1.86	120.49
Drying Loss										0.93							1.04			
$Cu(OH)_2$	0.58							0.58	0.58	0.58					0.00	0.00	0.00			
$Al(OH)_3$																				
$Co(OH)_2$								0.01	0.01	0.01					17.65	17.65	17.65			
$Ni(OH)_2$								6.12	6.12	6.12					0.09	0.09	0.09			
KOH	0.00							0.54	0.00	0.00	0.53				3.31	0.00	0.00	3.31	21.98	31.10
NH_3	0.00		0.00	0.00	0.00	0.00		2.04	0.01	0.01	2.04				59.98	0.01	0.01	59.97	2.58	
$Ni(NH_3)_6Cl_2$	0.00		15.36	0.07	0.00	15.30														
$Co(NH_3)_6Cl_2$	0.02		0.02	0.00	0.00	0.02														
DMG	0.22		15.62	15.62	0.78	0.00														
Ni-DMG	26.06		0.13	0.13	0.01	0.00														
Li_2CO_3																			0.59	0.59
Na_2CO_3																			6.22	6.22

Component	61	62	63	64	65	66	67	68	69	70	71	72	73	74	75	76	77	78	79	80
Total	5180.52	682.41	1926.83	12781.64	2447.21	10334.43	396.14	10727.63	741.51	21.58	1.63	769.46	2311.26	6.33	1548.55	542.51	3106.42	7400.74	2220.22	587.59
HCl	0.20			0.20		0.20	130.73	0.28				762.72	762.72					0.28	0.08	
H_2O	3121.55	4.17	1711.34	8646.72	2403.79	6242.94	265.41	6571.72					1548.55		1548.55	379.76	2112.36	4459.35	1337.81	399.56
LiCl	51.60	3.54		73.04		73.04		73.71										73.71	22.11	
$CoCl_2$	0.00			0.00		0.00		0.00										0.00	0.00	
NaCl	815.23	587.68		2372.28		2372.28		2379.14										1164.61	349.38	
$Mn(OH)_2$																				
$Fe(OH)_3$																				
NaOH																162.75	994.05			188.03
Na_3PO_4	23.57	1.62		33.67		33.67		33.67										33.67	10.10	
NH_4Cl	852.18	16.57		1062.51		1062.51		1217.40										1217.40	365.22	
NH_4OH	7.89		215.48	156.19	43.42	112.77		11.28										11.28	3.38	
$KMnO_4$	195.04	62.77		278.63		278.63		278.63										278.63	83.59	
Cl_2 gas									736.84											
KCl	113.27	0.78		120.49		120.49		161.81										161.81	48.54	
KOH		5.27		31.10		31.10														
Li_2CO_3				0.59		0.59														
Na_2CO_3				6.22		6.22														
H_2										21.58	1.63	2.08		1.66						
O_2									4.67			4.67		4.67						
CO_2																				

Component	81	82	83	84	85	86	87	88	89	90	91	92	93	94	95	96	97
Total	2.93	2889.12	459.57	459.57	2889.12	1926.83	962.29	852.99	170.58	109.30	117.88	4.18	222.44	209.70	41.92	12.73	12.73
HCl																	
H_2O		1737.41	451.41	451.41	1737.41	1711.34	26.06	5.21	1.04	20.85	81.02		103.57	103.47	20.69	0.10	
LiCl		22.11			22.11		22.11	4.42	0.88	17.69			2.48	2.47	0.49	0.00	0.00
$CoCl_2$													0.00	0.00			
NaCl		742.88			742.88		742.88	734.60	146.92	8.28			40.35	40.31	8.06	0.04	0.04
Na_3PO_4		10.10			10.10		10.10	2.02	0.40	8.08			8.08	8.07	1.61	0.01	0.01
NH_4Cl		36.52			36.52		36.52	20.72	4.14	15.80			6.77	6.76	1.35	0.01	0.01
NH_4OH		218.77	8.15	8.15	218.77	215.48	3.28			3.28			1.89	1.89	0.38	0.00	
$KMnO_4$		83.59			83.59		83.59	78.45	15.68	5.14			5.21	5.21	1.04	0.01	0.01
KCl		4.85			4.85		4.85	0.97	0.19	3.88			2.33	2.33	0.46	0.00	0.00
Drying Loss																	0.11
KOH		32.88			32.88		32.88	6.59	1.32	26.29			27.47	27.45	5.47	0.03	0.03
NH_3													3.23	3.23	0.65	0.00	
Li_2CO_3													13.26	0.73	0.15	12.53	12.53
Na_2CO_3											36.86		7.78	7.78	1.56	0.01	0.01
CO_2	2.93											4.18					

Process Flow Diagram of Mineral Acid Process Option 2 (MA-2)

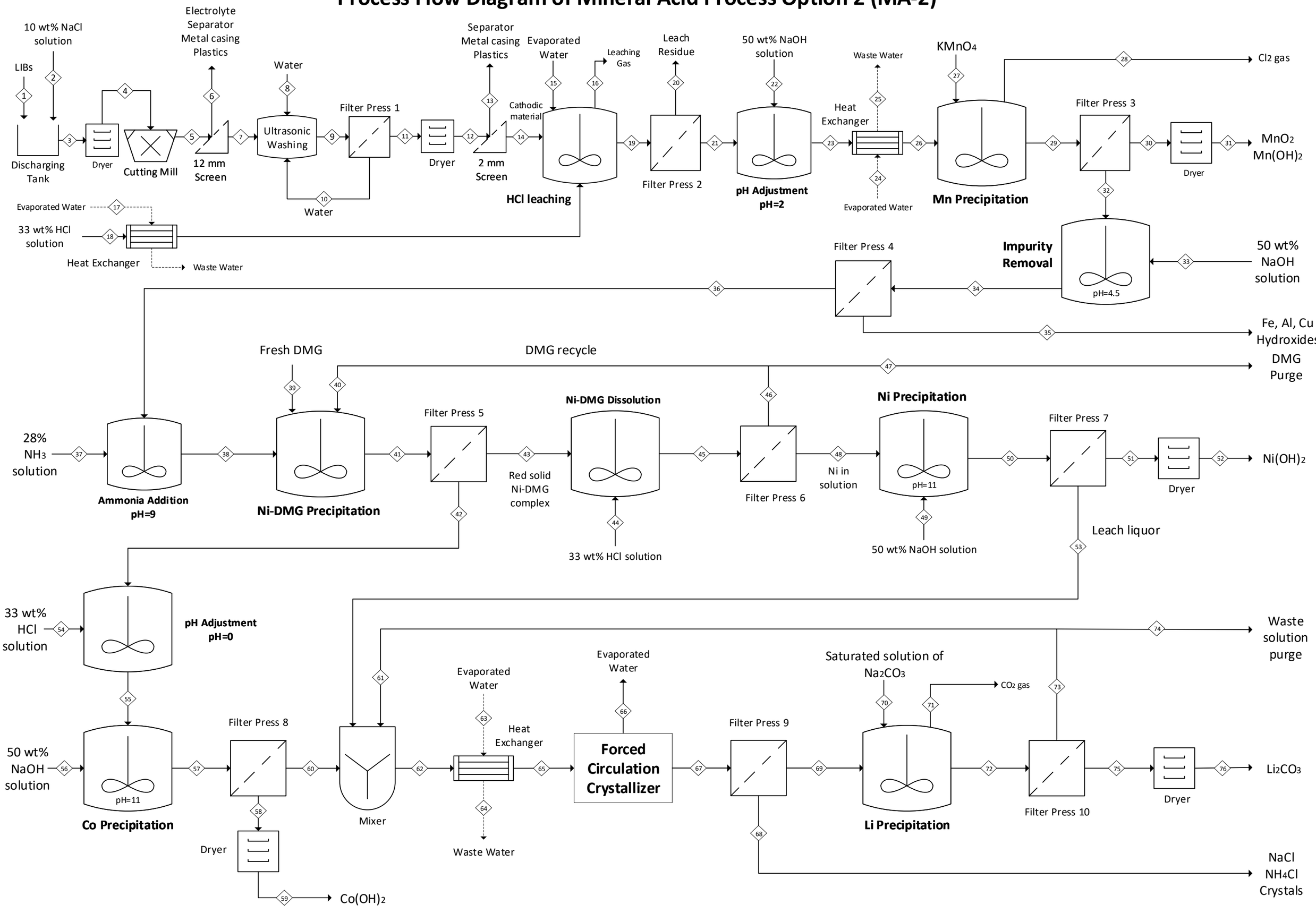

Table 63: Stream table for MA-2 (kg/hr)

Component	1	2	3	4	5	6	7	8	9	10	11	12	13	14	15	16	17	18	19	20
Total	107.70	161.49	123.85	107.70	107.70	29.76	77.94	4.97	249.41	166.49	82.92	77.94	23.33	54.61	1882.76	3.56	727.61	1206.67	3181.94	14.25
Plastics	5.13		5.13	5.13	5.13	4.88	0.26		0.26		0.26	0.26	0.26	0.00						
Electrolyte	3.37		3.37	3.37	3.37	3.37	0.00		0.00		0.00	0.00	0.00	0.00						
Metal Casing	22.64		22.64	22.64	22.64	21.51	1.13		1.13		1.13	1.13	1.13	0.00						
$LiCoO_2$	15.80		15.80	15.80	15.80		15.80		15.80		15.80	15.80	1.26	14.54					0.05	0.05
$LiNi_{0,33}Co_{0,33}Mn_{0,33}O_2$	12.32		12.32	12.32	12.32		12.32		12.32		12.32	12.32	0.99	11.33					0.08	0.08
$LiMn_2O_4$	9.09		9.09	9.09	9.09		9.09		9.09		9.09	9.09	0.73	8.36					0.02	0.02
$LiNiO_2$	3.06		3.06	3.06	3.06		3.06		3.06		3.06	3.06	0.24	2.81					0.00	0.00
$LiFePO_4$	2.21		2.21	2.21	2.21		2.21		2.21		2.21	2.21	0.18	2.03					0.08	0.08
Al	5.66		5.66	5.66	5.66		5.66		5.66		5.66	5.66	4.15	1.51					0.03	0.03
Cu	13.60		13.60	13.60	13.60		13.60		13.60		13.60	13.60	13.19	0.41					0.01	0.01
Fe	0.02		0.02	0.02	0.02		0.02		0.02		0.02	0.02	0.02	0.00					0.00	0.00
Co	0.46		0.46	0.46	0.46		0.46		0.46		0.46	0.46	0.04	0.42					0.00	0.00
Li	0.18		0.18	0.18	0.18		0.18		0.18		0.18	0.18	0.01	0.17					0.00	0.00
Ni	0.00		0.00	0.00	0.00		0.00		0.00		0.00	0.00	0.00	0.00					0.00	0.00
Carbon	14.15		14.15	14.15	14.15		14.15		14.15		14.15	14.15	1.13	13.02					13.02	13.02
NaCl		16.15	1.61																	
H_2O		145.34	14.53					4.97	171.47	166.49	4.97				1845.48		697.96	808.47	2704.55	0.81
HCl																		398.20	266.57	0.08
LiCl																			15.94	0.00
$CoCl_2$																			25.20	0.01
$NiCl_2$																			8.78	0.00
$MnCl_2$																			16.51	0.00
$FeCl_2$																			1.57	0.00
$FeCl_3$																			0.00	0.00
$AlCl_3$																			7.31	0.00
CuCl																			0.00	0.00
$CuCl_2$																			0.85	0.00
H_3PO_4																			1.21	0.00
O_2																3.35				
H_2																0.21				
NH_4OH															37.28		29.65			
NH_4Cl																			120.17	0.04

Component	21	22	23	24	25	26	27	28	29	30	31	32	33	34	35	36	37	38	39	40
Total	3167.70	774.57	3942.27	373.22	373.22	3942.27	36.06	4.65	3973.77	22.77	22.77	3951.00	28.27	3979.29	7.03	3972.27	395.01	4367.28	0.78	16.81
HCl	266.49		1.18			1.18			0.13	0.00		0.13		0.00	0.00	0.00		0.00		0.00
H_2O	2703.74	379.23	3214.75	358.01	358.01	3214.75			3214.68	1.29		3213.40	13.84	3227.82	0.48	3227.34	284.41	3422.36		1.13
LiCl	15.93		15.93			15.93			15.93	0.01	0.01	15.93		15.93	0.00	15.93		15.93		0.00
$CoCl_2$	25.19		25.19			25.19			25.19	0.01	0.01	25.18		24.67	0.00	24.67		0.12		0.00
$NiCl_2$	8.77		8.77			8.77			8.77	0.00	0.00	8.77		8.68	0.00	8.68		0.04		0.00
$MnCl_2$	16.50		14.36			14.36														
$FeCl_2$	1.57		1.57			1.57			1.57	0.00	0.00	1.57								
$AlCl_3$	7.31		7.31			7.31			7.31	0.00	0.00	7.31								0.00
$CuCl_2$	0.85		0.85			0.85			0.85	0.00	0.00	0.85		0.80	0.00	0.80				0.00
H_3PO_4	1.21		0.02			0.02			1.21	0.00		1.21								0.00
NaCl			551.93			551.93			554.06	0.22	0.22	553.83		571.89	0.09	571.81		285.90		0.00
$Mn(OH)_2$			1.52			1.52			1.52	1.52	1.52									
$Fe(OH)_3$			0.00			0.00			0.00	0.00	0.00			1.32	1.32	0.00				
NaOH		379.23											13.84					195.69		
Na_3PO_4			1.98			1.98								2.02	0.00	2.02		2.02		
NH_4Cl	120.14		6.01			6.01			6.01	0.00	0.00	6.00		0.30	0.00	0.30		265.63		0.06
NH_4OH		16.11	90.90	15.21	15.21	90.90			90.90	0.04		90.86	0.59	95.19	0.01	95.17		95.18		
$KMnO_4$							36.06		17.61	0.01	0.01	17.61		16.96	0.00	16.95		16.95		0.00
Cl_2 gas								4.65												
KCl									8.36	0.00	0.00	8.36		8.36	0.00	8.36		4.18		0.00
MnO_2									19.67	19.67	19.67			0.36	0.36	0.00				
Drying Loss											1.32									
CuOH														0.03	0.03	0.00				
$Cu(OH)_2$														0.03	0.03	0.00		0.58		0.58
$Al(OH)_3$														4.27	4.27	0.00				
$Co(OH)_2$														0.36	0.36	0.00				
$Ni(OH)_2$														0.06	0.06	0.00				
KOH														0.23	0.00	0.23		3.38		
NH_3																	110.60	0.00		0.00
$Ni(NH_3)_6Cl_2$																		15.45		0.07
$Co(NH_3)_6Cl_2$																		43.86		0.00
DMG																			0.78	14.84
Ni-DMG																				0.12

Component	41	42	43	44	45	46	47	48	49	50	51	52	53	54	55	56	57	58	59	60
Total	4383.71	4356.29	1.13	278.64	315.97	17.10	0.87	298.87	44.00	342.87	8.05	8.11	334.83	1154.61	5510.90	541.54	6052.44	19.26	19.26	6033.18
HCl	4.84	4.83	0.00	19.72	4.67	0.02	0.02	4.65		0.00	0.00			381.02	63.52					
H_2O	3423.49	3422.60	0.89	258.92	264.86	1.19	0.06	263.67	21.54	285.18	1.14		284.04	773.59	4334.33	265.14	4631.53	1.16		4630.37
LiCl	15.93	15.92	0.00		0.00	0.00	0.00	0.00		0.00	0.00	0.00	0.00		15.92		15.92	0.00	0.00	15.92
$CoCl_2$	0.12	0.12	0.00		0.00	0.00	0.00	0.00		0.00	0.00	0.00	0.00		24.66					
$NiCl_2$	0.04	0.04	0.00		0.00	0.00	0.00	0.00		0.00	0.00	0.00	0.00		0.12					
$CuCl_2$	0.00	0.00	0.00		0.80	0.00	0.00	0.80							0.00					
H_3PO_4	0.00	0.00	0.00		0.00	0.00	0.00	0.00							1.21					
NaCl	285.90	285.83	0.07		0.15	0.00	0.00	0.15		31.62	0.13	0.13	31.50		573.82		959.02	0.24	0.24	958.78
NaOH	195.69	195.64	0.05						21.54							265.14				
Na_3PO_4	2.02	2.02	0.00							0.00	0.00	0.00	0.00				2.02	0.00	0.00	2.02
NH_4Cl	265.69	265.62	0.07		14.36	0.06	0.00	14.29							471.70		235.85	0.06	0.06	235.79
NH_4OH	95.18	95.15	0.02						0.92	14.80	0.06	0.06	14.75			11.26	165.81	0.04		165.76
$KMnO_4$	16.95	16.95	0.00		0.00	0.00	0.00	0.00		0.00	0.00		0.00		16.95		16.95	0.00	0.00	16.94
KCl	4.18	4.18	0.00		0.00	0.00	0.00	0.00		0.00	0.00	0.00	0.00		8.66		4.33	0.00	0.00	4.33
Drying Loss												1.20							1.20	
$Cu(OH)_2$										0.58	0.58	0.58					0.00	0.00	0.00	0.00
$Co(OH)_2$										0.00	0.00	0.00					17.66	17.66	17.66	0.00
$Ni(OH)_2$										6.12	6.12	6.12					0.09	0.09	0.09	0.00
KOH	3.38	3.38	0.00							0.00	0.00	0.00	0.00				3.26	0.00	0.00	3.26
NH_3	0.00	0.00	0.00		0.00			0.00		4.55	0.02	0.02	4.53							
$Ni(NH_3)_6Cl_2$	0.14	0.14	0.00		15.37	0.07	0.00	15.30												
$Co(NH_3)_6Cl_2$	43.86	43.85	0.01		0.01	0.00	0.00	0.01												
DMG	0.22				15.62	15.62	0.78													
Ni-DMG	26.06				0.13	0.13	0.01													

Component	61	62	63	64	65	66	67	68	69	70	71	72	73	74	75	76
Total	349.41	6717.43	2095.19	2095.19	6717.43	5219.09	1498.33	1282.02	216.31	175.08	13.04	379.28	368.27	18.86	11.01	11.01
HCl								0.00								
H_2O	172.85	5072.34	2009.80	2009.80	5072.34	5006.40	65.94	13.19	52.75	124.16		182.25	181.89	9.03	0.36	
LiCl	2.36	18.28			18.28		18.28	3.66	14.62			2.49	2.48	0.12	0.00	0.00
$CoCl_2$	0.0000	0.0001			0.0001		0.0001	0.0000	0.0000							
$NiCl_2$	0.0000	0.0000			0.0000		0.0000	0.0000	0.0000							
NaCl	68.68	1058.97			1058.97		1058.97	1037.90	21.06			72.42	72.27	3.59	0.15	0.15
Na_3PO_4	6.37	8.39			8.39		8.39	1.68	6.71			6.71	6.70	0.33	0.01	0.01
NH_4Cl	10.03	245.81			245.81		245.81	205.41	40.40			10.56	10.54	0.52	0.02	0.02
NH_4OH	5.95	215.50	85.39	85.39	215.50	212.69	2.80	0.56	2.24	4.35		6.30	6.29	0.34	0.01	
$KMnO_4$	49.68	66.63			66.63		66.63	13.33	53.30			53.30	53.20	3.52	0.11	0.11
KCl	3.75	8.08			8.08		8.08	1.62	6.47			3.88	3.87	0.12	0.01	0.01
Drying Loss																0.40
KOH	18.94	22.20			22.20		22.20	4.44	17.76			19.71	19.67	0.73	0.04	0.04
NH_3	9.58				0.00		0.00					10.09	10.07	0.50	0.02	
Li_2CO_3	1.23	1.23			1.23		1.23	0.25	0.98			11.56	1.29	0.06	10.27	10.27
Na_2CO_3										46.57		0.00				
CO_2 gas											13.04					

Process Flow Diagram of Mineral Acid Process Option 3 (MA-3)

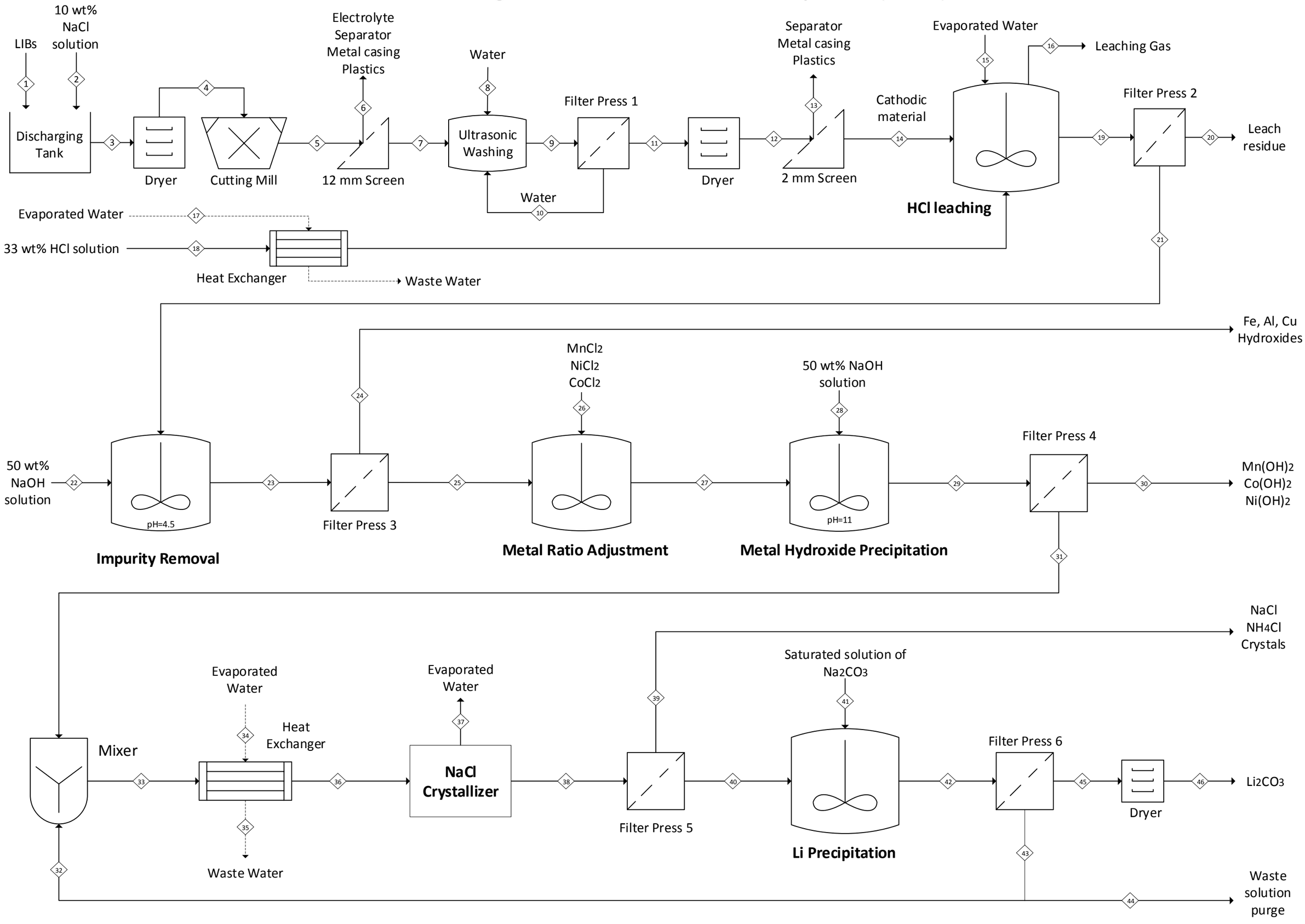

Table 64: Stream table for MA-3 (kg/hr)

Component	1	2	3	4	5	6	7	8	9	10	11	12	13	14	15	16	17	18	19	20
Total	107.70	161.49	123.85	107.70	107.70	29.76	77.94	4.97	249.41	166.49	82.92	77.94	23.33	54.61	1845.48	3.67	822.23	1206.67	3103.09	14.22
Plastics	5.13		5.13	5.13	5.13	4.88	0.26		0.26		0.26	0.26	0.26	0.00						
Electrolyte	3.37		3.37	3.37	3.37	3.37	0.00		0.00		0.00	0.00	0.00	0.00						
Metal Casing	22.64		22.64	22.64	22.64	21.51	1.13		1.13		1.13	1.13	1.13	0.00						
$LiCoO_2$	15.80		15.80	15.80	15.80		15.80		15.80		15.80	15.80	1.26	14.54					0.05	0.05
$LiNi_{0,33}Co_{0,33}Mn_{0,33}O_2$	12.32		12.32	12.32	12.32		12.32		12.32		12.32	12.32	0.99	11.33					0.08	0.08
$LiMn_2O_4$	9.09		9.09	9.09	9.09		9.09		9.09		9.09	9.09	0.73	8.36					0.02	0.02
$LiNiO_2$	3.06		3.06	3.06	3.06		3.06		3.06		3.06	3.06	0.24	2.81					0.00	0.00
$LiFePO_4$	2.21		2.21	2.21	2.21		2.21		2.21		2.21	2.21	0.18	2.03					0.08	0.08
Al	5.66		5.66	5.66	5.66		5.66		5.66		5.66	5.66	4.15	1.51					0.03	0.03
Cu	13.60		13.60	13.60	13.60		13.60		13.60		13.60	13.60	13.19	0.41					0.01	0.01
Fe	0.02		0.02	0.02	0.02		0.02		0.02		0.02	0.02	0.02	0.00					0.00	0.00
Co	0.46		0.46	0.46	0.46		0.46		0.46		0.46	0.46	0.04	0.42					0.00	0.00
Li	0.18		0.18	0.18	0.18		0.18		0.18		0.18	0.18	0.01	0.17					0.00	0.00
Ni	0.00		0.00	0.00	0.00		0.00		0.00		0.00	0.00	0.00	0.00					0.00	0.00
Carbon	14.15		14.15	14.15	14.15		14.15		14.15		14.15	14.15	1.13	13.02					13.02	13.02
NaCl		16.15	1.61																	
H_2O		145.34	14.53					4.97	171.47	166.49	4.97				1845.48		822.23	808.47	2663.95	0.80
HCl																		398.20	348.71	0.10
LiCl																			15.94	0.00
$CoCl_2$																			25.20	0.01
$NiCl_2$																			8.78	0.00
$MnCl_2$																			16.51	0.00
$FeCl_2$																			1.57	0.00
$FeCl_3$																			0.00	0.00
$AlCl_3$																			7.31	0.00
CuCl																			0.62	0.00
$CuCl_2$																			0.00	0.00
H_3PO_4																			1.21	0.00
O_2																3.45				
H_2																0.21				

Component	21	22	23	24	25	26	27	28	29	30	31	32	33	34	35
Total	3088.87	783.96	3872.82	6.53	3866.30	25.02	3891.32	93.60	3984.77	57.67	57.67	3927.11	173.82	4100.93	579.97
HCl	348.60		0.00	0.00	0.00		0.00					0.00	0.00	0.00	
H_2O	2663.15	391.98	3228.09	0.48	3227.60		3227.60	46.80	3274.27	3.27		3270.99	107.42	3378.41	579.97
LiCl	15.93		15.93	0.00	15.93		15.93		15.93	0.02	0.02	15.92	2.47	18.39	
$CoCl_2$	25.19		24.68	0.00	24.68	0.00	24.68								
$NiCl_2$	8.77		8.69	0.00	8.68	15.95	24.63								
$MnCl_2$	16.50		14.85	0.00	14.85	9.07	23.92								
$FeCl_2$	1.57		1.49	0.00	1.49		1.49								
$AlCl_3$	7.31		0.00	0.00	0.00		0.00								
CuCl	0.62		0.59	0.00	0.59		0.59								
$CuCl_2$	0.00		0.00	0.00	0.00		0.00								
H_3PO_4	1.21		0.00	0.00	0.00		0.00								
NaOH		391.98			0.00		0.00	46.80							
NaCl			570.52	0.09	570.44		570.44		638.81	0.64	0.64	638.17	42.68	680.86	
$Fe(OH)_2$			0.06	0.06	0.00		0.00		1.05	1.05	1.05	0.00			
CuOH			0.03	0.03	0.00		0.00		0.48	0.48	0.48	0.00			
$Al(OH)_3$			4.28	4.28	0.00		0.00		0.00	0.00					
$Co(OH)_2$			0.36	0.36	0.00		0.00		17.67	17.67	17.67	0.00			
$Ni(OH)_2$			0.06	0.06	0.00		0.00		17.62	17.62	17.62	0.00			
Na_3PO_4			2.02	0.00	2.02		2.02		2.02	0.00	0.00	2.02	5.98	8.00	
$Mn(OH)_2$			1.17	1.17	0.00		0.00		16.91	16.91	16.91	0.00			
Drying Loss											3.27	0.00			
Li2CO3													0.76	0.76	
Na2CO3													14.52	14.52	

Component	36	37	38	39	40	41	42	43	44	45	46	47
Total	579.97	4100.93	3287.19	813.74	686.74	127.00	57.36	184.35	173.96	0.13	10.40	10.83
HCl		0.00		0.00	0.00	0.00		0.00	0.00	0.00	0.00	
H_2O	579.97	3378.41	3287.19	91.22	22.80	68.41	39.51	107.93	107.50	0.08	0.43	0.43
LiCl		18.39		18.39	4.60	13.79		2.48	2.47	0.00	0.01	0.01
NaCl		680.86		680.86	653.52	27.33		42.92	42.71	0.03	0.21	0.21
Na_3PO_4		8.00		8.00	2.00	6.00		6.00	5.97		0.02	0.02
Drying Loss												0.43
Li2CO3		0.76		0.76	0.19	0.57		10.43	0.76	0.00	9.66	9.66
Na2CO3		14.52		14.52	3.63	10.89	17.84	14.60	14.54	0.02	0.06	0.06

Process Flow Diagram of Organic Acid Process Option 1 (OA-1)

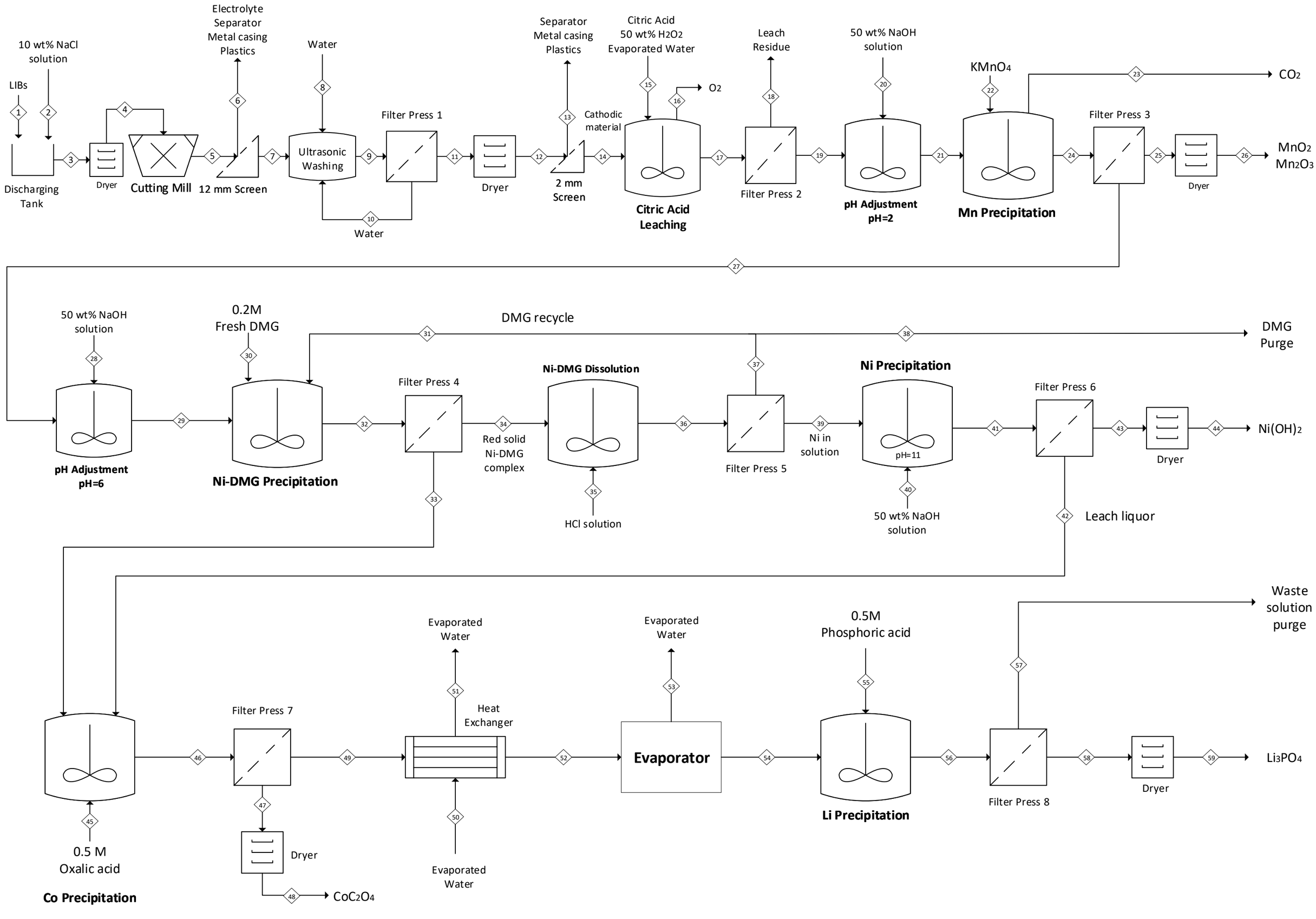

Table 65: Stream table for OA-1 (kg/hr)

Component	1	2	3	4	5	6	7	8	9	10	11	12	13	14	15	16	17	18	19
Total	107.70	161.49	123.85	107.70	107.70	29.76	77.94	4.97	249.41	166.49	82.92	77.94	23.33	54.61	2859.66	31.52	2942.94	18.39	2924.56
Plastics	5.13		5.13	5.13	5.13	4.88	0.26		0.26		0.26	0.26	0.26	0.00					
Electrolyte	3.37		3.37	3.37	3.37	3.37	0.00		0.00		0.00	0.00	0.00	0.00					
Metal Casing	22.64		22.64	22.64	22.64	21.51	1.13		1.13		1.13	1.13	1.13	0.00					
$LiCoO_2$	15.80		15.80	15.80	15.80		15.80		15.80		15.80	15.80	1.26	14.54			0.08	0.08	
$LiNi_{0,33}Co_{0,33}Mn_{0,33}O_2$	12.32		12.32	12.32	12.32		12.32		12.32		12.32	12.32	0.99	11.33			0.23	0.23	
$LiMn_2O_4$	9.09		9.09	9.09	9.09		9.09		9.09		9.09	9.09	0.73	8.36			0.29	0.29	
$LiNiO_2$	3.06		3.06	3.06	3.06		3.06		3.06		3.06	3.06	0.24	2.81			0.03	0.03	
$LiFePO_4$	2.21		2.21	2.21	2.21		2.21		2.21		2.21	2.21	0.18	2.03			0.01	0.01	
Al	5.66		5.66	5.66	5.66		5.66		5.66		5.66	5.66	4.15	1.51			1.39	1.39	
Cu	13.60		13.60	13.60	13.60		13.60		13.60		13.60	13.60	13.19	0.41			0.02	0.02	
Fe	0.02		0.02	0.02	0.02		0.02		0.02		0.02	0.02	0.02	0.00			0.00	0.00	
Co	0.46		0.46	0.46	0.46		0.46		0.46		0.46	0.46	0.04	0.42			0.00	0.00	
Li	0.18		0.18	0.18	0.18		0.18		0.18		0.18	0.18	0.01	0.17			0.00	0.00	
Ni	0.00		0.00	0.00	0.00		0.00		0.00		0.00	0.00	0.00	0.00			0.00	0.00	
Carbon	14.15		14.15	14.15	14.15		14.15		14.15		14.15	14.15	1.13	13.02			13.02	13.02	
$FePO_4$																	1.85	1.85	
NaCl		16.15	1.61																
H_2O		145.34	14.53					4.97	171.47	166.49	4.97				2537.99		2639.42	1.32	2638.10
Citric acid (H_3 Cit)															262.28		187.02	0.09	186.93
H_2O_2															59.39		0.00	0.00	0.00
Li_3Cit																	26.08	0.01	26.07
Co_3Cit_2																	35.76	0.02	35.74
Ni_3Cit_2																	12.37	0.01	12.36
Mn_3Cit_2																	23.10	0.01	23.09
AlCit																	0.97	0.00	0.97
Cu_3Cit_2																	1.16	0.00	1.16
Fe_3Cit_2																	0.09	0.00	0.09
H_3PO_4																	0.05	0.00	0.05
O_2																31.52			

Component	20	21	22	23	24	25	26	27	28	29	30	31	32	33	34	35	36	37	38	39	40
Total	118.19	3042.75	546.64	6.35	3583.04	33.52	33.52	3549.52	145.52	3695.47	34.11	15.73	3745.18	3724.54	20.64	201.42	222.18	16.56	0.83	205.62	26.30
H_2O	59.09	2723.81	506.32		3230.33	2.26	0.00	3228.07	72.76	3328.58	33.33	0.91	3365.22	3363.87	1.35	189.60	190.95	0.95	0.05	189.99	13.15
Citric acid (H_3 Cit)		92.42			87.80	0.06	0.06	87.73		0.00		0.00	0.00	0.00	0.00		0.00	0.00	0.00	0.00	
H_2O_2		0.00			0.00	0.00	0.00	0.00		0.00		0.00	0.00	0.00	0.00		0.00	0.00	0.00	0.00	
Li_3Cit		26.07			26.07	0.02	0.02	26.05		26.05		0.00	26.05	26.04	0.01		0.01	0.00	0.00	0.010	
Co_3Cit_2		35.74			35.74	0.03	0.03	35.71		35.71		0.00	35.68	35.66	0.01		0.01	0.00	0.00	0.014	
Ni_3Cit_2		12.36			12.36	0.01	0.01	12.35		12.35		0.00	0.19	0.19	0.00		0.00	0.00	0.00	0.00	
Mn_3Cit_2		23.09			0.00	0.00	0.00	0.00		0.00		0.00	0.00	0.00	0.00		0.00	0.00	0.00	0.00	
AlCit		0.97			0.97	0.00	0.00	0.97		0.97		0.00	0.97	0.97	0.00		0.00	0.00	0.00	0.00	
Cu_3Cit_2		1.16			1.16	0.00	0.00	1.16		1.16		0.00	1.16	1.15	0.00		0.00	0.00	0.00	0.00	
Fe_3Cit_2		0.09			0.09	0.00	0.00	0.09		0.09		0.00	0.09	0.09	0.00		0.00	0.00	0.00	0.00	
H_3PO_4		0.00			0.00	0.00	0.00	0.00		0.00		0.00	0.00	0.00	0.00		0.00	0.00	0.00	0.00	
Na_3PO_4		0.08			0.08	0.00	0.00	0.08		0.08		0.00	0.08	0.08	0.00		0.00	0.00	0.00	0.00	
Na_3Cit		126.96			126.96	0.09	0.09	126.87		244.72		0.00	256.09	255.98	0.10		0.10	0.001	0.000	0.102	
$KMnO_4$			40.32		4.08	0.00	0.00	4.07		4.05		0.00	4.05	4.05	0.00		0.00	0.00	0.00	0.002	
MnO_2					31.03	31.03	31.03	0.00		0.01		0.00	0.01	0.00	0.01		0.00	0.00	0.00	0.00	
KH_2Cit					19.58	0.01	0.01	19.57		0.00		0.00	0.00	0.00	0.00		0.00	0.00	0.00	0.00	
K_2O					6.80	0.00	0.00	6.79		0.00		0.00	0.00	0.00	0.00		0.00	0.00	0.00	0.00	
NaOH	59.09								72.76	5.39		0.00	0.07	0.07	0.00		0.00	0.00	0.00	0.00	13.15
KOH										4.05		0.00	4.05	4.05	0.00		0.00	0.00	0.00	0.00	
Na_2O										8.94		0.00	8.94	8.94	0.00		0.00	0.00	0.00	0.00	
KNa_2Cit										23.30		0.00	23.30	23.29	0.01		0.01	0.00	0.00	0.01	
DMG											0.78	14.75	0.19	0.00	0.19		15.53	15.53	0.78	0.00	
$Ni(C_4H_6N_2O_2)_2$												0.00	18.90	0.00	18.90		0.00	0.00	0.00	0.00	
$Co(C_4H_6N_2O_2)_2$												0.00	0.06	0.00	0.06		0.00	0.00	0.00	0.00	
HCl												0.03	0.00	0.00	0.00	11.82	6.98	0.03	0.00	6.95	
$NiCl_2$												0.04	0.04	0.04	0.00		8.54	0.04	0.00	8.49	
$CoCl_2$												0.00	0.00	0.00	0.00		0.03	0.00	0.00	0.02	
NaCl												0.00	0.05	0.05	0.00		0.01	0.00	0.00	0.01	
KCl												0.00	0.00	0.00	0.00		0.00	0.00	0.00	0.00	
$MnCl_2$												0.00	0.00	0.00	0.00		0.02	0.00	0.00	0.02	
CO_2				6.35																	
Vapour loss due to drying							2.26														

Component	41	42	43	44	45	46	47	48	49	50	51	52	53	54	55	56	57	58	59
Total	231.82	225.26	6.56	6.56		4225.72	30.01	30.00	4195.71	635.44	635.44	4195.71	3173.43	1022.28	259.48	1281.76	1267.44	14.32	14.32
H_2O	206.58	206.16	0.41		255.14	3825.33	1.91		3823.41	635.44	635.44	3823.41	3173.43	649.98	247.33	897.31	896.59	0.72	
Citric acid (H_3 Cit)	0.00	0.00	0.00			24.12	0.01	0.01	24.10			24.10		24.10		46.77	46.73	0.04	0.04
H_2O_2	0.00	0.00	0.00			0.00	0.00		0.00			0.00		0.00		0.00	0.00	0.00	
Li_3Cit	0.01	0.01	0.00			26.05	0.01	0.01	26.04			26.04		26.04		1.28	1.27	0.00	0.00
Co_3Cit_2	0.01	0.01	0.00			1.08	0.00	0.00	1.08			1.08		1.08		1.08	1.08	0.00	0.00
Ni_3Cit_2	0.00	0.00	0.00			0.19	0.00		0.19			0.19		0.19		0.19	0.18	0.00	
Mn_3Cit_2	0.00	0.00	0.00			0.00	0.00		0.00			0.00		0.00		0.00	0.00	0.00	
AlCit	0.00	0.00	0.00			0.73	0.00		0.73			0.73		0.73		0.73	0.73	0.00	0.00
Cu_3Cit_2	0.00	0.00	0.00			0.87	0.00		0.87			0.87		0.87		0.87	0.87	0.00	0.00
Fe_3Cit_2	0.00	0.00	0.00			0.07	0.00		0.07			0.07		0.07		0.07	0.07	0.00	
H_3PO_4	0.00	0.00	0.00			0.00	0.00		0.00			0.00		0.00	12.15	0.60	0.60	0.00	
Na_3PO_4	0.00	0.00	0.00			0.08	0.00		0.08			0.08		0.08		0.08	0.08	0.00	
Na_3Cit	0.00	0.00	0.00			256.33	0.13	0.13	256.21			256.21		256.21		256.21	256.00	0.20	0.20
$KMnO_4$	0.00	0.00	0.00			4.05	0.00	0.00	4.05			4.05		4.05		4.05	4.05	0.00	0.00
NaOH	0.26	0.26	0.00			0.00	0.00		0.00			0.00		0.00		0.00	0.00	0.00	
KOH	0.00	0.00	0.00			4.05	0.00	0.00	4.05			4.05		4.05		4.05	4.05	0.00	0.00
Na_2O	0.00	0.00	0.00			8.94	0.00	0.00	8.93			8.93		8.93		8.93	8.93	0.01	0.01
KNa_2Cit	0.01	0.01	0.00			23.30	0.01	0.01	23.29			23.29		23.29		23.29	23.27	0.02	0.02
NaCl	18.84	18.80	0.04	0.04		18.80	0.01	0.01	18.79			18.79		18.79		18.79	18.78	0.02	0.02
KCl	0.00	0.00	0.00	0.00		0.04	0.00		0.04			0.04		0.04		0.04	0.04	0.00	
$MnCl_2$	0.00	0.00	0.00	0.00		0.00	0.00		0.00			0.00		0.00		0.00	0.00	0.00	
$Ni(OH)_2$	6.08	0.00	6.08	6.08								0.00		0.00					
$Co(OH)_2$	0.02	0.00	0.02	0.02								0.00		0.00					
$Mn(OH)_2$	0.01	0.00	0.01	0.01								0.00		0.00					
$H_2C_2O_4$					20.83	3.51	0.00	0.00	3.51			3.51		3.51		3.51	3.50	0.00	0.00
CoC_2O_4						27.48	27.48	27.48	0.00			0.00		0.00		0.00	0.00	0.00	
$Na_2C_2O_4$						0.27	0.00	0.00	0.27			0.27		0.27		0.27	0.27	0.00	
$Al_2(C_2O_4)_3$						0.18	0.18	0.18				0.00		0.00					
CuC_2O_4						0.23	0.23	0.23				0.00		0.00					
FeC_2O_4						0.02	0.02	0.02				0.00		0.00					
Li_3PO_4																13.66	0.35	13.31	13.31
Vapour loss due to drying				0.41				1.91											0.72

Process Flow Diagram of Organic Acid Process Option 2 (OA-2)

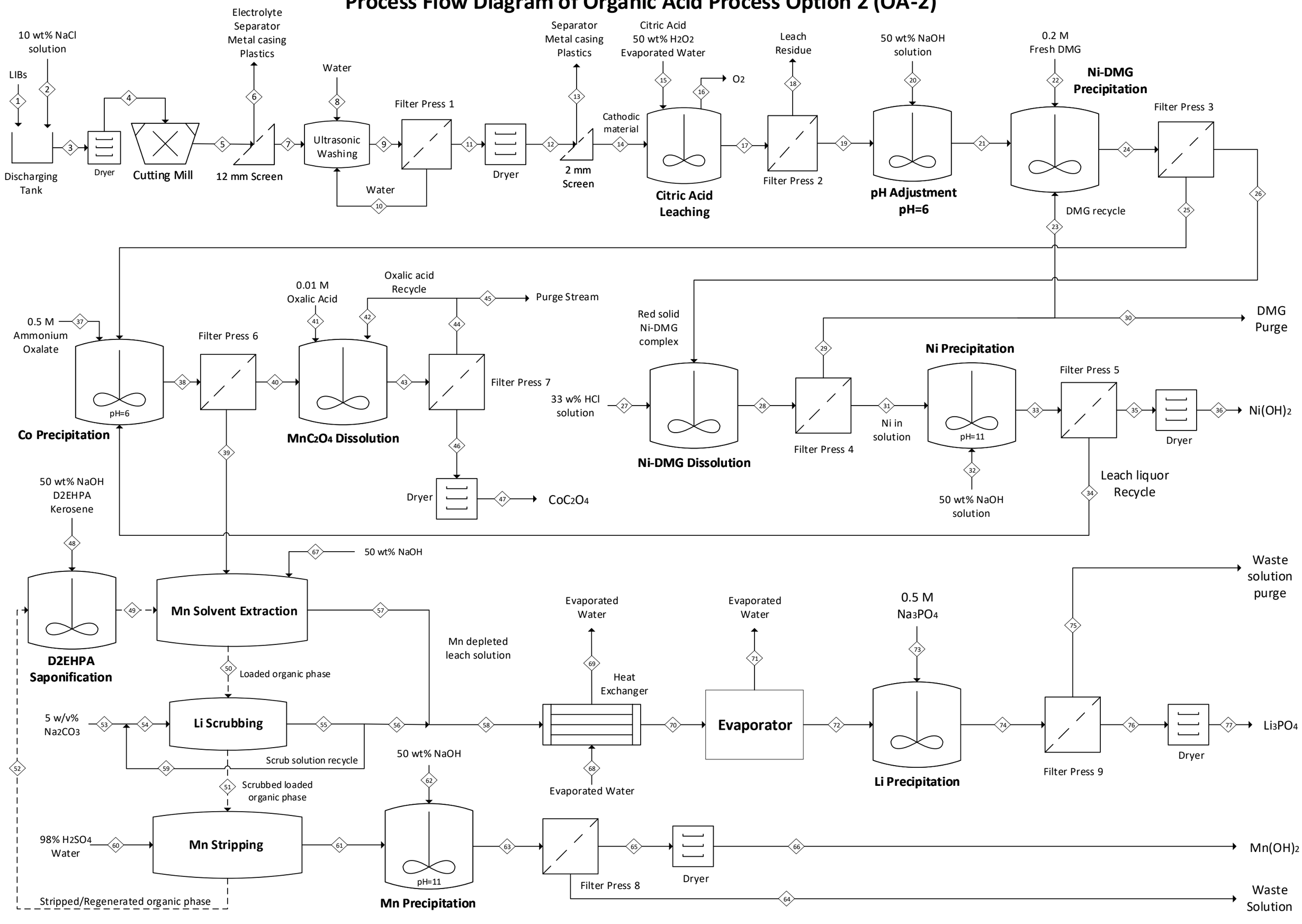

Table 66: Stream table for OA-2 (kg/hr)

Component	1	2	3	4	5	6	7	8	9	10	11	12	13	14	15	16	17	18	19
Total	107.70	161.49	123.85	107.70	107.70	29.76	77.94	4.97	249.41	166.49	82.92	77.94	23.33	54.61	2859.66	31.52	2942.94	18.39	2924.56
Plastics	5.13		5.13	5.13	5.13	4.88	0.26		0.26		0.26	0.26	0.26	0.00					
Electrolyte	3.37		3.37	3.37	3.37	3.37	0.00		0.00		0.00	0.00	0.00	0.00					
Metal Casing	22.64		22.64	22.64	22.64	21.51	1.13		1.13		1.13	1.13	1.13	0.00					
$LiCoO_2$	15.80		15.80	15.80	15.80		15.80		15.80		15.80	15.80	1.26	14.54			0.08	0.08	
$LiNi_{0,33}Co_{0,33}Mn_{0,33}O_2$	12.32		12.32	12.32	12.32		12.32		12.32		12.32	12.32	0.99	11.33			0.23	0.23	
$LiMn_2O_4$	9.09		9.09	9.09	9.09		9.09		9.09		9.09	9.09	0.73	8.36			0.29	0.29	
$LiNiO_2$	3.06		3.06	3.06	3.06		3.06		3.06		3.06	3.06	0.24	2.81			0.03	0.03	
$LiFePO_4$	2.21		2.21	2.21	2.21		2.21		2.21		2.21	2.21	0.18	2.03			0.01	0.01	
Al	5.66		5.66	5.66	5.66		5.66		5.66		5.66	5.66	4.15	1.51			1.39	1.39	
Cu	13.60		13.60	13.60	13.60		13.60		13.60		13.60	13.60	13.19	0.41			0.02	0.02	
Fe	0.02		0.02	0.02	0.02		0.02		0.02		0.02	0.02	0.02	0.00			0.00	0.00	
Co	0.46		0.46	0.46	0.46		0.46		0.46		0.46	0.46	0.04	0.42			0.00	0.00	
Li	0.18		0.18	0.18	0.18		0.18		0.18		0.18	0.18	0.01	0.17			0.00	0.00	
Ni	0.00		0.00	0.00	0.00		0.00		0.00		0.00	0.00	0.00	0.00			0.00	0.00	
Carbon	14.15		14.15	14.15	14.15		14.15		14.15		14.15	14.15	1.13	13.02			13.02	13.02	
$FePO_4$																	1.85	1.85	
NaCl		16.15	1.61																
H_2O		145.34	14.53					4.97	171.47	166.49	4.97				2537.99		2639.42	1.32	2638.10
Citric acid (H_3 Cit)															262.28		187.02	0.09	186.93
H_2O_2															59.39		0.00	0.00	0.00
Li_3Cit																	26.08	0.01	26.07
Co_3Cit_2																	35.76	0.02	35.74
Ni_3Cit_2																	12.37	0.01	12.36
Mn_3Cit_2																	23.10	0.01	23.09
AlCit																	0.97	0.00	0.97
Cu_3Cit_2																	1.16	0.00	1.16
Fe_3Cit_2																	0.09	0.00	0.09
H_3PO_4																	0.05	0.00	0.05
O_2																31.52			

Component	20	21	22	23	24	25	26	27	28	29	30	31	32	33	34	35	36	37	38	39	40
Total	245.32	3169.88	34.13	15.74	3219.63	3199.18	20.45	201.78	222.36	16.57	0.83	205.79	26.34	232.02	225.45	6.57	6.57	283.83	3708.42	3676.55	31.87
H_2O	122.66	2813.38	33.36	0.91	2850.05	2848.91	1.14	189.96	191.10	0.96	0.05	190.14	13.17	206.75	206.33	0.41		255.11	3310.36	3308.37	1.99
Citric acid (H_3 Cit)		0.00		0.00	0.00	0.00	0.00		0.00	0.00	0.00	0.00		0.00	0.00	0.00	0.00		0.00	0.00	0.00
H_2O_2		0.00		0.00	0.00	0.00	0.00		0.00	0.00	0.00	0.00		0.00	0.00	0.00	0.00		0.00	0.00	0.00
Li_3Cit		26.07		0.00	26.07	26.06	0.01		0.01	0.00	0.00	0.01		0.01	0.01	0.00	0.00		26.07	26.05	0.02
Co_3Cit_2		35.74		0.00	35.69	35.67	0.01		0.01	0.00	0.00	0.01		0.01	0.01	0.00	0.00		1.08	1.08	0.00
Ni_3Cit_2		12.36		0.00	0.19	0.19	0.00		0.00	0.00	0.00	0.00		0.00	0.00	0.00	0.00		0.19	0.19	0.00
Mn_3Cit_2		23.09		0.00	23.06	23.05	0.01		0.01	0.00	0.00	0.01		0.01	0.01	0.00	0.00		21.22	21.20	0.01
AlCit		0.97		0.00	0.97	0.97	0.00		0.00	0.00	0.00	0.00		0.00	0.00	0.00	0.00		0.56	0.56	0.00
Cu_3Cit_2		1.16		0.00	1.16	1.16	0.00		0.00	0.00	0.00	0.00		0.00	0.00	0.00	0.00		0.67	0.67	0.00
Fe_3Cit_2		0.09		0.00	0.09	0.09	0.00		0.00	0.00	0.00	0.00		0.00	0.00	0.00	0.00		0.05	0.05	0.00
H_3PO_4		0.00		0.00	0.00	0.00	0.00		0.00	0.00	0.00	0.00		0.00	0.00	0.00	0.00		0.00	0.00	0.00
Na_3PO_4		0.08		0.00	0.08	0.08	0.00		0.00	0.00	0.00	0.00		0.00	0.00	0.00	0.00		0.08	0.08	0.00
Na_3Cit		251.10		0.00	262.52	262.41	0.11		0.11	0.00	0.00	0.10		0.00	0.00	0.00	0.00		262.41	262.25	0.16
NaOH	122.66	5.84		0.00	0.50	0.50	0.00		0.00	0.00	0.00	0.00	13.17	0.26	0.26	0.00	0.00		0.75	0.75	0.00
DMG			0.78	14.76	0.13	0.00	0.13		15.54	15.54	0.78	0.00		0.00	0.00	0.00	0.00				
$Ni(C_4H_6N_2O_2)_2$				0.00	18.91	0.00	18.91		0.00	0.00	0.00	0.00		0.00	0.00	0.00	0.00				
$Co(C_4H_6N_2O_2)_2$				0.00	0.08	0.00	0.08		0.00	0.00	0.00	0.00		0.00	0.00	0.00	0.00				
HCl				0.03	0.00	0.00	0.00	11.83	6.99	0.03	0.00	6.95		0.00	0.00	0.00	0.00		0.00	0.00	0.00
$NiCl_2$				0.04	0.04	0.04	0.00		8.54	0.04	0.00	8.50		0.00	0.00	0.00	0.00		0.00	0.00	0.00
$CoCl_2$				0.00	0.00	0.00	0.00		0.04	0.00	0.00	0.03		0.00	0.00	0.00	0.00		0.00	0.00	0.00
NaCl				0.00	0.05	0.05	0.00		0.00	0.00	0.00	0.00		18.86	18.82	0.04	0.04		18.88	18.87	0.01
$MnCl_2$				0.00	0.00	0.00	0.00		0.02	0.00	0.00	0.02		0.00	0.00	0.00	0.00		0.00	0.00	0.00
$Mn(C_4H_6N_2O_2)_2$					0.05		0.05		0.00	0.00	0.00	0.00				0.00	0.00				
$Ni(OH)_2$														6.08	0.00	6.08	6.08				
$Co(OH)_2$														0.03	0.00	0.03	0.03				
$Mn(OH)_2$														0.02	0.00	0.02	0.02				
$(NH_4)_2C_2O_4$																		28.72	3.54	3.54	0.00
CoC_2O_4																			27.49		27.49
MnC_2O_4																			1.46		1.46
$Al_2(C_2O_4)_3$																			0.30		0.30
CuC_2O_4																			0.39		0.39
FeC_2O_4																			0.03		0.03
$(NH_4)_3Cit$																			32.89	32.87	0.02
Vapour loss due to drying																	0.41				

Component	41	42	43	44	45	46	47	48	49	50	51	52	53	54	55	56	57	58	59	60
Total	1016.68	927.25	1060.83	1030.28	103.03	30.55	30.55	42.51	5635.03	11196.95	11197.10	11185.05	328.64	6571.45	6571.37	328.57	3687.37	4015.94	6242.80	6566.96
H_2O	1015.76	914.14	1017.74	1015.71	101.57	2.04		7.42	10.77	80.08	80.08	0.80	326.77	6535.47	6535.47	326.77	3320.85	3647.62	6208.70	6502.66
Citric acid (H_3 Cit)																	0.01	0.01		
H_2O_2																	0.00	0.00		
Li_3Cit		0.14	0.15	0.15	0.02	0.00	0.00										25.53	25.53		
Co_3Cit_2		0.01	0.01	0.01	0.00	0.00	0.00										1.08	1.08		
Ni_3Cit_2																	0.19	0.19		
Mn_3Cit_2		0.11	0.13	0.12	0.01	0.00	0.00										0.64	0.64		
AlCit																	0.56	0.56		
Cu_3Cit_2																	0.67	0.67		
Fe_3Cit_2																	0.05	0.05		
H_3PO_4																	0.00	0.00		
Na_3PO_4																	0.08	0.08		
Na_3Cit		1.39	1.55	1.54	0.15	0.00	0.00										282.44	282.44		
NaOH		0.00	0.00	0.00	0.00	0.00	0.00	7.42									0.00	0.00		
NaCl		0.10	0.11	0.11	0.01	0.00	0.00										18.87	18.87		
$(NH_4)_2C_2O_4$		0.02	0.02	0.02	0.00	0.00	0.00										3.54	3.54		
CoC_2O_4			27.49			27.49	27.49													
MnC_2O_4		10.34	11.80	11.49	1.15	0.31	0.31													
$Al_2(C_2O_4)_3$			0.30			0.30	0.30													
CuC_2O_4			0.39			0.39	0.39													
FeC_2O_4			0.03			0.03	0.03													
$(NH_4)_3Cit$		0.17	0.19	0.19	0.02	0.00	0.00										32.87	32.87		
$H_2C_2O_4$	0.92	0.82	0.92	0.92	0.09	0.00	0.00													
Na_2CO_3													1.87	32.77	32.53	1.63	0.00	1.63	30.91	
Li_2CO_3														3.20	3.37	0.17	0.00	0.17	3.20	
Kerosene								21.50	4321.84	4300.34	4300.34	4300.34								
D2EHPA								6.17	325.40	304.87	304.87	379.07								
Na-D2EHPA									976.21	910.74	912.31	912.31								
Mn(D2EHPA)									0.80	2.45	0.96	0.01								
Li(D2EHPA)									0.01	5598.48	5598.55	5592.52								
Vapour loss due to drying							2.04													
H_2SO_4																				64.31

Component	61	62	63	64	65	66	67	68	69	70	71	72	73	74	75	76	77
Total	6573.17	104.86	6678.02	6667.15	10.88	10.88	3.18	434.82	434.82	4015.94	2972.81	1043.13	262.47	1305.59	1291.96	13.63	13.63
H_2O	6502.66	52.43	6574.57	6573.91	0.66		1.59	434.82	434.82	3647.62	2972.81	674.81	242.53	917.34	916.60	0.73	
Citric acid (H_3 Cit)										0.01		0.01		0.01	0.01	0.00	0.00
H_2O_2										0.00		0.00		0.00	0.00	0.00	0.00
Li_3Cit										25.53		25.53		2.04	2.04	0.00	0.00
Co_3Cit_2										1.08		1.08		1.08	1.08	0.00	0.00
Ni_3Cit_2										0.19		0.19		0.19	0.19	0.00	0.00
Mn_3Cit_2										0.64		0.64		0.64	0.64	0.00	0.00
AlCit										0.56		0.56		0.56	0.56	0.00	0.00
Cu_3Cit_2										0.67		0.67		0.67	0.67	0.00	0.00
Fe_3Cit_2										0.05		0.05		0.05	0.05	0.00	0.00
H_3PO_4										0.00		0.00		0.00	0.00	0.00	0.00
Na_3PO_4										0.08		0.08		1.68	1.68	0.00	0.00
Na_3Cit										282.44		282.44		311.31	311.06	0.25	0.25
NaOH		52.43					1.59			0.00		0.00		0.00	0.00	0.00	0.00
HCl										0.00		0.00		0.00	0.00	0.00	0.00
$NiCl_2$										0.00		0.00		0.00	0.00	0.00	0.00
$CoCl_2$										0.00		0.00		0.00	0.00	0.00	0.00
NaCl										18.87		18.87		18.87	18.85	0.02	0.02
$(NH_4)_2C_2O_4$										3.54		3.54		3.54	3.54	0.00	0.00
$(NH_4)_3Cit$										32.87		32.87		32.87	32.84	0.03	0.03
$H_2C_2O_4$																	
Na_2CO_3										1.63		1.63		1.63	1.63	0.00	0.00
Li_2CO_3										0.17		0.17		0.17	0.17	0.00	0.00
Li_3PO_4														12.96	0.36	12.60	12.60
Na_3PO_4													19.94				
Vapour loss due to drying						0.66											0.73
H_2SO_4	53.02		0.00	0.00	0.00	0.00											
$MnSO_4$	17.33		0.00	0.00	0.00	0.00											
Li_2SO_4	0.16		0.16	0.16	0.00	0.00											
Na2SO4			93.09	93.08	0.01	0.01											
Mn(OH)2			10.21	0.00	10.21	10.21											

Process Flow Diagram of Organic Acid Process Option 3 (OA-3)

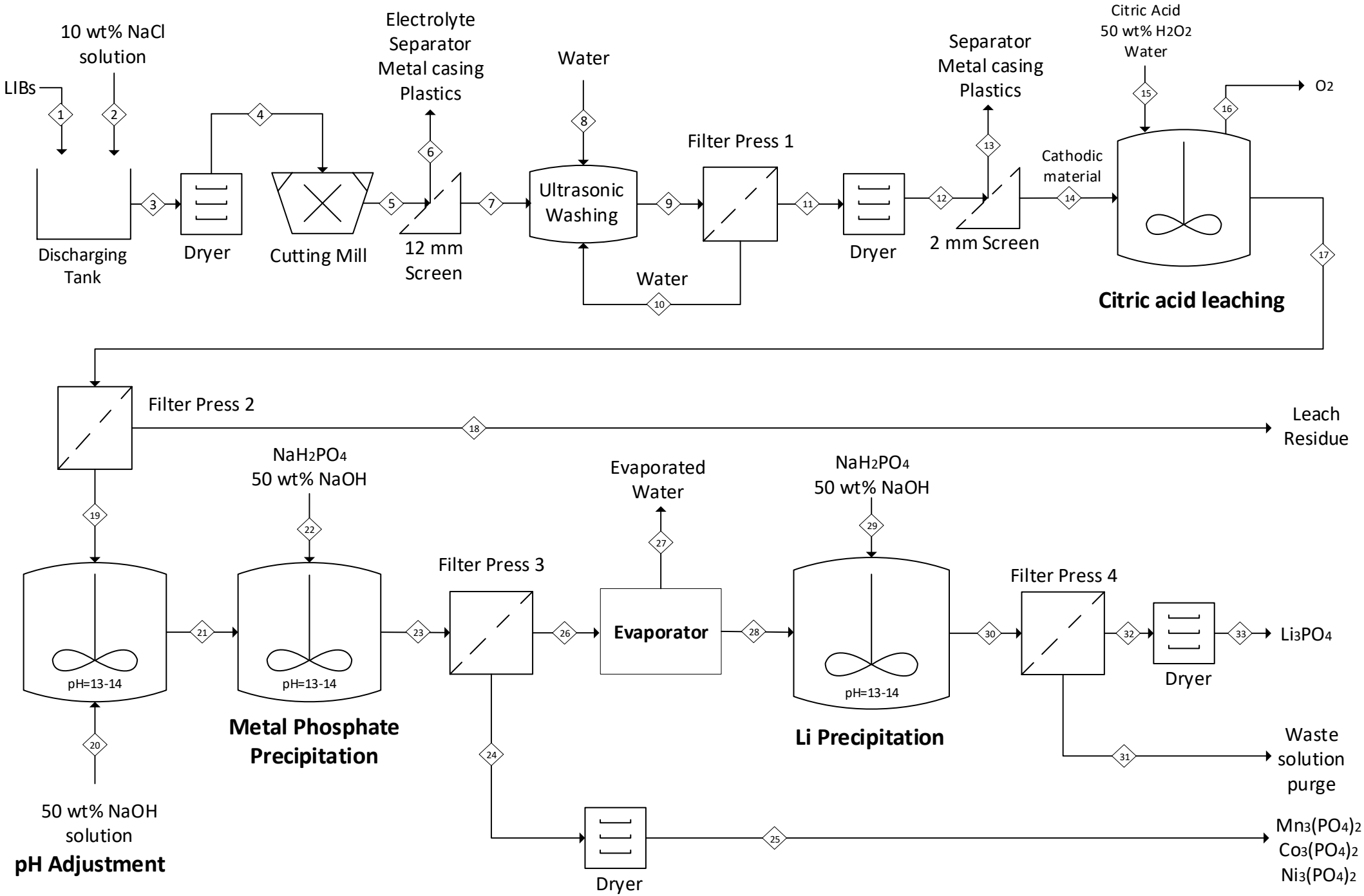

Table 67: Stream table for OA-3 (kg/hr)

Component	1	2	3	4	5	6	7	8	9	10	11	12	13	14	15	16	17	18	19
Total	107.70	161.49	123.85	107.70	107.70	29.76	77.94	4.97	249.41	166.49	82.92	77.94	23.33	54.61	2859.66	31.52	2942.94	18.39	2924.56
Plastics	5.13		5.13	5.13	5.13	4.88	0.26		0.26		0.26	0.26	0.26						
Electrolyte	3.37		3.37	3.37	3.37	3.37													
Metal Casing	22.64		22.64	22.64	22.64	21.51	1.13		1.13		1.13	1.13	1.13						
$LiCoO_2$	15.80		15.80	15.80	15.80		15.80		15.80		15.80	15.80	1.26	14.54			0.08	0.08	
$LiNi_{0,33}Co_{0,33}Mn_{0,33}O_2$	12.32		12.32	12.32	12.32		12.32		12.32		12.32	12.32	0.99	11.33			0.23	0.23	
$LiMn_2O_4$	9.09		9.09	9.09	9.09		9.09		9.09		9.09	9.09	0.73	8.36			0.29	0.29	
$LiNiO_2$	3.06		3.06	3.06	3.06		3.06		3.06		3.06	3.06	0.24	2.81			0.03	0.03	
$LiFePO_4$	2.21		2.21	2.21	2.21		2.21		2.21		2.21	2.21	0.18	2.03			0.01	0.01	
Al	5.66		5.66	5.66	5.66		5.66		5.66		5.66	5.66	4.15	1.51			1.39	1.39	
Cu	13.60		13.60	13.60	13.60		13.60		13.60		13.60	13.60	13.19	0.41			0.02	0.02	
Fe	0.02		0.02	0.02	0.02		0.02		0.02		0.02	0.02	0.02	0.00			0.00	0.00	
Co	0.46		0.46	0.46	0.46		0.46		0.46		0.46	0.46	0.04	0.42			0.00	0.00	
Li	0.18		0.18	0.18	0.18		0.18		0.18		0.18	0.18	0.01	0.17			0.00	0.00	
Ni	0.00		0.00	0.00	0.00		0.00		0.00		0.00	0.00	0.00	0.00			0.00	0.00	
Carbon	14.15		14.15	14.15	14.15		14.15		14.15		14.15	14.15	1.13	13.02			13.02	13.02	
$FePO_4$																	1.85	1.85	
NaCl		16.15	1.61																
H_2O		145.34	14.53					4.97	171.47	166.49	4.97				2537.99		2639.42	1.32	2638.10
Citric acid (H_3 Cit)															262.28		187.02	0.09	186.93
H_2O_2															59.39		0.00	0.00	0.00
Li_3Cit																	26.08	0.01	26.07
Co_3Cit_2																	35.76	0.02	35.74
Ni_3Cit_2																	12.37	0.01	12.36
Mn_3Cit_2																	23.10	0.01	23.09
AlCit																	0.97	0.00	0.97
Cu_3Cit_2																	1.16	0.00	1.16
Fe_3Cit_2																	0.09	0.00	0.09
H_3PO_4																	0.05	0.00	0.05
O_2																31.52			

Component	20	21	22	23	24	25	26	27	28	29	30	31	32	33
Total	233.64	3158.20	420.72	3578.92	51.48	51.48	3527.44	2215.88	1311.56	113.67	1425.23	1413.33	11.90	11.90
H_2O	116.82	2807.54	120.21	2981.91	3.58	0.00	2978.33	2215.88	762.45	32.48	809.56	809.08	0.49	
Citric acid (H_3 Cit)		0.00		0.00	0.00	0.00	0.00		0.00		0.00	0.00	0.00	0.00
H_2O_2		0.00		0.00	0.00	0.00	0.00		0.00		0.00	0.00	0.00	0.00
Li_3Cit		26.07		25.15	0.03	0.03	25.12		25.12		6.56	6.55	0.00	0.00
Co_3Cit_2		35.74		1.20	0.00	0.00	1.20		1.20		0.04	0.04	0.00	0.00
Ni_3Cit_2		12.36		0.23	0.00	0.00	0.23		0.23		0.00	0.00	0.00	0.00
Mn_3Cit_2		23.09		0.13	0.00	0.00	0.13		0.13		0.00	0.00	0.00	0.00
AlCit		0.97		0.02	0.00	0.00	0.02		0.02		0.01	0.01	0.00	0.00
Cu_3Cit_2		1.16		0.63	0.00	0.00	0.62		0.62		0.44	0.44	0.00	0.00
Fe_3Cit_2		0.09		0.09	0.00	0.00	0.09		0.09		0.09	0.09	0.00	0.00
H_3PO_4		0.00		0.00	0.00	0.00	0.00		0.00		0.00	0.00	0.00	0.00
Na_3PO_4		0.08		203.23	0.24	0.24	202.99		202.99		254.04	253.88	0.15	0.15
Na_3Cit		251.10		319.10	0.38	0.38	318.72		318.72		343.13	342.92	0.21	0.21
NaH_2PO_4			180.29	0.00	0.00	0.00	0.00			48.71	0.00	0.00	0.00	0.00
NaH_2Cit				0.00	0.00	0.00	0.00				0.00	0.00	0.00	0.00
Li_3PO_4				0.51	0.51	0.51	0.00				10.24	0.32	9.92	9.92
$Co_3(PO_4)_2$				22.82	22.82	22.82	0.00				0.77	0.00	0.77	0.77
$Ni_3(PO_4)_2$				8.01	8.01	8.01	0.00				0.15	0.00	0.15	0.15
$Mn_3(PO_4)_2$				15.00	15.00	15.00	0.00				0.08	0.00	0.08	0.08
$AlPO_4$				0.54	0.54	0.54	0.00				0.01	0.00	0.01	0.01
$Cu_3(PO_4)_2$				0.36	0.36	0.36	0.00				0.12	0.00	0.12	0.12
NaOH	116.82		120.21	0.00	0.00	0.00	0.00			32.48	0.00	0.00	0.00	0.00
Vapour loss due to drying						3.58								0.49

Appendix B – Sample Calculations

All sample calculations are shown for organic acid process option 1 (OA-1) unless stated otherwise.

LIB processing capacity

The LIB processing capacity was calculated based on the assumptions stated in section 3.2.

$$LIB\ Processing\ Capacity = 58.33 \times 10^6\ people \times \frac{6.2\ kg\ ewaste}{person} \times 8\%\ Recycling \times 3\%\ LIBs = 868\ ton/yr$$

The daily LIB feed rate was determined as shown below:

$$LIB\ feed\ rate = \frac{Annual\ LIB\ Processing\ Capacity}{Days\ in\ a\ year \times (1 - Down\ time)} = \frac{868\ ton/yr}{365 \times 92\%} = 2.58 \frac{ton}{day}$$

Energy balances

Energy balances were completed for units not operating at ambient temperature. Sample calculations for the citric acid leaching tank operating at 90℃ are shown below.

The inputs to the leaching tank are 54.6 kg/hr LIB electrode material (25℃), 262 kg/hr fresh citric acid (25℃), 2538 kg/hr evaporated water (94.15℃) and 119 kg/hr 50 wt% hydrogen peroxide solution (25℃). The energy contribution of the LIB waste was not considered in the calculations due to its small mass/volume in comparison to the rest of the tank contents and the lack of information regarding the specific heat capacity of the stream.

The following should be noted:

- Mass flowrates are in kg/hr, specific heat capacities in kJ/kg.K and temperatures are in ℃ and therefore converted Kelvin.
- The heat capacity of liquid phase water and leach solutions were calculated with the correlation shown below obtained from NIST where C_p^o is in J/mol.K and t is the Kelvin temperature divided by a 1000. The coefficients used in the correlation are tabulated in Table 68.

$$C_p^o = A + Bt + Ct^2 + Dt^3 + E/t^2$$

Table 68: Coefficients for the calculation of the liquid phase water heat capacity (Chase, 1998)

A	-203.6060
B	1523.290
C	-3196.413
D	2474.455
E	3.855326

- The heat capacity of the hydrogen peroxide solution (50 wt%) was calculated with the correlation used for the heat capacity of water.

An energy balance calculation was used to calculate how much energy should be supplied by using steam.

$$\dot{Q}_{in} = \dot{Q}_{citric\ acid} + \dot{Q}_{water} + \dot{Q}_{H_2O_2} + \dot{Q}_{steam}$$

$$\therefore \dot{Q}_{in} = \frac{262}{3600}(1.172)(25+273) + \frac{2538}{3600}(4.209)(94.15+273) + \frac{119}{3600}(4.18)(25+273) + \dot{Q}_{steam}$$

$$\therefore \dot{Q}_{in} = 1156\ kW + \dot{Q}_{steam}$$

Heat is also lost from the surface of the tank by convection. Based on the tank dimensions, the surface area was determined as 10.4 m^2. It was assumed that the surface temperature is equal to the temperature of the fluid in the tank and that T_∞ is 25°C. The convective heat transfer coefficient of air is typically 10-100 $W/m^2.K$ and was assumed as 55 $W/m^2.K$ (Engineers Edge, 2000).

$$\dot{Q_{loss}} = hA(T_s - T_\infty)$$

$$\dot{Q}_{loss} = 55\frac{W}{m^2.K} \times \frac{1\ kW}{1000\ W} \times 10.4\ m^2 \times (90℃ - 25℃) = 37\ kW$$

Therefore, the total energy leaving the system:

$$\dot{Q}_{out} = \dot{m}_{leach\ solution} C_p dT + \dot{Q}_{loss}$$

$$\dot{Q}_{out} = \frac{2943}{3600}(4.205)(90+273) + 37 = 1248\ kW$$

Finally, the energy demand that should be supplied by the steam was calculated by balancing the energy entering and leaving the system:

$$\dot{Q}_{in} = 1156\ kW + \dot{Q}_{steam} = \dot{Q}_{out}$$

$$\therefore \dot{Q}_{steam} = 1248\ kW - 1156\ kW = 128.8\ kW$$

Equipment Sizing: Tanks

The sample calculation shown is for the citric acid leaching tank. 119 kg/hr hydrogen peroxide (50 wt%) solution with a density of 1.197 kg/L and 2801 kg/hr citric acid solution (water and citric acid) with an assumed density of 0.96506 kg/L (density of water at 90°C) are fed to the tank with a residence time of 1 hour.

$$Effective\ Volume\ (L) = Volumetric\ feed\ rate\ \left(\frac{L}{hr}\right) \times Residence\ time\ (hr)$$

$$\therefore Effective\ Volume = \left(\frac{119\ kg/hr}{1.197\ kg/L} + \frac{2801 kg/hr}{0.96506\ kg/L}\right) \times 1\ hour = 3001\ L = 3\ m^3$$

A safety factor of 10% was added to obtain a final tank volume of 3.33 m^3.

Equipment Sizing: Heat Exchangers/ Evaporators

The sizing calculation of the shell-and-tube heat exchanger pre-heating the feed to the evaporator in OA-1 is shown as sample calculations.

635 kg/hr evaporated water at 94.2°C is available to pre-heat the feed stream to the evaporator in a shell-and tube heat exchanger. A summary of the stream properties of the hot and cold streams entering and leaving the heat exchanger is shown in Table 69 below. The heat capacities of both streams were calculated with the NIST correlation shown in the energy balance sample calculations.

Table 69: Summary of stream properties used in heat exchanger sizing calculations

Hot Stream		**Cold Stream**	
Mass flowrate	635 kg/hr	Mass flowrate	4196 kg/hr
T_{in}	94.2℃	T_{in}	25℃
Cp_{in}	4.21 kJ/kg.K	Cp_{in}	4.18 kJ/kg.K
T_{out}	?	T_{out}	?
Cp_{out}	$f(T_{out})$	Cp_{out}	$f(T_{out})$

Heat integration is only possible if the outlet temperature of the hot stream is higher than the outlet temperature of the cold stream to ensure that a temperature gradient always exist. The following steps were followed:

1. Select a hot stream outlet temperature and determine the available amount of heat that can be transferred. A hot stream temperature of 35℃ was selected.

$$\dot{Q} = \dot{m}C_p\Delta T$$

$$\therefore \dot{Q}_{hot\ stream} = \frac{635}{3600}(94.2 \times 4.21 - 35 \times 4.178) = 44.15\ kW$$

2. Calculate the cold stream outlet temperature if the heat is transferred assuming a constant cold stream heat capacity:

$$\dot{Q} = \dot{m}C_p(T_{out} - T_{in})$$

$$T_{out} = \frac{\dot{Q}}{\dot{m}C_p} + T_{in} = \frac{44.15}{\frac{4196}{3600}(4.18)} + 25 = 34.1℃$$

3. Check if the hot stream outlet temperature is higher than the cold stream outlet temperature else the calculation should be repeated with another hot stream outlet temperature guess.
4. Calculate the log mean temperature difference:

$$\Delta T_{lm} = \frac{\Delta T_1 - \Delta T_2}{ln\left(\frac{\Delta T_1}{\Delta T_2}\right)}$$

$$\Delta T_1 = T_{hot(in)} - T_{cold(out)} = 94.2 - 34.1 = 60.1℃$$

$$\Delta T_1 = T_{hot(out)} - T_{cold(in)} = 35 - 25 = 10℃$$

$$\therefore \Delta T_{lm} = \frac{\Delta T_1 - \Delta T_2}{ln\left(\frac{\Delta T_1}{\Delta T_2}\right)} = \frac{60.1 - 10}{\ln\left(\frac{60.1}{10}\right)} = 27.9℃$$

5. Calculate the required heat transfer area with the assumed overall heat transfer coefficient of 1700 W/m^2.K:

$$\therefore A = \frac{\dot{Q}}{U\Delta T_{lm}} = \frac{44.15\ kW \times 1000\frac{W}{kW}}{1700\frac{W}{m^2.K} \times 27.9℃} = 0.93\ m^2$$

Purchased Equipment Cost

The sample calculation is shown for the citric acid leaching tank. The base equipment cost of the majority of units were calculated with the cost correlation obtained from Turton *et al.* (2012). For process tanks with volumes between 0.3 and 520 m^3, the correlation constants were determined as follows: K_1=3.4974, K_2=0.4485 and K_3=0.1074. The size of the leaching tank was determined as 3.33 m^3.

$$\log_{10} C_p^0 = K_1 + K_2 \log_{10}(A) + K_3[\log_{10}(A)]^2$$

$$\therefore \log_{10} C_p^0 = 3.4974 - 0.4485 \log_{10}(3.33) + 0.1074[\log_{10}(3.33)]$$

$$\therefore C_p^0 = \$\ 5\ 772$$

The base equipment cost (C_p^0) should be adjusted to a present-day value with CEPCI values, scaling factors, material, temperature and pressure correction factors should be considered to determine the final purchased equipment cost of an unit. The CEPCI values used in calculations are tabulated in Table 70.

$$Purchased\ Equipment\ Cost = C_p^0 \times F_M \times F_P \times F_T \times \left(\frac{S_A}{S_B}\right)^n \times \frac{I_2}{I_1}$$

$$\therefore Purchased\ Equipment\ Cost = 5772 \times 1.8 \times 1 \times 1 \times \left(\frac{3.33}{3.33}\right)^{0.55} \times \frac{601.55}{394} = \$\ 15\ 863$$

Table 70: CEPCI indexes

Year	CEPCI	Year	CEPCI
2001	394	2010	550.8
2002	396	2011	585.7
2003	402	2012	584.6
2004	444	2013	567.3
2005	468	2014	576.1
2006	499.6	2015	556.8
2007	525.4	2016	541.7
2008	575.4	2017	567.5
2009	521.9	2018	601.55

Some units were not costed with the Turton *et al.* (2012) correlation but were scaled based on the same principles. The membrane cells are used as example. The capital cost of a membrane electrolysis system producing 544 ton Cl_2 gas per day was $ 32.2 million in 1980. The six-tenths rule was used to scale the capital cost to a facility with the capacity to produce 17.68 ton Cl_2 gas in 2019.

$$Capital\ cost\ of\ membrane\ cells = \$\ 32\ 200\ 000 \times \left(\frac{17.68}{544}\right)^{0.6} \times \frac{601.55}{261.2} = \$\ 9.49\ million\ in\ 2019$$

Raw material cost

The calculation of the cost associated with citric acid is shown below. The citric acid requirement in the leaching tank operating with a solid/liquid ratio of 20 g/L and citric acid molarity of 0.5 M was calculated as follows:

$$Liquid\ requirement(L) = \frac{Solids\ feedrate\ \left(\frac{kg}{hr}\right) \times \frac{1000g}{1kg}}{S/L\ ratio\ \left(\frac{g}{L}\right)}$$

$$\therefore Liquid\ requirement(L) = \frac{54.61 \times 1000}{20} = 2730.4\ L$$

Therefore, the amount of citric acid required in the tank is:

$$Citric\ acid\ required\ \left(\frac{kg}{hr}\right) = Liquid\ in\ tank\ (L) \times Molarity\ \left(\frac{mol}{L}\right) \times MW\ \left(\frac{g}{mol}\right) \times \frac{1\ kg}{1000\ g}$$

$$\therefore Citric\ acid\ required = 2730.4\ L \times 0.5\frac{mol}{L} \times 192.12\frac{g}{mol} \times \frac{1\ kg}{1000\ g} = 262.3\frac{kg}{hr}$$

Based on the desired federate of citric acid, the annual raw material cost was calculated:

$$Citric\ acid\ raw\ material\ cost = Feed\ rate\ \left(\frac{kg}{hr}\right) \times Operating\ hours \times Cost\ \left(\frac{\$}{kg}\right)$$

$$\therefore Citric\ acid\ cost = 262.3\frac{kg}{hr} \times 8059\frac{hr}{year} \times 719\frac{\$}{ton} \times \frac{1\ ton}{1000\ kg} = \$\ 1\ 519\ 280\ per\ year$$

Waste treatment cost

The correlation shown below from Ulrich and Vasudevan (2004) was used to determine waste treatment costs. A CEPCI value of 601.55 for 2018 was used in calculations. For a conservative estimation the average fuel price of heating oil between 2009 and 2019 (15.5 $/GJ) was used (index mundi, no date; Clarke, 2015).

$$C_{S,U} = a(CEPCI) + b(C_{S,f})$$

The cost of solid waste treatment was determined as $ 1203/tonne as discussed in section 4.3.2 in Chapter 4. A sample calculation for the solid leach residue stream are shown below:

$$Waste\ treatment\ cost = Waste\ generation\ rate\ \left(\frac{ton}{yr}\right) \times Operating\ hours \times Cost\ \left(\frac{\$}{ton}\right)$$

$$\therefore Waste\ treatment\ cost = 18.39\frac{kg}{hr} \times 8059\frac{hr}{yr} \times 1203\frac{\$}{ton} \times \frac{1ton}{1000\ kg} = \$\ 178\ 297\ per\ year$$

The waste water treatment cost was calculated with the correlation below. The value of a was estimated with the correlation below where q is the waste water flowrate in m^3/s and b is equal to 0.1 (Ulrich and Vasudevan, 2004).

$$a = 0.0005 + 1 \times 10^{-4} q^{-0.6}$$

The only waste water produced in OA-1 is the final leach solution because the entire water stream from the evaporator are recycled to units in the process. Therefore, the flowrate (q) was calculated as 0.00353 m^3/s.

$$\therefore a = 0.0005 + 1 \times 10^{-4} \times 0.00353 \frac{m^3}{s} = 0.01228$$

$$\therefore C_{S,U} = (0.01228 \times 601.55) + (0.1 \times 15.5) = \$\,8.94/m^3$$

The waste water treatment cost for treating the final leach solution produced after lithium precipitation are shown below. Assuming a waste water density of 1000 kg/m^3:

$$Waste\ treatment\ cost = Flow\ rate\ \left(\frac{kg}{yr}\right) \times \frac{1\ m^3}{1000\ kg} \times Operating\ hours \times Cost\ \left(\frac{\$}{m^3}\right)$$

$$\therefore Waste\ treatment\ cost = 1267.4 \frac{kg}{hr} \times 8059 \frac{hr}{yr} \times 18.94 \frac{\$}{m^3} \times \frac{1\ m^3}{1000\ kg} = \$\ 91\ 545\ per\ year$$

Operating Labour

Operating labour requirements were estimated based on the guidelines provided by Peters, Timmerhaus and West (2003). The calculation of the number of operators required per shift are summarized in Table 71. For each operator required per shift, 4.5 operators should be hired. The annual salary earned by plant operators were assumed as $13 184.

Table 71: Sample calculation of labour requirements for OA-1

Equipment	Workers/unit/shift	Number of units	Workers/shift
Crystallizer	0.16	1	0.16
Rotary dryer	0.5	3	1.5
Evaporator	0.25	1	0.25
Plate and Frame Filter	1	8	8
Heat Exchangers	0.1	3	0.3
Process Vessels	0.35	11	3.85
Auxiliary Pumps	0.35	30	10.5
Conveyor belts	1	7	7
Cutting mill	1	1	1
Screening	1	2	2
Total	-	67	34.56

$$C_{OL} = 4.5 N_{OL} \times Operator\ Salary/annum$$

$$C_{OL} = 4.5(35) \times \$\ 13\ 184 = \$\ 2\ 076\ 413/annum$$

Utilities

Electricity costs were calculated based on the power consumption of the specific unit. Sample calculations for the leaching tank are shown below.

The effective volume of the leaching tank is 3 m^3. The relationship between the power requirements and the effective volume obtained from Figure 30 below were used as follows:

$$Power\ requirement\ (kW) = 0.7204 \times Effective\ volume\ (m^3) + 3.4191$$

$$\therefore Power\ requirement\ (kW) = 0.7204 \times 3\ m^3 + 3.4191 = 5.58\ kW$$

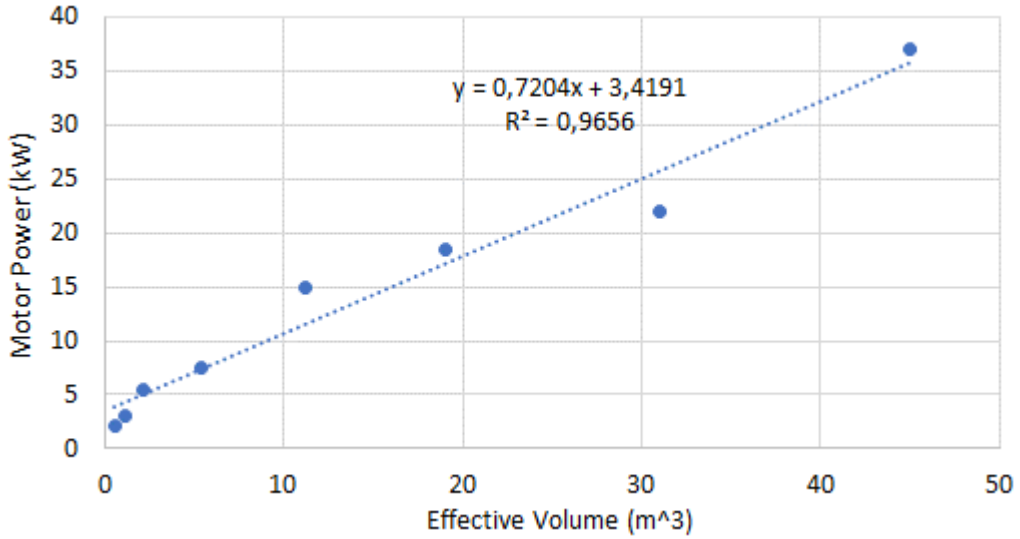

Figure 30: Agitation power requirements as a function of effective tank volume (based on data obtained from Xinhai Minerals Processing EPC)

Using the power requirement (kW) and assumed electricity cost of $ 0.08/kWh the annual electricity cost for operating the leaching tank was calculated as shown below:

$$Electricity\ cost = Power\ required\ (kW) \times Operating\ hours \times Electricity\ Cost$$

$$\therefore Electricity\ cost\ for\ leaching\ tank = 5.58\ kW \times 8059\frac{hr}{yr} \times 0.08\frac{\$}{kWh} = \$\ 3\ 461\ per\ year$$

The steam requirements of each unit were calculated and added determine the facility's overall steam requirements. A sample calculation of the steam required for heating the citric acid leaching tank are shown below. High-pressure steam (HPS) at 254°C are used and cooled down to 109°C. An energy balance over the citric acid leaching tank indicated that the energy required from steam is 128.8 kW.

$$\dot{Q} = \dot{m}C_p\Delta T$$

$$\therefore \dot{m_{steam}} = \frac{128.8\ kW \times 3600\frac{s}{hr}}{(254\ °C)\left(4.0566\frac{kJ}{kg.K}\right) - (109°C)\left(2.1191\frac{kJ}{kg.K}\right)} = 580.1\frac{kg}{hr}\ HPS$$

The total steam required for OA-1 is 2272 kg/hr. Assuming that the energy required to produce 1 kg of HPS from boiler feed water at 23.5℃ is 1159 Btu/lb. Also, the fuel cost related to the natural gas firing the boilers is $ 7.50/GJ.

$$Steam\ cost\ \left(\frac{\$}{ton}\right) = Energy\ required\ \left(\frac{kJ}{kg}\right) \times \frac{1\ GJ}{10^6\ kJ} \times Fuel\ Cost\left(\frac{\$}{GJ}\right) \times \frac{1000\ kg}{1\ ton}$$

$$\therefore Steam\ cost = 2696\frac{kJ}{kg} \times \frac{1\ GJ}{10^6\ kJ} \times 7.5\frac{\$}{GJ} \times \frac{1000\ kg}{1\ ton} = 20.22\frac{\$}{ton}\ HPS$$

$$Annual\ steam\ cost = Steam\ requirement\ \left(\frac{kg}{hr}\right) \times Operating\ hours \times Cost\ \left(\frac{\$}{ton}\right) \times \frac{1\ ton}{1000\ kg}$$

$$\therefore Annual\ steam\ cost = 2272\frac{kg}{hr} \times 8059\ hr \times 20.22\frac{\$}{ton}HPS \times \frac{1\ ton}{1000\ kg} = \$\ 370\ 250\ per\ year$$

Cooling water requirements were calculated in a similar fashion by first completing energy balances over units and then costing the cooling water required for the entire facility.

Depreciation

Straight-line depreciation was considered in economic analysis over an equipment lifetime of 10 years. The salvage value was assumed as 10% of the fixed capital investment.

$$d_k^{SL} = \frac{FCI_L - Salvage\ Value}{n}$$

$$d_k^{SL} = \frac{\$\ 19\ 793\ 813 - \$\ 1\ 979\ 381}{10} = \$\ 1\ 781\ 443$$

Product selling prices

No information was found with regards to the prices of $Mn(OH)_2$, $Mn_3(PO_4)_2$, $Co_3(PO_4)_2$, and $Ni_3(PO_4)_2$. The selling prices of these products were calculated from the known prices of MnO_2, $Co(OH)_2$, CoC_2O_4 and $Ni(OH)_2$ that were assumed based on data obtained from Alibaba.com (2019). Each base price was adjusted by multiplying with the mass fraction of the valuable metal in the compound with the unknown price and dividing by the mass fraction of the valuable metal in the known base price. The mass fractions of the valuable metals in each product are tabulated in Table 72 below.

The calculation for the price of $Mn(OH)_2$ is shown below. A similar procedure was followed for each of the products to calculate the prices summarized in Table 45 in Chapter 4.

$$Mass\ fraction\ Mn\ in\ MnO_2 = \frac{MW_{Mn}}{MW_{MnO_2}} = \frac{54.938}{86.94} = 63.2\%$$

$$Mass\ fraction\ Mn\ in\ Mn(OH)_2 = \frac{MW_{Mn}}{MW_{Mn(OH)_2}} = \frac{54.938}{88.95} = 61.8\%$$

$$\therefore Mn(OH)_2 selling\ price = MnO_2\ selling\ price \times \frac{Mass\ fraction\ Mn\ in\ Mn(OH)_2}{Mass\ fraction\ Mn\ in\ MnO_2}$$

$$\therefore Mn(OH)_2 selling\ price = \frac{\$\ 42.621}{kg} \times \frac{61.8\%}{63.2\%} = \frac{\$\ 41.677}{kg} Mn(OH)_2$$

Table 72: Mass fraction (wt%) of valuable metals in product streams

Co in $Co_3(PO_4)_2$	48.2%
Co in $Co(OH)_2$	63.4%
Co in CoC_2O_4	40.1%
Ni in $Ni_3(PO_4)_2$	48.1%
Ni in and $Ni(OH)_2$	63.3%
Mn in $Mn_3(PO_4)_2$	46.5%
Mn in MnO_2	63.2%
Mn in $Mn(OH)_2$	61.8%

Revenue

The estimated annual revenue was calculated by adding the expected income from the various product streams. For OA-1, 4 product streams contributed to the annual revenue. An example calculation for the income from CoC_2O_4 are shown below. The income from the other products were calculated in a similar way.

$$Revenue_{CoC_2O_4} = Production\ rate \times Operating\ hours \times Product\ purity \times Selling\ price$$

$$\therefore Revenue_{CoC_2O_4} = 28.1\frac{kg}{hr} \times 8059\frac{hr}{year} \times 97.8\% \times 50.625\frac{\$}{kg} = \$\ 11\ 211\ 358\ per\ year$$

The revenue earned per kilogram of LIB waste processed was calculated as shown below:

$$Revenue\ per\ kg\ LIBs\ treated = \frac{Total\ annual\ revenue}{kg\ LIBs\ treated\ per\ annum}$$

$$\therefore Revenue\ per\ kg\ LIBs\ treated = \frac{\$\ 25\ 451\ 031\ per\ annum}{868\ 000\ kg\ LIBs} = \$\ 29.32\ per\ kg\ LIBs\ treated$$

Profitability analysis

The cashflow sample calculations for the first year of plant operation (year 3) are shown for OA-1. The following steps were followed to calculate the annual NPV of each year:

1. Calculate the profit before tax (take note in year 3 only 85% of the calculated revenue is earned):

$$Profit\ before\ tax_{year3} = Revenue - Expenses = R - COM_d - d$$

$$\therefore Profit\ before\ tax_{year3} = 21\ 633\ 377 - 15\ 170\ 664 - 1\ 781\ 443 = \$\ 4\ 681\ 269$$

2. Calculate the after-tax cash flow (incorporating a tax rate of 28%):

$$After\ tax\ cash\ flow = Net\ Profit + Depreciation = (R - COM_d - d)(1 - t) + d$$

$$\therefore After\ tax\ cash\ flow_{year3} = 4\ 681\ 269\ (1 - 28\%) + 1\ 781\ 443 = \$\ 5\ 151\ 957$$

3. Calculate the annual non-discounted cash flow:

$$Non - discounted\ cash\ flow = Cash\ flow\ due\ to\ investments + After\ tax\ cash\ flow$$

$$\therefore Non-discounted\ cash\ flow_{year3} = 0 + 5\ 151\ 957 = \$\ 5\ 151\ 957$$

4. Calculate the annual discounted cash flow for the year:

$$Annual\ discounted\ cash\ flow = \frac{Estimated\ net\ cash\ flow\ in\ year\ n}{(1+r)^n}$$

$$\therefore Annual\ discounted\ cash\ flow_{year3} = \frac{5\ 151\ 957}{(1+0.15)^3} = \$\ 3\ 387\ 495$$

5. Calculate the cumulative NPV at the end of the year:

$$NPV = \sum_{n=1}^{n=project\ life} \frac{Estimated\ net\ cash\ flow\ in\ year\ n}{(1+r)^n}$$

$$\therefore NPV_{year3} = NPV_{year1} + NPV_{year2} + Annual\ discounted\ cash\ flow_{year3}$$

$$\therefore NPV_{year3} = -8\ 606\ 006 - 9\ 728\ 528 + 3\ 387\ 495 = \$ - 14\ 947\ 039$$

The above procedure shown above was repeated for every year to calculate the cumulative NPV at the end of 20 years. The PVR was calculated at the end of the project life to give an indication of the return on investment.

$$PVR = \frac{Present\ Value\ of\ all\ positive\ cash\ flows}{Present\ Value\ of\ all\ negative\ cash\ flows} = 1 + \frac{NPV}{FCI}$$

$$\therefore PVR_{year20} = 1 + \frac{16\ 439\ 761}{19\ 793\ 813} = 1.83$$

The DPBP was calculated at the end of the 20-year project lifetime by interpolating between the two years between which the initial fixed capital was paid back. The construction period of the plant was assumed two years and therefore the working capital was discounted by two years as shown below.

$$Discounted\ Working\ Capital = \frac{Working\ Capital}{(1+r)^2}$$

$$\therefore Discounted\ Working\ Capital = \frac{\$\ 2\ 969\ 072}{(1+15\%)^2} = \$\ 2\ 245\ 045$$

Therefore, the DPBP is the number of years corresponding to the time when the cumulative NPV was equal to $ -2 245 045. Interpolating the cumulative NPV between years 6 and 7 and subtracting the 2 construction years will give the DPBP:

$$DPBP = \frac{(6-7)}{(-\$3\ 086\ 100 - (-\$115\ 946))} \times \big(-\$\ 2\ 245\ 045 - (-\$3\ 086\ 100)\big) + 6 - 2 = 4.28\ years$$

Monte Carlo simulation product selling price maximum and minimum limits

Prices for pure Co, Li, Mn and Ni were obtained from Shanghai Metals Market and adjusted by multiplying with the mass fractions of the valuable metal in each compound (refer to Table 72) (Shanghai Metals Market, 2019). Table 73 below show how the bottom limit was calculated.

Table 73: Determination of Shanghai Metals Market (SMM) price minimums for Monte Carlo simulation

Shanghai Metals Market	SMM price (USD/ton)	Metal Product	Adjusted price (USD/ton)	Alibaba base price (USD/ton)	% below Alibaba base price
Refined cobalt	39375	CoC_2O_4	15791	50625	-69%
		$Co(OH)_2$	24965	55143	-55%
Manganese powder	36000	$Mn(OH)_2$	22235	41677	-47%
		MnO_2	22749	42621	-47%
Nickel powder	26250	$Ni(OH)_2$	16618	39500	-58%
Lithium carbonate	11625	Li_2CO_3	11625	16750	-31%
		Li_3PO_4	11128	15350	-28%

The historical fluctuations in the Co, Ni, Mn and Li prices are depicted in the graphs shown in Figure 31 below. Fluctuations in the pure metal prices will influence the value of products containing these metals.

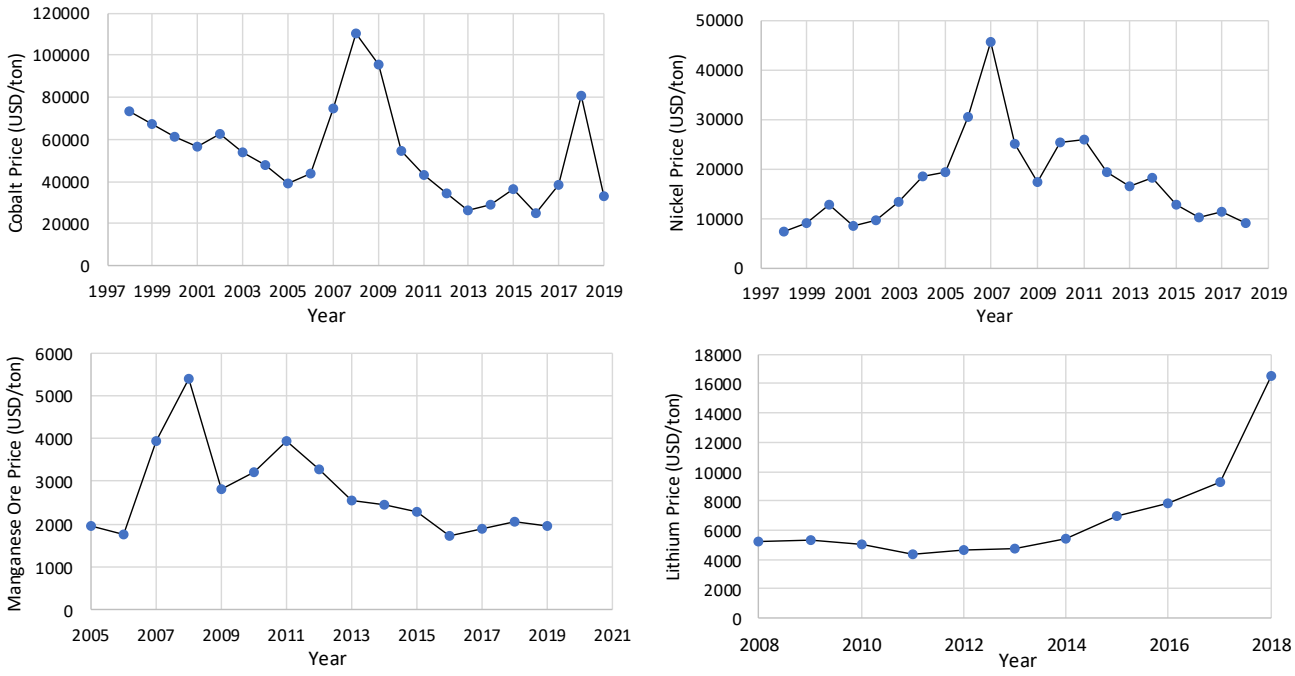

Figure 31: Historical fluctuation in pure metal market prices (data obtained from Metalary (2019))

For the calculation of the average price fluctuations in the pure metal prices, data regarding daily cobalt and nickel prices were obtained from Investing.com for the period April 2009 to May 2019. However, daily prices for Mn and Li were not available. Therefore, average yearly prices for manganese (period 2005-2018) and lithium (period 2008-2018) were obtained from Metalary.com. For each metal the average price over the entire period were calculated. The data percentiles were calculated as shown in

Table 74 and Table 75 respectively. The top and bottom 5% of the data were excluded to give a better representation of how much the metal prices fluctuated from their averages.

Table 74: Cobalt and Nickel percentiles based on data from Investing.com (2019)

Metal	**Cobalt**		**Nickel**	
Average	$38 086		$15 278	
Percentile	**Co Price**	**% above or below the average price**	**Ni Price**	**% above or below the average price**
Maximum 100%	$94 300	148%	$29 286	92%
99%	$91 050	139%	$27 366	79%
95%	$75 205	**97%**	$24 179	**58%**
90%	$60 997	60%	$22 039	44%
3rd Quartile 75%	$39 545	4%	$18 265	20%
Median 50%	$31 219	-18%	$14 512	-5%
1st Quartile 25%	$28 000	-26%	$11 564	-24%
10%	$25 251	-34%	$9 738	-36%
5%	$23 615	**-38%**	$8 899	**-42%**
1%	$22 500	-41%	$8 410	-45%
Minimum 0%	$21 666	-43%	$7 590	-50%

Table 75: Manganese and Lithium percentiles based on data from Metalary.com

Metal	**Manganese**		**Lithium**	
Average	$2 804		$6 866	
Percentile	**Mn Price**	**% above or below the average price**	**Li Price**	**% above or below the average price**
Maximum 100%	$5 402	93%	$16 500	140%
99%	$5 211	86%	$15 782	130%
95%	**$4 445**	**59%**	$12 909	**88%**
90%	$3 930	40%	$9 318	36%
3rd Quartile 75%	$3 252	16%	$7 398	8%
Median 50%	$2 498	-11%	$5 364	-22%
1st Quartile 25%	$1 990	-29%	$4 927	-28%
10%	$1 788	-36%	$4 668	-32%
5%	**$1 741**	**-38%**	$4 520	**-34%**
1%	$1 739	-38%	$4 401	-36%
Minimum 0%	$1 738	-38%	$4 371	-36%

The margin of error in the simulation results were determined as shown below. The sample calculation is based on the results of Simulation 1. A confidence level of 95% corresponding to a Z-value of 1.96 was used in all error calculations.

$$Margin\ of\ error = \frac{Z \times S}{\sqrt{n}}$$

$$Margin\ of\ error = \frac{1.96 \times \$\ 8\ 777\ 099}{\sqrt{100000}} = \$\ 54\ 401$$

The error was expressed as a percentage of the average NPV output:

$$\%\ Error = \frac{\$\ 54\ 401}{\$\ 1\ 579250} = 3.44$$

Appendix C – Mass Balances

Table 76: Overall mass balance MA-1

Mineral Acid Process Option 1			
Streams in	**kg/hr**	**Streams out**	**kg/hr**
LIB Feed	107.70	LIB waste (12 mm screen)	29.76
Ultrasonic washing water	4.97	Washing water loss	4.97
HCl, leaching water	3085.47	LIB waste (2 mm screen)	23.33
NaOH solution (pH=2)	1192.52	Leaching gas	3.56
$KMnO_4$	36.06	Leach residue	14.52
NaOH solution (pH=4,5)	35.16	Cl_2, CO_2 gas (Mn precipitation)	4.85
28% ammonia (pH=9)	394.91	Mn product powder	21.61
DMG	0.78	Drying loss (Mn)	1.46
Ni-DMG dissolution with HCl	276.74	Metal hydroxide impurities	6.85
NaOH solution (Ni precipitation)	50.11	Ni product powder	6.78
HCl (pH=0)	971.95	Drying loss (Ni)	0.93
NaOH solution (pH=11)	732.43	DMG purge	0.85
NaOH (membrane cells)	162.75	Co product powder	17.96
Water (membrane cells)	380.37	Drying loss (Co)	1.04
Demineralized water	1548.55	Evaporated water	1926.83
Cl_2 gas (HCl furnace)	741.69	Evaporated water	2447.21
H_2 gas (HCl furnace)	21.58	Cl_2 gas (membrane cells)	736.84
Excess H_2 fed	1.63	H_2 gas (membrane cells)	21.58
Sodium carbonate solution	117.88	32wt% NaOH solution (membrane cells)	3106.42
HCl Addition (pH adjustment)	396.14	33 wt% HCl (absorber)	2311.26
NaOH (pH Adjustment before Li precipitation)	668.89	Tail gas (tail gas tower)	6.33
		CO_2 gas (Li precipitation)	4.18
		Li product powder	12.60
		Drying loss (Li)	0.11
		NaCl crystal purge	170.58
		Final solution purge	41.94
		CO_2 gas (pH adjustment)	2.93
Total mass flowrate IN	**10928.3**	Total mass flowrate OUT	**10927.3**
Mass balance error %		**0.009%**	

Table 77: Overall mass balance MA-2

Mineral Acid Process Option 2			
Streams in	**kg/hr**	**Streams out**	**kg/hr**
LIB Feed	107.70	LIB waste (12 mm screen)	29.76
Ultrasonic washing water	4.97	Washing water loss	4.97
HCl, leaching water	3130.89	LIB waste (2 mm screen)	23.33
NaOH solution (pH=2)	774.57	Leaching gas	3.56
$KMnO_4$	36.06	Leach residue	14.21
NaOH solution (pH=4,5)	28.27	Cl_2, CO_2 gas (Mn precipitation)	4.65
28% ammonia (pH=9)	395.01	Mn product powder	21.49
DMG	0.78	Drying loss (Mn)	1.29
Ni-DMG dissolution with HCl	287.98	Metal hydroxide impurities	6.98
NaOH solution (Ni precipitation)	44.00	Ni product powder	6.83
HCl (pH=0)	1154.61	Drying loss (Ni)	1.22
NaOH solution (pH=11)	541.54	DMG purge	0.85
Sodium carbonate solution	153.28	Co product powder	18.05
Dilution Water	22.73	Drying loss (Co)	1.16
		Evaporated water	5219.09
		CO_2 gas (Li precipitation)	13.04
		Li product powder	10.57
		Drying loss (Li)	0.38
		NaCl crystal purge	1282.02
		Final solution purge	18.41
Total mass flowrate IN	**6682.4**	Total mass flowrate OUT	**6681.9**
Mass balance error %		**0.008%**	

Table 78: Overall mass balance MA-3

Mineral Acid Process Option 3			
Streams in	**kg/hr**	**Streams out**	**kg/hr**
LIB Feed	107.70	LIB waste (12 mm screen)	29.76
Ultrasonic washing water	4.97	Washing water loss	4.97
HCl, leaching water	3052.14	LIB waste (2 mm screen)	23.33
NaOH solution (pH=4,5)	783.96	Leaching gas	3.67
Metal Ratio Adjustment	25.02	Leach residue	14.22
50 wt% NaOH (Metal hydroxide precipitation)	93.60	Metal hydroxide impurities	6.53
Sodium carbonate solution	57.06	Metal hydroxide powder product	54.39
Dilution Water	0.30	Drying loss (metal hydroxides)	3.27
		Evaporated water	3287.19
		Li product powder	9.97
		Drying loss (Li)	0.43
		NaCl crystal purge	686.74
Total mass flowrate IN	**4124.8**	Total mass flowrate OUT	**4124.5**
Mass balance error %		**0.007%**	

Table 79: Overall mass balance OA-1

Organic Acid Process Option 1			
Streams in	**kg/hr**	**Streams out**	**kg/hr**
LIB Feed	107.70	LIB waste (12 mm screen)	29.76
Ultrasonic washing water	4.97	Washing water loss	4.97
Citric acid. leaching water	2800.27	LIB waste (2 mm screen)	23.33
50 wt% Hydrogen peroxide solution	118.77	Leaching gas	31.52
50 wt% NaOH solution (pH=2)	118.19	Leach residue purge	18.39
0.5 M KMnO4	546.64	CO_2 gas (Mn precipitation)	6.35
50 wt% NaOH solution (pH=6)	145.52	Mn product powder	31.26
0.2 M DMG	34.11	Drying loss (Mn)	2.26
33 wt% HCl (Ni-DMG dissolution)	201.42	Ni product powder	6.14
50 wt% NaOH (Ni precipitation)	26.30	Drying loss (Ni)	0.41
0.5 M Oxalic acid (Co precipitation)	275.97	DMG purge	0.83
0.5 M Phosphoric acid (Li precipitation)	259.48	Co product powder	28.09
		Drying loss (Co)	1.91
		Evaporated water	3173.43
		Li product powder	13.59
		Drying loss (Li)	0.72
		Final solution purge	1267.44
Total mass flowrate IN	**4639.3**	Total mass flowrate OUT	**4640.4**
Mass balance error %		**0.02%**	

Table 80: Overall mass balance OA-2

Organic Acid Process Option 2			
Streams in	**kg/hr**	**Streams out**	**kg/hr**
LIB Feed	107.70	LIB waste (12 mm screen)	29.76
Ultrasonic washing water	4.97	Washing water loss	4.97
Citric acid. leaching water	2800.27	LIB waste (2 mm screen)	23.33
50 wt% Hydrogen peroxide solution	118.77	Leaching gas	31.52
50 wt% NaOH solution (pH=6)	245.32	Leach residue purge	18.39
0.2 M DMG	34.13	Waste solution after Mn Precipitation	6667.15
33 wt% HCl (Ni-DMG dissolution)	201.78	Mn product powder	10.22
50 wt% NaOH (Ni precipitation)	26.34	Drying loss (Mn)	0.66
Ammonium oxalate solution	283.83	Ni product powder	6.16
Oxalic acid solution	101.71	Drying loss (Ni)	0.41
Fresh D2EHPA, kerosene	27.67	DMG purge	0.83
50 wt% NaOH (Saponification)	14.85	Co product powder	28.52
Scrub solution	328.64	Drying loss (Co)	2.04
98% sulfuric acid (stripping)	65.62	Evaporated water	2972.81
Stripping solution water make-up	6501.34	Oxalic acid purge stream	103.03
50 wt% NaOH (Solvent Extraction)	3.18	Li product powder	12.90
50 wt% NaOH (Mn Precipitation)	104.86	Drying loss (Li)	0.73
Sodium phosphate (Li precipitation)	262.47	Final solution purge	1291.96
		Organic extractant losses	27.98
Total mass flowrate IN	**11233.4**	Total mass flowrate OUT	**11233.4**
Mass balance error %		**0.001%**	

Table 81: Overall mass balance OA-3

Organic Acid Process Option 3			
Streams in	**kg/hr**	**Streams out**	**kg/hr**
LIB Feed	107.70	LIB waste (12 mm screen)	29.76
Ultrasonic washing water	4.97	Washing water loss	4.97
Citric acid, leaching water	2800.27	LIB waste (2 mm screen)	23.33
50 wt% Hydrogen peroxide solution	118.77	Leaching gas	31.52
50 wt% NaOH (pH=13)	233.64	Leach residue	18.39
NaH_2PO_4 solution (Ni,Co, Mn precipitation)	180.29	Mn, Ni, Co product powder	47.90
50 wt% NaOH (pH control in Ni, Co, Mn precipitation tank)	240.43	Drying loss (mixed product)	3.58
NaH_2PO_4 solution (Li precipitation)	48.71	Evaporated water	2215.88
50 wt% NaOH (pH control in Li precipitation tank)	64.96	Li product powder	11.41
		Drying loss (Li)	0.49
		Final solution purge	1413.33
Total mass flowrate IN	**3799.7**	Total mass flowrate OUT	**3800.6**
Mass balance error %		**0.022%**	

Appendix D – Capital Costs

Table 82: Breakdown of purchased equipment cost of MA-1

Process Unit/ Equipment piece	Base Case costs (Cp0)					FM	FT	FP	Scaling factor	Real size	Unit	Actual estimated equipment Cost ($)
	Size	Unit	Cost ($)	Year	Reference							
Retsch cutting mill	-	-	-	-	Retsch, 2019	-	-	-	-	-	-	37 514
12 mm screen	0.09	m^2	1 315	2018	Alibaba	1	1	1	0.6	0.09	m^2	1 315
2 mm screen	0.09	m^2	1 315	2018	Alibaba	1	1	1	0.6	0.09	m^2	1 315
Discharging tank	1.00	m^3	3 139	2001	R. Turton, 2012	1.8	1	1	0.55	1.00	m^3	8 628
Ultrasonic washing tank	0.18	m^3	2 100	2018	Alibaba	1	1	1	0.55	0.11	m^3	1 607
Ultrasonic washing tank agitator	0.76	kW	5 846	2001	R. Turton, 2012	1.8	1	1	0.5	0.76	kW	16 067
HCl leaching tank	3.28	m^3	5 716	2001	R. Turton, 2012	1.8	1	1	0.55	3.28	m^3	15 709
HCl leaching tank agitator	5.54	kW	23 564	2001	R. Turton, 2012	1.8	1	1	0.5	5.54	kW	64 759
pH Adjustment (pH=2) tank	1.69	m^3	4 034	2001	R. Turton, 2012	1.8	1	1	0.55	1.69	m^3	11 086
pH Adjustment (pH=2) agitator	4.52	kW	20 417	2001	R. Turton, 2012	1.8	1	1	0.5	4.52	kW	56 110
Mn Precipitation tank	4.17	m^3	6 557	2001	R. Turton, 2012	1.8	1	1	0.55	4.17	m^3	18 020
Mn Precipitation agitator	6.12	kW	25 259	2001	R. Turton, 2012	1.8	1	1	0.5	6.12	kW	69 417
Impurity Removal tank	1.75	m^3	4 098	2001	R. Turton, 2012	1.8	1	1	0.55	1.75	m^3	11 261
Impurity Removal agitator	4.55	kW	20 528	2001	R. Turton, 2012	1.8	1	1	0.5	4.55	kW	56 415
Ammonia addition tank	3.51	m^3	5 943	2001	R. Turton, 2012	1.8	1	1	0.55	3.51	m^3	16 333
Ammonia addition agitator	5.70	kW	24 016	2001	R. Turton, 2012	1.8	1	1	0.5	5.70	kW	66 002
Ni-DMG Precipitation tank	4.42	m^3	6 783	2001	R. Turton, 2012	1.8	1	1	0.55	4.42	m^3	18 641
Ni-DMG Precipitation agitator	6.28	kW	25 723	2001	R. Turton, 2012	1.8	1	1	0.5	6.28	kW	70 693
Ni-DMG dissolution tank	0.30	m^3	1 959	2001	R. Turton, 2012	1.8	1	1	0.55	0.30	m^3	5 384
Ni-DMG dissolution agitator	0.96	kW	6 899	2001	R. Turton, 2012	1.8	1	1	0.5	0.96	kW	18 960
Ni precipitation tank	0.59	m^3	2 520	2001	R. Turton, 2012	1.8	1	1	0.55	0.59	m^3	6 926
Ni precipitation agitator	3.80	kW	18 101	2001	R. Turton, 2012	1.8	1	1	0.5	3.80	kW	49 746
pH Adjustment (pH=0) tank	1.32	m^3	3 568	2001	R. Turton, 2012	1.8	1	1	0.55	1.32	m^3	9 805

Process Unit/ Equipment piece	Size	Unit	Cost (US $)	Year	Reference	FM	FT	FP	Scaling factor	Real size	Unit	Actual estimated equipment Cost ($)
pH Adjustment (pH=0) agitator	4.27	kW	19 634	2001	R. Turton, 2012	1.8	1	1	0.5	4.27	kW	53 958
Co precipitation tank	10.82	m^3	11 917	2001	R. Turton, 2012	1.8	1	1	0.55	10.82	m^3	32 751
Co precipitation agitator	10.44	kW	36 700	2001	R. Turton, 2012	1.8	1	1	0.5	10.44	kW	100 860
Mixer	1.82	m^3	4 177	2001	R. Turton, 2012	1.8	1	1	0.55	1.82	m^3	11 479
Mixer agitator	4.60	kW	20 667	2001	R. Turton, 2012	1.8	1	1	0.5	4.60	kW	56 796
pH Adjustment tank	0.20	m^3	1 732	2001	R. Turton, 2012	1.8	1	1	0.55	0.20	m^3	4 760
pH Adjustment agitator	0.86	kW	6 381	2001	R. Turton, 2012	1.8	1	1	0.5	0.86	kW	17 535
pH Adjustment tank	3.88	m^3	6 291	2001	R. Turton, 2012	1.8	1	1	0.55	3.88	m^3	17 288
pH Adjustment agitator	5.93	kW	24 716	2001	R. Turton, 2012	1.8	1	1	0.5	5.93	kW	67 925
Li precipitation tank	0.14	m^3	1 572	2001	R. Turton, 2012	1.8	1	1	0.55	0.14	m^3	4 320
Li precipitation agitator	0.80	kW	6 055	2001	R. Turton, 2012	1.8	1	1	0.5	0.80	kW	16 640
NaCl make-up tank	0.17	m^3	1 636	2001	R. Turton, 2012	1.8	1	1	0.55	0.17	m^3	4 496
NaCl make-up tank agitation	0.82	kW	6 181	2001	R. Turton, 2012	1.8	1	1	0.5	0.82	kW	16 986
Na_2CO_3 solution make-up tank	0.24	m^3	1 817	2001	R. Turton, 2012	1.8	1	1	0.55	0.24	m^3	4 992
Na_2CO_3 make-up agitator	0.89	kW	6 566	2001	R. Turton, 2012	1.8	1	1	0.5	0.89	kW	18 046
Filter press 1	29.22	m^2	88 091	2001	R. Turton, 2012	1.8	1	1	0.6	29.22	m^2	242 091
Filter press 2	50.10	m^2	120 293	2001	R. Turton, 2012	1.8	1	1	0.6	50.10	m^2	330 588
Filter press 3	58.84	m^2	132 476	2001	R. Turton, 2012	1.8	1	1	0.6	58.84	m^2	364 070
Filter press 4	58.93	m^2	132 595	2001	R. Turton, 2012	1.8	1	1	0.6	58.93	m^2	364 397
Filter press 5	61.86	m^2	136 552	2001	R. Turton, 2012	1.8	1	1	0.6	61.86	m^2	375 272
Filter press 6	29.64	m^2	88 788	2001	R. Turton, 2012	1.8	1	1	0.6	29.64	m^2	244 007
Filter press 7	29.88	m^2	89 190	2001	R. Turton, 2012	1.8	1	1	0.6	29.88	m^2	245 111
Filter press 8	73.97	m^2	152 381	2001	R. Turton, 2012	1.8	1	1	0.6	73.97	m^2	418 773
Filter press 9	34.38	m^2	96 579	2001	R. Turton, 2012	1.8	1	1	0.6	34.38	m^2	265 419
Filter press 10	29.03	m^2	87 760	2001	R. Turton, 2012	1.8	1	1	0.6	29.03	m^2	241 183
Dryer after discharging tank	800.00	kg/hr	6 500	2019	Alibaba	1	1	1	0.6	107.70	kg/hr	1 952

Process Unit/ Equipment piece	Size	Unit	Cost (US $)	Year	Reference	FM	FT	FP	Scaling factor	Real size	Unit	Actual estimated equipment Cost ($)
Continuous dryer (LIBs feed)	800.00	kg/hr	6 500	2019	Alibaba	1	1	1	0.6	82.92	kg/hr	1 668
Product powder dryer	800.00	kg/hr	6 500	2019	Alibaba	1	1	1	0.6	161.60	kg/hr	2 490
Crystallizer	0.06	m^3	31 453	2001	R. Turton, 2012	1.8	1	1	0.54	0.06	m^3	86 438
Evaporator 1	2.38	m^2	146 103	2001	R. Turton, 2012	1.8	1	1,1	0.6	2.38	m^2	443 092
Evaporator 2	1.25	m^2	114 299	2001	R. Turton, 2012	1.8	1	1,1	0.6	1.25	m^2	346 638
Heat Exchanger (Evaporator 1 pre-heat)	5.00	m^2	10 400	2014	Matches	1.8	1	1	0.6	2.25	m^2	12 116
Heat Exchanger (Evaporator 2 pre-heat)	0.46	m^2	4 600	2014	Matches	1.8	1	1	0.6	0.52	m^2	9 274
Heat Exchanger (HCl pre-heat)	5.00	m^2	10 400	2014	Matches	1.8	1	1	0.6	0.95	m^2	7 235
LIBs feed storage tank	24.07	m^3	20 986	2001	R. Turton, 2012	1.8	1	1	0.55	24.07	m^3	57 673
$KMnO_4$ Hopper	10.68	m^3	11 815	2001	R. Turton, 2012	1.8	1	1	0.55	10.68	m^3	32 470
DMG Hopper	0.46	m^3	2 279	2001	R. Turton, 2012	1.8	1	1	0.55	0.46	m^3	6 263
NaOH Hopper	14.25	m^3	14 384	2001	R. Turton, 2012	1.8	1	1	0.55	14.25	m^3	39 531
Na_2CO_3 Hopper	11.61	m^3	12 496	2001	R. Turton, 2012	1.8	1	1	0.55	11.61	m^3	34 340
NaCl Hopper	5.98	m^3	8 139	2001	R. Turton, 2012	1.8	1	1	0.55	5.98	m^3	22 369
Fresh HCl (33 wt% solution) Storage tank	49.42	m^3	36 752	2001	R. Turton, 2012	1.8	1	1	0.55	49.42	m^3	101 002
28% Ammonia Storage tank	164.18	m^3	104 245	2001	R. Turton, 2012	1.8	1	1	0.55	164.18	m^3	286 486
Intermediate HCl storage tank	4.47	m^3	6 829	2001	R. Turton, 2012	1.8	1	1	0.55	4.47	m^3	18 768
Intermediate 32wt% NaOH storage tank	4.41	m^3	6 779	2001	R. Turton, 2012	1.8	1	1	0.55	4.41	m^3	18 631
Mn product prior to drying	0.90	m^3	2 999	2001	R. Turton, 2012	1.8	1	1	0.55	0.90	m^3	8 243
Ni product prior to drying	0.30	m^3	1 958	2001	R. Turton, 2012	1.8	1	1	0.55	0.30	m^3	5 382
Co product prior to drying	0.99	m^3	3 130	2001	R. Turton, 2012	1.8	1	1	0.55	0.99	m^3	8 601
Li product prior to drying	1.12	m^3	3 314	2001	R. Turton, 2012	1.8	1	1	0.55	1.12	m^3	9 108
Battery waste tank	12.80	m^3	13 352	2001	R. Turton, 2012	1.8	1	1	0.55	12.80	m^3	36 694
Leach Residue Storage tank	5.45	m^3	7 693	2001	R. Turton, 2012	1.8	1	1	0.55	5.45	m^3	21 142
Metal Hydroxide Storage tank	2.19	m^3	4 600	2001	R. Turton, 2012	1.8	1	1	0.55	2.19	m^3	12 641
DMG Purge Collection tank	0.50	m^3	2 363	2001	R. Turton, 2012	1.8	1	1	0.55	0.50	m^3	6 495

Process Unit/ Equipment piece	Size	Unit	Cost (US $)	Year	Reference	FM	FT	FP	Scaling factor	Real size	Unit	Actual estimated equipment Cost ($)
NaCl crystal purge collection tank	28.27	m^3	23 690	2001	R. Turton, 2012	1.8	1	1	0.55	28.27	m^3	65 104
Final solution purge collection tank	47.93	m^3	35 852	2001	R. Turton, 2012	1.8	1	1	0.55	47.93	m^3	98 528
Ammonia waste water tank	4.47	m^3	6 829	2001	R. Turton, 2012	1.8	1	1	0.55	4.47	m^3	18 768
Mn-Product storage tank	3.61	m^3	6 037	2001	R. Turton, 2012	1.8	1	1	0.55	3.61	m^3	16 591
Ni-Product storage tank	1.22	m^3	3 443	2001	R. Turton, 2012	1.8	1	1	0.55	1.22	m^3	9 462
Co-Product storage tank	4.01	m^3	6 409	2001	R. Turton, 2012	1.8	1	1	0.55	4.01	m^3	17 614
Li-Product storage tank	4.76	m^3	7 093	2001	R. Turton, 2012	1.8	1	1	0.55	4.76	m^3	19 493
Combustion Furnace	1.60	m^3	3 138	2001	R. Turton, 2012	5.8	2,1	1	0.6	1.60	m^3	58 347
HCl Absorber	49.00	m^2	73 400	2014	Matches.com	5.8	2,1	1	0.6	22.13	m^2	579 461
Tail gas Absorber	0.003	m^3	1 118	2001	R. Turton, 2012	5.8	2,1	1	0.6	0.00	m^3	20 796
Total Purchased Equipment Cost												**6 673 592**

Table 83: Breakdown of purchased equipment cost of MA-2

Process Unit/ Equipment piece	Base Case costs (Cp0)					FM	FT	FP	Scaling factor	Real size	Unit	Actual estimated equipment Cost ($)
	Size	Unit	Cost (US $)	Year	Reference							
Retsch cutting mill												37 514
12 mm screen	0.09	m^2	1 315	2018	Alibaba	1	1	1	0.6	0.09	m^2	1 315
2 mm screen	0.09	m^2	1 315	2018	Alibaba	1	1	1	0.6	0.09	m^2	1 315
Discharging tank	1.00	m^3	3 139	2001	R. Turton, 2012	1.8	1	1	0.55	1.00	m^3	8 628
Ultrasonic washing tank	0.18	m^3	2 100	2018	Alibaba	1	1	1	0.55	0.11	m^3	1 607
Ultrasonic washing tank agitator	0.76	kW	5 846	2001	R. Turton, 2012	1.8	1	1	0.5	0.76	kW	16 067
HCl leaching tank	3.28	m^3	5 716	2001	R. Turton, 2012	1.8	1	1	0.55	3.28	m^3	15 709
HCl leaching tank agitator	5.54	kW	23 564	2001	R. Turton, 2012	1.8	1	1	0.5	5.54	kW	64 759
pH Adjustment (pH=2) tank	0.73	m^3	2 749	2001	R. Turton, 2012	1.8	1	1	0.55	0.73	m^3	15 112
pH Adjustment (pH=2) agitator	1.42	kW	9 066	2001	R. Turton, 2012	1.8	1	1	0.5	1.42	kW	49 828
Mn Precipitation tank	3.67	m^3	6 099	2001	R. Turton, 2012	1.8	1	1	0.55	3.67	m^3	16 760
Mn Precipitation agitator	5.80	kW	24 328	2001	R. Turton, 2012	1.8	1	1	0.5	5.80	kW	66 857
Impurity Removal tank	0.80	m^3	2 846	2001	R. Turton, 2012	1.8	1	1	0.55	0.80	m^3	15 644
Impurity Removal agitator	1.48	kW	9 358	2001	R. Turton, 2012	1.8	1	1	0.5	1.48	kW	51 438
Ammonia addition tank	1.57	m^3	3 881	2001	R. Turton, 2012	1.8	1	1	0.55	1.57	m^3	21 331
Ammonia addition agitator	2.29	kW	12 698	2001	R. Turton, 2012	1.8	1	1	0.5	2.29	kW	69 792
Ni-DMG Precipitation tank	3.91	m^3	6 321	2001	R. Turton, 2012	1.8	1	1	0.55	3.91	m^3	17 372
Ni-DMG Precipitation agitator	5.96	kW	24 778	2001	R. Turton, 2012	1.8	1	1	0.5	5.96	kW	68 095
Ni-DMG dissolution tank	0.31	m^3	1 971	2001	R. Turton, 2012	1.8	1	1	0.55	0.31	m^3	5 417
Ni-DMG dissolution agitator	0.97	kW	6 928	2001	R. Turton, 2012	1.8	1	1	0.5	0.97	kW	19 039
Ni precipitation tank	0.29	m^3	1 937	2001	R. Turton, 2012	1.8	1	1	0.55	0.29	m^3	10 645
Ni precipitation agitator	0.95	kW	6 845	2001	R. Turton, 2012	1.8	1	1	0.5	0.95	kW	37 624
pH Adjustment (pH=0) tank	1.19	m^3	3 404	2001	R. Turton, 2012	1.8	1	1	0.55	1.19	m^3	9 354
pH Adjustment (pH=0) agitator	1.90	kW	11 118	2001	R. Turton, 2012	1.8	1	1	0.5	1.90	kW	30 555

Process Unit/ Equipment piece	Size	Unit	Cost (US $)	Year	Reference	FM	FT	FP	Scaling factor	Real size	Unit	Actual estimated equipment Cost ($)
Co precipitation tank	4.90	m^3	7 209	2001	R. Turton, 2012	1.8	1	1	0.55	4.90	m^3	39 625
Co precipitation agitator	6.59	kW	26 608	2001	R. Turton, 2012	1.8	1	1	0.5	6.59	kW	146 248
Mixer	1.75	m^3	4 102	2001	R. Turton, 2012	1.8	1	1	0.55	1.75	m^3	11 272
Mixer agitator	2.49	kW	13 444	2001	R. Turton, 2012	1.8	1	1	0.5	2.49	kW	36 946
Li precipitation tank	0.20	m^3	1 734	2001	R. Turton, 2012	1.8	1	1	0.55	0.20	m^3	4 766
Li precipitation agitator	0.86	kW	6 385	2001	R. Turton, 2012	1.8	1	1	0.5	0.86	kW	17 547
Saturated Na_2CO_3 solution make-up tank	0.30	m^3	1 960	2001	R. Turton, 2012	1.8	1	1	0.55	0.30	m^3	5 387
Na_2CO_3 make-up agitator	0.96	kW	6 901	2001	R. Turton, 2012	1.8	1	1	0.5	0.96	kW	18 966
50 wt% NaOH solution make-up tank	1.96	m^3	4 342	2001	R. Turton, 2012	1.8	1	1	0.55	1.96	m^3	11 933
NaOH solution make-up tank agitator	4.69	kW	20 961	2001	R. Turton, 2012	1.8	1	1	0.5	4.69	kW	57 604
NaCl make-up tank	0.17	m^3	1 636	2001	R. Turton, 2012	1.8	1	1	0.55	0.17	m^3	4 496
NaCl make-up tank agitation	0.82	kW	6 181	2001	R. Turton, 2012	1.8	1	1	0.5	0.82	kW	16 986
Filter press 1	29.22	m^2	88 091	2001	R. Turton, 2012	1.8	1	1	0.6	29.22	m^2	242 091
Filter press 2	50.43	m^2	120 761	2001	R. Turton, 2012	1.8	1	1	0.6	50.43	m^2	331 876
Filter press 3	56.15	m^2	128 789	2001	R. Turton, 2012	1.8	1	1	0.6	56.15	m^2	353 937
Filter press 4	56.19	m^2	128 844	2001	R. Turton, 2012	1.8	1	1	0.6	56.19	m^2	354 089
Filter press 5	59.12	m^2	132 855	2001	R. Turton, 2012	1.8	1	1	0.6	59.12	m^2	365 111
Filter press 6	29.70	m^2	88 903	2001	R. Turton, 2012	1.8	1	1	0.6	29.70	m^2	244 322
Filter press 7	29.90	m^2	89 230	2001	R. Turton, 2012	1.8	1	1	0.6	29.90	m^2	245 221
Filter press 8	71.18	m^2	148 807	2001	R. Turton, 2012	1.8	1	1	0.6	71.18	m^2	408 951
Filter press 9	38.25	m^2	102 694	2001	R. Turton, 2012	1.8	1	1	0.6	38.25	m^2	282 224
Filter press 10	30.16	m^2	89 671	2001	R. Turton, 2012	1.8	1	1	0.6	30.16	m^2	246 434
Dryer after discharging	800.00	kg/hr	6 500	2019	Alibaba	1	1	1	0.6	107.70	kg/hr	1 952
Continuous dryer (LIBs feed)	800.00	kg/hr	6 500	2019	Alibaba	1	1	1	0.6	82.92	kg/hr	1 668
Product powder dryer	800.00	kg/hr	6 500	2019	Alibaba	1	1	1	0.6	159.41	kg/hr	2 469
Forced Circulation Crystallizer	1.67	m^3	35 881	2001	R. Turton, 2012	1.8	1	1	0.37	1.67	m^3	98 607

Process Unit/ Equipment piece	Size	Unit	Cost (US $)	Year	Reference	FM	FT	FP	Scaling factor	Real size	Unit	Actual estimated equipment Cost ($)
Forced Circulation Evaporator	5.00	m^2	200 004	2001	R. Turton, 2012	1.8	1	1,10	0.54	1.71	m^2	339 500
Shell and tube Heat Exchanger (33 wt% HCl pre-heating)	1.20	m^2	6 400	2014	Matches	1.8	1	1	0.6	0.60	m^2	7 902
Shell and tube Heat Exchanger (Mn precipitation tank pre-heat)	0.46	m^2	4 600	2014	Matches	1.8	1	1	0.6	0.43	m^2	8 277
Shell and tube Heat Exchanger (Brine pre-heating)	5.00	m^2	10 400	2014	Matches	1.8	1	1	0.6	3.36	m^2	15 389
LIBs feed storage tank	24.07	m^3	20 986	2001	R. Turton, 2012	1.8	1	1	0.55	24.07	m^3	57 673
$KMnO_4$ Hopper	10.68	m^3	11 816	2001	R. Turton, 2012	1.8	1	1	0.55	10.68	m^3	32 473
DMG Hopper	0.46	m^3	2 279	2001	R. Turton, 2012	1.8	1	1	0.55	0.46	m^3	6 263
NaOH Hopper	119.14	m^3	77 878	2001	R. Turton, 2012	1.8	1	1	0.55	119.14	m^3	214 025
Na_2CO_3 Hopper	14.67	m^3	14 677	2001	R. Turton, 2012	1.8	1	1	0.55	14.67	m^3	40 336
NaCl Hopper	5.98	m^3	8 139	2001	R. Turton, 2012	1.8	1	1	0.55	5.98	m^3	22 369
Fresh HCl (33 wt% solution) Storage Tank	388.19	m^3	239 057	2001	R. Turton, 2012	1.8	1	1	0.55	388.19	m^3	656 975
28% Ammonia Storage Tank	164.22	m^3	104 268	2001	R. Turton, 2012	1.8	1	1	0.55	164.22	m^3	286 550
Mn product prior to drying	0.89	m^3	2 980	2001	R. Turton, 2012	1.8	1	1	0.55	0.89	m^3	8 189
Ni product prior to drying	0.34	m^3	2 048	2001	R. Turton, 2012	1.8	1	1	0.55	0.34	m^3	5 629
Co product prior to drying	1.00	m^3	3 148	2001	R. Turton, 2012	1.8	1	1	0.55	1.00	m^3	8 651
Li product prior to drying	0.96	m^3	3 086	2001	R. Turton, 2012	1.8	1	1	0.55	0.96	m^3	8 480
Battery waste tank	12.80	m^3	13 352	2001	R. Turton, 2012	1.8	1	1	0.55	12.80	m^3	36 694
Leach Residue Storage Tank	5.24	m^3	7 513	2001	R. Turton, 2012	1.8	1	1	0.55	5.24	m^3	20 647
Metal Hydroxide Storage Tank	2.29	m^3	4 710	2001	R. Turton, 2012	1.8	1	1	0.55	2.29	m^3	12 943
DMG Purge Collection Tank	0.50	m^3	2 364	2001	R. Turton, 2012	1.8	1	1	0.55	0.50	m^3	6 497
NaCl Crystal Purge Collection Tank	226.24	m^3	140 878	2001	R. Turton, 2012	1	1	1	0.55	226.24	m^3	215 090
Waste Water Container	4.97	m^3	7 270	2001	R. Turton, 2012	1	1	1	0.55	4.97	m^3	11 100
Final Solution Purge Collection Tank	21.04	m^3	19 004	2001	R. Turton, 2012	1.8	1	1	0.55	21.04	m^3	52 227
Mn-Product storage tank	3.58	m^3	6 012	2001	R. Turton, 2012	1.8	1	1	0.55	3.58	m^3	16 522

Process Unit/ Equipment piece	Size	Unit	Cost (US $)	Year	Reference	FM	FT	FP	Scaling factor	Real size	Unit	Actual estimated equipment Cost ($)
Ni-Product storage tank	1.24	m^3	3 470	2001	R. Turton, 2012	1.8	1	1	0.55	1.24	m^3	9 537
Co-Product storage tank	4.03	m^3	6 430	2001	R. Turton, 2012	1.8	1	1	0.55	4.03	m^3	17 671
Li-Product storage tank	3.95	m^3	6 355	2001	R. Turton, 2012	1.8	1	1	0.55	3.95	m^3	17 465
Total Purchased Equipment Cost												**6 337 580**

Table 84: Breakdown of purchased equipment cost of MA-3

Process Unit/ Equipment piece	Base Case costs (Cp0)					FM	FT	FP	Scaling factor	Real size	Unit	Actual estimated equipment Cost ($)
	Size	Unit	Cost (US $)	Year	Reference							
Retsch cutting mill												37 514
12 mm screen	0.09	m^2	1 315	2018	Alibaba	1	1	1	0.6	0.09	m^2	1 315
2 mm screen	0.09	m^2	1 315	2018	Alibaba	1	1	1	0.6	0.09	m^2	1 315
Discharging tank	1.00	m^3	3 139	2001	R. Turton, 2012	1.8	1	1	0.55	1.00	m^3	8 628
Ultrasonic washing tank	0.18	m^3	2 100	2018	Alibaba	1	1	1	0.55	0.11	m^3	1 607
Ultrasonic washing tank agitator	0.76	kW	5 846	2001	R. Turton, 2012	1.8	1	1	0.5	0.76	kW	16 067
HCl leaching tank	3.28	m^3	5 716	2001	R. Turton, 2012	1.8	1	1	0.55	3.28	m^3	15 709
HCl leaching tank agitator	4.09	kW	19 051	2001	R. Turton, 2012	1.8	1	1	0.5	4.09	kW	52 357
Impurity Removal tank	1.52	m^3	3 823	2001	R. Turton, 2012	1.8	1	1	0.55	1.52	m^3	10 507
Impurity Removal agitator	2.24	kW	12 504	2001	R. Turton, 2012	1.8	1	1	0.5	2.24	kW	34 362
Metal Hydroxide Precipitation tank	2.04	m^3	4 427	2001	R. Turton, 2012	1.8	1	1	0.55	2.04	m^3	12 165
Metal Hydroxide Precipitation agitator	2.79	kW	14 554	2001	R. Turton, 2012	1.8	1	1	0.5	2.79	kW	39 998
Ratio Adjustment tank	7.38	m^3	9 281	2001	R. Turton, 2012	1.8	1	1	0.55	7.38	m^3	25 507
Ratio Adjustment agitator	8.41	kW	31 549	2001	R. Turton, 2012	1.8	1	1	0.5	8.41	kW	86 702
Mixer	1.26	m^3	3 493	2001	R. Turton, 2012	1.8	1	1	0.55	1.26	m^3	9 600
Mixer agitator	1.97	kW	11 411	2001	R. Turton, 2012	1.8	1	1	0.5	1.97	kW	31 358

Process Unit/ Equipment piece	Size	Unit	Cost (US $)	Year	Reference	FM	FT	FP	Scaling factor	Real size	Unit	Actual estimated equipment Cost ($)
Li precipitation Tank	0.13	m^3	1 539	2001	R. Turton, 2012	1.8	1	1	0.55	0.13	m^3	4 229
Li precipitation tank	0.79	kW	5 992	2001	R. Turton, 2012	1.8	1	1	0.5	0.79	kW	16 467
Li precipitation agitator	0.11	m^3	1 482	2001	R. Turton, 2012	1.8	1	1	0.55	0.11	m^3	4 073
Na_2CO_3 solution make-up tank	0.77	kW	5 888	2001	R. Turton, 2012	1.8	1	1	0.5	0.77	kW	16 182
Na_2CO_3 make-up agitator	1.28	m^3	3 520	2001	R. Turton, 2012	1.8	1	1	0.55	1.28	m^3	9 672
50 wt% NaOH solution make-up tank agitator	1.99	kW	11 497	2001	R. Turton, 2012	1.8	1	1	0.5	1.99	kW	31 596
NaCl make-up tank	0.17	m^3	1 636	2001	R. Turton, 2012	1.8	1	1	0.55	0.17	m^3	4 496
NaCl make-up tank agitation	0.82	kW	6 181	2001	R. Turton, 2012	1.8	1	1	0.5	0.82	kW	16 986
Filter press 1	29.22	m^2	88 091	2001	R. Turton, 2012	1.8	1	1	0.6	29.22	m^2	242 091
Filter press 2	49.86	m^2	119 947	2001	R. Turton, 2012	1.8	1	1	0.6	49.86	m^2	329 639
Filter press 3	55.42	m^2	127 779	2001	R. Turton, 2012	1.8	1	1	0.6	55.42	m^2	351 163
Filter press 4	56.23	m^2	128 899	2001	R. Turton, 2012	1.8	1	1	0.6	56.23	m^2	354 239
Filter press 5	33.30	m^2	94 846	2001	R. Turton, 2012	1.8	1	1	0.6	33.30	m^2	260 656
Filter press 6	28.75	m^2	87 293	2001	R. Turton, 2012	1.8	1	1	0.6	28.75	m^2	239 897
Dryer after discharging	800.00	kg/hr	6 500	2019	Alibaba	1	1	1	0.6	107.70	kg/hr	1 952
Continuous dryer (LIBs feed)	800.00	kg/hr	6 500	2019	Alibaba	1	1	1	0.6	82.92	kg/hr	1 668
Product powder dryer	800.00	kg/hr	6 500	2019	Alibaba	1	1	1	0.6	57.67	kg/hr	1 342
Forced Circulation Crystallizer	1.01	m^3	32 410	2001	R. Turton, 2012	1.8	1	1	0.37	1.01	m^3	89 070
Forced Circulation Evaporator	5.00	m^2	200 004	2001	R. Turton, 2012	1.8	1	1,104	0.54	1.25	m^2	286 418
Shell and tube Heat Exchanger (33 wt% HCl pre-heating)	1.20	m^2	6 400	2014	Matches	1.8	1	1	0.6	0.66	m^2	8 428
Shell and tube Heat Exchanger (Brine pre-heating)	1.20	m^2	6 400	2014	Matches	1.8	1	1	0.6	1.03	m^2	10 993
LIBs feed storage tank	24.07	m^3	20 986	2001	R. Turton, 2012	1.8	1	1	0.55	24.07	m^3	57 673
NaOH Hopper	76.91	m^3	53 121	2001	R. Turton, 2012	1.8	1	1	0.55	76.91	m^3	145 987
Na_2CO_3 Hopper	5.62	m^3	7 834	2001	R. Turton, 2012	1.8	1	1	0.55	5.62	m^3	21 531

Process Unit/ Equipment piece	Size	Unit	Cost (US $)	Year	Reference	FM	FT	FP	Scaling factor	Real size	Unit	Actual estimated equipment Cost ($)
NaCl hopper	5.98	m^3	8 139	2001	R. Turton, 2012	1.8	1	1	0.55	5.98	m^3	22 369
Fresh HCl (33 wt% solution) Storage Tank	193.48	m^3	121 482	2001	R. Turton, 2012	1.8	1	1	0.55	193.48	m^3	333 856
Metal Hydroxides prior to drying	2.97	m^3	5 412	2001	R. Turton, 2012	1.8	1	1	0.55	2.97	m^3	14 873
Li product prior to drying	0.91	m^3	3 016	2001	R. Turton, 2012	1.8	1	1	0.55	0.91	m^3	8 288
Battery waste tank	12.80	m^3	13 352	2001	R. Turton, 2012	1.8	1	1	0.55	12.80	m^3	36 694
Leach Residue Storage Tank	5.23	m^3	7 505	2001	R. Turton, 2012	1.8	1	1	0.55	5.23	m^3	20 624
Metal Hydroxide Storage Tank	2.21	m^3	4 622	2001	R. Turton, 2012	1.8	1	1	0.55	2.21	m^3	12 703
NaCl Crystal Purge Collection Tank	55.69	m^3	40 524	2001	R. Turton, 2012	1.8	1	1	0.55	55.69	m^3	111 367
Waste Water Container	2.15	m^3	4 551	2001	R. Turton, 2012	1.8	1	1	0.55	2.15	m^3	12 506
Metal Hydroxide storage tank	12.00	m^3	12 780	2001	R. Turton, 2012	1.8	1	1	0.55	12.00	m^3	35 122
Li-Product storage tank	3.74	m^3	6 161	2001	R. Turton, 2012	1.8	1	1	0.55	3.74	m^3	16 933
Total Purchased Equipment Cost												**3 516 491**

Table 85: Breakdown of purchased equipment cost of OA-1

Process Unit/ Equipment piece	Base Case costs (Cp0)					FM	FT	FP	Scaling factor	Real size	Unit	Actual estimated equipment Cost ($)
	Size	Unit	Cost (US $)	Year	Reference							
Retsch cutting mill	-	-	-	-	Retsch, 2019	-	-	-	-	-	-	37 514
12 mm screen	0.09	m^2	1 315	2018	Alibaba	1	1	1	0.6	0.09	m^2	1 315
2 mm screen	0.09	m^2	1 315	2018	Alibaba	1	1	1	0.6	0.09	m^2	1 315
Discharging tank	1.00	m^3	3 139	2001	R. Turton, 2012	1.8	1	1	0.55	1.00	m^3	8 628
Ultrasonic washing tank	0.18	m^3	2 100	2018	Alibaba	1	1	1	0.55	0.11	m^3	1 607
Ultrasonic washing tank agitator	0.76	kW	5 846	2001	R. Turton, 2012	1.8	1	1	0.5	0.76	kW	16 067
Citric acid leaching tank	3.33	m^3	5 772	2001	R. Turton, 2012	1.8	1	1	0.55	3.33	m^3	15 863
Leaching tank agitator	5.58	kW	23 676	2001	R. Turton, 2012	1.8	1	1	0.5	5.58	kW	65 065
pH Adjustment (pH=2) tank	0.11	m^3	1 482	2001	R. Turton, 2012	1.8	1	1	0.55	0.11	m^3	4 073
pH Adjustment (pH=2) agitator	0.77	kW	5 888	2001	R. Turton, 2012	1.8	1	1	0.5	0.77	kW	16 182
Mn Precipitation tank	3.68	m^3	6 104	2001	R. Turton, 2012	1.8	1	1	0.55	3.68	m^3	16 775
Mn Precipitation agitator	5.81	kW	24 339	2001	R. Turton, 2012	1.8	1	1	0.5	5.81	kW	66 888
pH Adjustment (pH=6) tank	0.73	m^3	2 742	2001	R. Turton, 2012	1.8	1	1	0.55	0.73	m^3	15 070
pH Adjustment (pH=6) agitator	1.41	kW	9 042	2001	R. Turton, 2012	1.8	1	1	0.5	1.41	kW	49 701
Ni-DMG precipitation tank	3.75	m^3	6 166	2001	R. Turton, 2012	1.8	1	1	0.55	3.75	m^3	16 946
Ni-DMG precipitation agitator	5.85	kW	24 464	2001	R. Turton, 2012	1.8	1	1	0.5	5.85	kW	67 232
Ni-DMG dissolution tank	0.22	m^3	1 768	2001	R. Turton, 2012	1.8	1	1	0.55	0.22	m^3	4 859
Ni-DMG dissolution agitator	0.87	kW	6 459	2001	R. Turton, 2012	1.8	1	1	0.5	0.87	kW	17 751
Ni precipitation tank	0.21	m^3	1 753	2001	R. Turton, 2012	1.8	1	1	0.55	0.21	m^3	9 635
Ni precipitation agitator	0.87	kW	6 426	2001	R. Turton, 2012	1.8	1	1	0.5	0.87	kW	35 319
Co precipitation tank	4.36	m^3	6 731	2001	R. Turton, 2012	1.8	1	1	0.55	4.36	m^3	18 499
Co precipitation agitator	6.25	kW	25 617	2001	R. Turton, 2012	1.8	1	1	0.5	6.25	kW	70 400
Li precipitation tank	4.54	m^3	6 891	2001	R. Turton, 2012	1.8	1	1	0.55	4.54	m^3	18 937
Li precipitation agitator	6.36	kW	25 946	2001	R. Turton, 2012	1.8	1	1	0.5	6.36	kW	71 304
$KMnO_4$ make-up tank	0.57	m^3	2 474	2001	R. Turton, 2012	1.8	1	1	0.55	0.57	m^3	6 799

Process Unit/ Equipment piece	Size	Unit	Cost (US $)	Year	Reference	FM	FT	FP	Scaling factor	Real size	Unit	Actual estimated equipment Cost ($)
$KMnO_4$ make-up tank agitator	1.24	kW	8 260	2001	R. Turton, 2012	1.8	1	1	0.5	1.24	kW	22 700
50 wt% NaOH solution make-up tank	0.21	m^3	1 752	2001	R. Turton, 2012	1.8	1	1	0.55	0.21	m^3	4 815
NaOH solution make-up tank agitator	0.87	kW	6 424	2001	R. Turton, 2012	1.8	1	1	0.5	0.87	kW	17 654
DMG make-up tank	0.04	m^3	1 190	2001	R. Turton, 2012	1.8	1	1	0.55	0.04	m^3	3 271
DMG make-up tank agitator	0.68	kW	5 440	2001	R. Turton, 2012	1.8	1	1	0.5	0.68	kW	14 949
Oxalic acid make-up tank	0.51	m^3	2 381	2001	R. Turton, 2012	1.8	1	1	0.55	0.51	m^3	6 544
Oxalic acid make-up tank agitator	1.19	kW	7 999	2001	R. Turton, 2012	1.8	1	1	0.5	1.19	kW	21 982
NaCl make-up tank	0.17	m^3	1 636	2001	R. Turton, 2012	1.8	1	1	0.55	0.17	m^3	4 496
NaCl make-up Tank agitator	0.82	kW	6 181	2001	R. Turton, 2012	1.8	1	1	0.5	0.82	kW	16 986
Filter press 1	29.22	m^2	88 091	2001	R. Turton, 2012	1.8	1	1	0.6	29.22	m^2	242 091
Filter press 2	48.70	m^2	118 285	2001	R. Turton, 2012	1.8	1	1	0.6	48.70	m^2	325 072
Filter press 3	53.33	m^2	124 860	2001	R. Turton, 2012	1.8	1	1	0.6	53.33	m^2	343 139
Filter press 4	54.50	m^2	126 498	2001	R. Turton, 2012	1.8	1	1	0.6	54.50	m^2	347 640
Filter press 5	29.03	m^2	87 757	2001	R. Turton, 2012	1.8	1	1	0.6	29.03	m^2	241 174
Filter press 6	29.10	m^2	87 875	2001	R. Turton, 2012	1.8	1	1	0.6	29.10	m^2	241 499
Filter press 7	57.97	m^2	131 291	2001	R. Turton, 2012	1.8	1	1	0.6	57.97	m^2	360 815
Filter press 8	36.69	m^2	100 248	2001	R. Turton, 2012	1.8	1	1	0.6	36.69	m^2	275 503
Dryer after discharging	800.00	kg/hr	6 500	2019	Alibaba	1	1	1	0.6	107.70	kg/hr	1 952
Continuous dryer (LIBs feed)	800.00	kg/hr	6 500	2019	Alibaba	1	1	1	0.6	82.92	kg/hr	1 668
Product powder dryer	800.00	kg/hr	6 500	2019	Alibaba	1	1	1	0.6	234.63	kg/hr	3 114
Forced Circulation Evaporator	5.00	m^2	200 004	2001	R. Turton, 2012	1.8	1	1,1035	0.54	0.78	m^2	222 851
Shell and tube heat exchanger	0.46	m^2	4 600	2014	Matches	1.8	1	1	0.6	0.93	m^2	13 111
LIBs feed storage tank	24.07	m^3	20 986	2001	R. Turton, 2012	1.8	1	1	0.55	24.07	m^3	57 673
Citric acid hopper	58.99	m^3	42 496	2001	R. Turton, 2012	1.8	1	1	0.55	58.99	m^3	116 787
$KMnO_4$ Hopper	11.95	m^3	12 741	2001	R. Turton, 2012	1.8	1	1	0.55	11.95	m^3	35 014
DMG Hopper	0.45	m^3	2 270	2001	R. Turton, 2012	1.8	1	1	0.55	0.45	m^3	6 238

Process Unit/ Equipment piece	Size	Unit	Cost (US $)	Year	Reference	FM	FT	FP	Scaling factor	Real size	Unit	Actual estimated equipment Cost ($)
NaOH Hopper	25.42	m^3	21 859	2001	R. Turton, 2012	1.8	1	1	0.55	25.42	m^3	60 073
Oxalic acid Hopper	8.77	m^3	10 371	2019	R. Turton, 2012	1.8	1	1	0.55	8.77	m^3	28 501
Hydrogen Peroxide Storage Tank	79.38	m^3	54 578	2001	R. Turton, 2012	1.8	1	1	0.55	79.38	m^3	149 991
Fresh 33 wt% HCl Storage Tank	11.49	m^3	12 407	2001	R. Turton, 2012	1.8	1	1	0.55	11.49	m^3	34 098
Phosphoric acid Storage Tank	12.74	m^3	13 312	2001	R. Turton, 2012	1.8	1	1	0.55	12.74	m^3	36 583
Mn product prior to drying	1.23	m^3	3 463	2001	R. Turton, 2012	1.8	1	1	0.55	1.23	m^3	9 516
Ni product prior to drying	0.30	m^3	1 961	2001	R. Turton, 2012	1.8	1	1	0.55	0.30	m^3	5 389
Co product prior to drying	1.82	m^3	4 182	2001	R. Turton, 2012	1.8	1	1	0.55	1.82	m^3	11 492
Li product prior to drying	1.10	m^3	3 284	2001	R. Turton, 2012	1.8	1	1	0.55	1.10	m^3	9 025
Battery waste tank	12.80	m^3	13 352	2001	R. Turton, 2012	1.8	1	1	0.55	12.80	m^3	36 694
Leach Residue Storage Tank	6.55	m^3	8 614	2001	R. Turton, 2012	1.8	1	1	0.55	6.55	m^3	23 674
DMG Purge Collection Tank	0.49	m^3	2 340	2001	R. Turton, 2012	1.8	1	1	0.55	0.49	m^3	6 432
Final Solution Purge Collection Tank	33.90	m^3	27 237	2001	R. Turton, 2012	1.8	1	1	0.55	33.90	m^3	74 852
Mn-Product storage tank	4.94	m^3	7 244	2001	R. Turton, 2012	1.8	1	1	0.55	4.94	m^3	19 908
Ni-Product storage tank	1.21	m^3	3 425	2001	R. Turton, 2012	1.8	1	1	0.55	1.21	m^3	9 412
Co-Product storage tank	7.30	m^3	9 221	2001	R. Turton, 2012	1.8	1	1	0.55	7.30	m^3	25 341
Li-Product storage tank	4.48	m^3	6 838	2001	R. Turton, 2012	1.8	1	1	0.55	4.48	m^3	18 792
Total Purchased Equipment Cost												**4 162 250**

Table 86: Breakdown of purchased equipment cost of OA-2

Process Unit/ Equipment piece	Base Case costs (Cp0)					FM	FT	FP	Scaling factor	Real size	Unit	Actual estimated equipment Cost ($)
	Size	Unit	Cost ($)	Year	Reference							
Retsch cutting mill	-	-	-	-	Retsch, 2019	-	-	-	-	-	-	37 514
12 mm screen	0.09	m^2	1 315	2018	Alibaba	1	1	1	0.6	0.09	m^2	1 315
2 mm screen	0.09	m^2	1 315	2018	Alibaba	1	1	1	0.6	0.09	m^2	1 315
Discharging tank	1.00	m^3	3 139	2001	R. Turton, 2012	1.8	1	1	0.55	1.00	m^3	8 628
Ultrasonic washing tank	0.18	m^3	2 100	2018	Alibaba	1	1	1	0.55	0.11	m^3	1 607
Ultrasonic washing tank agitator	0.76	kW	5 846	2001	R. Turton, 2012	1.8	1	1	0.5	0.76	kW	16 067
Citric acid leaching tank	3.33	m^3	5 772	2001	R. Turton, 2012	1.8	1	1	0.55	3.33	m^3	15 863
Leaching tank agitator	5.58	kW	23 676	2001	R. Turton, 2012	1.8	1	1	0.5	5.58	kW	65 065
pH Adjustment (pH=6) tank	1.12	m^3	3 315	2001	R. Turton, 2012	1.8	1	1	0.55	1.12	m^3	18 219
pH Adjustment (pH=6) agitator	1.83	kW	10 830	2001	R. Turton, 2012	1.8	1	1	0.5	1.83	kW	59 528
Ni-DMG precipitation tank	3.25	m^3	5 693	2001	R. Turton, 2012	1.8	1	1	0.55	3.25	m^3	15 646
Ni-DMG precipitation agitator	5.53	kW	23 519	2001	R. Turton, 2012	1.8	1	1	0.5	5.53	kW	64 635
Ni-DMG dissolution tank	0.22	m^3	1 772	2001	R. Turton, 2012	1.8	1	1	0.55	0.22	m^3	4 869
Ni-DMG dissolution agitator	0.88	kW	6 467	2001	R. Turton, 2012	1.8	1	1	0.5	0.88	kW	17 772
Ni precipitation Tank	0.21	m^3	1 753	2001	R. Turton, 2012	1.8	1	1	0.55	0.21	m^3	9 638
Ni precipitation agitator	0.87	kW	6 427	2001	R. Turton, 2012	1.8	1	1	0.5	0.87	kW	35 324
Co precipitation tank	4.00	m^3	6 403	2001	R. Turton, 2012	1.8	1	1	0.55	4.00	m^3	17 598
Co precipitation agitator	6.01	kW	24 945	2001	R. Turton, 2012	1.8	1	1	0.5	6.01	kW	68 554
MnC_2O_4 dissolution tank	1.13	m^3	3 325	2001	R. Turton, 2012	1.8	1	1	0.55	1.13	m^3	9 139
MnC_2O_4 dissolution agitator	4.15	kW	19 248	2001	R. Turton, 2012	1.8	1	1	0.5	4.15	kW	52 899
D2EHPA saponification tank	7.42	m^3	9 312	2001	R. Turton, 2012	1.8	1	1	0.55	7.42	m^3	25 590
D2EHPA saponification tank agitator	8.23	kW	31 072	2001	R. Turton, 2012	1.8	1	1	0.5	8.23	kW	85 392
Mn Precipitation tank	4.03	m^3	6 428	2001	R. Turton, 2012	1.8	1	1	0.55	4.03	m^3	35 331
Mn Precipitation agitator	4.88	kW	21 559	2001	R. Turton, 2012	1.8	1	1	0.5	4.88	kW	118 497
Li precipitation tank	3.96	m^3	6 363	2001	R. Turton, 2012	1.8	1	1	0.55	3.96	m^3	17 486

Process Unit/ Equipment piece	Size	Unit	Cost ($)	Year	Reference	FM	FT	FP	Scaling factor	Real size	Unit	Actual estimated equipment Cost ($)
Li precipitation agitator	5.98	kW	24 863	2001	R. Turton, 2012	1.8	1	1	0.5	5.98	kW	68 328
NaOH solution make-up tank	0.29	m^3	1 929	2001	R. Turton, 2012	1.8	1	1	0.55	0.29	m^3	5 303
NaOH solution make-up tank agitator	3.60	kW	17 431	2001	R. Turton, 2012	1.8	1	1	0.5	3.60	kW	47 903
NaCl make-up tank	0.17	m^3	1 636	2001	R. Turton, 2012	1.8	1	1	0.55	0.17	m^3	4 496
NaCl make-up tank agitator	0.82	kW	6 181	2001	R. Turton, 2012	1.8	1	1	0.5	0.82	kW	16 986
DMG make-up tank	0.04	m^3	1 190	2001	R. Turton, 2012	1.8	1	1	0.55	0.04	m^3	3 272
DMG make-up tank agitator	0.68	kW	5 440	2001	R. Turton, 2012	1.8	1	1	0.5	0.68	kW	14 949
Ammonium oxalate make-up tank	0.28	m^3	1 925	2001	R. Turton, 2012	1.8	1	1	0.55	0.28	m^3	5 291
Ammonium oxalate make-up tank agitator	0.94	kW	6 817	2001	R. Turton, 2012	1.8	1	1	0.5	0.94	kW	18 736
Oxalic acid make-up tank	0.11	m^3	1 477	2001	R. Turton, 2012	1.8	1	1	0.55	0.11	m^3	4 058
Oxalic acid make-up tank agitator	0.76	kW	5 878	2001	R. Turton, 2012	1.8	1	1	0.5	0.76	kW	16 155
Na_2CO_3 make-up tank	0.36	m^3	2 096	2001	R. Turton, 2012	1.8	1	1	0.55	0.36	m^3	5 759
Na_2CO_3 make-up tank agitator	1.03	kW	7 237	2001	R. Turton, 2012	1.8	1	1	0.5	1.03	kW	19 889
Na_3PO_4 make-up tank	0.27	m^3	1 893	2001	R. Turton, 2012	1.8	1	1	0.55	0.27	m^3	5 203
Na_3PO_4 make-up tank agitator	0.93	kW	6 743	2001	R. Turton, 2012	1.8	1	1	0.5	0.93	kW	18 530
Filter press 1	29.22	m^2	88 091	2001	R. Turton, 2012	1.8	1	1	0.6	29.22	m^2	242 091
Filter press 2	48.70	m^2	118 285	2001	R. Turton, 2012	1.8	1	1	0.6	48.70	m^2	325 072
Filter press 3	50.70	m^2	121 149	2001	R. Turton, 2012	1.8	1	1	0.6	50.70	m^2	332 942
Filter press 4	29.03	m^2	87 759	2001	R. Turton, 2012	1.8	1	1	0.6	29.03	m^2	241 180
Filter press 5	29.10	m^2	87 878	2001	R. Turton, 2012	1.8	1	1	0.6	29.10	m^2	241 506
Filter press 6	54.23	m^2	126 127	2001	R. Turton, 2012	1.8	1	1	0.6	54.23	m^2	346 622
Filter press 7	35.09	m^2	97 719	2001	R. Turton, 2012	1.8	1	1	0.6	35.09	m^2	268 551
Filter press 8	75.70	m^2	154 586	2001	R. Turton, 2012	1.8	1	1	0.6	75.70	m^2	424 833
Filter press 9	36.86	m^2	100 519	2001	R. Turton, 2012	1.8	1	1	0.6	36.86	m^2	276 247
Dryer after discharging	800.00	kg/hr	6 500	2019	Alibaba	1	1	1	0.6	107.70	kg/hr	1 952
Continuous dryer (LIBs feed)	800.00	kg/hr	6 500	2019	Alibaba	1	1	1	0.6	82.92	kg/hr	1 668

Process Unit/ Equipment piece	Size	Unit	Cost ($)	Year	Reference	FM	FT	FP	Scaling factor	Real size	Unit	Actual estimated equipment Cost ($)
Product powder dryer	800.00	kg/hr	6 500	2019	Alibaba	1	1	1	0.6	213.88	kg/hr	2 946
Forced Circulation Evaporator	5.00	m^2	200 004	2001	R. Turton, 2012	1.8	1	1,1	0.54	0.71	m^2	210 784
Shell and tube heat exchanger	0.46	m^2	4 600	2014	Matches	1.8	1	1	0.6	0.62	m^2	10 302
LIBs feed storage tank	24.07	m^3	20 986	2001	R. Turton, 2012	1.8	1	1	0.55	24.07	m^3	57 673
Citric acid hopper	58.99	m^3	42 496	2001	R. Turton, 2012	1.8	1	1	0.55	58.99	m^3	116 787
Ammonium Oxalate Hopper	22.59	m^3	20 022	2001	R. Turton, 2012	1.8	1	1	0.55	22.59	m^3	55 024
DMG Hopper	0.45	m^3	2 270	2001	R. Turton, 2012	1.8	1	1	0.55	0.45	m^3	6 240
NaOH Hopper	34.58	m^3	27 660	2001	R. Turton, 2012	1.8	1	1	0.55	34.58	m^3	76 014
Oxalic acid Hopper	0.04	m^3	1 200	2019	R. Turton, 2012	1.8	1	1	0.55	0.04	m^3	3 298
Na_2CO_3 Hopper	0.59	m^3	2 511	2001	R. Turton, 2012	1.8	1	1	0.55	0.59	m^3	6 900
Na_3PO_4 hopper	9.85	m^3	11 190	2019	R. Turton, 2012	1.8	1	1	0.55	9.85	m^3	30 753
NaCl Hopper	5.98	m^3	8 139	2019	R. Turton, 2012	1.8	1	1	0.55	5.98	m^3	22 369
D2EHPA storage tank	5.06	m^3	7 349	2001	R. Turton, 2012	1.8	1	1	0.55	5.06	m^3	20 196
Kerosene storage tank	21.24	m^3	19 131	2019	R. Turton, 2012	1.8	1	1	0.55	21.24	m^3	52 576
Fresh 33 wt% HCl storage tank	11.49	m^3	12 410	2001	R. Turton, 2012	1.8	1	1	0.55	11.49	m^3	34 105
Sulfuric acid Storage Tank	28.67	m^3	23 943	2001	R. Turton, 2012	1.8	1	1	0.55	28.67	m^3	65 800
Hydrogen peroxide Storage Tank	79.38	m^3	54 578	2001	R. Turton, 2012	1.8	1	1	0.55	79.38	m^3	149 991
Mn product prior to drying	0.62	m^3	2 569	2001	R. Turton, 2012	1.8	1	1	0.55	0.62	m^3	7 061
Ni product prior to drying	0.30	m^3	1 963	2001	R. Turton, 2012	1.8	1	1	0.55	0.30	m^3	5 394
Co product prior to drying	1.93	m^3	4 309	2001	R. Turton, 2012	1.8	1	1	0.55	1.93	m^3	11 842
Li product prior to drying	1.05	m^3	3 216	2001	R. Turton, 2012	1.8	1	1	0.55	1.05	m^3	8 838
Battery waste tank	12.80	m^3	13 352	2001	R. Turton, 2012	1.8	1	1	0.55	12.80	m^3	36 694
Leach Residue Storage Tank	6.55	m^3	8 614	2001	R. Turton, 2012	1.8	1	1	0.55	6.55	m^3	23 674
DMG Purge Collection Tank	0.49	m^3	2 341	2001	R. Turton, 2012	1.8	1	1	0.55	0.49	m^3	6 434
Final Solution Purge Collection Tank	215.63	m^3	134 581	2001	R. Turton, 2012	1.8	1	1	0.55	215.63	m^3	369 855
Mn-Product storage tank	2.51	m^3	4 941	2001	R. Turton, 2012	1.8	1	1	0.55	2.51	m^3	13 578

Process Unit/ Equipment piece	Size	Unit	Cost ($)	Year	Reference	FM	FT	FP	Scaling factor	Real size	Unit	Actual estimated equipment Cost ($)
Ni-Product storage tank	1.21	m^3	3 429	2001	R. Turton, 2012	1.8	1	1	0.55	1.21	m^3	9 425
Co-Product storage tank	7.41	m^3	9 304	2001	R. Turton, 2012	1.8	1	1	0.55	7.41	m^3	25 568
Li-Product storage tank	4.26	m^3	6 645	2001	R. Turton, 2012	1.8	1	1	0.55	4.26	m^3	18 263
Extraction: Mixer	0.11	m^3	16 800	2015	Arroyo *et al.* (2015)	1	1	1	0.6	0.91	m^3	63 558
Extraction: Settler	0.23	m^3	5 600	2015	Arroyo *et al.* (2015)	1	1	1	0.6	2.74	m^3	26 669
Scrubbing: Mixer	0.02	m^3	8 711	2015	Arroyo *et al.* (2015)	1	1	1	0.6	1.20	m^3	101 039
Scrubbing: Settler	0.01	m^3	3 733	2015	Arroyo *et al.* (2015)	1	1	1	0.6	3.61	m^3	149 636
Stripping: Mixer	0.02	m^3	8 711	2015	Arroyo *et al.* (2015)	1	1	1	0.6	0.60	m^3	66 896
Stripping: Settler	0.01	m^3	3 733	2015	Arroyo *et al.* (2015)	1	1	1	0.6	1.81	m^3	99 071
Total Purchased Equipment Cost												**5 450 016**

Table 87: Breakdown of purchased equipment cost of OA-3

Process Unit/ Equipment piece	Base Case costs (Cp0)					FM	FT	FP	Scaling factor	Real size	Unit	Actual estimated equipment Cost ($)
	Size	Unit	Cost (US $)	Year	Reference							
Retsch cutting mill	-	-	-	-	Retsch, 2019	-	-	-	-	-	-	37 514
12 mm screen	0.09	m^2	1 315	2018	Alibaba	1	1	1	0.6	0.09	m^2	1 315
2 mm screen	0.09	m^2	1 315	2018	Alibaba	1	1	1	0.6	0.09	m^2	1 315
Discharging tank	1.00	m^3	3 139	2001	R. Turton, 2012	1.8	1	1	0.55	1.00	m^3	8 628
Ultrasonic washing tank	0.11	m^3	2 100	2018	Alibaba	1	1	1	0.55	0.11	m^3	1 607
Ultrasonic washing tank agitator	0.76	kW	5 846	2001	R. Turton, 2012	1.8	1	1	0.5	0.76	kW	16 067
Citric acid leaching tank	3.33	m^3	5 772	2001	R. Turton, 2012	1.8	1	1	0.55	3.33	m^3	15 863
Leaching tank agitator	5.58	kW	23 676	2001	R. Turton, 2012	1.8	1	1	0.5	5.58	kW	65 065
pH Adjustment (pH=13) tank	2.98	m^3	5 422	2001	R. Turton, 2012	1.8	1	1	0.55	2.98	m^3	29 804
pH Adjustment (pH=13) agitator	3.78	kW	18 019	2001	R. Turton, 2012	1.8	1	1	0.5	3.78	kW	99 042
Mixed product precipitation tank	6.68	m^3	8 716	2001	R. Turton, 2012	1.8	1	1	0.55	6.68	m^3	23 953
Mixed product precipitation agitator	7.75	kW	29 795	2001	R. Turton, 2012	1.8	1	1	0.5	7.75	kW	81 883
Li precipitation tank	1.80	m^3	4 163	2001	R. Turton, 2012	1.8	1	1	0.55	1.80	m^3	11 441
Li precipitation agitator	4.59	kW	20 643	2001	R. Turton, 2012	1.8	1	1	0.5	4.59	kW	56 730
NaOH solution make-up tank	0.39	m^3	2 153	2001	R. Turton, 2012	1.8	1	1	0.55	0.39	m^3	5 916
NaOH solution make-up tank agitator	1.06	kW	7 385	2001	R. Turton, 2012	1.8	1	1	0.5	1.06	kW	20 294
NaCl make-up tank	0.17	m^3	1 636	2001	R. Turton, 2012	1.8	1	1	0.55	0.17	m^3	4 496
NaCl make-up tank agitator	0.82	kW	6 181	2001	R. Turton, 2012	1.8	1	1	0.5	0.82	kW	16 986
Filter press 1	29.22	m^2	88 091	2001	R. Turton, 2012	1.8	1	1	0.6	29.22	m^2	242 091
Filter press 2	48.70	m^2	118 285	2001	R. Turton, 2012	1.8	1	1	0.6	48.70	m^2	325 072
Filter press 3	53.30	m^2	124 818	2001	R. Turton, 2012	1.8	1	1	0.6	53.30	m^2	343 024
Filter press 4	37.72	m^2	101 872	2001	R. Turton, 2012	1.8	1	1	0.6	37.72	m^2	279 965
Dryer after discharging	800.00	kg/hr	6 500	2019	Alibaba	1	1	1	0.6	107.70	kg/hr	1 952
Continuous dryer (LIBs feed)	800.00	kg/hr	6 500	2019	Alibaba	1	1	1	0.6	82.92	kg/hr	1 668
Product powder dryer	800.00	kg/hr	6 500	2019	Alibaba	1	1	1	0.6	360.35	kg/hr	4 028
Forced circulation evaporator	5.00	m^2	200 004	2001	R. Turton, 2012	1.8	1	1,1	0.54	0.67	m^2	205 222

Process Unit/ Equipment piece	Size	Unit	Cost ($)	Year	Reference	FM	FT	FP	Scaling factor	Real size	Unit	Actual estimated equipment Cost ($)
LIBs feed storage tank	24.07	m^3	20 986	2001	R. Turton, 2012	1.8	1	1	0.55	24.07	m^3	57 673
Citric acid hopper	58.99	m^3	42 496	2001	R. Turton, 2012	1.8	1	1	0.55	58.99	m^3	116 787
NaCl Hopper	5.98	m^3	8 139	2001	R. Turton, 2012	1.8	1	1	0.55	5.98	m^3	22 369
NaH2PO4 Hopper	77.63	m^3	53 545	2001	R. Turton, 2012	1.8	1	1	0.55	77.63	m^3	147 153
NaOH Hopper	47.24	m^3	35 432	2001	R. Turton, 2012	1.8	1	1	0.55	47.24	m^3	97 373
Hydrogen Peroxide Storage Tank	79.38	m^3	54 578	2001	R. Turton, 2012	1.8	1	1	0.55	79.38	m^3	149 991
Mixed product prior to drying	2.40	m^3	4 827	2001	R. Turton, 2012	1.8	1	1	0.55	2.40	m^3	13 266
Li product prior to drying	0.87	m^3	2 951	2001	R. Turton, 2012	1.8	1	1	0.55	0.87	m^3	8 111
Battery waste tank	12.80	m^3	13 352	2001	R. Turton, 2012	1.8	1	1	0.55	12.80	m^3	36 694
Leach residue storage tank	6.55	m^3	8 614	2001	R. Turton, 2012	1.8	1	1	0.55	6.55	m^3	23 674
Final solution purge collection tank	37.80	m^3	29 660	2001	R. Turton, 2012	1.8	1	1	0.55	37.80	m^3	81 511
Co, Ni, Mn Product container	9.58	m^3	10 990	2001	R. Turton, 2012	1.8	1	1	0.55	9.58	m^3	30 203
Li-product container	3.56	m^3	5 993	2001	R. Turton, 2012	1.8	1	1	0.55	3.56	m^3	16 470
Total purchased equipment cost												**2 702 215**

Table 88: Summary of purchased equipment cost (US $) of 6 process alternatives

Equipment/ Unit Operation	**Mineral Acid Process Options**			**Organic Acid Process Options**		
	MA-1	**MA-2**	**MA-3**	**OA-1**	**OA-2**	**OA-3**
Crushing and Screening	40 144	40 144	40 144	40 144	40 144	40 144
Agitated Tanks	1 020 401	983 411	448 268	726 995	1 018 205	457 776
Filter presses	3 090 911	3 074 256	1 777 685	2 376 932	2 422 796	1 190 152
Dryers, Evaporators, Heat Exchangers and Crystallizers	910 902	475 764	399 870	242 695	227 651	212 870
Storage Tanks and Hoppers	648 866	1 347 613	604 575	560 378	730 860	612 721
Waste Containers	240 604	355 198	193 895	141 652	436 657	141 880
Product Containers	63 161	61 194	52 054	73 453	66 833	46 673
HCl Production	658 604	0	0	0	0	0
Solvent Extraction	0	0	0	0	506 870	0
Total Purchased Equipment Cost	6 673 592	6 337 580	3 516 491	4 162 250	5 450 016	2 702 215

Table 89: Capital Expenditure (CAPEX) of 6 evaluated process options

CAPEX (US $)	Mineral Acid Process Options			Organic Acid Process Options		
	MA-1	MA-2	MA-3	OA-1	OA-2	OA-3
Direct Costs	40 997 470	21 266 101	11 799 782	13 966 663	18 287 832	9 067 433
Delivered Equipment Cost	7 415 103	7 041 755	3 907 213	4 624 723	6 055 573	3 002 461
Equipment Installation	2 891 890	2 746 285	1 523 813	1 803 642	2 361 674	1 170 960
Instrumentation and controls	1 927 927	1 830 856	1 015 875	1 202 428	1 574 449	780 640
Piping (Installed)	2 298 682	2 182 944	1 211 236	1 433 664	1 877 228	930 763
Electrical Systems (Installed)	741 510	704 176	390 721	462 472	605 557	300 246
Membrane Cells	9 491 766	0	0	0	0	0
Buildings	4 902 992	2 042 109	1 133 092	1 341 170	1 756 116	870 714
Yard Improvements	2 028 824	845 011	468 866	554 967	726 669	360 295
Service Facilities	9 298 778	3 872 966	2 148 967	2 543 598	3 330 565	1 651 354
Indirect Costs	21 302 654	8 872 612	4 923 088	5 827 151	7 630 022	3 783 101
Engineering and supervision	5 410 198	2 253 362	1 250 308	1 479 911	1 937 783	960 788
Construction and Expenses	5 748 335	2 394 197	1 328 452	1 572 406	2 058 895	1 020 837
Legal Expenses	676 275	281 670	156 289	184 989	242 223	120 098
Contractor's fee	3 212 305	1 337 934	742 370	878 697	1 150 559	570 468
Contingency	6 255 541	2 605 450	1 445 669	1 711 147	2 240 562	1 110 911
Fixed Capital Investment (FCI)	62 300 124	30 138 713	16 722 870	19 793 813	25 917 854	12 850 534
Working Capital	9 345 019	4 520 807	2 508 431	2 969 072	3 887 678	1 927 580
Total Capital Investment	71 645 143	34 659 520	19 231 301	22 762 885	29 805 532	14 778 114
CAPEX/kg LIB treated	4.59	2.22	1.23	1.46	1.91	0.95

Appendix E – Operating Costs

Refer to Chapter 4 (section 4.3) for the assumptions made regarding specific operating expenses.

Table 90: Breakdown of waste treatment costs

Mineral Acid Process Option 1				
Waste Stream	**Flowrate (kg/hr)**	**Phase**	**Cost ($/ton or $/m^3)**	**Cost ($/yr)**
Battery waste	53.1	Solid	1203	514 752
Leach residue	14.5	Solid	1203	140 828
Impurities/Metal hydroxides	6.9	Solid	1203	66 432
DMG purge stream	0.9	Solid	1203	8 268
Final leach solution	41.9	Liquid	6.96	2 055
Waste water	2303.8	Liquid	6.96	129 964
Carbon dioxide gas emissions	7.1	Gas	889	50 911
TOTAL				**913 211**
Mineral Acid Process Option 2				
Waste Stream	**Flowrate (kg/hr)**	**Phase**	**Cost ($/ton or $/ m^3)**	**Cost ($/yr)**
Battery waste	53.1	Solid	1203	514 752
Leach residue	14.2	Solid	1203	137 780
Impurities/Metal hydroxides	7.0	Solid	1203	67 699
DMG purge stream	0.9	Solid	1203	8 289
Final leach solution	18.4	Liquid	6.85	886
Waste water	2389.2	Liquid	6.85	133 578
Carbon dioxide gas emissions	13.0	Gas	889	93 374
TOTAL				**956 358**
Mineral Acid Process Option 2				
Waste Stream	**Flowrate (kg/hr)**	**Phase**	**Cost ($/ton or $/ m^3)**	**Cost ($/yr)**
Battery waste	53.1	Solid	1203	514 752
Leach residue	14.2	Solid	1203	137 900
Impurities/Metal hydroxides	6.5	Solid	1203	63 289
Waste water	1124.9	Liquid	4.73	43 099
TOTAL				**759 040**
Organic Acid Process Option 1				
Waste Stream	**Flowrate (kg/hr)**	**Phase**	**Cost ($/ton or $/ m^3)**	**Cost ($/yr)**
Battery waste	53.1	Solid	1203	514 752
Leach residue	18.4	Solid	1203	178 297
DMG purge stream	0.8	Solid	1203	8 029
Final leach solution	1267.4	Liquid	8.94	91 545
Carbon dioxide gas emissions	6.4	Gas	889	45 483
TOTAL				**838 106**

Table 90 continued

Organic Acid Process Option 2				
Waste Stream	**Flowrate (kg/hr)**	**Phase**	**Cost ($/ton or $/ m³)**	**Cost ($/yr)**
Battery waste	53.1	Solid	1203	514 752
Leach residue	18.4	Solid	1203	178 297
DMG purge stream	0.8	Solid	1203	8 035
Oxalic acid purge stream	103.0	Liquid	4.18	3 484
Leach solution after Mn precipitation	6667.1	Liquid	4.18	225 445
Final leach solution	1292.0	Liquid	4.18	43 687
TOTAL				**973 700**
Organic Acid Process Option 3				
Waste Stream	**Flowrate (kg/hr)**	**Phase**	**Cost ($/ton or $/ m³)**	**Cost ($/yr)**
Battery waste	53.1	Solid	1203	514 752
Leach residue	18.4	Solid	1203	178 297
Final leach solution	1413.3	Liquid	8.49	96 958
TOTAL				**790 007**

Table 91: Breakdown of utility costs of organic acid processes

Electricity						
Process Option	**OA-1**		**OA-2**		**OA-3**	
Equipment	**kWh/yr**	**Cost ($/yr)**	**kWh/yr**	**Cost ($/yr)**	**kWh/yr**	**Cost ($/yr)**
Cutting Mill	24 178	1 860	24 178	1 860	24 178	1 860
Ultrasonic washing	15 561	1 197	15 561	1 197	15 561	1 197
Agitation	334 823	26 272	455 886	38 935	233 140	17 939
Filter presses	52 856	4 067	50 818	3 910	56 407	4 340
Drying	33 672	2 591	32 979	2 538	37 715	2 902
Equipment Electricity Consumption	461 089	35 988	579 421	48 440	367 001	28 239
General Plant electricity	51 964	3 999	69 945	5 382	40 775	3 138
Total electricity	519 640	**39 986**	699 448	**53 822**	407 753	**31 377**
Steam and Cooling Water						
Process Option	**OA-1**		**OA-2**		**OA-3**	
Steam	**kg/hr**	**Cost ($/yr)**	**kg/hr**	**Cost ($/yr)**	**kg/hr**	**Cost ($/yr)**
Citric acid leaching	580	94 545	583	95 027	716	116 701
Evaporation	1 544	251 592	1 408	229 446	1 239	201 932
Li precipitation	148	24 113	133	21 757	75	12 173
Combined phosphate precipitation	0	0	0	0	450	73 272
Total steam requirement	2 272	**370 250**	2 124	**346 230**	2 479	**404 078**
Cooling water	2 156	**437 444**	0	**0**	0	**0**
Total Utilities ($/yr)	**847 680**		**400 053**		**435 455**	

Table 92: Breakdown of utility costs of mineral acid processes

Electricity						
Process Option	**MA-1**		**MA-2**		**MA-3**	
Equipment	**kWh/yr**	**Cost ($/yr)**	**kWh/yr**	**Cost ($/yr)**	**kWh/yr**	**Cost ($/yr)**
Cutting Mill	24 178	1 860	24 178	1 860	24 178	1 860
Ultrasonic washing	15 561	1 197	15 561	1 197	15 561	1 197
Agitation	538 740	41 453	453 082	34 862	238 965	18 387
Filter presses	365 162	28 097	511 152	39 331	294 040	22 625
Drying	39 885	3 069	30 679	2 361	52 998	4 078
Membrane Cell	12 619 035	970 975	0	0	0	0
Equipment Electricity Consumption	13 602 560	1 046 652	1 034 651	79 611	625 741	48 148
General Plant electricity	1 511 302	116 295	114 954	8 846	69 522	5 350
Total electricity	15 113 022	**1 162 947**	1 149 541	**88 457**	695 225	**53 498**
Steam and Cooling Water						
Process Option	**MA-1**		**MA-2**		**MA-3**	
Steam	**kg/hr**	**Cost ($/yr)**	**kg/hr**	**Cost ($/yr)**	**kg/hr**	**Cost ($/yr)**
HCl leaching tank	316	51 526	0	0	73	11 866
Mn Precipitation	0	0	38	6 262		
Evaporation	4 843	789 368	3 453	562 740	2 527	411 821
Na_2CO_3 make-up tank	0	0	108	17 682	49	7 927
Li precipitation	21	3 400	30	4 930	31	5 058
Total steam requirement	5 180	**844 294**	3 630	**591 614**	2 679	**436 673**
Cooling water	64 344	**578 844**	0	**0**	0	**0**
Total Utilities ($/yr)	**2 586 085**		**680 071**		**490 171**	

Table 93: Breakdown of raw material costs (US $)

Raw Materials	Mineral Acid Process Options			Organic Acid Process Options			
	MA-1	MA-2	MA-3	OA-1	OA-2	OA-3	OA-3: Na_3PO_4 as precipitant
LIB waste	169 250	169 250	169 250	169 250	169 250	169 250	169 250
Water	19 272	1 705	1 705	9 818	85 962	8 417	9 197
Potassium permanganate	668 365	668 432	0	747 402	0	0	0
28% Ammonia	986 636	986 876	0	0	0	0	0
Dimethylglyoxime (DMG)	230 823	230 835	0	228 399	228 559	0	0
Sodium Hydroxide	180 198	2 784 786	1 797 595	594 053	808 162	1 104 121	478 577
Hydrochloric Acid	459 548	3 609 649	1 799 086	53 418	53 435	0	0
Sodium Carbonate	52 979	66 937	25 643	0	2 685	0	0
Hydrogen	183 329	0	0	0	0	0	0
Sodium Chloride	12 413	12 413	0	12 413	12 413	12 413	12 413
Manganese Chloride	0	0	149 837	0	0	0	0
Nickel Chloride	0	0	554 908	0	0	0	0
Oxalic acid	0	0	0	121 817	546	0	0
Citric acid	0	0	0	1 519 280	1 519 280	1 519 280	1 519 280
Phosphoric acid	0	0	0	87 659	0	0	0
Hydrogen Peroxide	0	0	0	587 487	587 487	587 487	587 487
Ammonium oxalate	0	0	0	0	354 378	0	0
D2EHPA	0	0	0	0	228 584	0	0
Kerosene	0	0	0	0	49 518	0	0
Sodium phosphate	0	0	0	0	59 938	0	697 240
Sulfuric Acid	0	0	0	0	145 427	0	0
Mono-sodium phosphate	0	0	0	0	0	1 879 836	0
Total raw material cost	**2 962 814**	**8 530 883**	**4 498 025**	**4 130 995**	**4 305 625**	**5 280 804**	**3 473 445**

Table 94: Breakdown of operating expenditure (US $/annum)

Cost Component	Cost factor	Mineral Acid Process Options			Organic Acid Process Options			
		MA-1	MA-2	MA-3	OA-1	OA-2	OA-3	OA-3: Na_3PO_4 as precipitant
Direct Operating Costs (US $/annum)		14 706 003	15 245 225	9 347 128	9 944 183	10 860 568	9 128 833	7 279 428
Raw Materials	1 CRM	2 962 814	8 530 883	4 498 025	4 130 995	4 305 625	5 280 804	3 473 445
Waste treatment	1 CWT	913 211	956 358	759 040	838 106	973 700	790 007	787 083
Utilities	1CUT	2 586 085	680 071	490 171	847 680	400 053	435 455	410 982
Operating labour	1 COL	2 966 304	2 254 391	1 839 109	2 076 413	2 551 021	1 305 174	1 305 174
Direct Supervisory and Labour	0.18 COL	533 935	405 790	331 040	373 754	459 184	234 931	234 931
Maintenance and Repairs	0.06 FCI	3 738 007	1 808 323	1 003 372	1 187 629	1 555 071	771 032	758 293
Operating Supplies	0.009 FCI	560 701	271 248	150 506	178 144	233 261	115 655	113 744
Laboratory Charges	0.15 COL	444 946	338 159	275 866	311 462	382 653	195 776	195 776
Fixed Operating Costs (US $/annum)		11 943 563	6 358 026	3 944 302	4 597 523	5 901 144	2 954 447	2 920 902
Depreciation	Apart	5 607 011	2 712 484	1 505 058	1 781 443	2 332 607	1 156 548	1 137 440
Local Taxes and Insurance	0.032 FCI	1 993 604	964 439	535 132	633 402	829 371	411 217	404 423
Plant Overhead Costs	0.708 COL+ 0.036 FCI	4 342 948	2 681 103	1 904 112	2 182 678	2 739 166	1 386 682	1 379 039
General Operating Expenses (US $/annum)		4 513 696	3 423 183	2 177 624	2 410 401	2 841 101	1 882 957	1 648 085
Administration Costs	0.177 COL + 0.009 FCI	1 085 737	670 276	476 028	545 669	684 791	346 671	344 760
Distribution and Selling Costs	0.11 CTOC	3 427 959	2 752 908	1 701 596	1 864 732	2 156 309	1 536 286	1 303 326
Total Operating Cost (TOC) (US $/annum)		**31 163 262**	**25 026 433**	**15 469 054**	**16 952 107**	**19 602 813**	**13 966 237**	**11 848 414**

Appendix F – Profitability Analysis

Table 95: Metal recovery, product purity and annual income

Mineral Acid Process Options						
Option 1 - Membrane electrolysis	**Products**		**Metal recovery**	**Purity**	**Production (ton/yr)**	**Income ($/yr)**
	Mn	MnO_2	66.1%	98.8%	174.2	7 334 724
	Ni	$Ni(OH)_2$	89.2%	90.2%	54.6	1 947 651
	Co	$Co(OH)_2$	89.8%	98.3%	144.8	7 170 861
	Li	Li_2CO_3	82.5%	99.4%	101.5	1 691 210
						18 144 447
Option 2 - Without membrane electrolysis	**Products**		**Metal recovery**	**Purity**	**Production (ton/yr)**	**Income ($/yr)**
	Mn	MnO_2	65.5%	98.6%	173.2	7 278 670
	Ni	$Ni(OH)_2$	89.2%	89.6%	55.0	1 947 745
	Co	$Co(OH)_2$	89.9%	97.8%	145.4	7 846 674
	Li	Li_2CO_3	67.7%	97.2%	85.2	1 386 872
						18 459 960
Option 3 - Mixed Product	**Products**		**Metal recovery**	**Purity**	**Production (ton/yr)**	**Income ($/yr)**
	Mixed Mn, Co, Ni	$Mn(OH)_2$, $Ni(OH)_2$, $Co(OH)_2$	-	96.0%	438.4	18 366 627
	Li	Li_2CO_3	63.7%	97.1%	80.3	1 305 845
	NaCl	NaCl	-	98.4%	5220.7	490 109
						20 162 581
Organic Acid Process Options						
Option 1 - Mn Precipitation	**Products**		**Metal recovery**	**Purity**	**Production (ton/yr)**	**Income ($/yr)**
	Mn	MnO_2	89.6%	99.3%	251.9	10 659 286
	Ni	$Ni(OH)_2$	88.6%	98.9%	49.5	1 934 096
	Co	CoC_2O_4	88.5%	97.8%	226.4	11 211 358
	Li	Li_3PO_4	83.9%	97.9%	109.5	1 646 291
						25 451 031
Option 2 - Mn Solvent Extraction	**Products**		**Metal recovery**	**Purity**	**Production (ton/yr)**	**Income ($/yr)**
	Mn	$Mn(OH)_2$	80.4%	99.9%	82.4	3 427 475
	Ni	$Ni(OH)_2$	88.7%	98.7%	49.6	1 935 451
	Co	CoC_2O_4	88.5%	96.4%	229.8	11 214 719
	Li	Li_3PO_4	79.4%	97.7%	103.9	1 558 520
						18 136 166
Option 3 - Mixed Product	**Products**		**Metal recovery**	**Purity**	**Production (ton/yr)**	**Income ($/yr)**
	Mixed Mn, Co, Ni	Mixed phosphate	-	95.7%	386.0	14 528 299
	Li	Li_3PO_4	62.6%	86.9%	92.0	1 227 531
						15 755 830

Table 96: Profitability analysis of mineral acid process option 1

End of year	Investment	Depreciation	Book Value	Yearly Revenue	Cost of Manufacturing	Profit before tax	After Tax Cash flow	Non-discounted Cash Flow	Discounted cash flow (NPV)	Cumulative NPV
k	FCI	d_k	FCI-d_k	R	COM_d	R-COM_d-d_k				
0	0	0	0	0	0	0	0	0	0	0
1	-31 150 062	0	31 150 062	0	0	0	0	-31 150 062	-27 087 011	-27 087 011
2	-40 495 081	0	62 300 124	0	0	0	0	-40 495 081	-30 620 099	-57 707 110
3	0	5 607 011	56 693 113	15 422 780	25 556 251	-15 740 482	-10 133 470	-10 133 470	-6 662 921	-64 370 031
4	0	5 607 011	51 086 102	18 144 447	25 556 251	-13 018 815	-7 411 803	-7 411 803	-4 237 723	-68 607 754
5	0	5 607 011	45 479 091	18 144 447	25 556 251	-13 018 815	-7 411 803	-7 411 803	-3 684 976	-72 292 730
6	0	5 607 011	39 872 080	18 144 447	25 556 251	-13 018 815	-7 411 803	-7 411 803	-3 204 327	-75 497 057
7	0	5 607 011	34 265 068	18 144 447	25 556 251	-13 018 815	-7 411 803	-7 411 803	-2 786 371	-78 283 428
8	0	5 607 011	28 658 057	18 144 447	25 556 251	-13 018 815	-7 411 803	-7 411 803	-2 422 932	-80 706 360
9	0	5 607 011	23 051 046	18 144 447	25 556 251	-13 018 815	-7 411 803	-7 411 803	-2 106 897	-82 813 257
10	0	5 607 011	17 444 035	18 144 447	25 556 251	-13 018 815	-7 411 803	-7 411 803	-1 832 084	-84 645 341
11	0	5 607 011	11 837 024	18 144 447	25 556 251	-13 018 815	-7 411 803	-7 411 803	-1 593 117	-86 238 458
12	0	5 607 011	6 230 012	18 144 447	25 556 251	-13 018 815	-7 411 803	-7 411 803	-1 385 319	-87 623 777
13	0	5 607 011	623 001	18 144 447	25 556 251	-13 018 815	-7 411 803	-7 411 803	-1 204 625	-88 828 403
14	0	623 001	0	18 144 447	25 556 251	-8 034 805	-7 411 803	-7 411 803	-1 047 500	-89 875 903
15	0	0	0	18 144 447	25 556 251	-7 411 803	-7 411 803	-7 411 803	-910 870	-90 786 773
16	0	0	0	18 144 447	25 556 251	-7 411 803	-7 411 803	-7 411 803	-792 061	-91 578 833
17	0	0	0	18 144 447	25 556 251	-7 411 803	-7 411 803	-7 411 803	-688 748	-92 267 582
18	0	0	0	18 144 447	25 556 251	-7 411 803	-7 411 803	-7 411 803	-598 912	-92 866 493
19	0	0	0	18 144 447	25 556 251	-7 411 803	-7 411 803	-7 411 803	-520 793	-93 387 286
20	15 575 031	0	0	18 144 447	25 556 251	-7 411 803	-7 411 803	8 163 228	498 775	**-92 888 511**

Table 97: Profitability analysis of mineral acid process option 2

End of year	Investment	Depreciation	Book Value	Yearly Revenue	Cost of Manufacturing	Profit before tax	After Tax Cash flow	Non-discounted Cash Flow	Discounted cash flow (NPV)	Cumulative NPV
k	FCI	d_k	FCI-d_k	R	COM_d	R-COM_d-d_k				
0	0	0	0	0	0	0	0	0	0	0
1	-15 069 357	0	15 069 357	0	0	0	0	-15 069 357	-13 103 788	-13 103 788
2	-19 590 164	0	30 138 713	0	0	0	0	-19 590 164	-14 812 978	-27 916 767
3	0	2 712 484	27 426 229	15 690 966	22 313 949	-9 335 467	-6 622 983	-6 622 983	-4 354 719	-32 271 485
4	0	2 712 484	24 713 745	18 459 960	22 313 949	-6 566 473	-3 853 989	-3 853 989	-2 203 531	-34 475 016
5	0	2 712 484	22 001 261	18 459 960	22 313 949	-6 566 473	-3 853 989	-3 853 989	-1 916 114	-36 391 130
6	0	2 712 484	19 288 777	18 459 960	22 313 949	-6 566 473	-3 853 989	-3 853 989	-1 666 186	-38 057 316
7	0	2 712 484	16 576 292	18 459 960	22 313 949	-6 566 473	-3 853 989	-3 853 989	-1 448 857	-39 506 173
8	0	2 712 484	13 863 808	18 459 960	22 313 949	-6 566 473	-3 853 989	-3 853 989	-1 259 876	-40 766 049
9	0	2 712 484	11 151 324	18 459 960	22 313 949	-6 566 473	-3 853 989	-3 853 989	-1 095 544	-41 861 593
10	0	2 712 484	8 438 840	18 459 960	22 313 949	-6 566 473	-3 853 989	-3 853 989	-952 647	-42 814 240
11	0	2 712 484	5 726 356	18 459 960	22 313 949	-6 566 473	-3 853 989	-3 853 989	-828 389	-43 642 629
12	0	2 712 484	3 013 871	18 459 960	22 313 949	-6 566 473	-3 853 989	-3 853 989	-720 338	-44 362 967
13	0	2 712 484	301 387	18 459 960	22 313 949	-6 566 473	-3 853 989	-3 853 989	-626 381	-44 989 348
14	0	301 387	0	18 459 960	22 313 949	-4 155 376	-3 853 989	-3 853 989	-544 679	-45 534 027
15	0	0	0	18 459 960	22 313 949	-3 853 989	-3 853 989	-3 853 989	-473 634	-46 007 661
16	0	0	0	18 459 960	22 313 949	-3 853 989	-3 853 989	-3 853 989	-411 856	-46 419 517
17	0	0	0	18 459 960	22 313 949	-3 853 989	-3 853 989	-3 853 989	-358 135	-46 777 652
18	0	0	0	18 459 960	22 313 949	-3 853 989	-3 853 989	-3 853 989	-311 422	-47 089 074
19	0	0	0	18 459 960	22 313 949	-3 853 989	-3 853 989	-3 853 989	-270 802	-47 359 876
20	7 534 678	0	0	18 459 960	22 313 949	-3 853 989	-3 853 989	3 680 689	224 891	**-47 134 985**

Table 98: Profitability analysis of mineral acid process option 3

End of year	Investment	Depreciation	Book Value	Yearly Revenue	Cost of Manufacturing	Profit before tax	After Tax Cash flow	Non-discounted Cash Flow	Discounted cash flow (NPV)	Cumulative NPV
k	FCI	d_k	FCI-d_k	R	COM_d	R-COM_d-d_k				
0	0	0	0	0	0	0	0	0	0	0
1	-8 361 435	0	8 361 435	0	0	0	0	-8 361 435	-7 270 813	-7 270 813
2	-10 869 866	0	16 722 870	0	0	0	0	-10 869 866	-8 219 180	-15 489 993
3	0	1 505 058	15 217 812	17 138 194	13 963 996	1 669 140	2 706 839	2 706 839	1 779 791	-13 710 203
4	0	1 505 058	13 712 754	20 162 581	13 963 996	4 693 527	4 884 398	4 884 398	2 792 670	-10 917 532
5	0	1 505 058	12 207 695	20 162 581	13 963 996	4 693 527	4 884 398	4 884 398	2 428 409	-8 489 123
6	0	1 505 058	10 702 637	20 162 581	13 963 996	4 693 527	4 884 398	4 884 398	2 111 660	-6 377 464
7	0	1 505 058	9 197 579	20 162 581	13 963 996	4 693 527	4 884 398	4 884 398	1 836 226	-4 541 238
8	0	1 505 058	7 692 520	20 162 581	13 963 996	4 693 527	4 884 398	4 884 398	1 596 718	-2 944 519
9	0	1 505 058	6 187 462	20 162 581	13 963 996	4 693 527	4 884 398	4 884 398	1 388 451	-1 556 069
10	0	1 505 058	4 682 404	20 162 581	13 963 996	4 693 527	4 884 398	4 884 398	1 207 348	-348 720
11	0	1 505 058	3 177 345	20 162 581	13 963 996	4 693 527	4 884 398	4 884 398	1 049 868	701 148
12	0	1 505 058	1 672 287	20 162 581	13 963 996	4 693 527	4 884 398	4 884 398	912 929	1 614 077
13	0	1 505 058	167 229	20 162 581	13 963 996	4 693 527	4 884 398	4 884 398	793 851	2 407 928
14	0	167 229	0	20 162 581	13 963 996	6 031 357	4 509 805	4 509 805	637 365	3 045 293
15	0	0	0	20 162 581	13 963 996	6 198 585	4 462 981	4 462 981	548 476	3 593 769
16	0	0	0	20 162 581	13 963 996	6 198 585	4 462 981	4 462 981	476 935	4 070 704
17	0	0	0	20 162 581	13 963 996	6 198 585	4 462 981	4 462 981	414 726	4 485 430
18	0	0	0	20 162 581	13 963 996	6 198 585	4 462 981	4 462 981	360 632	4 846 062
19	0	0	0	20 162 581	13 963 996	6 198 585	4 462 981	4 462 981	313 593	5 159 655
20	4 180 718	0	0	20 162 581	13 963 996	6 198 585	4 462 981	8 643 699	528 132	**5 687 787**

Table 99: Profitability analysis of organic acid process option 1

End of year	Investment	Depreciation	Book Value	Yearly Revenue	Cost of Manufacturing	Profit before tax	After Tax Cash flow	Non-discounted Cash Flow	Discounted cash flow (NPV)	Cumulative NPV
k	FCI	d_k	FCI-d_k	R	COM_d	R-COM_d-d_k				
0	0	0	0	0	0	0	0	0	0	0
1	-9 896 907	0	9 896 907	0	0	0	0	-9 896 907	-8 606 006	-8 606 006
2	-12 865 979	0	19 793 813	0	0	0	0	-12 865 979	-9 728 528	-18 334 534
3	0	1 781 443	18 012 370	21 633 377	15 170 664	4 681 269	5 151 957	5 151 957	3 387 495	-14 947 039
4	0	1 781 443	16 230 927	25 451 031	15 170 664	8 498 924	7 900 669	7 900 669	4 517 233	-10 429 806
5	0	1 781 443	14 449 484	25 451 031	15 170 664	8 498 924	7 900 669	7 900 669	3 928 029	-6 501 777
6	0	1 781 443	12 668 041	25 451 031	15 170 664	8 498 924	7 900 669	7 900 669	3 415 677	-3 086 100
7	0	1 781 443	10 886 597	25 451 031	15 170 664	8 498 924	7 900 669	7 900 669	2 970 154	-115 946
8	0	1 781 443	9 105 154	25 451 031	15 170 664	8 498 924	7 900 669	7 900 669	2 582 743	2 466 796
9	0	1 781 443	7 323 711	25 451 031	15 170 664	8 498 924	7 900 669	7 900 669	2 245 863	4 712 659
10	0	1 781 443	5 542 268	25 451 031	15 170 664	8 498 924	7 900 669	7 900 669	1 952 924	6 665 584
11	0	1 781 443	3 760 825	25 451 031	15 170 664	8 498 924	7 900 669	7 900 669	1 698 195	8 363 779
12	0	1 781 443	1 979 381	25 451 031	15 170 664	8 498 924	7 900 669	7 900 669	1 476 691	9 840 470
13	0	1 781 443	197 938	25 451 031	15 170 664	8 498 924	7 900 669	7 900 669	1 284 080	11 124 550
14	0	197 938	0	25 451 031	15 170 664	10 082 429	7 457 287	7 457 287	1 053 928	12 178 478
15	0	0	0	25 451 031	15 170 664	10 280 367	7 401 864	7 401 864	909 648	13 088 127
16	0	0	0	25 451 031	15 170 664	10 280 367	7 401 864	7 401 864	790 999	13 879 125
17	0	0	0	25 451 031	15 170 664	10 280 367	7 401 864	7 401 864	687 825	14 566 950
18	0	0	0	25 451 031	15 170 664	10 280 367	7 401 864	7 401 864	598 109	15 165 059
19	0	0	0	25 451 031	15 170 664	10 280 367	7 401 864	7 401 864	520 094	15 685 153
20	4 948 453	0	0	25 451 031	15 170 664	10 280 367	7 401 864	12 350 318	754 608	**16 439 761**

Table 100: Profitability analysis of organic acid process option 2

End of year	Investment	Depreciation	Book Value	Yearly Revenue	Cost of Manufacturing	Profit before tax	After Tax Cash flow	Non-discounted Cash Flow	Discounted cash flow (NPV)	Cumulative NPV
k	FCI	d_k	FCI-d_k	R	COM_d	R-COM_d-d_k				
0	0	0	0	0	0	0	0	0	0	0
1	-12 958 927	0	12 958 927	0	0	0	0	-12 958 927	-11 268 632	-11 268 632
2	-16 846 605	0	25 917 854	0	0	0	0	-16 846 605	-12 738 454	-24 007 086
3	0	2 332 607	23 585 247	15 415 741	17 270 207	-4 187 072	-1 854 465	-1 854 465	-1 219 341	-25 226 427
4	0	2 332 607	21 252 640	18 136 166	17 270 207	-1 466 647	865 960	865 960	495 115	-24 731 312
5	0	2 332 607	18 920 034	18 136 166	17 270 207	-1 466 647	865 960	865 960	430 535	-24 300 777
6	0	2 332 607	16 587 427	18 136 166	17 270 207	-1 466 647	865 960	865 960	374 378	-23 926 399
7	0	2 332 607	14 254 820	18 136 166	17 270 207	-1 466 647	865 960	865 960	325 546	-23 600 853
8	0	2 332 607	11 922 213	18 136 166	17 270 207	-1 466 647	865 960	865 960	283 084	-23 317 769
9	0	2 332 607	9 589 606	18 136 166	17 270 207	-1 466 647	865 960	865 960	246 160	-23 071 609
10	0	2 332 607	7 256 999	18 136 166	17 270 207	-1 466 647	865 960	865 960	214 052	-22 857 557
11	0	2 332 607	4 924 392	18 136 166	17 270 207	-1 466 647	865 960	865 960	186 132	-22 671 425
12	0	2 332 607	2 591 785	18 136 166	17 270 207	-1 466 647	865 960	865 960	161 854	-22 509 571
13	0	2 332 607	259 179	18 136 166	17 270 207	-1 466 647	865 960	865 960	140 743	-22 368 829
14	0	259 179	0	18 136 166	17 270 207	606 781	696 061	696 061	98 373	-22 270 455
15	0	0	0	18 136 166	17 270 207	865 960	623 491	623 491	76 624	-22 193 832
16	0	0	0	18 136 166	17 270 207	865 960	623 491	623 491	66 629	-22 127 202
17	0	0	0	18 136 166	17 270 207	865 960	623 491	623 491	57 938	-22 069 264
18	0	0	0	18 136 166	17 270 207	865 960	623 491	623 491	50 381	-22 018 883
19	0	0	0	18 136 166	17 270 207	865 960	623 491	623 491	43 810	-21 975 073
20	6 479 464	0	0	18 136 166	17 270 207	865 960	623 491	7 102 954	433 992	**-21 541 080**

Table 101: Profitability analysis of organic acid process option 3

End of year	Investment	Depreciation	Book Value	Yearly Revenue	Cost of Manufacturing	Profit before tax	After Tax Cash flow	Non-discounted Cash Flow	Discounted cash flow (NPV)	Cumulative NPV
k	FCI	d_k	FCI-d_k	R	COM_d	R-COM_d-d_k				
0	0	0	0	0	0	0	0	0	0	0
1	-6 425 267	0	6 425 267	0	0	0	0	-6 425 267	-5 587 188	-5 587 188
2	-8 352 847	0	12 850 534	0	0	0	0	-8 352 847	-6 315 952	-11 903 141
3	0	1 156 548	11 693 986	13 392 455	12 809 689	-573 782	582 766	582 766	383 178	-11 519 962
4	0	1 156 548	10 537 437	15 755 830	12 809 689	1 789 593	2 445 055	2 445 055	1 397 968	-10 121 994
5	0	1 156 548	9 380 889	15 755 830	12 809 689	1 789 593	2 445 055	2 445 055	1 215 624	-8 906 370
6	0	1 156 548	8 224 341	15 755 830	12 809 689	1 789 593	2 445 055	2 445 055	1 057 065	-7 849 305
7	0	1 156 548	7 067 793	15 755 830	12 809 689	1 789 593	2 445 055	2 445 055	919 187	-6 930 118
8	0	1 156 548	5 911 245	15 755 830	12 809 689	1 789 593	2 445 055	2 445 055	799 293	-6 130 826
9	0	1 156 548	4 754 697	15 755 830	12 809 689	1 789 593	2 445 055	2 445 055	695 037	-5 435 788
10	0	1 156 548	3 598 149	15 755 830	12 809 689	1 789 593	2 445 055	2 445 055	604 380	-4 831 408
11	0	1 156 548	2 441 601	15 755 830	12 809 689	1 789 593	2 445 055	2 445 055	525 548	-4 305 860
12	0	1 156 548	1 285 053	15 755 830	12 809 689	1 789 593	2 445 055	2 445 055	456 998	-3 848 862
13	0	1 156 548	128 505	15 755 830	12 809 689	1 789 593	2 445 055	2 445 055	397 390	-3 451 472
14	0	128 505	0	15 755 830	12 809 689	2 817 636	2 157 203	2 157 203	304 875	-3 146 598
15	0	0	0	15 755 830	12 809 689	2 946 141	2 121 221	2 121 221	260 686	-2 885 911
16	0	0	0	15 755 830	12 809 689	2 946 141	2 121 221	2 121 221	226 684	-2 659 227
17	0	0	0	15 755 830	12 809 689	2 946 141	2 121 221	2 121 221	197 116	-2 462 111
18	0	0	0	15 755 830	12 809 689	2 946 141	2 121 221	2 121 221	171 406	-2 290 705
19	0	0	0	15 755 830	12 809 689	2 946 141	2 121 221	2 121 221	149 048	-2 141 657
20	3 212 633	0	0	15 755 830	12 809 689	2 946 141	2 121 221	5 333 855	325 900	**-1 815 757**

Appendix G – Sensitivity Analysis

Effect of individual variables

Table 102: Sensitivity analysis to investigate the effect of the CAPEX on the NPV and PVR of OA-1

% Change in CAPEX	CAPEX	NPV	PVR
-60%	$9 105 154	$33 010 466	5.17
-40%	$13 657 731	$27 486 898	3.31
-20%	$18 210 308	$21 963 329	2.39
0	$22 762 885	$16 439 761	1.83
20%	$27 315 462	$10 916 192	1.46
40%	$31 868 040	$5 392 624	1.19
60%	$36 420 617	-$130 945	1.00
80%	$40 973 194	-$5 654 513	0.84
100%	$45 525 771	-$11 282 548	0.71

Table 103: Effect of salvage value, working capital and fixed capital investment on NPV of OA-1

Salvage Value		Working Capital		Fixed Capital Investment	
% Change in Salvage Value	NPV	% Change in Working Capital	NPV	% Change in Fixed Capital Investment	NPV
-60%	$16 398 128	-60%	$17 677 941	-60%	$31 813 919
-40%	$16 412 006	-40%	$17 265 214	-40%	$26 689 199
-20%	$16 425 883	-20%	$16 852 488	-20%	$21 564 480
0%	$16 439 761	0%	$16 439 761	0%	$16 439 761
20%	$16 453 638	20%	$16 027 034	20%	$11 315 041
40%	$16 467 516	40%	$15 614 307	40%	$6 190 322
60%	$16 481 393	60%	$15 201 580	60%	$1 065 603

Table 104: Effect of waste treatment costs, utility costs and the overall OPEX on NPV of OA-1

Waste Treatment		Utilities		OPEX		
% Change in Waste Treatment	NPV	% Change in Utilities	NPV	% Change in OPEX	NPV	PVR
-60%	$18 324 770	-60%	$18 346 302	-60%	$50 373 217	3.54
-40%	$17 696 433	-40%	$17 710 789	-40%	$39 062 065	2.97
-20%	$17 068 097	-20%	$17 075 275	-20%	$27 750 913	2.40
0%	$16 439 761	0%	$16 439 761	0%	$16 439 761	1.83
20%	$15 811 424	20%	$15 804 247	20%	$5 128 609	1.26
40%	$15 183 088	40%	$15 168 733	40%	-$6 569 084	0.67
60%	$14 554 752	60%	$14 533 219	60%	-$20 053 150	-0.01

Table 105: Effect of raw material and operating labour costs on the NPV and PVR of OA-1

Raw materials					Operating Labour				
% Change in Raw Materials	OPEX	Revenue	NPV	PVR	% Change in Operating Labour	OPEX	Revenue	NPV	PVR
-60%	$14 167 167	$25 451 031	$25 730 902	2.30	-60%	$13 851 486	$25 451 031	$26 784 078	2.35
-40%	$15 095 480	$25 451 031	$22 633 855	2.14	-40%	$14 885 027	$25 451 031	$23 335 972	2.18
-20%	$16 023 794	$25 451 031	$19 536 808	1.99	-20%	$15 918 567	$25 451 031	$19 887 867	2.00
0%	$16 952 107	$25 451 031	$16 439 761	1.83	0%	$16 952 107	$25 451 031	$16 439 761	1.83
20%	$17 880 421	$25 451 031	$13 342 714	1.67	20%	$17 985 648	$25 451 031	$12 991 655	1.66
40%	$18 808 734	$25 451 031	$10 245 667	1.52	40%	$19 019 188	$25 451 031	$9 543 549	1.48
60%	$19 737 048	$25 451 031	$7 148 619	1.36	60%	$20 052 728	$25 451 031	$6 095 444	1.31
80%	$20 665 361	$25 451 031	$4 051 572	1.20	80%	$21 086 268	$25 451 031	$2 647 338	1.13
100%	$21 593 675	$25 451 031	$954 525	1.05	100%	$22 119 809	$25 451 031	-$890 322	0.96

Table 106: Effect of LIB feed capacity on profitability of OA-1

% Change in Feed capacity	Feed Capacity (ton/yr)	CAPEX	OPEX	Revenue	NPV	PVR
-80%	174	15 958 743	10 608 914	5 090 206	-32 928 613	-1.37
-60%	347	17 862 989	12 248 985	10 180 413	-18 261 982	-0.18
-40%	521	19 587 126	13 840 672	15 270 619	-5 169 248	0.70
-20%	694	21 209 629	15 405 461	20 360 825	5 668 842	1.31
0%	868	22 762 885	16 952 107	25 451 031	16 439 761	1.83
20%	1042	24 264 439	18 485 304	30 541 238	27 278 505	2.29
40%	1215	25 725 236	20 007 957	35 631 444	38 170 525	2.71
60%	1389	27 152 722	21 522 029	40 721 650	49 105 962	3.08
80%	1562	28 552 276	23 028 929	45 811 856	60 077 726	3.42

Table 107: Effect of metal product selling prices and revenue on the NPV and PVR of OA-1

MnO_2 Selling Price				$Ni(OH)_2$ Selling Price			
% Change in Mn Price	Revenue	NPV	PVR	% Change in Ni Price	Revenue	NPV	PVR
-80%	16 923 602	-11 902 913	0.40	-80%	23 903 754	11 387 597	1.58
-60%	19 055 460	-4 582 031	0.77	-60%	24 290 573	12 650 638	1.64
-40%	21 187 317	2 517 895	1.13	-40%	24 677 393	13 913 679	1.70
-20%	23 319 174	9 478 828	1.48	-20%	25 064 212	15 176 720	1.77
0%	25 451 031	16 439 761	1.83	0%	25 451 031	16 439 761	1.83
20%	27 582 889	23 400 694	2.18	20%	25 837 851	17 702 802	1.89
40%	29 714 746	30 361 626	2.53	40%	26 224 670	18 965 843	1.96
60%	31 846 603	37 322 559	2.89	60%	26 611 489	20 228 884	2.02
80%	33 978 460	44 283 492	3.24	80%	26 998 308	21 491 924	2.09
$Co(OH)_2$ Selling Price				Li_3PO_4 Selling Price			
% Change in Co price	Revenue	NPV	PVR	% Change in Li price	Revenue	NPV	PVR
-80%	16 481 945	-13 822 207	0.30	-80%	24 133 999	12 139 390	1.61
-60%	18 724 217	-5 715 440	0.71	-60%	24 463 257	13 214 483	1.67
-40%	20 966 488	1 796 846	1.09	-40%	24 792 515	14 289 576	1.72
-20%	23 208 760	9 118 303	1.46	-20%	25 121 773	15 364 668	1.78
0%	25 451 031	16 439 761	1.83	0%	25 451 031	16 439 761	1.83
20%	27 693 303	23 761 218	2.20	20%	25 780 289	17 514 853	1.88
40%	29 935 574	31 082 675	2.57	40%	26 109 548	18 589 946	1.94
60%	32 177 846	38 404 133	2.94	60%	26 438 806	19 665 039	1.99
80%	34 420 118	45 725 590	3.31	80%	26 768 064	20 740 131	2.05
Total Revenue							
% Change in Total Revenue	Revenue	NPV	PVR				
-60%	10 180 413	-42 159 192	-1.13				
-40%	15 270 619	-19 090 101	0.04				
-20%	20 360 825	-180 763	0.99				
0%	25 451 031	16 439 761	1.83				
20%	30 541 238	33 060 284	2.67				
40%	35 631 444	49 680 808	3.51				
60%	40 721 650	66 301 332	4.35				

Table 108: Effect of cathode material feed distribution on the NPV of OA-1

$LiFePO_4$						
% Change LFP	**Wt% LCO**	**Wt% NMC**	**Wt% LMO**	**Wt% LNO**	**Wt% LFP**	**NPV**
-60%	38.4%	30.0%	22.1%	7.4%	**2.1%**	18 366 593
-40%	38.0%	29.6%	21.9%	7.4%	**3.1%**	17 724 278
-20%	37.6%	29.3%	21.6%	7.3%	**4.2%**	17 082 000
0%	37.2%	29.0%	21.4%	7.2%	**5.2%**	16 439 761
20%	36.8%	28.7%	21.2%	7.1%	**6.2%**	15 797 559
40%	36.4%	28.4%	20.9%	7.0%	**7.3%**	15 155 395
60%	36.0%	28.0%	20.7%	7.0%	**8.3%**	14 513 270

$LiMn_2O_4$						
% Change in LMO	**Wt% LCO**	**Wt% NMC**	**Wt% LMO**	**Wt% LNO**	**Wt% LFP**	**NPV**
-60%	43.3%	33.7%	**8.6%**	8.4%	6.0%	16 816 264
-40%	41.3%	32.2%	**12.8%**	8.0%	5.8%	16 689 492
-20%	39.2%	30.6%	**17.1%**	7.6%	5.5%	16 564 506
0%	37.2%	29.0%	**21.4%**	7.2%	5.2%	16 439 761
20%	35.2%	27.4%	**25.7%**	6.8%	4.9%	16 315 137
40%	33.1%	25.8%	**30.0%**	6.4%	4.6%	16 191 882
60%	31.1%	24.3%	**34.2%**	6.0%	4.4%	16 069 937

$LiNi_{0.33}Mn_{0.33}Co_{0.33}O_2$						
% Change in NMC	**Wt% LCO**	**Wt% NMC**	**Wt% LMO**	**Wt% LNO**	**Wt% LFP**	**NPV**
-60%	46.3%	**11.6%**	26.6%	9.0%	6.5%	17 452 037
-40%	43.3%	**17.4%**	24.9%	8.4%	6.0%	17 114 409
-20%	40.2%	**23.2%**	23.1%	7.8%	5.6%	16 776 799
0%	37.2%	**29.0%**	21.4%	7.2%	5.2%	16 439 761
20%	34.2%	**34.8%**	19.7%	6.6%	4.8%	16 103 238
40%	31.1%	**40.6%**	17.9%	6.0%	4.4%	15 767 186
60%	28.1%	**46.4%**	16.2%	5.4%	3.9%	15 431 566

$LiNiO_2$						
% Change in LNO	**Wt% LCO**	**Wt% NMC**	**Wt% LMO**	**Wt% LNO**	**Wt% LFP**	**NPV**
-60%	38.9%	30.4%	22.4%	**2.9%**	5.4%	17 749 287
-40%	38.4%	29.9%	22.1%	**4.3%**	5.4%	17 312 226
-20%	37.8%	29.5%	21.7%	**5.8%**	5.3%	16 875 737
0%	37.2%	29.0%	21.4%	**7.2%**	5.2%	16 439 761
20%	36.6%	28.6%	21.1%	**8.6%**	5.1%	16 004 250
40%	36.0%	28.1%	20.7%	**10.1%**	5.0%	15 569 165
60,0%	35.5%	27.7%	20.4%	**11.5%**	5.0%	15 134 471

$LiCoO_2$						
% Change in LCO	**Wt% LCO**	**Wt% NMC**	**Wt% LMO**	**Wt% LNO**	**Wt% LFP**	**NPV**
-60%	**14.9%**	39.3%	29.0%	9.8%	7.0%	10 001 277
-40%	**22.3%**	35.9%	26.5%	8.9%	6.4%	12 144 135
-20%	**29.8%**	32.4%	23.9%	8.1%	5.8%	14 290 360
0%	**37.2%**	29.0%	21.4%	7.2%	5.2%	16 439 761
20%	**44.6%**	25.6%	18.9%	6.3%	4.6%	18 588 749
40%	**52.1%**	22.1%	16.3%	5.5%	4.0%	20 739 691
60%	**59.5%**	18.7%	13.8%	4.6%	3.4%	22 894 257

Table 109: Effect of pre-treatment losses on profitability of OA-1

% Change in pre-treatment losses	Pre-treatment Losses	CAPEX	OPEX	Revenue	NPV	PVR
-100%	0%	23 353 419	17 474 036	27 650 966	21 619 508	2.06
-75%	2%	23 206 564	17 343 757	27 100 982	20 323 548	2.01
-50%	4%	23 059 199	17 213 345	26 550 998	19 028 259	1.95
-25%	6%	22 911 311	17 082 796	26 001 015	17 733 657	1.89
0%	8%	22 762 885	16 952 107	25 451 031	16 439 761	1.83
25%	10%	22 613 909	16 821 275	24 901 048	15 146 589	1.77
50%	12%	22 464 368	16 690 294	24 351 064	13 854 161	1.71
75%	14%	22 314 246	16 559 162	23 801 080	12 562 499	1.65
100%	16%	22 163 526	16 427 873	23 251 097	11 271 623	1.58

Monte Carlo Simulation Histograms

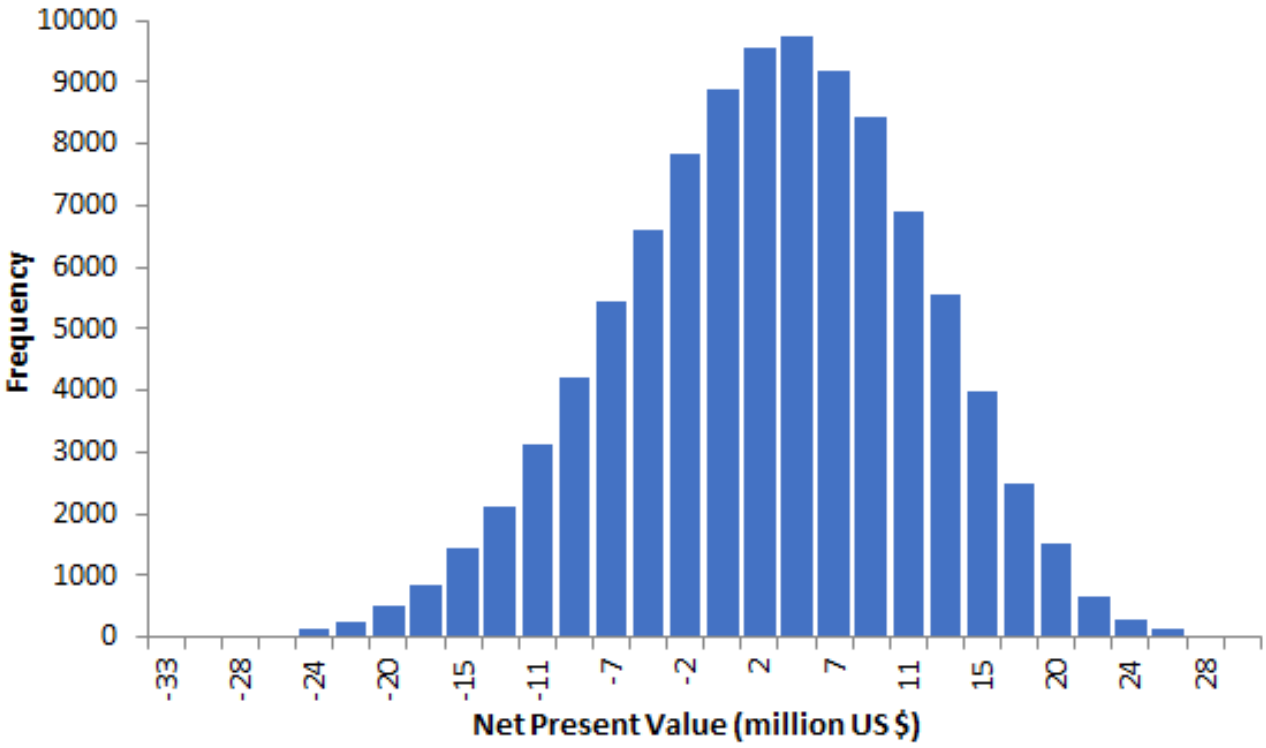

Figure 32: Histogram representing the data of Monte Carlo Simulation 1

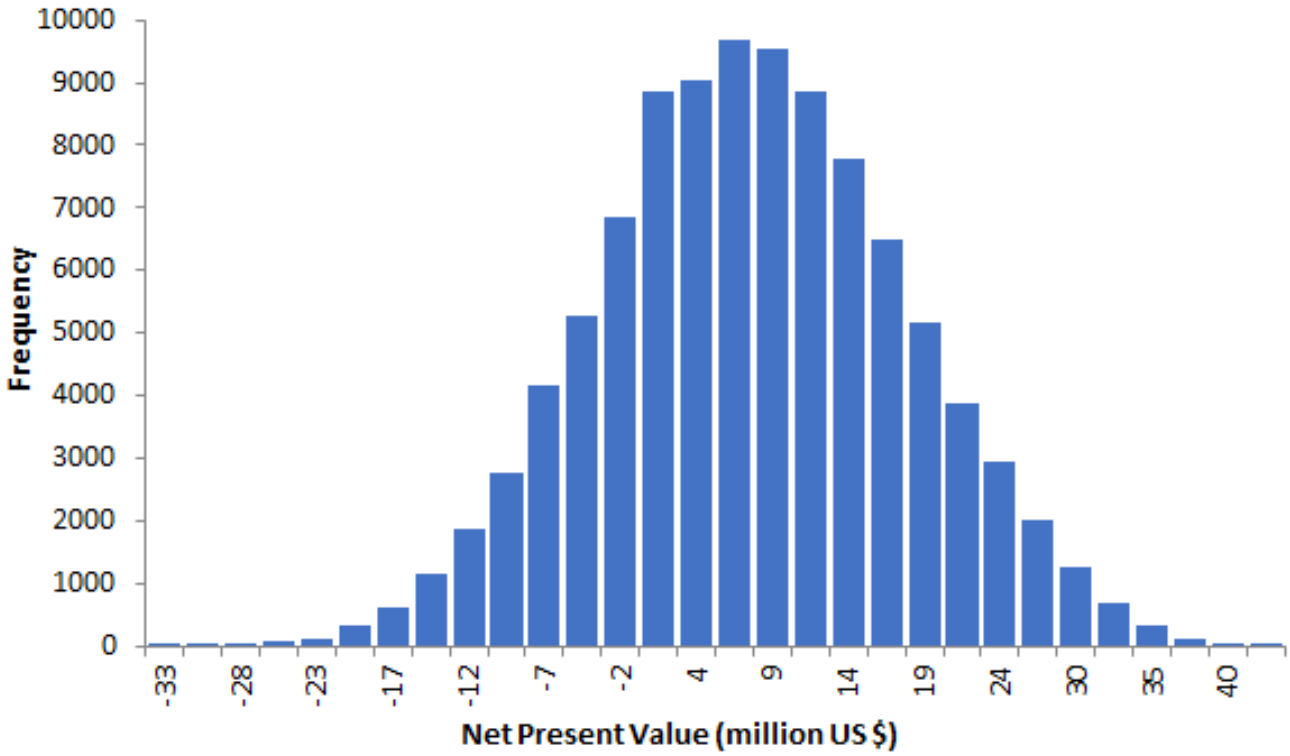

Figure 33: Histogram representing the data of Monte Carlo Simulation 2

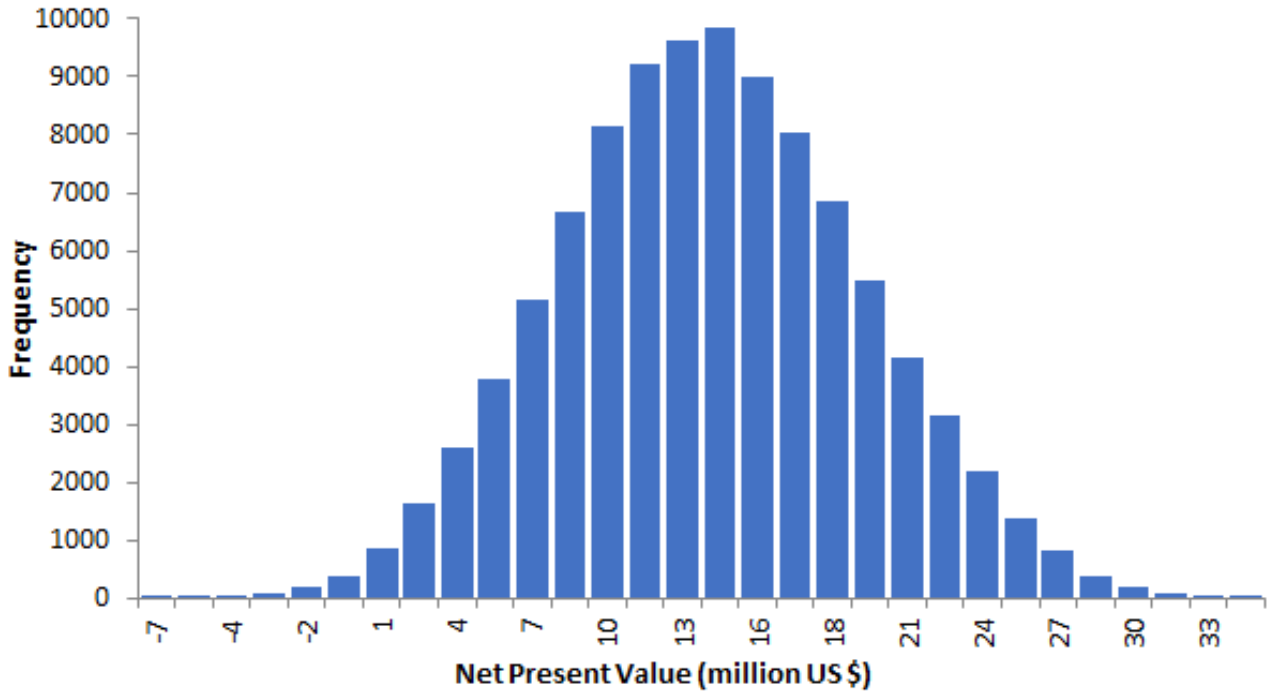

Figure 34: Histogram representing the data of Monte Carlo Simulation 3

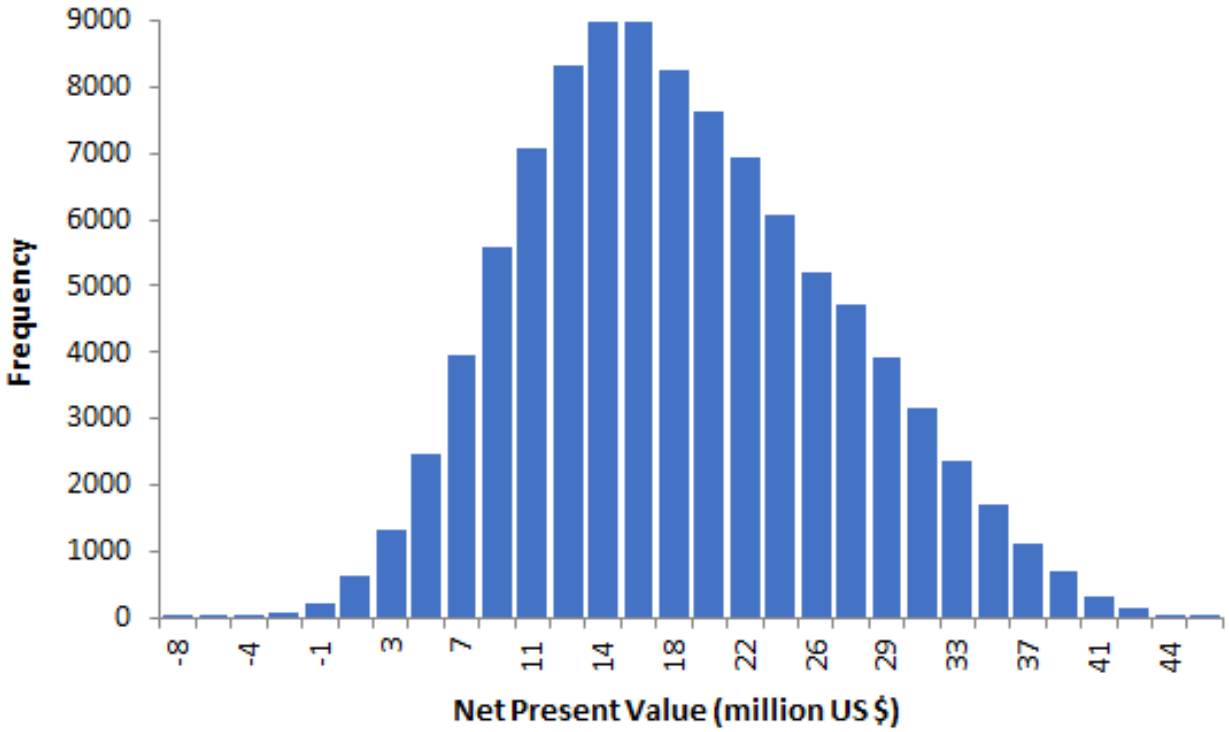

Figure 35: Histogram representing the data of Monte Carlo Simulation 4

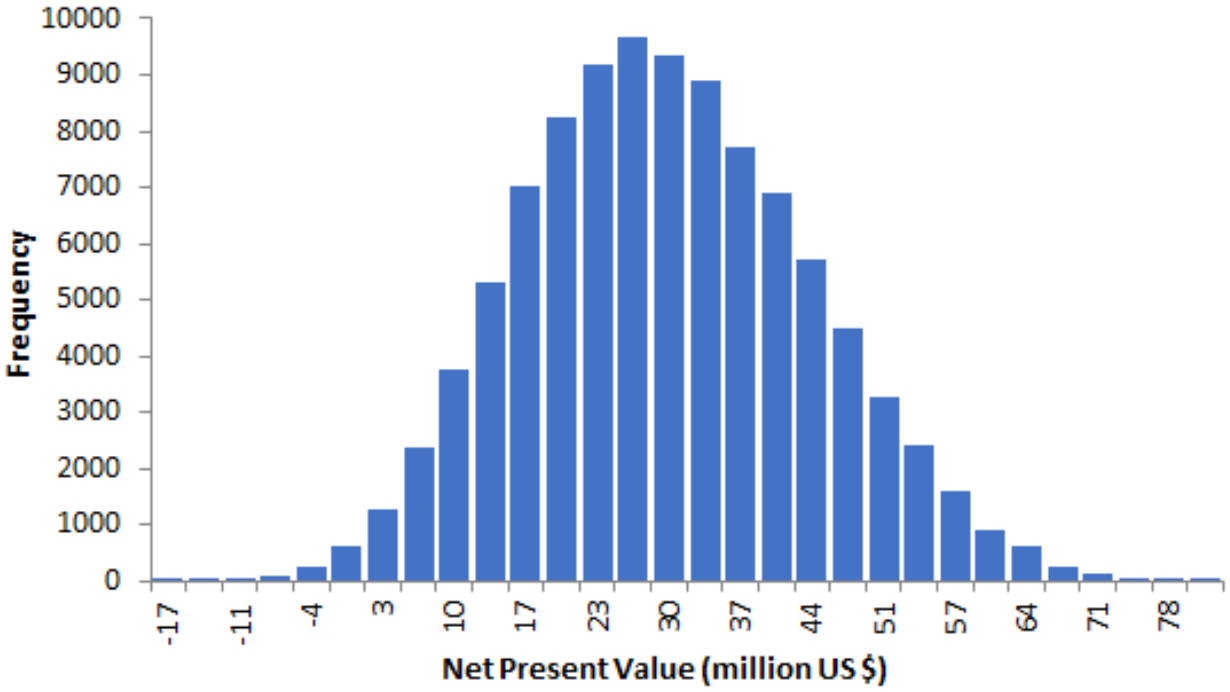

Figure 36: Histogram representing the data of Monte Carlo Simulation 5

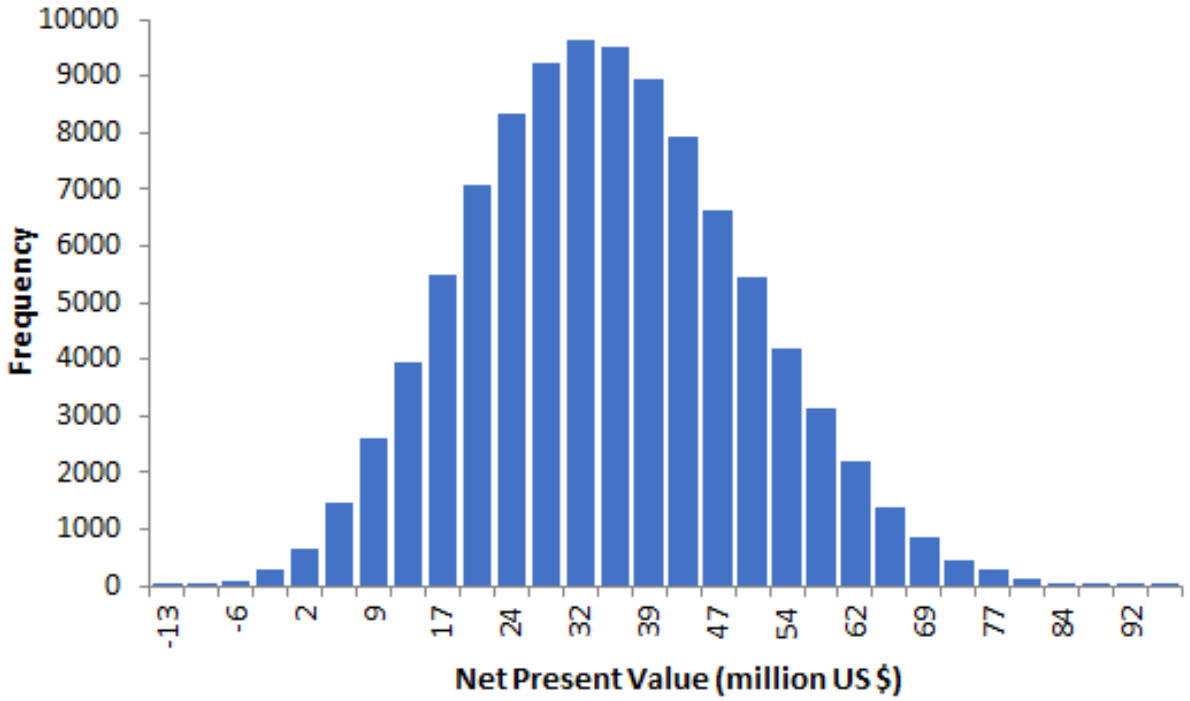

Figure 37: Histogram representing the data of Monte Carlo Simulation 6